HSRI THREE DIMENSIONAL CRASH VICITIM SIMULATOR:: ANALYSIS, VERIFICATION, USER'S MANUAL AND PICTORIAL SECTION

EDC Library Ref. No. 1018

DISCLAIMER

DOT HS-800 551

HSRI THREE DIMENSIONAL CRASH VICTIM SIMULATOR: ANALYSIS, VERIFICATION, AND USERS' MANUAL, AND PICTORIAL SECTION

Highway Safety Research Institute
The University of Michigan
Huron Parkway and Baxter Road
Ann Arbor, Michigan 48105

Contract No. FH-11-6962
June 30, 1971
Final Report

PREPARED FOR:
U.S. DEPARTMENT OF TRANSPORTATION
NATIONAL HIGHWAY TRAFFIC SAFETY ADMINISTRATION
WASHINGTON, D.C. 20590

17245

1. Report No.	2. Government Accession No.	3. Recipient's Catalog No.

4. Title and Subtitle	5. Report Date
HSRI Three-Dimensional Crash Victim Simulator: Analysis, Verification, and Users' Manual, and Pictorial Section	June 30, 1971
	6. Performing Organization Code
7. Author(s)	8. Performing Organization Report No.
D.H. Robbins, R.O. Bennett, and V.L. Roberts	Bio M-70-9
9. Performing Organization Name and Address	10. Work Unit No.
Highway Safety Research Institute The University of Michigan Huron Parkway and Baxter Road Ann Arbor, Michigan 48105	
	11. Contract or Grant No.
	FH-11-6962
12. Sponsoring Agency Name and Address	13. Type of Report and Period Covered
National Highway Traffic Safety Administration U.S. Department of Transportation Federal Highway Administration 7th and E Streets, S.W. Washington, D.C. 20590	Final Report January 1, 1969 - June 30, 1971
	14. Sponsoring Agency Code

15. Supplementary Notes

16. Abstract

This report deals with the development and use of mathematical models for the simulation of automotive occupant kinematics in the event of a collision. This model was developed as a tool to study advanced concepts and designs of seat-restraint systems from the viewpoint of occupant protection. After a discussion of the state-of-the-art of mathematical modeling of the crash victim, an analytical description of the HSRI Three-Dimensional Crash Victim Simulator is presented. This model consists of a segmented, three-mass dynamic model of a human interacting with the interior of a vehicle in a full six degree-of-freedom crash. The degree to which predictions of the model agree with experimental impact sled test data is presented along with a detailed Users' Manual for those individuals desiring to exercise the HSRI Three-Dimensional Crash Victim Simulator. The report concludes with a description of the pictorial section.

17. Key Words	18. Distribution Statement

19. Security Classif.(of this report)	20. Security Classif.(of this page)	21. No. of Pages	22. Price

Form DOT F 1700.7 (8-69)

TABLE OF CONTENTS

17245

TABLE OF CONTENTS (Cont'd.)

LIST OF FIGURES

TABLES

TABLES (Continued)

ACKNOWLEDGMENTS

This research program was carried out by staff of the Biosciences Division of the Highway Safety Research Institute, The University of Michigan. The program was under the direction of Dr. D. H. Robbins, Dr. V. L. Roberts, and Mr. R. O. Bennett.

Mrs. J. M. Becker deserves special mention for her contributions to this work.

1.0 INTRODUCTION

This report deals with the development and use of a mathematical model for the simulation of automobile occupant kinematics in three dimensions in event of a collision. The model was developed as a tool to study advanced concepts and designs of seat restraint systems from the viewpoint of occupant protection.

A schematic for the three-dimensional model is shown in Figure 1. The three parts of the model are the occupant, the vehicle, and the deceleration profile. The occupant is represented by three mass elements located in the head, torso, and extermities. Attached to the various body elements are ellipitical surfaces serving to outline the body in order that contact between the occupant and the interior or exterior of a vehicle can be predicted. The vehicle is represented by a series of planar contact surfaces which can be arranged to represent either a vehicle interior for occupant kinematics studies or the exterior for pedestrian studies. Belt restraints are included in the model if their use is desired. Forces are applied to the body of the occupant whenever interaction is sensed between the occupant and the vehicle. In order to produce occupant motions, a six degree of freedom deceleration can be applied to the vehicle. The resulting occupant motions are listed as computer program output.

In addition to an analytical description of the model, a User's Guide is included as a part of this report. Sections are included describing preparation of input data decks and the options available in studying the output produced by the computer program. The techniques which can be used in operating the model at a teletype terminal remote from The University of Michigan

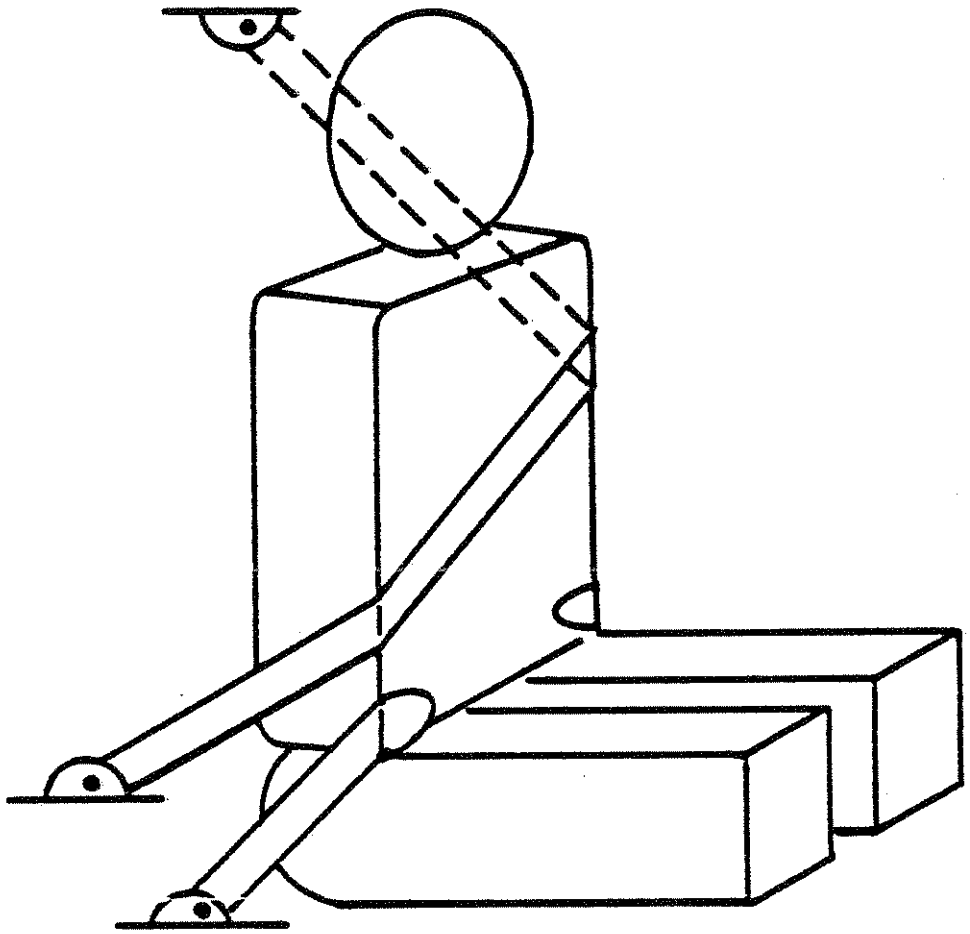

FIG. 1

THREE-MASS, THREE-DIMENSIONAL MODEL

are described in a Teletype Users' Guide. Documentation of the program includes an overall program description and flow diagrams, subroutine descriptions and a complete symbol dictionary.

The comparison of the predictions of the model with experimental impact sled tests is the subject of part 3.0 of the report. The complex problem of gathering a set of input data describing the occupant and the vehicle is discussed and the technique by which this is carried out are described. The equally difficult task of obtaining appropriate experimental data is also considered. Comparisons between a 30 mph impact sled test involving a belt-restrained 50th percentile male dummy and the predictions of the model conclude part 3.0.

The model which is described in this report is proposed as a powerful tool for studying and designing advanced integrated seat-restraint systems. It has been exercised several hundred times to study belt restraint systems, various deceleration profiles, headrest and seatback shape, pedestrian kinematics, occupant size and position, etc., and represents the current state of the art in three-dimensional crash victim simulators.

As a secondary output, the program produces a file of stored data which is used in preparing pictorial displays of occupant motions on a sequence of ink plots, a television screen, or as 16mm motion pictures. The calling routines for operating on this file are described in part 5.0.

1.1 STATE OF THE ART

Mathematical models have been developed for the motion of the human body in several environments, including auto occupant dynamics*[1-8], human gait, and

*Note: Only a small number of representative papers published on this are included in this list.

the motions experienced by the legs and arms during walking.[9-11] This work is often applied to the design, development and use of prosthetic devices. In connection with aerospace applications, analytical studies of self-generated motions possible in free-fall[12-14] and 0-gravity environments are being carried out and find application in such activities as sky-diving and space-walking. Also, studies are being made of such work tasks as lifting[15,16] resulting in the development of work capability amplifiers.

Fundamental theoretical work has been carried out in the field of mathematical models for more than sixty years, as seen in the work of Fischer.[17] However, it is only with the coming-of-age of the high speed computer in the last twenty years that practical solutions of equations as complex as those proposed by Fischer have been realized. Hence, the mathematical simulation of human body motions has become a very active research topic in the last ten years.

Generally, two approaches have been used in analyses simulating auto occupant protection. On one hand, various researchers have adopted relatively simple physical models for studying specific aspects of human kinematics. Weaver[18] has used a two-mass, two-degree-of-freedom model to simulate belt loadings and head impact velocity in the case of a lap-belted occupant. Similar models have been developed by Aldman[19] and Renneker[20] for studying slack in restraint systems and the effect of various input deceleration profiles. Other authors, including Martinez[21], Mertz[22], and Roberts[23] have used somewhat more sophisticated models for studying the phenomenon of whiplash. Roberts has added an additional complicating factor to his model—the motion of the brain mass inside the brain case.

On the other hand, several authors[1-8] have developed more complex models of human kinematics utilizing several masses for simulating body motions. In

addition, complex vehicle geometry is introduced in these simulations to provide an intricate array of forces acting on the segmented occupant. Particularly noteworthy in the early development of these models are the efforts of McHenry.[2] All these models are marked by extensive development programs requiring at least two years from project initiation to the production of a functioning computer program.

Most of the modeling work mentioned above has been concerned with simulations of occupant motion in two dimensions. The only known published simulations involving three dimensions are those of Roberts,[1] Thompson,[4] Robbins,[6] and Young.[7] The first of these is a simple-one-mass model capable of simulating belt loads and upper torso motions in three dimensions, while the second is part of a large program involving vehicle crush characteristics. The third model simulates a three-dimensional occupant by three masses and twelve degrees-of-freedom while the recently completed fourth model describes the occupant by twelve masses and thirty-one degrees-of-freedom while possessing a less sophisticated model of occupant-vehicle interactions than that of Robbins.[6]

Even with the advent of the highly complex computer programs described here, there still exist major problem areas such as:

1. Verification of the model by experiment;
2. Lack of highly controlled tests;
3. Lack of anthropometric data and verification of the models using human volunteers;
4. Lack of impact test data reduction techniques specifically oriented towards mathematical model verification.
5. Difficulty in using the models because of the complex input data requirements; and

6. Difficulty in using the model at locations other than the laboratories of the developer.

These problems can be classified into two general types: (a) lack of closely coordinated efforts to insure that the mathematical models predict and anticipate physical reality, and (b) ease of use. The latter problem is somewhat easier to approach than the first one. One needs to identify the user and his capabilities and then write a program which is user-oriented. Computer programs of this nature are in actual use, particularly in styling and design laboratories in the auto industry. The users need not be highly trained computer experts.

In assigning staff to the various subject areas of the current research project, a concerted effort was made to coordinate the sled test program and the analytical program. One group was assigned the task of analysis; another group was responsible for the impact sled test program; and a new key group was formed to bridge the gap which was found to exist between the analytical and experimental groups. The task of the key group was to insure that meaningful data was generated in the tests and to establish techniques for reducing this data into a form which could be compared with the output of a mathematical model.

This discussion is intended to show that the current state of the art is quite advanced from the viewpoint of producing computer programs which predict vehicle occupant motions in a crash environment. However, considerable research must be carried out to make programs of this nature easily usable. Additionally, it is recommended that experimental work accompany the development of future models to make assessment of their validity more straightforward.

by stops located at the limit of practical motion of each joint. The stops are modeled by linear, viscoelastic torsional springs possessing a high degree of stiffness. Third, body geometry is represented by the moments of inertia of the three rigid masses and by body contact ellipsoids. These ellipsoids, which are rigidly attached to the head, torso, and lower extremities, allow the user of the model to ascertain if a body part contacts any part of the vehicle interior (or exterior) and with what force.

The external system restraining an occupant is ordinarily defined in terms of specific devices such as a seat belt or an airbag. One common feature of all these devices is the fact that they can be described in terms of a dynamic force-deformation profile. For example, an acceleration-dependent inertial reel used in conjunction with a shoulder harness will have a different characteristic curve than a controlled permanent deformation device or one of the harnesses used in most current production vehicles. In each case a different formula must be used which computes force as a function of deformation and deformation rate. Therefore, provisions must be made for forces to be applied to the occupant in a rather general manner in order that they can be used in modeling any one of the proposed restraint devices.

Two types of interactions are possible between the occupant and vehicle: (a) the occupant with a system of belts attached to both the vehicle and himself, i.e., the seat belt and/or shoulder harness, and (b) a collection of ellipsoids representing body parts with a collection of geometric surfaces representing the profile of a vehicle interior or exterior. These surfaces, each represented by a different dynamic force-deformation relationship, interact with the contact ellipsoids fixed to the body of the occupant to generate a complex interaction of forces and occupant motions representing the collision of the occupant with seat, restraint system, or vehicle structural member.

An example of a complex set of force interactions between an occupant and a vehicle interior is represented by simulating the airbag restraint system. The occupant is represented in the usual way and may or may not be restrained by a lap belt. Vehicle components such as the seat back, seat cushion, floor, windshield, and lower dash panel are described in terms of contact surfaces. It is necessary to know the force-motion interrelationship between the head or torso and the bag before the simulation can be carried out as the model itself cannot predict any force-deformation relationships. They must be obtained using experimental procedures and be provided as input data for the operation of the computer simulation.

It should also be noted that this general formulation allows studies of much more than a seated occupant restrained in some manner inside the vehicle. Studies have been carried out of more esoteric concepts such as the collapsing airbag, the oblique rolling collision, and the pedestrian. Also, studies of the dynamics of a child in any one of the large number of seats and restraint devices available on today's market are possible.

The deceleration profile of the crashing vehicle which is used in this model can provide a completely general six-degree-of-freedom motion input to the occupant compartment. The motions can include front (or rear), lateral, and vertical linear decelerations as well as pitching, spinning, and rolling angular decelerations. These input decelerations may be used separately or in any combination. The shape of each deceleration profile input to the model is limited to 100 piecewise linear segments. Typical examples are shown in Figures 2 and 3.

2.2 FORMULATION OF THE MODEL

The equations of motion are derived by Lagrangian techniques[24]:

$$\frac{d}{dt}\left[\frac{\partial(KE)}{\partial \dot{Z}_i}\right] - \frac{\partial(KE)}{\partial Z_i} + \frac{\partial(PE)}{\partial Z_i} + \frac{\partial(DE)}{\partial \dot{Z}_i} = F_{Z_i} \qquad (2.2.1)$$

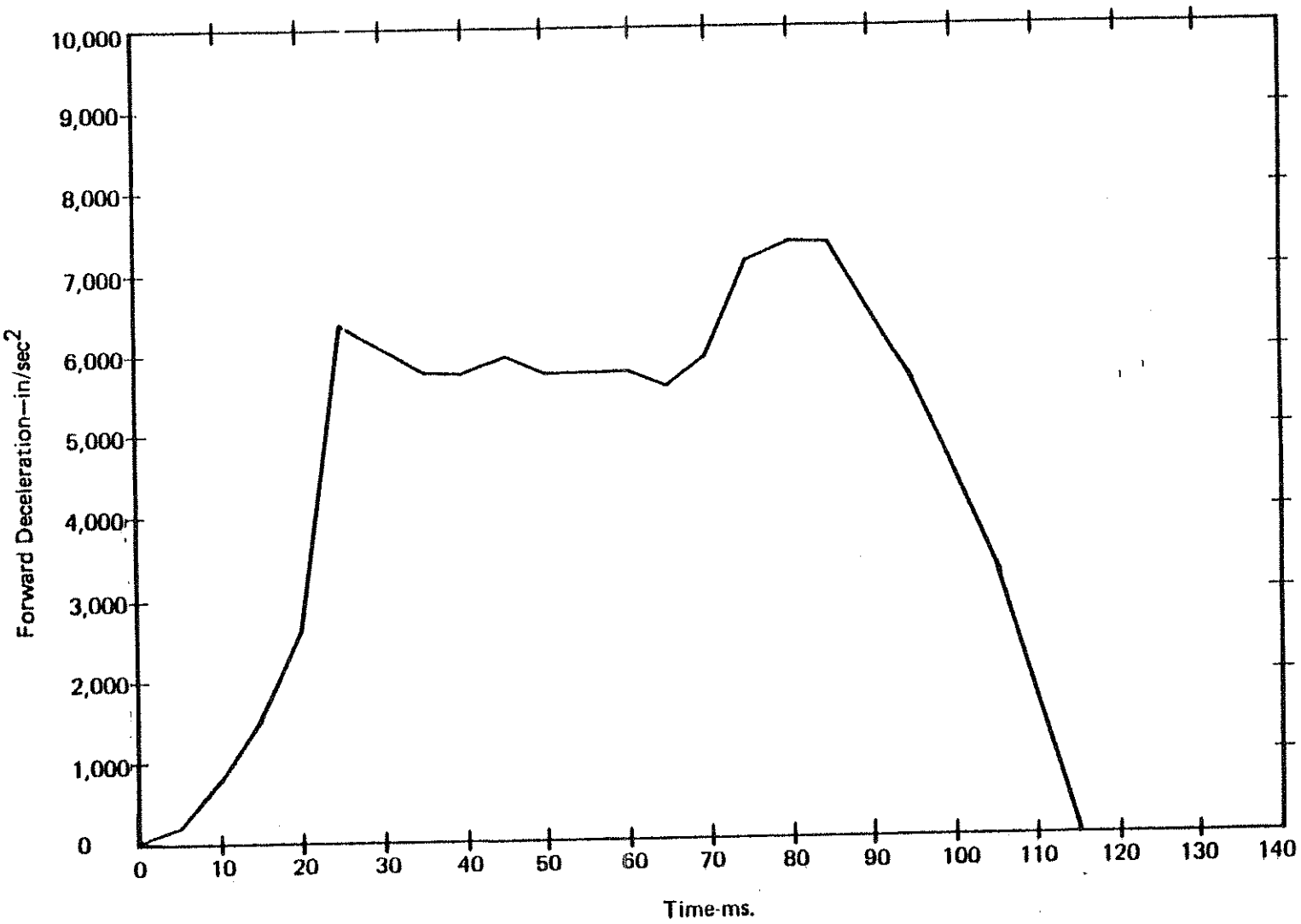

Figure 2. AMA Frontal Deceleration Profile

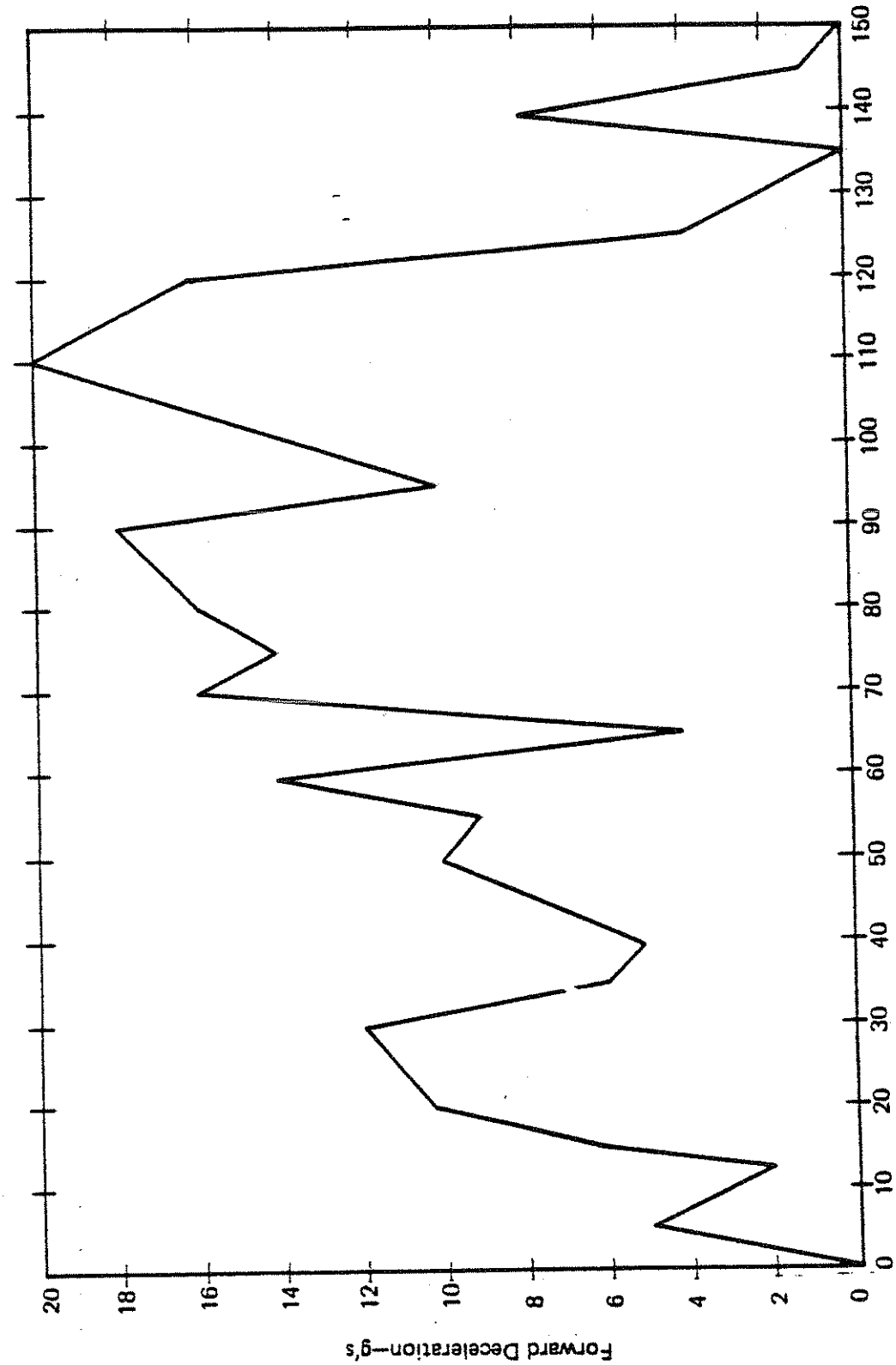

Figure 3. Complex Frontal Deceleration Trace

where

KE is the system kinetic energy

PE is the system potential energy

DE is the system dissipated energy rate

F_{Z_i} are the classical generalized forces

Z_i are the classical generalized coordinates or degrees of freedom of the model

Since the only driving force is applied to the vehicle and not directly to the body, the F_{Z_i} terms are all zero. After the energy terms have been written, the resulting equations of motion are rearranged so that all the terms containing generalized accelerations appear on the left-hand side and all other terms appear on the right-hand side. Thus rearranged, these equations are of the form

$$m \ddot{\vec{Z}} = \vec{Q} \tag{2.2.2}$$

where m is the matrix of generalized acceleration coefficients and $\ddot{\vec{Z}}$ is the generalized acceleration vector. In this analysis the right-hand side of the equation, $\vec{Q}$, will be called the "generalized force" and contributions to it from the kinetic, potential, and dissipative energies in Equation (2.2.1) will be referred to as the generalized force from that part of the model. The total "generalized force" is the vectorial sum of each contributing component (gravity, joints, belts and contacts). The kinetic energy contributions to the "generalized force" are centrifugal and Coriolis force terms.

Kinetic energy alone determines the left-hand side of the equations of motion. In the computational procedure, the inverse of the matrix, m^{-1}, multiplied by the generalized vector, $\vec{Q}$, yields the solution for the generalized accelerations, i.e.,

$$\ddot{\vec{Z}} = m^{-1}\vec{Q} \tag{2.2.3}$$

The generalized force vector may be expanded to show the various contributions

$$\vec{Q} = \vec{Q}_G + \vec{Q}_T + \vec{Q}_C + \vec{Q}_J + \vec{Q}_B \qquad (2.2.4)$$

where

$\vec{Q}_T$ is due to kinetic energy
$\vec{Q}_G$ is due to gravity
$\vec{Q}_C$ is due to contact forces
$\vec{Q}_J$ is due to joints
$\vec{Q}_B$ is due to belts

are there any other restraining or effecting forces we might want to consider down stream?

2.3 BODY

The crash victim is simulated by three body segments: the head, the torso (with attached arms), and the lower extremities (right and left legs combined). Figure 1 shows a crash victim in a typical seating configuration restrained by a lap belt and shoulder harness. Figure 4 illustrates the body segments and their lengths, centers of gravity, and moments of inertia.

The basic inertial coordinate system has unit vector $\vec{I}$ pointed forward, $\vec{J}$ pointed right, and $\vec{K}$ pointed downward and positioned at an arbitrary point in space.

Let

$$e = \begin{bmatrix} \vec{I} \\ \vec{J} \\ \vec{K} \end{bmatrix} \qquad (2.3.1)$$

The coordinate systems imbedded in the torso, head, legs, and vehicle will be referred to as e_1, e_2, e_3, and e_4 respectively where

$$e_n = \begin{bmatrix} \vec{i}_n \\ \vec{j}_n \\ \vec{k}_n \end{bmatrix} \quad \text{for } n = 1, 2, 3, \text{ or } 4 \qquad (2.3.2)$$

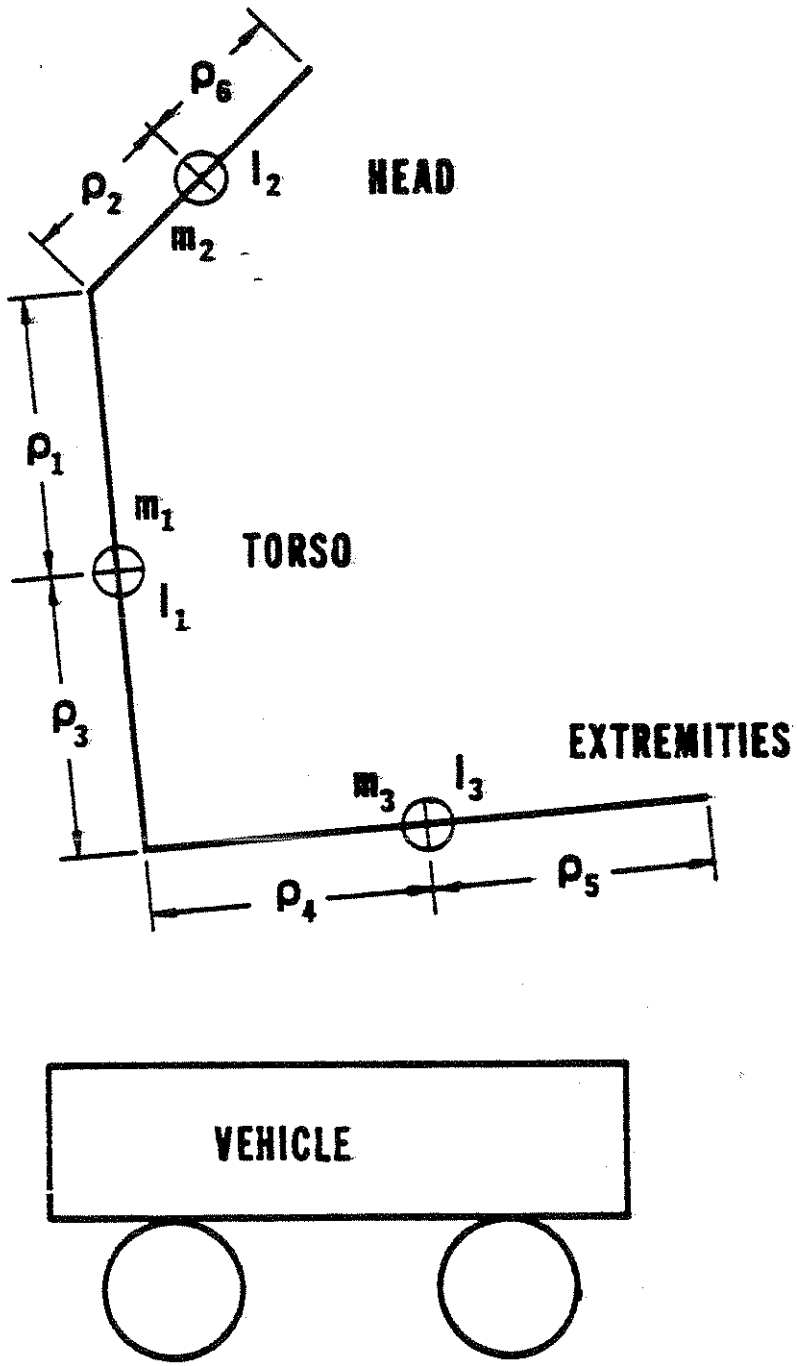

FIG. 4

DETAIL OF THREE-MASS BODY SHOWING LENGTHS, CENTERS OF GRAVITY, AND MOMENTS OF INERTIA

e_1 is positioned at the torso center of gravity so that $\vec{i}_1$ points out of the chest, $\vec{j}_1$ points out the right arm, and $\vec{k}_1$ points out the bottom of the torso.

e_2 is positioned at the head center of gravity so that $\vec{i}_2$ points out the nose, $\vec{j}_2$ points out the right ear, and $\vec{k}_2$ points down the neck.

e_3 is positioned at the center of gravity of the lower extremities so that $\vec{i}_3$ protrudes forward from the knees, $\vec{j}_3$ points out the right side, and $\vec{k}_3$ points out the bottom of the upper legs.

e_4 is positioned at a point "O" which is arbitrarily positioned in the vehicle with $\vec{e}_4$ extending forward, $\vec{j}_4$ extending right, and $\vec{k}_4$ extending downward.

Figure 5 shows the relationships between the five basic coordinate systems, their positions, and orientations. Note that the vector $\vec{R}_n$ points from the inertial system to the origin of the n^{th} movable coordinate system for each of the four values of n.

The rotations of each of the movable coordinate systems are described by a set of Euler angles as illustrated in Figure 6. It should be noted that any of the systems of movable coordinates, e_n, are positioned initially parallel to the inertial system and the angles are applied in the order yaw, pitch, and roll. The arrows in Figure 6 show the direction of positive rotation. When the individual rotations are applied to a coordinate system, it will be true that

$$e_n = \begin{bmatrix} \cos\psi_n\cos\theta_n & \sin\psi_n\cos\theta_n & -\sin\theta_n \\ \cos\psi_n\sin\theta_n\sin\phi_n - \sin\psi_n\cos\phi_n & \sin\psi_n\sin\theta_n\sin\phi_n + \cos\psi_n\cos\phi_n & \cos\theta_n\sin\phi_n \\ \cos\psi_n\sin\theta_n\cos\phi_n + \sin\psi_n\sin\phi_n & \sin\psi_n\sin\theta_n\cos\phi_n - \cos\psi_n\sin\phi_n & \cos\theta_n\cos\phi_n \end{bmatrix} e \qquad (2.3.3)$$

for each n = 1, 4

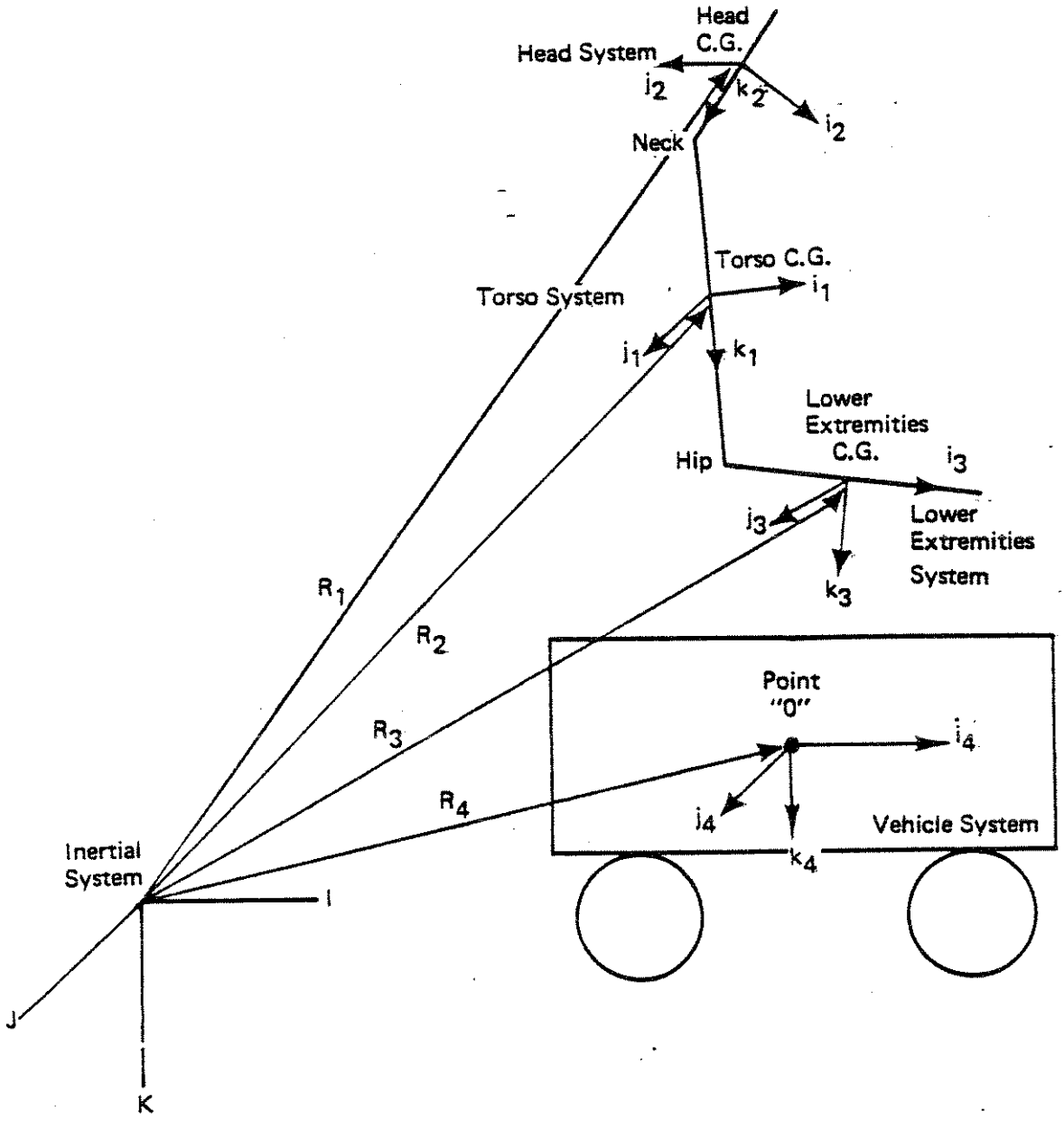

Fig. 5. Detail Showing the Coordinate Systems Used in This Simulation

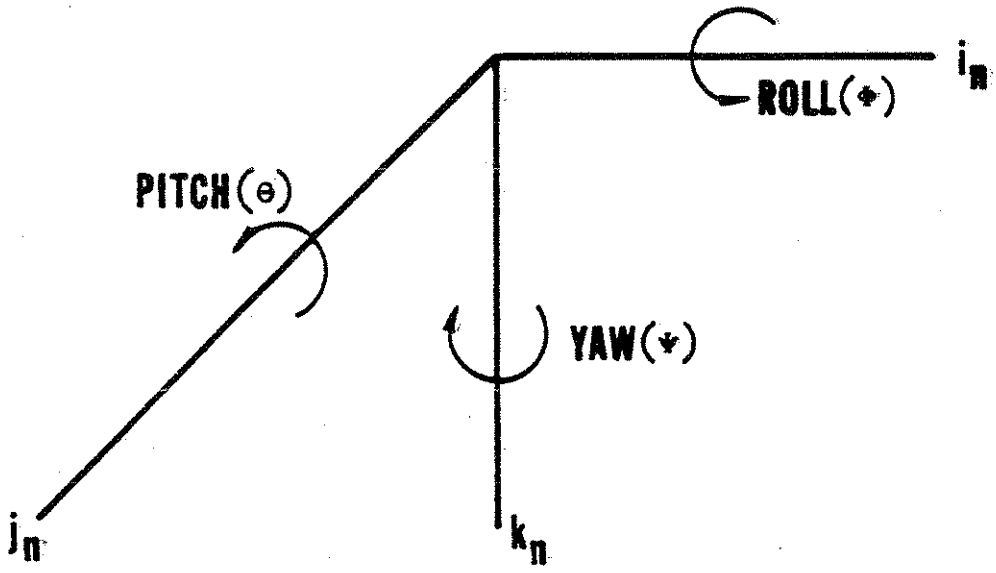

FIG. 6

DEFINITION OF EULER ANGLES

The rotational kinetic energy is

$$T_{rot} = \frac{1}{2} \sum_{n=1}^{3} \sum_{m=1}^{3} I_{mn}\alpha_{mn}^2 \tag{2.3.4}$$

where

I_{1n} is the moment of inertia about $\vec{i}_n$

I_{2n} about $\vec{j}_n$

I_{3n} about $\vec{k}_n$

and "n" is the body segment index (n=1 for torso, n=2 for head, n=3 for lower extremities). The quantities α_{1n}, α_{2n}, and α_{3n} shown in Equation (2.3.5)

$$\begin{aligned} \alpha_{1n} &= \dot{\phi}_n - \dot{\psi}_n \sin\theta_n \\ \alpha_{2n} &= \dot{\psi}_n \sin\phi_n \cos\theta_n + \dot{\theta}_n \cos\phi_n \\ \alpha_{3n} &= \dot{\psi}_n \cos\phi_n \cos\theta_n - \dot{\theta}_n \sin\phi_n \end{aligned} \tag{2.3.5}$$

are the components of the angular velocity vector $\vec{\omega}_n$ shown in Equation (2.3.6).

$$\vec{\omega}_n = \alpha_{1n}\vec{i}_n + \alpha_{2n}\vec{j}_n + \alpha_{3n}\vec{k}_n \tag{2.3.6}$$

The translational kinetic energy for the body is

$$T_{trans} = \frac{1}{2} \sum_{\ell=1}^{3} m_\ell(\dot{x}_\ell^2 + \dot{y}_\ell^2 + \dot{z}_\ell^2) \tag{2.3.7}$$

where m_ℓ is the mass of the ℓ^{th} body segment and x_ℓ, y_ℓ, z_ℓ are the components of the position vector of the body segment center of gravity as shown in Figure 5 and Equation (2.3.8).

$$\vec{R}_n = x_n\vec{I} + y_n\vec{J} + z_n\vec{K} \tag{2.3.8}$$

The total kinetic energy is then just the sum of T_{rot} and T_{trans}.

A three mass structure connected by ball joints will exhibit twelve degrees of freedom. The twelve generalized coordinates used in this simulation are x_1, y_1, z_1, ψ_1, θ_1, ϕ_1, ψ_2, θ_2, ϕ_2, ψ_3, θ_3, and ϕ_3 in that order.

It is true that

$$\vec{R}_2 = \vec{R}_1 - \rho_1\vec{k}_1 - \rho_2\vec{k}_2$$

and

$$\vec{R}_3 = \vec{R}_1 + \rho_3\vec{k}_1 + \rho_4\vec{i}_3 \qquad (2.3.9)$$

where ρ_i is the distance along the centerline from the center of gravity of one of the body segments to one of the joints or the end of the body segment as shown in Figure 4. Equation (2.3.10) shows Equation (2.3.9) rewritten in terms of generalized coordinates.

$$x_2 = x_1 - \sum_{\ell=1}^{2} \rho_\ell[\cos\psi_\ell\sin\theta_\ell\cos\phi_\ell + \sin\psi_\ell\sin\phi_\ell]$$

$$y_2 = y_1 - \sum_{\ell=1}^{2} \rho_\ell[\sin\psi_\ell\sin\theta_\ell\cos\phi_\ell - \cos\psi_\ell\sin\phi_\ell]$$

$$z_2 = z_1 - \sum_{\ell=1}^{2} \rho_\ell[\cos\theta_\ell\cos\phi_\ell] \qquad (2.3.10)$$

$$x_3 = x_1 + \rho_3(\cos\psi_1\sin\theta_1\cos\phi_1 + \sin\psi_1\sin\phi_1) + \rho_4\cos\psi_3\cos\theta_3$$

$$y_3 = y_1 + \rho_3(\sin\psi_1\sin\theta_1\cos\phi_1 - \cos\psi_1\sin\phi_1) + \rho_4\sin\psi_3\cos\theta_3$$

$$z_3 = z_1 + \rho_3\cos\theta_1\cos\phi_1 - \rho_4\sin\theta_3$$

When Equation (2.3.10) is substituted into Equation (2.3.7) and then, along with Equation (2.3.4), substituted into Equation (2.2.1) and rearranged into the form of Equation (2.2.2), the resulting matrix, m, has the elements shown in Equation (2.3.11).

Since the matrix, m, is symmetric, only the diagonal and the terms above the diagonal are whown in Equation (2.3.11). Certain trigonometric functions used in the matrix and throughout this report are given in Equation (2.3.12).

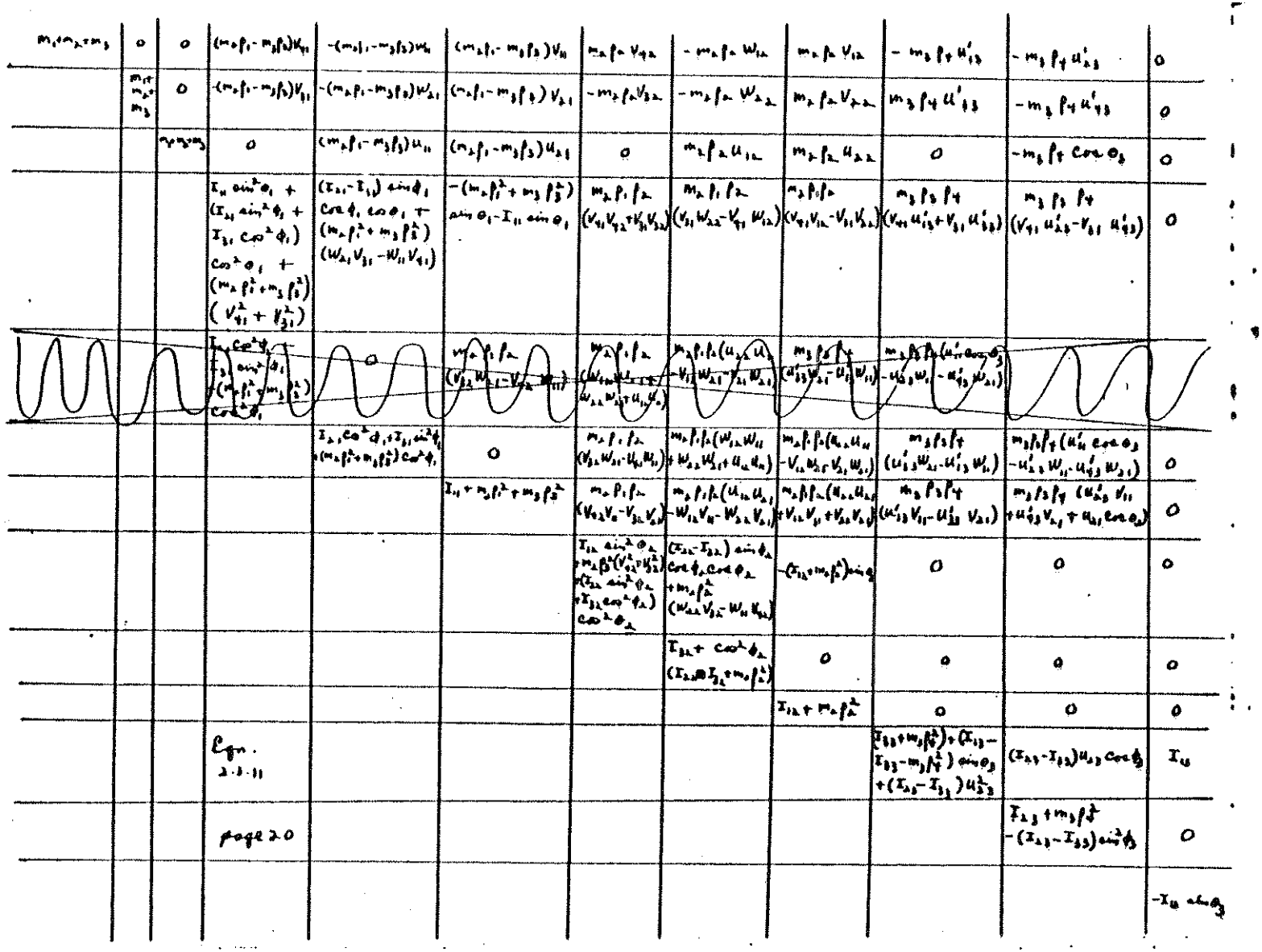

Eqn. 2.3.11

page 20

$$
\begin{aligned}
V_{1k} &= \cos\psi_k \sin\theta_k \sin\phi_k - \sin\psi_k \cos\phi_k \\
V_{2k} &= \sin\psi_k \sin\theta_k \sin\phi_k + \cos\psi_k \cos\phi_k \\
V_{3k} &= \cos\psi_k \sin\theta_k \cos\phi_k + \sin\psi_k \sin\phi_k \\
V_{4k} &= \sin\psi_k \sin\theta_k \cos\phi_k - \cos\psi_k \sin\phi_k \\
W_{1k} &= \cos\psi_k \cos\theta_k \cos\phi_k \\
W_{2k} &= \sin\psi_k \cos\theta_k \cos\phi_k \\
W_{3k} &= \cos\psi_k \cos\theta_k \sin\phi_k \\
W_{4k} &= \sin\psi_k \cos\theta_k \sin\phi_k \\
W_{5k} &= \cos\psi_k \sin\theta_k \cos\phi_k \\
W_{6k} &= \sin\psi_k \sin\theta_k \cos\phi_k \\
W_{7k} &= \cos\psi_k \sin\theta_k \sin\phi_k \\
W_{8k} &= \sin\psi_k \sin\theta_k \sin\phi_k \\
u_{1k} &= \sin\theta_k \cos\phi_k \\
u_{2k} &= \cos\theta_k \sin\phi_k \\
u_{3k} &= \cos\theta_k \cos\phi_k \\
u_{4k} &= \sin\theta_k \sin\phi_k \\
u'_{1k} &= \sin\psi_k \cos\theta_k \\
u'_{2k} &= \cos\psi_k \sin\theta_k \\
u'_{3k} &= \cos\psi_k \cos\theta_k \\
u'_{4k} &= \sin\psi_k \sin\theta_k
\end{aligned}
\qquad (2.3.12)
$$

where k = 1, 2, 3, 4 refers to a particular moving coordinate system.

After the matrix, m, has been formed out of the kinetic energy terms, the remaining terms are collected on the right-hand side to form $\vec{Q}_T$. Physically these terms represent the forces due to Coriolis and centrifugal effects. The components of $\vec{Q}_T$ are given as Equation (2.3.13).

$$
\begin{aligned}
-Q_{T1} &= (m_2\rho_1 - m_3\rho_3)[\dot{\theta}_1^2 W_{51} + (\dot{\psi}_1^2 + \dot{\phi}_1^2)V_{31} \\
&\quad + 2\dot{\psi}_1\dot{\theta}_1 W_{21} - 2\dot{\psi}_1\dot{\phi}_1 V_{21} + 2\dot{\theta}_1\dot{\phi}_1 W_{31}] \\
&\quad + m_2\rho_2[\dot{\theta}_2^2 W_{52} + (\dot{\psi}_2^2 + \dot{\phi}_2^2)V_{32} + 2\dot{\psi}_2\dot{\theta}_2 W_{22} \\
&\quad - 2\dot{\psi}_2\dot{\phi}_2 V_{22} + 2\dot{\theta}_2\dot{\phi}_2 W_{32}] \\
&\quad - m_3\rho_4[(\dot{\psi}_3^2 + \dot{\theta}_3^2)u'_{33} - 2\dot{\psi}_3\dot{\theta}_3 u'_{43}] \\
-Q_{T2} &= (m_2\rho_1 - m_3\rho_3)[\dot{\theta}_1^2 W_{61} + (\dot{\psi}_1^2 + \dot{\phi}_1^2)V_{41} \\
&\quad - 2\dot{\psi}_1\dot{\theta}_1 W_{11} + 2\dot{\psi}_1\dot{\phi}_1 V_{11} + 2\dot{\theta}_1\dot{\phi}_1 W_{41}] \\
&\quad + m_2\rho_2[\dot{\theta}_2^2 W_{62} + (\dot{\psi}_2^2 + \dot{\phi}_2^2)V_{42} \\
&\quad - 2\dot{\psi}_2\dot{\theta}_2 W_{12} + 2\dot{\psi}_2\dot{\phi}_2 V_{12} + 2\dot{\theta}_2\dot{\phi}_2 W_{42}] \\
&\quad - m_3\rho_4[(\dot{\psi}_3^2 + \dot{\theta}_3^2)u'_{13} + 2\dot{\psi}_3\dot{\theta}_3 u'_{23}] \\
-Q_{T3} &= (m_2\rho_1 - m_3\rho_3)[(\dot{\theta}_1^2 + \dot{\phi}_1^2)u_{31} - 2\dot{\theta}_1\dot{\phi}_1 u_{41}] \\
&\quad + m_2\rho_2[(\dot{\theta}_2^2 + \dot{\phi}_2^2)u_{32} - 2\dot{\theta}_2\dot{\phi}_2 u_{42}] \\
&\quad + m_3\rho_4\dot{\theta}_3^2 \sin\theta_3 \\
-Q_{T4} &= -(I_{21} - I_{31} + m_2\rho_1^2 + m_3\rho_3^2)\dot{\theta}_1^2\, {}_{41}\cos\phi_1 \\
&\quad + 2\dot{\psi}_1\dot{\theta}_1[I_{11} - I_{31} + m_2\rho_1^2 + m_3\rho_3^2 \\
&\quad - (I_{21} - I_{31} + m_2\rho_1^2 + m_3\rho_3^2)\sin^2\phi_1]\sin\theta_1\cos\theta_1 \\
&\quad + 2(I_{21} - I_{31} + m_2\rho_1^2 + m_3\rho_3^2)\dot{\psi}_1\dot{\phi}_1 u_{21}u_{31} \\
&\quad + \dot{\theta}_1\dot{\phi}_1(I_{21} - I_{31} - I_{11} - 2\sin\phi_1[I_{21} - I_{31} + m_2\rho_1^2 + m_3\rho_3^2])\cos\theta_1 \\
&\quad + m_2\rho_1\rho_2[\dot{\psi}_2^2(V_{41}V_{32} - V_{42}V_{31}) + \dot{\theta}_2^2(V_{41}W_{52} - V_{31}W_{62}) \\
&\quad + \dot{\phi}_2^2(V_{41}V_{22} - V_{31}V_{42}) - 2\dot{\psi}_2\dot{\phi}_2(V_{41}V_{22} + V_{31}V_{12}) \\
&\quad + 2\dot{\psi}_2\dot{\theta}_2(V_{41}W_{22} + V_{31}W_{12}) + 2\dot{\theta}_2\dot{\phi}_2(V_{41}W_{32} - V_{31}W_{42})] \\
&\quad + m_3\rho_3\rho_4[(\dot{\psi}_3^2 + \dot{\theta}_3^2)(V_{41}u'_{33} - V_{31}u'_{13}) - 2\dot{\psi}_3\dot{\theta}_3(V_{41}u'_{43} + V_{31}u'_{12})]
\end{aligned}
\tag{2.3.13}
$$

$$
\begin{aligned}
-Q_{T5} &= \dot{\psi}_1^2[(I_{21} - I_{31} + m_2\rho_1^2 + m_3\rho_3^2)\sin^2\phi_1 - I_{11} + I_{31} - m_2\rho_1^2 \\
&\quad - m_3\rho_3^2]\sin\theta_1\cos\theta_1 \\
&\quad + \dot{\psi}_1\dot{\phi}_1[I_{11} + I_{21} - I_{31} + 2(m_2\rho_1^2 + m_3\rho_3^2) \\
&\quad - 2(I_{21} - I_{31} + m_2\rho_1^2 + m_3\rho_3^2)\sin^2\phi_1]\cos\theta_1 \\
&\quad - 2\dot{\theta}_1\dot{\phi}_1(I_{21} - I_{31} + m_2\rho_1^2 + m_3\rho_3^2)\sin\phi_1\cos\phi_1 \\
&\quad + m_2\rho_1\rho_2[\dot{\theta}_2^2(u_{11}u_{32} - W_{11}W_{52} - W_{21}W_{62}) \\
&\quad - \dot{\psi}_2^2(W_{11}V_{32} + W_{21}V_{42}) + \dot{\phi}_2^2(u_{11}u_{32} - W_{11}V_{32} - W_{21}V_{42}) \\
&\quad + 2\dot{\psi}_2\dot{\phi}_2(W_{11}V_{22} - W_{21}V_{12}) + 2\dot{\psi}_2\dot{\theta}_2(W_{12}W_{21} - W_{11}W_{22}) \\
&\quad - 2\dot{\theta}_2\dot{\phi}_2(u_{11}u_{42} + W_{11}W_{32} + W_{21}W_{42})] \\
&\quad - m_3\rho_3\rho_4[\dot{\theta}_3^2(\sin\theta_3 u_{11} + W_{11}u'_{33} + W_{21}u'_{13}) \\
&\quad + \dot{\psi}_3^2(W_{11}u'_{33} + W_{21}u'_{13}) + 2\dot{\psi}_3\dot{\theta}_3(W_{21}u'_{23} - W_{11}u'_{43})] \\
-Q_{T6} &= (I_{21} - I_{31} + m_2\rho_1^2 + m_3\rho_3^2)(\dot{\theta}_1^2\sin\phi_1\cos\phi_1 - \dot{\psi}_1^2 u_{21}u_{31}) \\
&\quad - \dot{\psi}_1\dot{\theta}_1[I_{11} + I_{21} - I_{31} + 2m_2\rho_1^2 + 2m_3\rho_3^2 \\
&\quad -2\sin^2\phi_1(I_{21} - I_{31} + m_2\rho_1^2 + m_3\rho_3^2)]\cos\theta_1 \qquad \text{(2.3.13 continued)} \\
&\quad + m_2\rho_1\rho_2[\dot{\psi}_2^2(V_{11}V_{32} + V_{21}V_{42}) + \dot{\theta}_2^2(u_{21}u_{32} + V_{11}W_{52} + V_{21}W_{62}) \\
&\quad + \dot{\phi}_2^2(u_{21}u_{32} + V_{11}V_{32} + V_{21}V_{42}) + 2\dot{\psi}_2\dot{\phi}_2(V_{12}V_{21} - V_{11}V_{22}) \\
&\quad + 2\dot{\psi}_2\dot{\theta}_2(V_{11}W_{22} - V_{21}W_{12}) + 2\dot{\theta}_2\dot{\phi}_2(V_{11}W_{32} + V_{21}W_{42} - u_{21}u_{42})] \\
&\quad + m_3\rho_3\rho_4[\dot{\psi}_3^2(V_{11}u'_{33} + V_{21}u'_{13}) + \dot{\theta}_3^2(V_{11}u'_{33} + V_{21}u'_{13} - u_{21}\sin\theta_3) \\
&\quad + 2\dot{\psi}_3\dot{\theta}_3(V_{21}u'_{23} - V_{11}u'_{43})] \\
-Q_{T7} &= m_2\rho_1\rho_2[\dot{\psi}_1^2(V_{31}V_{42} - V_{41}V_{32}) + \dot{\theta}_1^2(V_{42}W_{51} - V_{32}W_{61}) \\
&\quad + \dot{\phi}_1^2(V_{31}V_{42} - V_{41}V_{32}) - 2\dot{\psi}_1\dot{\phi}_1(V_{21}V_{42} + V_{11}V_{32}) \\
&\quad + 2\dot{\psi}_1\dot{\theta}_1(V_{42}W_{21} + V_{32}W_{11}) + 2\dot{\theta}_1\dot{\phi}_1(V_{42}W_{31} - V_{32}W_{41})] \\
&\quad - \dot{\theta}_2^2(I_{22} - I_{32} + m_2\rho_2^2)u_{42}\cos\phi_2 \\
&\quad - 2\dot{\psi}_2\dot{\theta}_2[(I_{12} - I_{32} + m_2\rho_2^2) - (I_{22} - I_{32} + m_2\rho_2^2)\sin^2\phi_2]\sin\theta_2\cos\theta_2 \\
&\quad + 2\dot{\psi}_2\dot{\phi}_2(I_{22} - I_{32} + m_2\rho_2^2)u_{22}u_{32} \\
&\quad + \dot{\theta}_2\dot{\phi}_2[I_{22} - I_{32} - I_{12} - 2(I_{22} - I_{32} + m_2\rho_2^2)\sin^2\phi_2]\cos\theta_2
\end{aligned}
$$

$$-Q_{T8} = m_2\rho_1\rho_2[\dot{\theta}_1^2(u_{31}u_{12} - W_{51}W_{12} - W_{61}W_{22})$$
$$- \dot{\psi}_1^2(V_{41}W_{22} + V_{31}W_{12}) + \dot{\phi}_1^2(u_{31}u_{12} - V_{31}W_{12} - V_{41}W_{22})$$
$$+ 2\dot{\psi}_1\dot{\theta}_1(W_{11}W_{22} - W_{21}W_{12}) + 2\dot{\psi}_1\dot{\phi}_1(V_{21}W_{12} - V_{11}W_{22})$$
$$- 2\dot{\theta}_1\dot{\phi}_1(u_{41}u_{12} + W_{31}W_{12} + W_{41}W_{22})]$$
$$- \dot{\psi}_2^2[I_{12} - I_{32} + m_2\rho_2^2 - (I_{22} - I_{32} + m_2\rho_2^2)\sin^2\phi_2]\sin\theta_2\cos\theta_2$$
$$+ \dot{\psi}_2\dot{\phi}_2[I_{12} + I_{22} - I_{32} + 2m_2\rho_2^2 - 2(I_{22} - I_{32} + m_2\rho_2^2)\sin^2\phi_2]\cos\theta_2$$
$$- 2\dot{\theta}_2\dot{\phi}_2(I_{22} - I_{32} + m_2\rho_2^2)\sin\phi_2\cos\phi_2$$

$$-Q_{T9} = m_2\rho_1\rho_2[\dot{\theta}_1^2(u_{31}u_{22} + W_{51}V_{12} + W_{61}V_{22})$$
$$+ \dot{\psi}_1^2(V_{31}V_{12} + V_{41}V_{22}) + \dot{\phi}_1^2(u_{31}u_{22} + V_{31}V_{12} + V_{41}V_{22})$$
$$+ 2\dot{\psi}_1\dot{\phi}_1(V_{11}V_{22} - V_{21}V_{12}) + 2\dot{\psi}_1\dot{\theta}_1(W_{21}V_{12} - W_{11}V_{22})$$
$$+ 2\dot{\theta}_1\dot{\phi}_1(W_{31}V_{12} + W_{41}V_{22} - u_{41}u_{22})]$$
$$- \dot{\psi}_2^2(I_{22} - I_{32} + m_2\rho_2^2)u_{22}u_{32} \qquad \text{(2.3.13 continued)}$$
$$+ \dot{\theta}_2^2(I_{22} - I_{32} + m_2\rho_2^2)\sin\phi_2\cos\phi_2$$
$$- \dot{\psi}_2\dot{\theta}_2[I_{12} + I_{22} - I_{32} + 2m_2\rho_2^2 - 2(I_{22} - I_{32} + m_2\rho_3^2)\sin^2\phi_2]\cos\theta_2$$

$$-Q_{T10} = m_3\rho_3\rho_4[\dot{\theta}_1^2(W_{51}u_{13}' - W_{61}u_{33}') + (\dot{\psi}_1^2 + \dot{\phi}_1^2)(V_{31}u_{13}' - V_{41}u_{33}')$$
$$+ 2\dot{\psi}_1\dot{\theta}_1(W_{11}u_{33}' + W_{21}u_{13}') - 2\dot{\psi}_1\dot{\phi}_1(V_{11}u_{33}' + V_{21}u_{13}')$$
$$- 2\dot{\theta}_1\dot{\phi}_1(W_{41}u_{33}' - W_{31}u_{13}')] - \dot{\theta}_3^2(I_{23} - I_{33})u_{43}\cos\phi_3$$
$$- 2\dot{\psi}_3\dot{\theta}_3[I_{33} - I_{13} + m_3\rho_4^2 + (I_{23} - I_{33})\sin^2\phi_3]\sin\theta_3\cos\theta_3$$
$$+ 2\dot{\psi}_3\dot{\phi}_3(I_{23} - I_{33})u_{23}u_{33}$$
$$- \dot{\theta}_3\dot{\phi}_3[I_{13} - I_{23} + I_{33} + 2(I_{23} - I_{33})\sin^2\phi_3]\cos\theta_3$$

$$-Q_{T11} = m_3\rho_3\rho_4[\dot{\theta}_1^2(W_{51}u_{23}' + W_{61}u_{43}' + u_{31}\cos\theta_3)$$
$$+ \dot{\psi}_1^2(V_{31}u_{23}' + V_{41}u_{43}') + \dot{\phi}_1^2(V_{31}u_{23}' + V_{41}u_{43}' + u_{31}\cos\theta_3)$$
$$- 2\dot{\psi}_1\dot{\theta}_1(W_{11}V_{43}' - W_{21}u_{23}') + 2\dot{\psi}_1\dot{\phi}_1(V_{11}u_{43}' - V_{21}u_{23}')$$
$$+ 2\dot{\theta}_1\dot{\phi}_1(W_{31}u_{23}' + W_{41}u_{43}' - u_{41}\cos\theta_3)]$$
$$+ \dot{\psi}_3^2[(I_{33} - I_{13} + m_3\rho_4^2)\sin\theta_3\cos\theta_3 + (I_{23} - I_{33})u_{43}u_{23}]$$
$$+ \dot{\psi}_3\dot{\phi}_3[I_{13} + I_{23} - I_{33} - 2(I_{23} - I_{33})\sin^2\phi_3]\cos\theta_3$$
$$- 2\dot{\theta}_3\dot{\phi}_3(I_{23} - I_{33})\sin\phi_3\cos\phi_3$$

$$-Q_{T_{12}} = \dot{\theta}_3^2(I_{23} - I_{33})\sin\phi_3\cos\phi_3 - \dot{\psi}_3^2(I_{23} - I_{33})u_{23}u_{33} - \dot{\psi}_3\dot{\theta}_3[I_{13} + I_{23} - I_{33} - 2(I_{23} - I_{33})\sin^2\phi_3]\cos\theta_3 \quad \text{(2.3.13 concluded)}$$

For all of the body segments, formulation of the gravitational potential energy and substitution in Equation (2.2.1) will yield $\vec{Q}_G$.

$$\vec{Q}_G = \begin{bmatrix} 0 \\ 0 \\ -g(m_1 + m_2 + m_3) \\ 0 \\ -g(m_2\rho_1 u_{11} - m_3\rho_3 u_{11}) \\ -g(m_2\rho_1 u_{21} - m_3\rho_3 u_{21}) \\ 0 \\ -g(m_2\rho_2 u_{12}) \\ -g(m_2\rho_2 u_{22}) \\ 0 \\ g(m_3\rho_4\cos\theta_3) \\ 0 \end{bmatrix} \quad (2.3.14)$$

2.4 ADDITION OF FORCES TO THE EQUATIONS OF MOTION

Each of the remaining sections of this part of the report concerns itself with the effect upon the equations of motion from one of the force-producing features (contacts, belts and joints) of the vehicle or body modeled in this simulation. The determination of force is unique to each of these features but the way in which the resulting force is applied to the equations of motion is common to all and will be discussed here.

Consider a typical force-producer and call it feature F. In this simulation, the magnitude of the force produced by F will be a function of deflection and deflection rate where deflection is defined appropriately for each feature.

For example, belt deflection is elongation of the belt beyond the zero slack condition. The direction of the force in each case is that which will tend to maximally decrease deflection. The force produced can be separated into a collection of deflection-dependent terms which will be called the spring force and a collection of deflection rate-dependent terms which will be called the damping force.

$$\vec{F}_F = {}_S\vec{F}_F + {}_D\vec{F}_F \tag{2.4.1}$$

where

$\vec{F}_F$ is the total force produced by feature F

${}_S\vec{F}_F$ is the spring force for feature F

${}_D\vec{F}_F$ is the damping force for feature F

Further

$$|{}_S\vec{F}_F| = f(\delta)$$

and, (2.4.2)

$$|{}_D\vec{F}_F| = g(\dot{\delta})$$

where $f(\delta)$ is an analytical third-order polynomial function of displacement, δ, and $g(\dot{\delta})$ is a linear function of displacement rate, $\dot{\delta}$. The deflection and deflection rate (δ and $\dot{\delta}$) are computed as functions of the twelve generalized coordinates.

The spring force, ${}_S\vec{F}_F$, will do work in the classical sense and yield a potential energy

$$V_F = \int_0^{\delta} f(x)dx \tag{2.4.3}$$

and the contributions to (2.2.1) will be of the form

$$\frac{\partial V}{\partial Z_i} = \frac{\partial V}{\partial \delta}\frac{\partial \delta}{\partial Z_i} = |{}_S\vec{F}_F|\frac{\partial \delta}{\partial Z_i} \tag{2.4.4}$$

for $i = 1, 12$.

The quantity $\frac{\partial \delta}{\partial Z_i}$ will be referred to as the "lever arm." If the generalized coordinate is rotational and the force for the feature F such that it tends to physically push or pull the body segment in a direction perpendicular to the line joining the center of rotation to the point of application of the force, then this quantity will be the actual length of that line and hence, the lever arm. In other cases, it contains factors which yield the perpendicular component of the force as well and is an "effective lever arm". In general, since

$$ {}_S Q_{Fi} = |{}_S \vec{F}_F| \frac{\partial \delta}{\partial Z_i} \tag{2.4.5} $$

(where ${}_S \vec{Q}_F$ is the generalized force vector contribution due to the spring force of feature F) strongly resembles the relation,

Torque = Force x Lever arm

this nomenclature has been adopted.

The quantity ${}_D \vec{F}_F$ is dissipative in nature and will yield a dissipative energy rate.

$$ D_F = \int_o^{\dot{\delta}} g(x)dx \tag{2.4.6} $$

and the contributions to (2.2.1) will be of the form

$$ \frac{\partial D}{\partial \dot{Z}_i} = \frac{\partial D}{\partial \delta} \frac{\partial \dot{\delta}}{\partial \dot{Z}_i} = |{}_D \vec{F}_F| \frac{\partial \dot{\delta}}{\partial \dot{Z}_i} \tag{2.4.7} $$

for i = 1, 12.

But it is also true that

$$ \frac{\partial \dot{\delta}}{\partial \dot{Z}_i} = \frac{\partial}{\partial \dot{Z}_i} \left(\sum_{j=1}^{12} \frac{\partial \delta}{\partial Z_j} \dot{Z}_j \right) = \frac{\partial \delta}{\partial Z_i} + \sum_{j=1}^{12} \dot{Z}_j \frac{\partial}{\partial \dot{Z}_i} \left(\frac{\partial \delta}{\partial Z_j} \right) = \frac{\partial \delta}{\partial Z_i} \tag{2.4.8} $$

since δ is a function only of the generalized coordinates and not their rates.

Therefore (2.4.7) will take the form of (2.4.5) and recalling (2.4.1) as well as correcting signs, it can be shown that

$$ Q_{Fi} = |\vec{F}_F| \frac{\partial \delta}{\partial Z_i} \tag{2.4.9} $$

where $\vec{Q}_F$ is the generalized force vector contribution for feature F.

Equation (2.4.9) will hold true if it is agreed that the magnitude may reverse signs when the force reverses directions.

One last property of lever arms should be noted. Using the chain rule,

$$\frac{d}{dt}[\delta(q_1, \ldots, q_N) = \sum_{k=1}^{N} \frac{\partial \delta}{\partial q_k} \frac{dq_k}{dt} \qquad (2.4.10)$$

where the q's are the parameters including generalized coordinate upon which deflection depends

Hence the terms of $\dot{\delta}$ due to body motion can be computed by summing up each lever arm times the corresponding generalized velocity. In most cases, this is the actual technique employed.

So the labor of either deriving or presenting the implications of feature F on the equations of motion can be simplified to the consideration of deflection and lever arms. In the sections which follow concerning the individual force-producers, deflection and lever arms will be explicitly defined. It will be left to the reader to substitute these quantities into the "feature F" equations given in this section.

Deflection rate will be discussed in terms of body motion, vehicle motion, and motion relative to the vehicle. The exact form of equation (2.4.10) which applies for the feature under consideration will also be presented.

Figure 7 illustrates the load-deflection characteristics of a typical feature F. Curve MAA'BC represents an instance of a force versus deflection plot of $|\vec{F}_F|$ defined in Equation (2.4.1) where

$$\begin{aligned} |_S\vec{F}_F| &= k_1\delta + k_2\delta^2 + k_3\delta^3 \\ \text{and} \quad |_D\vec{F}_F| &= c\dot{\delta} \end{aligned} \qquad (2.4.11)$$

This basic model is modified in three ways to achieve greater realism, computer stability, and special material properties respectively.

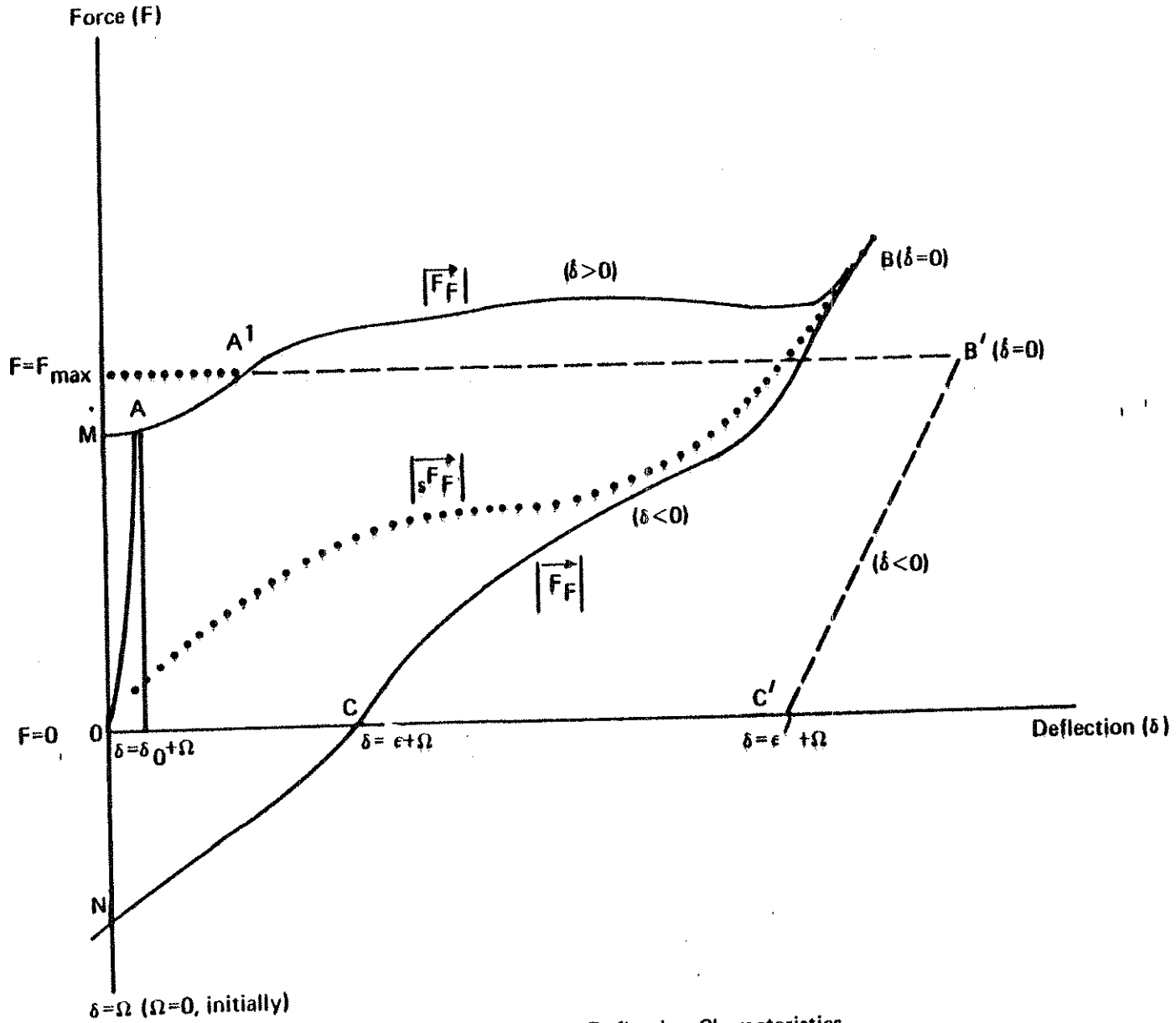

Figure 7. Load-Deflection Characteristics

Production of negative force by feature F is unrealistic for the kinds of force-producers that are being discussed. Therefore, any segment, CN, of a load-deflection curve is replaced by segment CO. In terms of computational manipulations, if a negative force is computed, it is set to zero. Further, the deflection (ε) at which the force first goes zero is added to the permanent deformation (Ω). The deflection must exceed the permanent deformation before any force will be computed during reloading.

The form of $|\vec{F}_F|$ embodied in Equation (2.4.11) leads to a step function at point O as the curve is zero on the left side of point O and continues from point M on the right side. This condition is intolerable to the numerical procedures employed for integration and so segment MA is replaced by segment OA.

The dissipative force, $|_D\vec{F}_F|$, is multiplied by a coefficient which varies linearly from zero at point O to unity at a specified deflection, δ_o, beyond point O.

In order to model special energy-absorbing materials or structures which undergo large deformations at a constant load, the program accepts as input a maximum limiting force and a special slope for the force-deformation curve when the material unloads. This is applicable to the belt and contact surface force-producers. The normal OABCO curve is used until force is predicted to exceed the specified maximum force, F_{max}. The force is then held at this level until unloading is predicted to begin. A permanent deformation, ε', is added to Ω in this case. Hence, if "saturation" of the maximum force occurs, the load-deflection curve takes the shape OAA'B'C'O as shown in Figure 7.

The resulting analytical forms are

$$|\vec{D_F}| = Kc\dot{\delta} \text{ where } K = \begin{cases} 0 \text{ for } \delta' < 0 \\ \delta'/\delta_o \text{ for } 0 \le \delta' \le \delta_o \\ 1 \text{ for } \delta' > \delta_o \end{cases}$$

$$|\vec{S_F}| = \begin{cases} k_1\delta' + k_2(\delta')^2 + k_3(\delta')^3 \text{ for } \delta' \ge 0 \\ 0 \text{ for } \delta' < 0 \end{cases} \qquad (2.4.12)$$

$$|\vec{F_F}| = \begin{cases} F_{max} \text{ if } |\vec{D_F}| + |\vec{S_F}| \ge F_{max} \text{ and } \dot{\delta} \ge 0 \\ |\vec{D_F}| + |\vec{S_F}| \text{ if } 0 \le |\vec{D_F}| + |\vec{S_F}| < F_{max} \\ 0 \text{ if } |\vec{D_F}| + |\vec{S_F}| < 0 \text{ or } \delta' \le \varepsilon' \\ (\delta' - \varepsilon')D \text{ if } F_{max} \text{ has been reached, } \delta' > \varepsilon', \text{ and } \dot{\delta} < 0. \end{cases}$$

where

$\delta' = \delta - \Omega$

δ_o = damping term full on deflection (set to one inch if units are inches or .1 radian if units are radians).

Ω = permanent deflection which is initially zero and accumulated for each interaction separately

c = damping constant

k_1, k_2, k_3 = non-linear spring constants

F_{max} = specified maximum force

$\varepsilon' = \omega - \frac{F_{max}}{D}$

D = specified unloading slope

ω = value of deflection at which $\dot{\delta} = 0$ after F_{max} has been exceeded

2.5 CONTACT FORCES

Interactions of the crash victim with the vehicle interior are modeled by impingement of ellipsoids attached to body segments into planar surfaces attached to the vehicle as shown in Figure 8. Neither the ellipsoid nor the contact surface is considered to deform as such although in effect the contact surface will move away in response to "deformations" due to the effect of permanent deformation as discussed in Part 2.4 of this report. The force from such an encounter is taken to be deflection and deflection-rate dependent where deflection is defined as the maximum perpendicular distance, δ, the ellipsoid extends into the contact surface. The force acts to push the ellipsoid outward perpendicular to the contact plane at the point of maximum impingement.

A total of ten ellipsoids is allowed. Each ellipsoid can be attached to any of the body segments, centered at an arbitrary displacement from the body segment center of gravity, but always located with principle axes parallel to the body segment coordinate system (see Figure 9). Twenty-five planar contact surfaces in the shape of parallelograms can be attached to the vehicle and moved relative to the vehicle as a function of time to represent occupant compartment deformation or intrusion. Each contact surface is specified by three consecutive corner points, given as a function of time in tabular form relative to the vehicle coordinate system (see Figure 10). Only the initial location need be specified if the contact is stationary relative to the vehicle.

The spring constants and damping constant used are considered to be properties of the contact surface alone in this simulation. Contact surfaces are endowed with other special properties some of which are illustrated in Figure 11. The three points in Figure 11 which define the shape of the contact surface are specified in the following order:

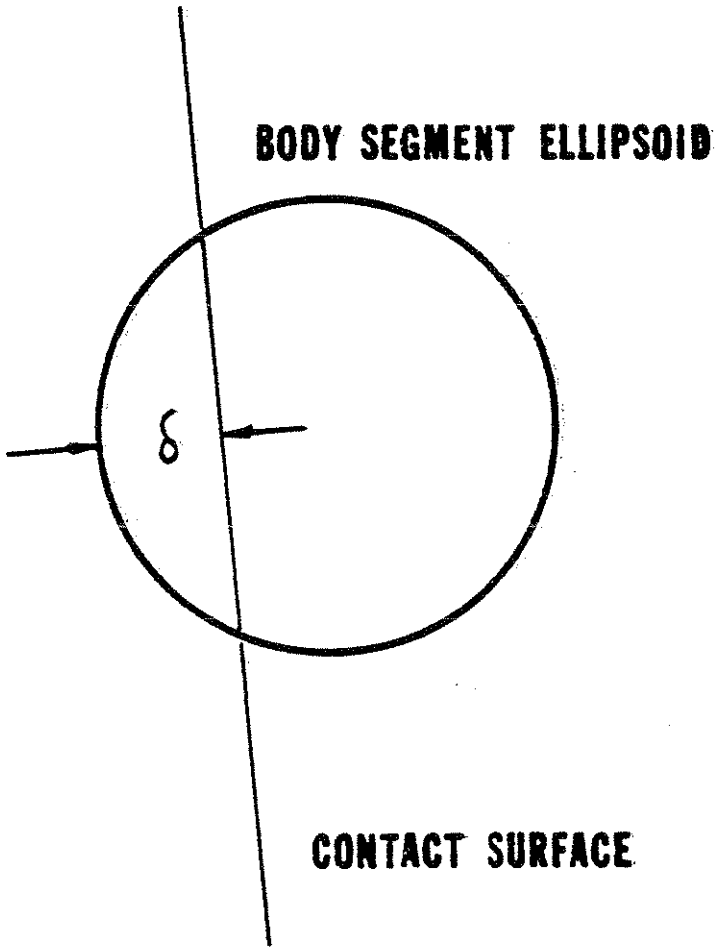

FIG. 8
CONTACT FORCE

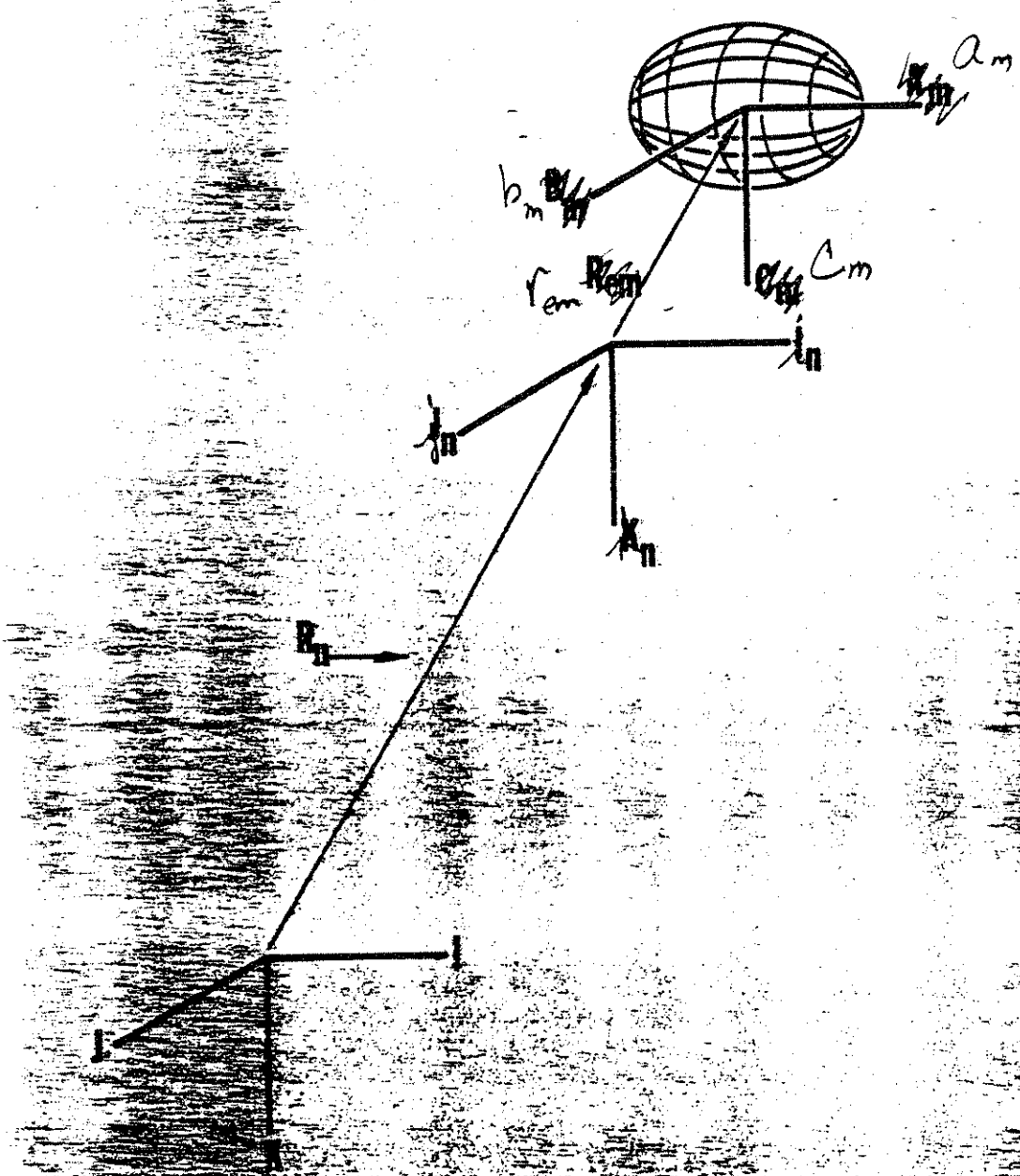

FIG. 9

ELLIPSOID 'm' ATTACHED TO BODY SEGMENT 'n'

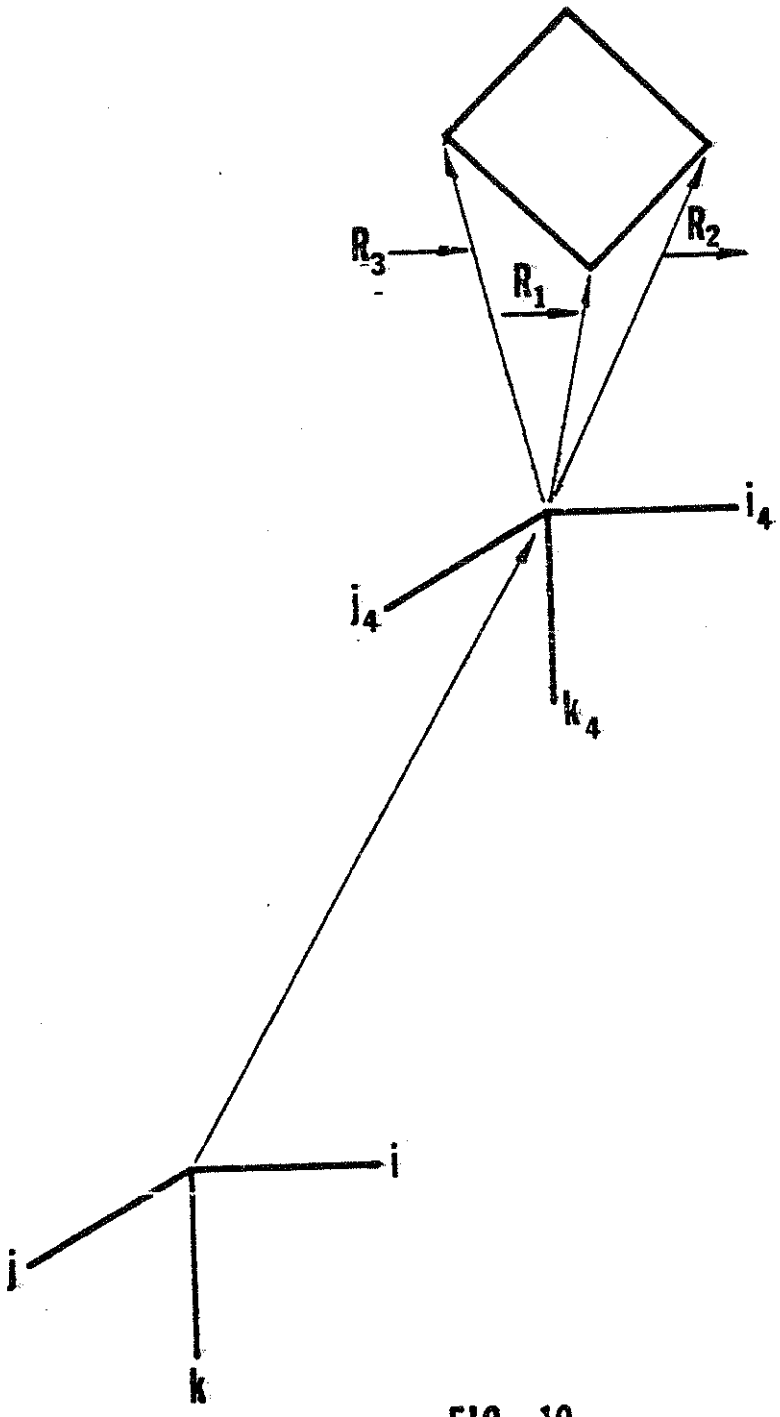

FIG. 10

CONTACT SURFACE ATTACHED TO THE VEHICLE

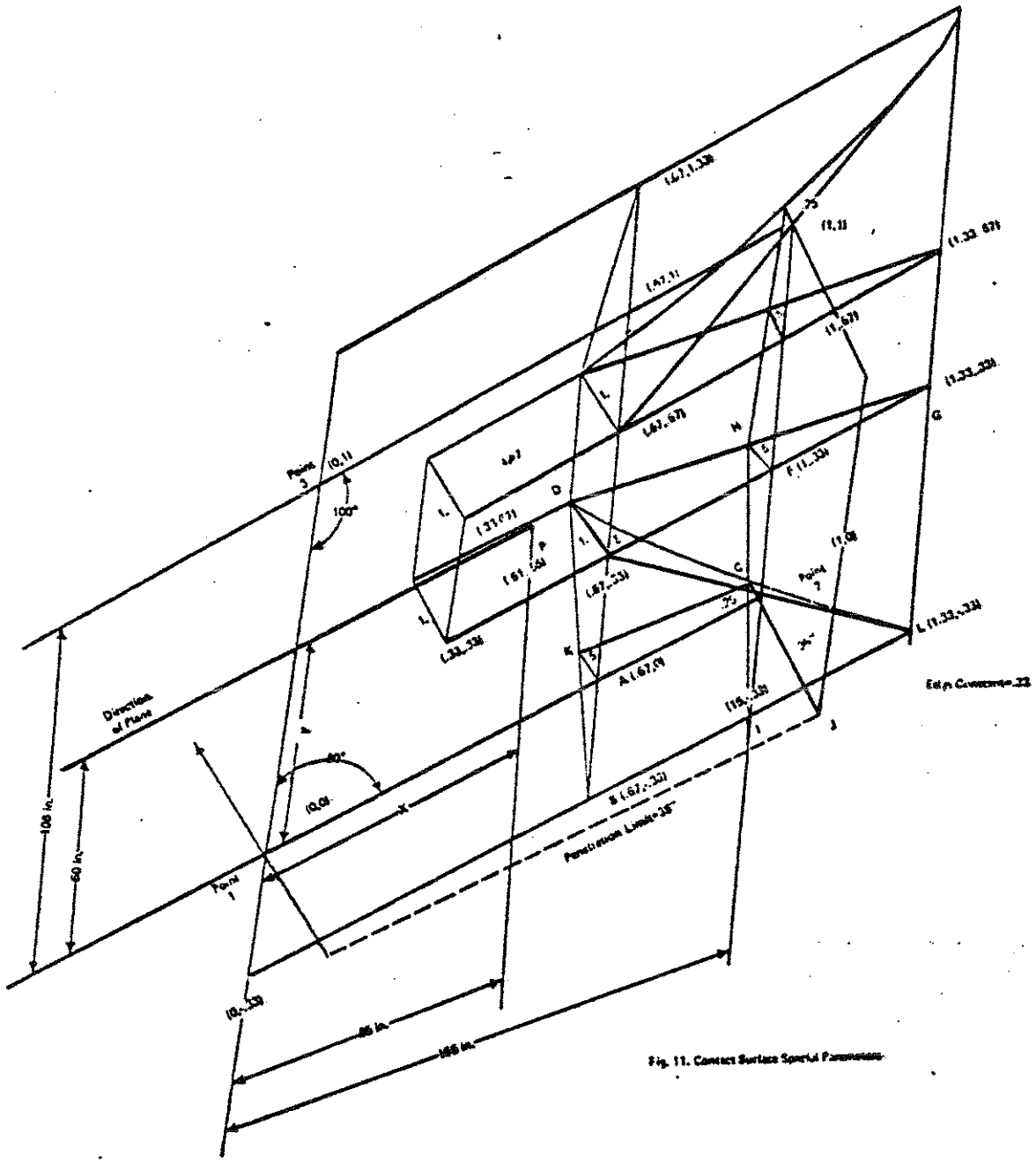

Fig. 11. Contact Surface Spatial Parameters

(1) Point 1. Any of the four corner points;

(2) Point 2. Either adjacent corner point; and,

(3) Point 3. The other corner point adjacent to Point 1.

The contact surface illustrated is 165 inches from Point 1 to Point 2 and 108 inches from Point 1 to Point 3. The included angle is eighty degrees. A surface coordinate system is set up by the computer program with Point 1 serving as the origin, Point 2 as Point (1,0) and Point 3 as Point (0,1) with the axes taken parallel to the edges. This coordinate system sees all contact surfaces as a unit square regardless of shape or size. The point on the contact surface at which the maximum impingement takes place is represented in this system. When the coordinates of the point are reported in the printed output, each of the coordinates are multiplied by the length of its respective side so that printed results are in inches. Thus, if Point P represents the point of maximum impingement, it has internal surface coordinates of (.51,.56) and will be reported as (85,60).

Since the total interaction of the ellipsoid with the parallelogram is represented by what happens at the point of maximum impingement, a quantity called the "edge constant" was introduced to handle cases where an ellipsoid interacted with the edge of a contact surface or at a corner where contact surfaces meet. In this case, maximum impingement lies outside the region defined by the parallelogram but yet the ellipsoid makes firm contact with the surface. It is assumed in developing an analytical tool to handle this problem that the contact force decreases as the point of maximum impingement moves away from the edge of the contact surface. The computer simulation approximately resolves these edge problems by employing the following device. The force is computed using the deflection and deflection rate in the normal manner. The resulting force is multiplied by an "effectiveness factor" which ranges from one in a region in the middle of the contact surface down to zero

in the regions outside the contact surface. The effectiveness factor is illustrated in Figure 11 by plotting its value corresponding to the various points on and near the contact surface above the level of the plane. For example:

(1) Effectiveness factor for contact surface Point P is shown as Point P' above the surface and has the value of unity;

(2) Effectiveness factor for Point E is represented by Point D, also unity;

(3) Point A on the edge of the contact surface has an effectiveness factor of 1/2 shown as Point K; and,

(4) Outside the contact surface at Point B, the effectiveness factor is reduced to zero indicating that no contact will be predicted between an ellipsoid and a contact surface.

The line BKD is a trace of the values of the factor as the point of maximum impingement of an ellipsoid into the surface moves toward and beyond the edge of the contact surface along line EAB. The result is that for a given deflection, force will be reduced to zero as the ellipsoid moves off the edge of the surface. The effectiveness factor is linear along lines such as BKD, GHD, KC, and HCI but parabolic along DCL. The exact definition of the effectiveness factor is given below:

$$E = R \cdot S \tag{2.5.1}$$

where

E is the effectiveness factor

$$R = \begin{cases} 0 \text{ for } X \leq -\lambda \\ .5 + \frac{.5X}{\lambda} \text{ for } -\lambda < X < \lambda \\ 1 \text{ for } \lambda \leq X \leq 1 - \lambda \\ .5 + .5\left(\frac{1-X}{\lambda}\right) \text{ for } 1 - \lambda < X < 1 + \lambda \\ 0 \text{ for } X \geq 1 + \lambda \end{cases} \tag{2.5.2}$$

(Continued on next page)

$$S = \begin{cases} 0 \text{ for } Y \leq -\lambda \\ .5 + \frac{.5Y}{\lambda} \text{ for } -\lambda < Y < \lambda \\ 1 \text{ for } \lambda \leq Y \leq 1-\lambda \\ .5 + .5\left(\frac{1-Y}{\lambda}\right) \text{ for } 1-\lambda < Y < 1+\lambda \\ 0 \text{ for } Y \geq 1+\lambda \end{cases} \qquad \begin{matrix} (2.5.2 \\ \text{concluded}) \end{matrix}$$

where X, Y are the contact surface coordinates of the maximum impingement

λ is the edge constants specified as input to the computer program, which must lie in the range $0 < \lambda \leq .5$

The edge constant is the mechanism by which a user of the HSRI model specifies the interaction of a body ellipsoid with the edge of a contact surface and must be provided as input data for each contact surface in order to exercise the model. It should be selected on the basis of a comparison of the geometries of a particular contact surface and the body ellipsoid which is most likely to interact with the surface. For instance, the surface shown in Figure 11 is 165 inches long along its x-coordinate. If it is assumed that a body ellipsoid with a semi-major axis length of 54.45 inches is the most likely or important interaction, then the edge constant should be selected as

$$\lambda = 54.45/165 = 0.33$$

If this value is used, a contact force equal to zero will be predicted if the contact ellipsoid just misses the surface, but when any part of the ellipsoid touches an edge of the contact surface, a small force will be computed. This force will be at a maximum when the contact ellipsoid interacts with the center region of the contact surface.

Occasionally a body ellipsoid can approach a contact surface from either side. Consider the case of a contact surface representing the top of a dash panel and a body ellipsoid attached to the knee of an unrestrained occupant. In some vehicles the top of the dash panel is directly above the knees. Consider a hypothetical case where the vehicle is impacted in the rear and is pushed into the path of an

oncoming truck. During the rear-end part of the collision, the occupant is often propelled upward along the slope of the seat back. During the frontal collision, the occupant then moves forward. In this series of events it is possible that the knees of the occupant could impact very high on the instrument panel due to the unusual initial positioning for the frontal crash event. It is desired in this case that the knee feel a force from contact with the top of the dash panel and not a large force due to the initial seating position where the knee is below the panel. Another example of this kind of problem is the rear seat passenger which vaults the front seat, striking the front seat back.

This simulation resolves this kind of difficulty by requiring the user to assign a positive or front side to each contact surface. No force will be generated unless the ellipsoid approaches from the front side. In order to determine simply whether an ellipsoid has approached from the front or back, the user is required to specify the "penetration limit," a parameter which represents the maximum penetration into the surface which can occur in one integration time step. Then, if an ellipsoid's first deflection into the surface is greater than this value, the ellipsoid is assumed to be coming up from behind and no force is computed until the ellipsoid gets totally in front of the contact surface and then comes back and hits the surface.

The penetration limit is illustrated in Figure 11 by a plane in dotted lines drawn underneath the contact plane. CJ represents the penetration limit. The value of 38 inches is about ten times the normal size of this parameter and is exaggerated only for illustrative purposes.

The positive side specification is made by telling the program whether the inertial origin lies behind or in front of the contact surface. The inertial origin should not lie exactly on the infinite extension of any of the contact surfaces although it is permissible to get arbitrarily close. The front of the contact surface is shown in Figure 11 by an arrow passing through Point 1.

The analytical expression for deflection is

$$\delta = \frac{Ax_o + By_o + Cz_o + D}{\pm\sqrt{A^2+B^2+C^2}} \tag{2.5.3}$$

where (x_o, y_o, z_o) is the location of that point in inertial coordinates on the ellipsoid which is tangent to a surface, parallel to the contact surface, and which represents the point of maximum penetration of the ellipsoid into the contact surface. The quantities A, B, C, D are computed from the generalized motion coordinates at each point of time in the simulation. The various quantities are defined in the following analytical expressions.

$$\begin{aligned} x_o &= \mu_7 + k(\mu_2 A + \mu_2 B + \mu_3 C) \\ y_o &= \mu_8 + k(\mu_1 A + \mu_4 B + \mu_5 C) \\ z_o &= \mu_9 + k(\mu_3 A + \mu_5 B + \mu_6 C) \end{aligned} \tag{2.5.4}$$

$$k = \pm\sqrt{\frac{2}{\mu_2 A^2+\mu_4 B^2+\mu_6 C^2+2\mu_1 AB+2\mu_3 AC+2\mu_5 BC}} \tag{2.5.5}$$

$$\begin{aligned} \mu_1 &= \tfrac{1}{2}[c_m^2 V_{3n} V_{4n} + b_m^2 V_{1n} V_{2n} + a_m^2 u'_{1n} u'_{3n}] \\ \mu_2 &= \tfrac{1}{2}[c_m^2 V_{3n}^2 + b_m^2 V_{1n}^2 + a_m^2 (u'_{3n})^2] \\ \mu_3 &= \tfrac{1}{2}[c_m^2 V_{3n} u_{3n} + b_m^2 V_{1n} u_{2n} - a_m^2 u'_{3n} \sin\theta_n] \\ \mu_4 &= \tfrac{1}{2}[c_m^2 V_{4n}^2 + b_m^2 V_{2n}^2 + a_m^2 (u'_{1n})^2] \\ \mu_5 &= \tfrac{1}{2}[c_m^2 V_{4n} u_{3n} + b_m^2 V_{2n} u_{2n} - a_m^2 u'_{1n} \sin\theta_n] \\ \mu_6 &= \tfrac{1}{2}[c_m^2 u_{3n}^2 + b_m^2 u_{2n} + a_m^2 \sin^2\theta_n] \end{aligned} \tag{2.5.6}$$

$$\begin{aligned} A &= u'_{34} r + u'_{14} q - \sin\theta_4 p \\ B &= V_{14} r + V_{24} q + u_{24} p \\ C &= V_{34} r + V_{44} q + u_{34} p \\ D &= s - Ax_4 - By_4 - Cz_4 \end{aligned} \tag{2.5.7}$$

The quantities A, B, C, D are the coefficients of the contact plane according to the inertial system.

$$
\begin{aligned}
p &= \hat{x}_1(\hat{y}_2 - \hat{y}_3) + \hat{x}_2(\hat{y}_3 - \hat{y}_1) + \hat{x}_3(\hat{y}_1 - \hat{y}_2) \\
q &= \hat{x}_1(\hat{z}_3 - \hat{z}_2) + \hat{x}_2(\hat{z}_1 - \hat{z}_3) + \hat{x}_3(\hat{z}_2 - \hat{z}_1) \\
r &= \hat{y}_1(\hat{z}_2 - \hat{z}_3) + \hat{y}_2(\hat{z}_3 - \hat{z}_1) + \hat{y}_3(\hat{z}_1 - \hat{z}_2) \\
s &= \hat{z}_1(\hat{x}_3\hat{y}_2 - \hat{x}_2\hat{y}_3) + \hat{z}_2(\hat{x}_1\hat{y}_3 - \hat{x}_3\hat{y}_1) \\
&\quad + \hat{z}_3(\hat{x}_2\hat{y}_1 - \hat{x}_1\hat{y}_2)
\end{aligned}
\tag{2.5.8}
$$

The quantities p, q, r, s are coefficients of the contact plane according to the vehicle system.

$$
\begin{aligned}
\mu_7 &= x_n + x_{em}u'_{3n} + y_{em}V_{1n} + z_{em}V_{3n} \\
\mu_8 &= y_n + x_{em}u'_{1n} + y_{em}V_{2n} + z_{em}V_{4n} \\
\mu_9 &= z_n - x_{em}\sin\theta_n + y_{em}u_{2n} + z_{em}u_{3n}
\end{aligned}
\tag{2.5.9}
$$

The quantities μ_7, μ_8, μ_9 are the inertial coordinates of the ellipsoid center. The remaining quantities are defined as

m is ellipsoid index,

n is body segment index,

a_m, b_m, c_m are the semimajor axes of ellipsoid m,

x_{em}, y_{em}, z_{em} are the components of $\vec{R}_{em}$ or the coordinates of the ellipsoid center in the body segment coordinate system (see Figure 9),

$\hat{x}_i, \hat{y}_i, \hat{z}_i$ are the components of vector $\vec{R}_i$ for i=1,2,3 or contact surface corner position vectors in vehicle system (see Figure 10).

Lever arms are as follows:

$$\frac{\partial\delta}{\partial Z_1} = \frac{A}{\pm\sqrt{p^2+q^2+r^2}} \tag{2.5.10}$$

$$\frac{\partial\delta}{\partial Z_2} = \frac{B}{\pm\sqrt{p^2+q^2+r^2}} \tag{2.5.11}$$

$$\frac{\partial\delta}{\partial Z_3} = \frac{C}{\pm\sqrt{p^2+q^2+r^2}} \tag{2.5.12}$$

$$(\sqrt{p^2+q^2+r^2})\frac{\partial\delta}{\partial Z_4} = \begin{cases} B(u'_{31}x_{em} + V_{11}y_{em} + V_{31}z_{em}) - A(u'_{11}x_{em} + V_{21}y_{em} \\ \quad + V_{41}z_{em}) + k[(B^2 - A^2)\mu_1 + AB(\mu_2 - \mu_4) - AC\mu_5 + BC\mu_3] \\ \qquad\qquad \text{when } n=1 \\ \rho_1(AV_{41} - BV_{31}) \qquad \text{when } n=2 \\ \rho_3(BV_{31} - AV_{41}) \qquad \text{when } n=3 \end{cases} \tag{2.5.13}$$

$$\begin{aligned}(\sqrt{p^2+q^2+r^2})\frac{\partial\delta}{\partial Z_5} &= A(-u'_{21}x_{em} + W_{31}y_{em} + W_{11}z_{em}) + B(-u'_{41}x_{em} + W_{41}y_{em} + W_{21}z_{em}) \\ &+ C(-\cos\theta_1 x_{em} - u_{41}y_{em} - u_{11}z_{em}) + \tfrac{1}{2}k[A^2(c_m^2V_{31}W_{11} \\ &+ b_m^2V_{11}W_{31} - a_m^2u'_{21}u'_{31}) + B^2(c_m^2V_{41}W_{21} + b_m^2V_{21}W_{41} - a_m^2u'_{11}u'_{41}) \\ &+ C^2(-c_m^2u_{11}u_{31} - b_m^2u_{21}u_{41} + a_m^2\sin\theta_1\cos\theta_1) \\ &+ AB\{c_m^2(V_{31}W_{21} + W_{11}V_{41}) + b_m^2(V_{11}W_{41} + V_{21}W_{31}) \\ &- a_m^2(u'_{11}u'_{21} + u'_{31}u_{41})\} + AC\{c_m^2(u_{31}W_{11} - V_{31}u_{31}) \\ &+ b_m^2(u_{21}W_{31} - V_{11}u_{41}) + a_m^2(u'_{21}\sin\theta_1 - u'_{31}\cos\theta_1)\} \\ &+ BC\{c_m^2(u_{31}W_{21} - V_{41}u_{11}) + b_m^2(u_{21}W_{41} - V_{21}u_{41}) \\ &+ a_m^2(u'_{41}\sin\theta_1 - u'_{11}\cos\theta_1)\}] \\ &\qquad\qquad \text{when } n=1\end{aligned} \tag{2.5.14}$$

$$(\sqrt{p^2+q^2+r^2})\frac{\partial\delta}{\partial Z_5} = \begin{cases} \rho_1(Cu_{11} - BW_{21} - AW_{11}) & \text{when } n=2 \\ \rho_3(AW_{11} + BW_{21} - Cu_{11}) & \text{when } n=3 \end{cases} \tag{2.5.15}$$

$$(\sqrt{p^2+q^2+r^2})\frac{\partial\delta}{\partial Z_6} = \begin{cases} A(V_{31}y_{em} - V_{11}z_{em}) + B(V_{41}y_{em} - V_{21}z_{em}) \\ + C(u_{31}y_{em} - u_{21}z_{em}) + \frac{1}{2}k(b_m^2 - c_m^2)[A^2V_{11}V_{31} \\ + B^2V_{21}V_{41} + C^2u_{21}u_{31} + AB(V_{11}V_{41} + V_{21}V_{31}) \\ + AC(V_{11}u_{31} + V_{31}u_{21}) + BC(V_{21}u_{31} + V_{41}u_{21})] \quad \text{when } n=1 \\ \rho_1(AV_{11} + BV_{21} + Cu_{21}) \qquad \text{when } n=2 \\ -\rho_3(AV_{11} + BV_{21} + Cu_{21}) \qquad \text{when } n=3 \end{cases} \tag{2.5.16}$$

Note: The lever arms for generalized coordinates 7, 8 and 9 (ψ_2, θ_2, and ϕ_2) are zero when n=1 or 3.

$$(\sqrt{p^2+q^2+r^2})\frac{\partial \delta}{\partial Z_7} = B(u'_{32}x_{em} + V_{12}y_{em} + V_{32}z_{em}) - A(u'_{12}x_{em} + V_{22}y_{em} + V_{41}z_{em}) + \rho_2(AV_{42} - BV_{32}) + k[(B^2 - A^2)u_1 + AB(u_2 - u_4) - ACu_5 + BCu_3] \quad \text{when } n=2 \tag{2.5.17}$$

$$(\sqrt{p^2+q^2+r^2})\frac{\partial \delta}{\partial Z_8} = A(-u'_{22}x_{em} + W_{32}y_{em} + W_{12}z_{em}) + B(-u'_{42}x_{em} + W_{42}y_{em} + W_{22}z_{em}) + C(-\cos\theta_2 x_{em} - u_{42}y_{em} - u_{12}z_{em}) + \rho_2(Cu_{12} - BW_{22} - AW_{12}) + \tfrac{1}{2}k[A^2(c_m^2V_{32}W_{12} + b_m^2V_{12}W_{32} - a_m^2u'_{22}u'_{32}) + B^2(c_m^2V_{42}W_{22} + b_m^2V_{22}W_{42} - a_m^2u'_{22}u'_{42}) + C^2(-c_m^2u_{12}u_{32} - b_m^2u_{22}u_{42} + a_m^2\sin\theta_2\cos\theta_2) + AB\{c_m^2(V_{32}W_{22} + V_{42}W_{12}) + b_m^2(V_{12}W_{42} + V_{32}W_{32}) - a_m^2(u'_{12}u'_{22} + u'_{32}u'_{42})\} + AC\{c_m^2(u_{32}W_{12} - V_{32}u_{12}) + b_m^2(u_{22}W_{32} - V_{12}u_{42}) + a_m^2(u'_{22}\sin\theta_2 - u'_{32}\cos\theta_2)\} + BC\{c_m^2(u_{32}W_{22} - V_{42}u_{12}) + b_m^2(u_{22}W_{42} - V_{22}u_{42}) + a_m^2(u'_{42}\sin\theta_2 - u'_{12}\cos\theta_2)\} \quad \text{when } n=2 \tag{2.5.18}$$

$$(\sqrt{p^2+q^2+r^2})\frac{\partial \delta}{\partial Z_9} = A(V_{32}y_{em} - V_{12}z_{em}) + B(V_{42}y_{em} - V_{22}z_{em}) + C(u_{32}y_{em} - u_{22}z_{em}) + \rho_2(AV_{12} + BV_{22} + Cu_{22}) + \tfrac{1}{2}k(b_m^2 - c_m^2)[A^2V_{12}V_{32} + B^2V_{22}V_{42} + C^2u_{22}u_{32} + AB(V_{12}V_{42} + V_{22}V_{32}) + AC(V_{12}u_{32} + V_{32}u_{22}) + BC(V_{22}u_{32} + V_{42}u_{22})] \quad \text{when } n=2 \tag{2.5.19}$$

Note: The lever arms for generalized coordinates 10, 11, and 12 (ψ_3, θ_3, and ϕ_3) are zero when n=1 or 2.

$$(\sqrt{p^2+q^2+r^2})\frac{\partial \delta}{\partial Z_{10}} = B(u'_{33}x_{em} + V_{13}y_{em} + V_{33}z_{em}) - A(u'_{13}x_{em} + V_{23}y_{em} + V_{43}z_{em}) + \rho_4(Bu'_{33} - Au'_{13}) + k[(B^2 - A^2)u_1 + AB(u_2 - u_4) - ACu_5 + BCu_3] \quad \text{when } n=3 \tag{2.5.20}$$

$$(\sqrt{p^2+q^2+r^2})\frac{\partial \delta}{\partial Z_{11}} = A(-u'_{23}x_{em} + W_{33}y_{em} + W_{13}z_{em}) + B(-u'_{43}x_{em} + W_{43}y_{em} + W_{23}z_{em})$$
$$+ C(-\cos\theta_3 x_{em} - u_{43}y_{em} - u_{13}z_{em}) - \rho_4(Au'_{23} + Bu'_{43} + C\cos\theta_3)$$
$$+ \frac{1}{2}k(A^2(c_m^2V_{33}W_{13} + b_m^2V_{13}W_{33} - a_m^2u'_{23}u'_{33}) + B^2(c_m^2V_{43}W_{23}$$
$$+ b_m^2V_{23}W_{43} - a_m^2u'_{13}u'_{43}) + C^2(-c_m^2u_{13}u_{33} - b_m^2u_{23}u_{43}$$
$$+ a_m^2\sin\theta_3\cos\theta_3) + AB[c_m^2(V_{33}W_{23} + V_{43}W_{13}) + b_m^2(V_{13}W_{43} + V_{23}W_{33})$$
$$- a_m^2(u'_{13}u'_{23} + u'_{33}u'_{43})] + AC[c_m^2(u_{33}W_{13} - V_{33}u_{13})$$
$$+ b_m^2(u_{23}W_{33} - V_{13}u_{43}) + a_m^2(u'_{23}\sin\theta_3 - u'_{33}\cos\theta_3)]$$
$$+ BC[c_m^2(u_{33}W_{23} - V_{43}u_{13}) + b_m^2(u_{23}W_{43} - V_{23}u_{43})$$
$$+ a_m^2(u'_{43}\sin\theta_3 - u'_{13}\cos\theta_3)]) \qquad \text{when } n=3 \tag{2.5.21}$$

$$(\sqrt{p^2+q^2+r^2})\frac{\partial \delta}{\partial Z_{12}} = A(V_{33}y_{em} - V_{13}z_{em}) + B(V_{43}y_{em} - V_{23}z_{em})$$
$$+ C(u_{33}y_{em} - u_{23}z_{em}) + \frac{1}{2}(b_m^2 - c_m^2)[A^2V_{13}V_{33}$$
$$+ B^2V_{23}V_{43} + C^2u_{23}u_{33} + AB(V_{13}V_{43} + V_{23}V_{33})$$
$$+ AC(V_{13}u_{33} + V_{33}u_{23}) + BC(V_{23}u_{33} + V_{43}u_{23})]$$
$$\text{when } n=3 \tag{2.5.22}$$

The deflection time rate is dependent on not only the movement of the crash victim but also on both the movement of the vehicle and the movement of the contact surface with respect to the vehicle. Therefore, Equation (2.4.10) here becomes

$$\dot{\delta} = \sum_{k=1}^{12} \frac{\partial \delta}{\partial Z_k}\dot{Z}_k + \sum_{i=1}^{6} \frac{\partial \delta}{\partial \sigma_i}\dot{\sigma} + \sum_{j=1}^{4} \frac{\partial \delta}{\partial n_j}\dot{n}_j \tag{2.5.23}$$

The first term of (2.5.23) represents the movement of the body and is the sum of each lever arm already presented times the corresponding generalized velocity. The second term of (2.5.23) represents the movement of the vehicle where

$$\vec{\sigma} = \begin{bmatrix} x_4 \\ y_4 \\ z_4 \\ \psi_4 \\ \theta_4 \\ \phi_4 \end{bmatrix} \tag{2.5.24}$$

The vehicle "lever arms" are given below.

$$\frac{\partial \delta}{\partial \sigma_1} = -\frac{A}{\sqrt{p^2+q^2+r^2}} \tag{2.5.25}$$

$$\frac{\partial \delta}{\partial \sigma_2} = -\frac{B}{\sqrt{p^2+q^2+r^2}} \tag{2.5.26}$$

$$\frac{\partial \delta}{\partial \sigma_3} = -\frac{C}{\sqrt{p^2+q^2+r^2}} \tag{2.5.27}$$

$$\frac{\partial \delta}{\partial \sigma_4} = \frac{(y_o-y_4)A - (x_o-x_4)B}{\sqrt{p^2+q^2+r^2}} \tag{2.5.28}$$

$$\begin{aligned}(\sqrt{p^2+q^2+r^2})\frac{\partial \delta}{\partial \sigma_5} = {} & (x_o - x_4)(W_{14}p + W_{34}q - u'_{24}r) \\ & + (y_o - y_4)(W_{24}p + W_{44}q - u'_{44}r) \\ & - (z_o - z_4)(u_{14}p + u_{44}q + \cos\theta_4 r)\end{aligned} \tag{2.5.29}$$

$$\begin{aligned}(\sqrt{p^2+q^2+r^2})\frac{\partial \delta}{\partial \sigma_6} = {} & (x_o - x_4)(V_{34}q - V_{14}p) + (y_o - y_4)(V_{44}q - V_{24}p) \\ & + (z_o - z_4)(u_{34}q - u_{24}p)\end{aligned} \tag{2.5.30}$$

The third term of (2.5.23) represents the motion of the contact with respect to the vehicle where

$$\vec{n} = \begin{bmatrix} p \\ q \\ r \\ s \end{bmatrix} \text{ as defined in (2.5.8)} \tag{2.5.31}$$

These contact coefficients or "lever arms" are defined below.

$$(\sqrt{p^2+q^2+r^2})\frac{\partial \delta}{\partial n_1} = (x_o - x_4)V_{34} + (y_o - y_4)V_{44} + (z_o - z_4)u_{34} - \frac{p\delta}{\sqrt{p^2+q^2+r^2}} \tag{2.5.32}$$

$$(\sqrt{p^2+q^2+r^2})\frac{\partial \delta}{\partial n_2} = (x_o - x_4)V_{14} + (y_o - y_4)V_{24} + (z_o - z_4)u_{24} - \frac{q\delta}{\sqrt{p^2+q^2+r^2}} \tag{2.5.33}$$

$$(\sqrt{p^2+q^2+r^2})\frac{\partial \delta}{\partial n_3} = (x_o - x_4)u'_{34} + (y_o - y_4)u'_{14} - (z_o - z_4)\sin\theta_4 - \frac{r\delta}{\sqrt{p^2+q^2+r^2}} \tag{2.5.34}$$

$$\frac{\partial \delta}{\partial n_4} = \frac{1}{\sqrt{p^2+q^2+r^2}} \tag{2.5.35}$$

The motion of any of the contact surfaces is specified as input data to the crash victim simulator by presenting the positions of the three defining corner points at a sequence of time points. Implicit in this type of specification is the ability to change size, shape and orientation as well as position of a contact surface as a function of time. Figure 12 illustrates this general type of motion in a contact surface specified at three time points. The arrow eminating from the contact surface shows the forward side of the surface.

The contact surface starts out in the form of a square in the plane of the figure at t=0, moves forward, sideways, rotates, and becomes a rectangle by $t=t_1$, and moves back into the plane of the figure as a diamond shape oriented in the other direction by $t=t_2$. The three defining points are numbered with arrows showing their movements during the intervening times between specifications.

Each of the nine coordinates defining the position of the corner points are treated as piece-wise linear functions of time. A typical coordinate, the x-coordinate of Point 1, is shown in Figure 13. The coordinate rate is a step function but is made continuous by adding ramps from one level to the next within a small time interval. Values for corner coordinates and coordinate rates together with the derivatives of Equation (2.5.8) determine the $\dot{n}_j$ for j=1-4 used in Equation (2.5.23).

2.6 BELTS

The belt model is illustrated in Figure 14. The belts are represented by four independent segments, each anchored to the vehicle at an arbitrary point and pinned to the torso at an arbitrary point. Deflection is defined as elongation beyond the effective length of the belt segment at time zero and is formulated as

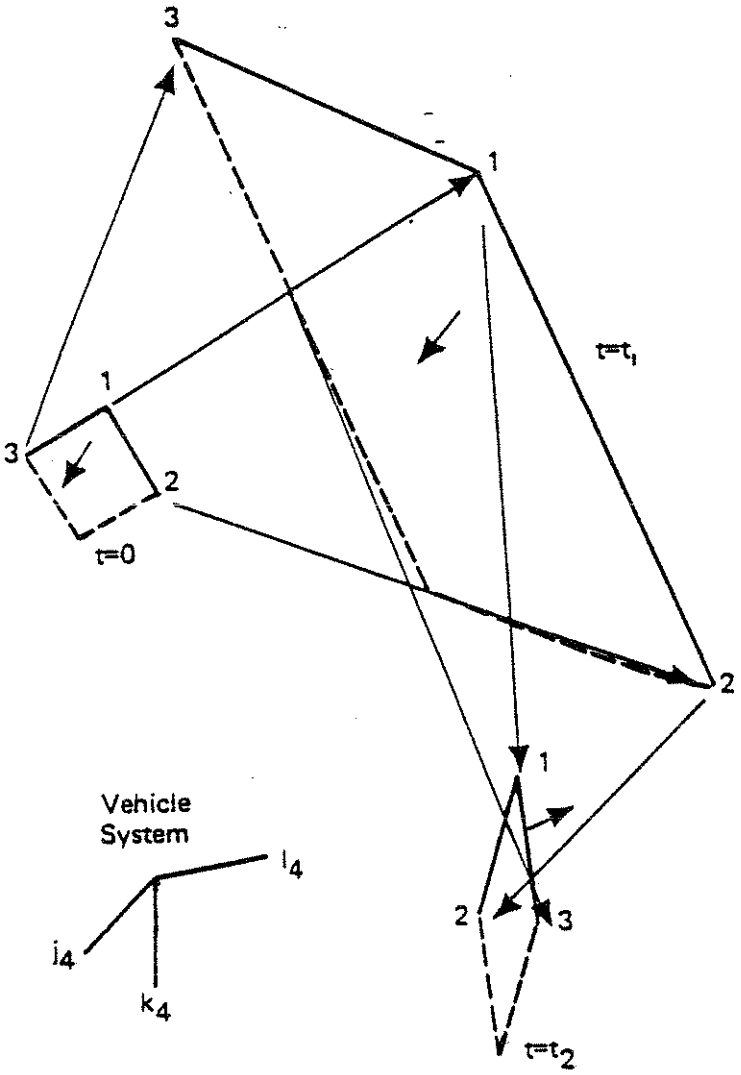

Fig. 12. A Moving Contact at Three Time Points

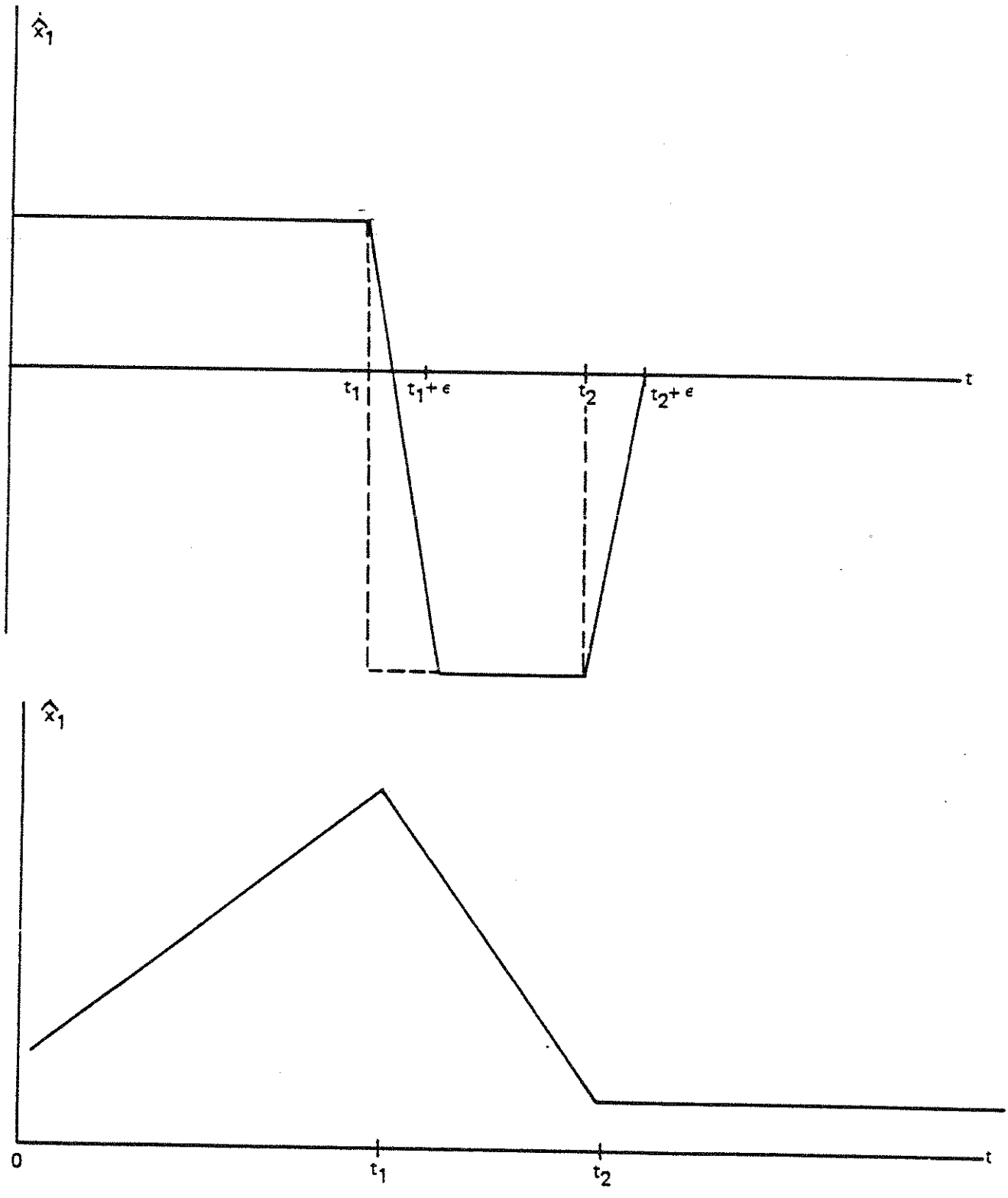

Fig. 13. A Corner Coordinate Value and Rate as a Function of Time

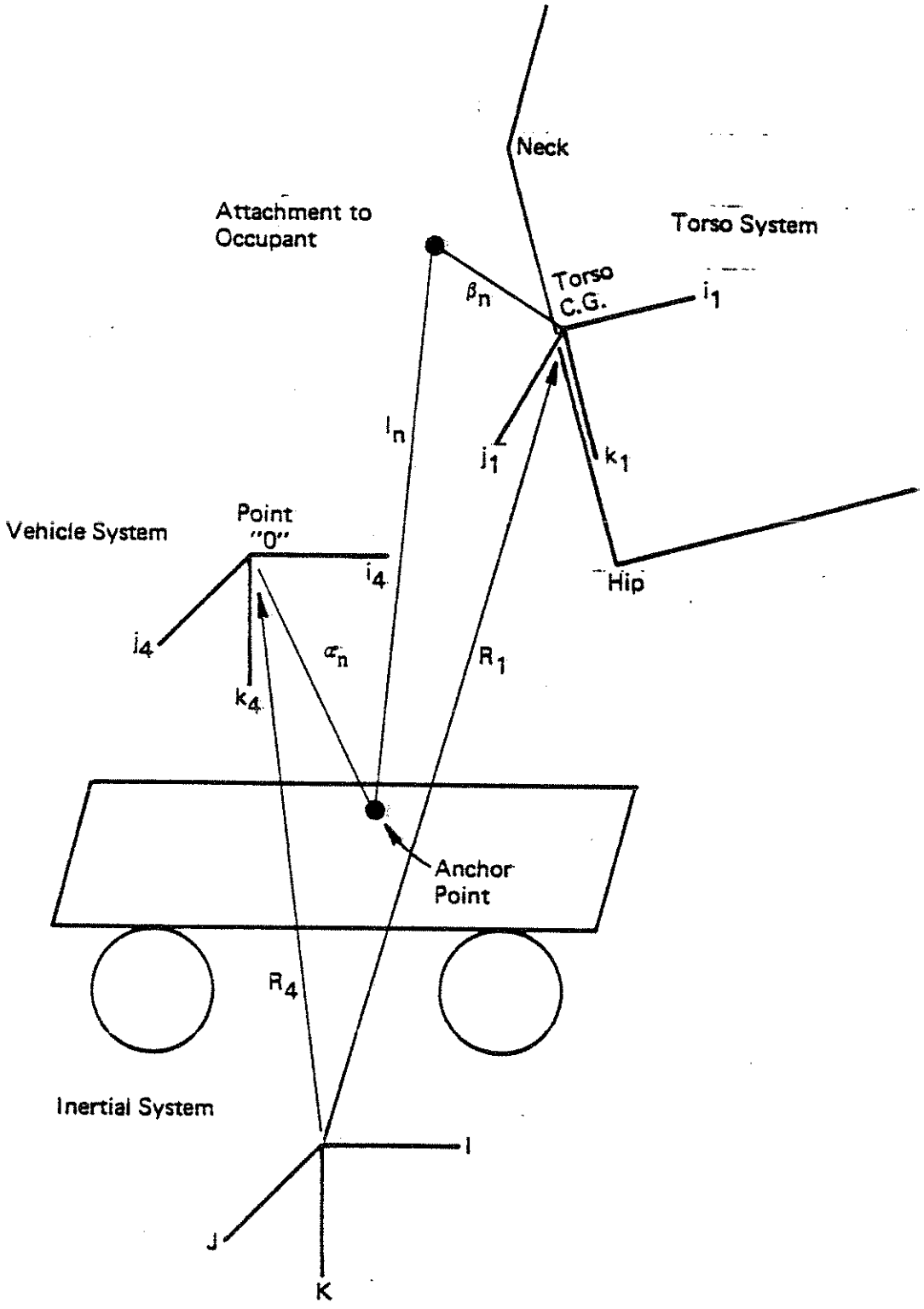

Figure 14. Belt Segment N

$$\delta_n = \ell_n(t) - \ell_n(o) \tag{2.6.1}$$

where $\ell_n(o) = [|\vec{R}_1 + \vec{\beta}_n - \vec{R} - \alpha_n|]_{t=0} - \Delta_n$

$\ell_n(t) = |\vec{R} + \vec{\beta}_n - \vec{R} - \vec{\alpha}_n|$

n is belt segment number

$\vec{\alpha}_n$ is anchor position vector (see Figure 12)

$\vec{\beta}_n$ is attachment position vector

Δ_n is the specified slack in the belt

TABLE I. BELT INDEX SPECIFICATIONS	
Belt Index	Belt Segment Name
1	Left Shoulder
2	Right Shoulder
3	Left Lap
4	Right Lap

The components of $\vec{\alpha}_n$ and $\vec{\beta}_n$ are taken according to vehicle and torso respectively as shown in Eq. (2.6.2).

$$\begin{aligned} \vec{\alpha}_n &= \lambda_n \vec{i}_4 + \mu_n \vec{j}_4 + \nu_n \vec{k}_4 \\ \vec{\beta}_n &= r_n \vec{i}_1 + s_n \vec{j}_1 + t_n \vec{k}_1 \end{aligned} \tag{2.6.2}$$

Then the inertial position of the anchor point is

$$\begin{aligned} \hat{\underline{X}}_n &= x_4 + \lambda_n \cos\psi_4 \cos\theta_4 + \mu_n \sin\psi_4 \cos\theta_4 - \nu_n \sin\theta_4 \\ \hat{\underline{Y}}_n &= y_4 + \lambda_n(\cos\psi_4 \sin\theta_4 \sin\phi_4 - \sin\psi_4 \cos\phi_4) + \mu_n(\sin\psi_4 \sin\theta_4 \sin\phi_4 + \cos\psi_4 \cos\phi_4) \\ &\quad + \nu_n \cos\theta_4 \sin\phi_4 \\ \hat{\underline{Z}}_n &= z_4 + \lambda_n(\cos\psi_4 \sin\theta_4 \cos\phi_4 + \sin\psi_4 \sin\phi_4) + \mu_n(\sin\psi_4 \sin\theta_4 \cos\phi_4 - \cos\psi_4 \sin\phi_4) \\ &\quad + \nu_n \cos\theta_4 \cos\phi_4 \end{aligned} \tag{2.6.3}$$

and the inertial position of the attachment point on the torso is

$$\hat{x}_n = x_1 + r_n\cos\psi_1\cos\theta_1 + s_n\sin\psi_1\cos\theta_1 - t_n\sin\theta_1$$

$$\hat{y}_n = y_1 + r_n(\cos\psi_1\sin\theta_1\sin\phi_1 - \sin\psi_1\cos\phi_1) + s_n(\sin\psi_1\sin\theta_1\sin\phi_1 + \cos\psi_1\cos\phi_1)$$
$$+ t_n\cos\theta_1\sin\phi_1 \qquad (2.6.4)$$

$$\hat{z}_n = z_1 + r_n(\cos\psi_1\sin\theta_1\cos\phi_1 + \sin\psi_1\sin\phi_1) + s_n(\sin\psi_1\sin\theta_1\cos\phi_1 - \cos\psi_1\sin\phi_1)$$
$$+ t_n\cos\theta_1\cos\phi_1$$

and

$$\ell_n = \sqrt{(\hat{\underline{X}}_n - \hat{x}_n)^2 + (\hat{\underline{Y}}_n - \hat{y}_n)^2 + (\hat{\underline{Z}}_n - \hat{z}_n)^2} \qquad (2.6.5)$$

Further, lever arms take the form

$$\frac{\partial\delta}{\delta Z_j} = \frac{\hat{x}_n - \hat{\underline{X}}_n}{\ell_n}\frac{\hat{x}_n}{\partial Z_j} + \frac{\hat{y}_n - \hat{\underline{Y}}_n}{\ell_n}\frac{\hat{y}_n}{\partial Z_j} + \frac{\hat{z}_n - \hat{\underline{Z}}_n}{\ell_n}\frac{\hat{z}_n}{\partial Z_j} \qquad (2.6.6)$$

for j=1,12

where

$$\frac{\partial x_n}{\partial Z_i} = \begin{bmatrix} 1 \\ 0 \\ 0 \\ (s_n\cos\psi_1 - r_n\sin\psi_1)\cos\theta_1 \\ -(s_n\sin\psi_1 + r_n\cos\psi_1)\sin\theta_1 - t_n\cos\theta_1 \\ 0 \\ 0 \\ 0 \\ 0 \\ 0 \\ 0 \\ 0 \end{bmatrix} \qquad (2.6.7)$$

$$\frac{\partial \hat{y}_n}{\partial Z_j} = \begin{bmatrix} 0 \\ 1 \\ 0 \\ (s_n\cos\psi_1 - r_n\sin\psi_1)\sin\theta_1\sin\phi_1 - (s_n\sin\psi_1 + r_n\cos\psi_1)\cos\phi_1 \\ [(s_n\sin\psi_1 + r_n\cos\psi_1)\cos\theta_1 - t_n\sin\theta_1]\sin\phi_1 \\ (s_n\sin\psi_1 + r_n\cos\psi_1)\sin\theta_1\cos\phi_1 - (s_n\cos\psi_1 - r_n\sin\psi_1)\sin\phi_1 \\ + t_n\cos\theta_1\cos\phi_1 \\ 0 \\ 0 \\ 0 \\ 0 \\ 0 \\ 0 \end{bmatrix} \qquad (2.6.8)$$

$$\frac{\partial \hat{z}_n}{\partial Z_j} = \begin{bmatrix} 0 \\ 0 \\ 1 \\ (s_n\cos\psi_1 - r_n\sin\psi_1)\sin\theta_1\cos\phi_1 + (s_n\sin\psi_1 + r_n\cos\psi_1)\sin\phi_1 \\ [(s_n\sin\psi_1 + r_n\cos\psi_1)\cos\theta_1 - t_n\sin\theta_1]\cos\phi_1 \\ - (s_n\sin\psi_1 + r_n\cos\psi_1)\sin\theta_1\sin\phi_1 - (s_n\cos\psi_1 - r_n\sin\psi_1)\cos\phi_1 \\ - t_n\cos\theta_1\sin\phi_1 \\ 0 \\ 0 \\ 0 \\ 0 \\ 0 \\ 0 \end{bmatrix} \qquad (2.6.9)$$

For belts, deflection rate is computed by Equation

$$\dot{\delta} = \sum_{k=1}^{12} \frac{\partial \delta}{\partial Z_k} \dot{Z}_k + \sum_{i=1}^{6} \frac{\partial \delta}{\partial \sigma_i} \dot{\sigma}_i \tag{2.6.10}$$

where the second term represents vehicle motion and $\vec{\sigma}$ is defined in (2.5.24).

Then
$$\frac{\partial \delta}{\partial \sigma_j} = \frac{\hat{x}_n - \hat{\underline{X}}_n}{\ell_n} \frac{\partial \hat{\underline{X}}_n}{\partial \sigma_j} + \frac{\hat{y}_n - \hat{\underline{Y}}_n}{\ell_n} \frac{\partial \hat{\underline{Y}}_n}{\partial \sigma_j} + \frac{\hat{z}_n - \hat{\underline{Z}}_n}{\ell_n} \frac{\partial \hat{\underline{Z}}_n}{\partial \sigma_j} \tag{2.6.11}$$

where

$$\frac{\partial \hat{\underline{X}}_n}{\partial \sigma_j} = \begin{bmatrix} 1 \\ 0 \\ 0 \\ -\lambda_n \sin\psi_4 \cos\theta_4 + \mu_n \cos\psi_4 \cos\theta_4 \\ -\lambda_n \cos\psi_4 \sin\theta_4 - \mu_n \sin\psi_4 \sin\theta_4 - \nu_4 \cos\theta_4 \\ 0 \end{bmatrix} \tag{2.6.12}$$

$$\frac{\partial \hat{\underline{Y}}_n}{\partial \sigma_j} = \begin{bmatrix} 0 \\ 1 \\ 0 \\ -\lambda_n V_{24} + \mu_n V_{14} \\ \lambda_n W_{34} + W_{44}\mu_n - u_{44}\nu_n \\ \lambda_n V_{34} + \mu_n V_{44} + u_{34}\nu_n \end{bmatrix} \tag{2.6.13}$$

$$\frac{\partial \hat{\underline{Z}}_n}{\partial \sigma_j} = \begin{bmatrix} 0 \\ 0 \\ 1 \\ -\lambda_n V_{44} + V_{34}\mu_n \\ \lambda_n W_{14} + W_{24}\mu_n - u_{14}\nu_n \\ -\lambda_n V_{14} - V_{24}\mu_n - u_{24}\nu_n \end{bmatrix} \tag{2.6.14}$$

2.7 JOINTS

The motion resisting torques which exist at the two joint structures (neck and hip) have been modeled by linear elastic torsional springs which tend to hold the body in its position at time zero (representing muscular action tending to hold the body in an equilibrium position) and stiff linear elastic torsional springs which are applied only at the end of the practical range of joint motion. In addition, the torques associated with the joint stops include linear damping effects. At each joint, separate torques are applied to resist pitch, roll and yaw motions. A schematic of joint structures is included as Figure 15.

The motion resisting torques are computed from relative angular motions between the various body segments. These are represented as a series of relative Euler angles shown in Figure 16 which transforms a system of coordinates parallel to the torso coordinate system to a system of coordinates parallel to the head coordinate system. The relative angles are named

$\Delta\psi_{ij}$ = relative yaw,

$\Delta\theta_{ij}$ = relative pitch, and

$\Delta\phi_{ij}$ = relative roll,

where the subscripts define the two body elements, i and j, between which the motions take place. The order of application of these angles is yaw, pitch, then roll.

To derive these equations, reference is made to Equation (2.3.3) which shows the transformation between e_i, a coordinate system fixed in one of the body segments, and e, the coordinate system fixed in inertial space. Equation (2.3.3) can be rewritten to show this transformation.

$$e_i = A_i e \qquad (2.7.1)$$

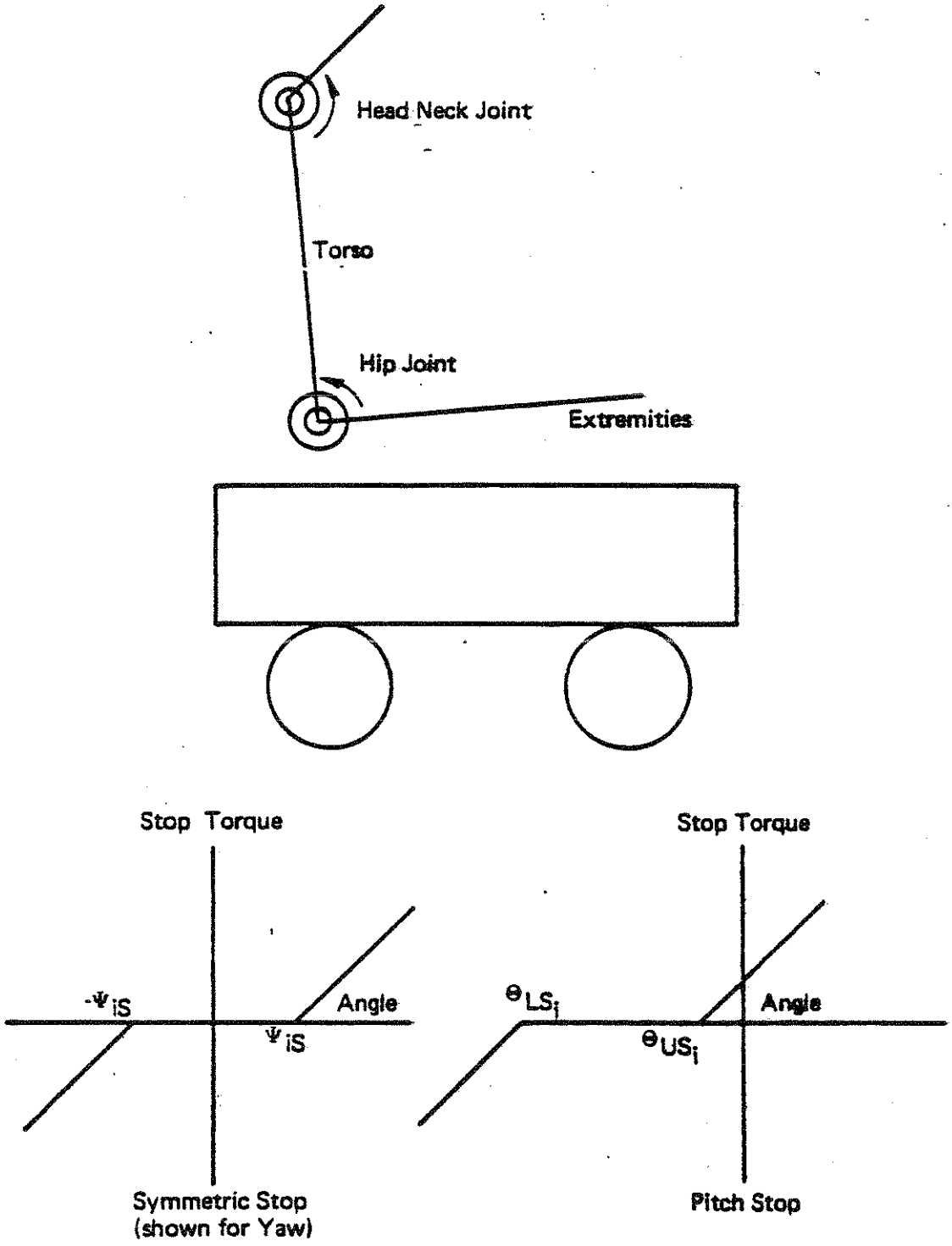

Fig. 16. Joints

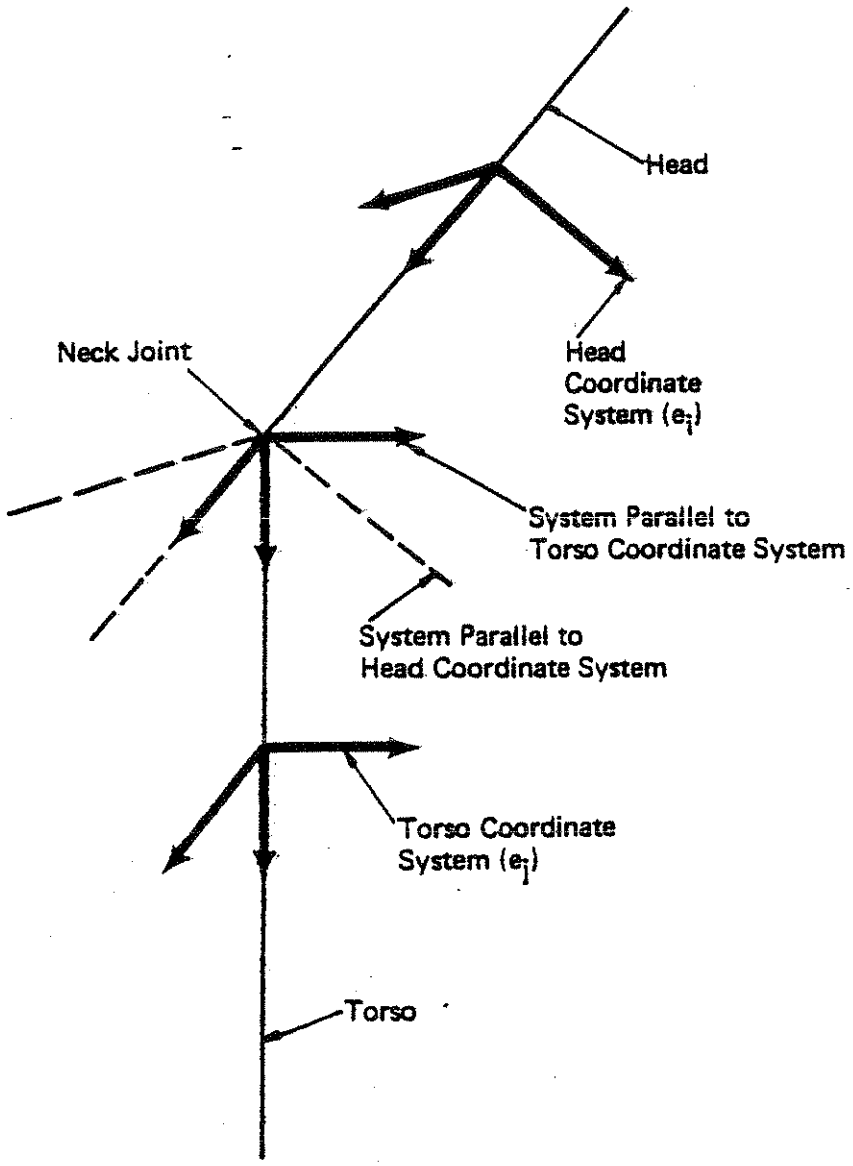

Fig. 16. Relative Euler Angles for Computing Joint Torques.

For orthogonal transformations the inverse of A_i is the same as the transpose.

$$A_i^{-1} = A_i^T \tag{2.7.2}$$

Let e_j represent the coordinate system attached to the body segment adjacent to the body segment orientated by e_i. Equation (2.7.1) becomes

$$e_j = A_j e \tag{2.7.3}$$

The system of relative Euler angles $\Delta\psi_{ij}$, $\Delta\theta_{ij}$, and $\Delta\phi_{ij}$ is defined from a transformation of the same form as Equation (2.3.3) which rotates a system parallel to e_j into a system parallel to e_i as illustrated in Figure 16.

Recalling Equations (2.7.3) and (2.7.2), it is apparent that

$$e = A_j^{-1} e_j = A_j^T e_j \quad \text{and} \tag{2.7.4}$$

substituting into Equation (2.7.1), it will be seen that

$$e_i = A_i A_j^T e_j \tag{2.7.5}$$

So it is true that

$$A_i A_j^T = \begin{bmatrix} \cos\Delta\psi_{ij}\cos\Delta\theta_{ij} & \sin\Delta\psi_{ij}\cos\Delta\theta_{ij} & -\sin\Delta\theta_{ij} \\ \cos\Delta\psi_{ij}\sin\Delta\theta_{ij}\sin\Delta\phi_{ij} - \sin\Delta\psi_{ij}\cos\Delta\phi_{ij} & \sin\Delta\psi_{ij}\sin\Delta\theta_{ij}\sin\Delta\phi_{ij} + \cos\Delta\psi_{ij}\cos\Delta\phi_{ij} & \cos\Delta\theta_{ij}\sin\Delta\phi_{ij} \\ \cos\Delta\psi_{ij}\sin\Delta\theta_{ij}\cos\Delta\phi_{ij} + \sin\Delta\psi_{ij}\sin\Delta\phi_{ij} & \sin\Delta\psi_{ij}\sin\Delta\theta_{ij}\cos\Delta\phi_{ij} - \cos\Delta\psi_{ij}\sin\Delta\phi_{ij} & \cos\Delta\theta_{ij}\cos\Delta\phi_{ij} \end{bmatrix} \tag{2.7.6}$$

The quantities $\Delta\psi_{ij}$, $\Delta\theta_{ij}$, and $\Delta\phi_{ij}$ must be written in terms of the generalized coordinates describing occupant motion. To do this one must use the original forms of A_i and A_j described by Equation (2.3.3) in terms of the pitch, roll, and yaw generalized coordinates in order to form an equation equivalent to Equation (2.7.6). When this has been done, various elements of the matrix in Equation (2.7.6) and its equivalent can be used to define the relative Euler angles as follows:

$$\Delta\psi_{ij} = \tan^{-1}\left(\frac{\sin\Delta\psi_{ij}\cos\Delta\theta_{ij}}{\cos\Delta\psi_{ij}\cos\Delta\theta_{ij}}\right) = \tan^{-1}\left(\frac{N\psi_{ij}}{D\psi_{ij}}\right) \tag{2.7.7}$$

where $N\psi_{ij}$ and $D\psi_{ij}$ are given in terms of the generalized motion coordinates as defined in Equation (2.3.12).

$$\begin{aligned} N\psi_{ij} &= V_{1j}u'_{3i} + V_{2j}u'_{1i} - u_{2j}\sin\theta_i \\ D\psi_{ij} &= u'_{3i}u'_{3j} + u'_{1i}u'_{1j} + \sin\theta_i\sin\theta_j \end{aligned} \tag{2.7.8}$$

Similarly, $\Delta\theta_{ij}$ is formed from the third element in the first row of the matrix,

$$\Delta\theta_{ij} = \sin^{-1}(A\theta_{ij}) \tag{2.7.9}$$

where

$$A\theta_{ij} = u_{3j}\sin\theta_i - V_{3j}u'_{3i} - V_{4j}u'_{1i} \tag{2.7.10}$$

and $\Delta\phi_{ij}$ is formed from the second and third elements in the third column of the matrix,

$$\Delta\phi_{ij} = \tan^{-1}\left(\frac{N\theta_{ij}}{D\phi_{ij}}\right) \tag{2.7.11}$$

where

$$\begin{aligned} N\phi_{ij} &= V_{1i}V_{3j} + V_{2i}V_{4j} + u_{2i}u_{3j} \\ D\phi_{ij} &= V_{3i}V_{3j} + V_{4i}V_{4j} + u_{3i}u_{3j} \end{aligned} \tag{2.7.12}$$

In order to compute the torques acting at all joints, it is necessary to define the angular deflection for use in the equations given in Section 2.4 of this report. For computation of elastic forces, the deflections are given relative to the initial position of the occupant at the beginning of the simulation, or

$$\begin{aligned} e^{\delta_{\psi_i}} &= \Delta\psi_{i1} - [\Delta\psi_{i1}]_{t=0} \\ e^{\delta_{\theta_i}} &= \Delta\theta_{i1} - [\Delta\theta_{i1}]_{t=0} \\ e^{\delta_{\phi_i}} &= \Delta\phi_{i1} - [\Delta\phi_{i1}]_{t=0} \end{aligned} \tag{2.7.13}$$

where the subscript 1 refers to the torso element and the subscript i can have the values i=2,3 depending on whether the motion is relative to the head or the lower extremities. The torsional reactions which occur as a result of interaction with the motion resisting stops are based on the relative and stop angles as follows.

$$s^{\delta}\psi_i = |\Delta\psi_{i1}| - \psi_{is}$$

$$s^{\delta}\theta_i = \begin{cases} \Delta\theta_{i_1} - \theta_{ius} & \text{, interaction with upper stop} \\ \Delta\theta_{i\ell s} - \Delta\theta_i & \text{, interaction with lower stop} \end{cases} \qquad (2.7.14)$$

$$s^{\delta}\phi_i = |\Delta\phi_{i1}| - \phi_{is}$$

where ψ_{is}, θ_{ius}, $\theta_{i\ell s}$, and ϕ_{is} are the various stop angles illustrated in Figure 15.

Based on the deflections given in Equations (2.7.13) and (2.7.14), it is possible to determine the "lever arms" used in computing the contributions to the generalized force vector from joint forces. For i=2,3 indicating either the head or lower extremities, the lever arms are given in the following table of equations.

Generalized Coordinate Subscript = n	Constant x Lever Arm = $[(N\phi_{i1})^2 + (D\phi_{i1})^2]\frac{\partial\Delta\phi_{i1}}{\partial Z_n}$
4	$\sin\theta_i - u_{31}A\theta_{i1}$
5	$- N\psi_{i1}$
6	$- D\psi_{i1}$
3i + 1	$u_{31}A\theta_{i1} - \sin\theta_i$
3i + 2	$u_{31}(V_{41}u'_{3i} - V_{31}u'_{4i}) + [(V_{31}^2 - V_{41}^2)\cos\psi_i + 2V_{31}V_{41}\sin\psi_i]u'_{1i} - V_{31}V_{41}\cos\theta_i$
3i + 3	$(N\phi_{i1})^2 + (D\phi_{i1})^2$

(zero for all other n) (2.7.15)

Generalized Coordinate Subscript = n	Constant x Lever Arm = $[1-(A\theta_{ij})^2]^{1/2}\frac{\partial\Delta\theta_{i1}}{\partial Z_n}$
4	$V_{41}u'_{3i} - V_{31}u'_{1i}$
5	$-(u_{11}\sin\theta_i + W_{11}u'_{3i} + W_{21}u'_{1i})$
6	$V_{11}u'_{3i} + V_{21}u'_{1i} - u_{21}\sin\theta_i$
3i + 1	$V_{31}u'_{1i} - V_{41}u'_{3i}$
3i + 2	$u_{31}\cos\theta_i + V_{31}u'_{2i} + V_{41}u'_{4i}$

(zero for all other n) (2.7.16)

Generalized Coordinate Subscript = n	Constant x Lever Arm = $[(N\psi_{i1})^2 + (D\psi_{i1})^2]\frac{\partial\Delta\psi_{i1}}{Z_n}$
4	$-\cos\theta_i(u_{31}\cos\theta_i + V_{31}u'_{2i} + V_{41}u'_{4i})$
5	$\sin\phi_1\sin^2\theta_i - [V_{41}\cos\psi_1 - (\sin\phi_1 + 2V_{41}\cos\psi_1)\sin^2\psi_i + (2V_{41}\sin\psi_1 - V_{11})\sin\psi_i\cos\psi_i]\cos^2\theta_i + (W_{21}\cos\psi_i - W_{11}\sin\psi_i)\sin\theta_i\cos\theta_i$
6	$-(D\psi_{i1})(A\theta_{i1})$
3i + 1	$\cos\theta_i(u_{31}\cos\theta_i + V_{31}u'_{2i} + V_{41}u'_{4i})$
3i + 2	$V_{41}\cos\psi_i - V_{31}\sin\psi_i$

(zero for all other n) (2.7.17)

Equations (2.7.13 - 2.7.17) are used to form the contributions to the generalized force vector, $\vec{Q}_F$, due to the joint structures using the formulas set forth in Section 2.4 of this report.

3.0 EXPERIMENTAL VERIFICATION OF THE MODEL

In this part of the report comparisons are made between the predictions of the model and experiments involving anthropometric dummies which have been carried out on the HSRI impact sled. Beginning with a section outlining the criteria on which the validation is based, the report continues with a description of the sled tests and concludes with sections describing the degree to which the models describe the real test situation.

3.1 CHOICE OF CRITERIA FOR VERIFICATION

The choice of a criterion of verification of the mathematical model describing human body impact is based on three premises: (a) whether or not the mathematical analysis and computer program are correct; (b) the extraction of appropriate experimental data on which the validation procedures can be based; and (c) the observation that the mathematical model consists of parameters describing the occupant, the force field consisting of belts and contact surfaces which acts on the occupant, and the externally applied deceleration forcing function.

The use of a Lagrangian formulation of Newtonian mechanics as a basis for the model is based on a long history of successful applications to problems in impact, and hence,offers no cause for concern. Thus, sources of problems can arise only in writing down the particular equations and computer programs which apply to the present analyses. All equations and computer programs have been derived independently by two or more persons leading to a very low incidence of errors in the final programs.

The second premise, which is concerned with the extraction of appropriate experimental data on which the validation can be based, has been the basis for a major research effort. The acquisition of the necessary transducer and photometric data is straightforward and requires only the proper useage of the appropriate high speed cameras, data tape recorders, and light beam oscillographs. The processing of the transducer data is also relatively simple. For example, the determination of the magnitude of the linear acceleration of the head of the dummy requires computation of the simple vector sum of the three linear acceleration components.

The processing of the photometric data is much more complex. Although procedures for plotting the trajectory of a point in space, using various automatic or operator-controlled photometric analyzers, are widely applied in the field of motion analysis, they were not developed for determining the angular orientation of a body in space. Thus, it was necessary to develop techniques for determining the pitch, roll, and yaw angles of the body of the test subject before proceeding to a comparison of experimental and theoretical results.

Analysis and graphing of the test data is only part of the problem because preparation of a well-founded set of input data is necessary for the successful operation of any computer analysis. Therefore, a description of the mass, geometric, and inertial properties of the test subject is required. This must be supplemented by a geometrical profile of the vehicle components with which the test subject is expected to interact. Finally, the force-deformation characteristics of the interactions between the test subject and the vehicle components must be measured in order to specify the proper balance between subject motions and loadings.

In order to define the test subject, eight basic body elements (head, two arm elements, two leg elements, and three torso elements) were weighed and moments of inertia were either measured using a trifilar pendulum or predicted using formulas similar to those of Hanavan[25] and Patten.[26] This data was combined to describe the three mass elements of the current model. After geometry of the test sled and the initial position of the dummy subject were carefully measured, it was then necessary to develop test procedures defining the force-motion relationships between the test subject and vehicle elements. This was carried out for the seat and for a belt restraint system using a combination of photometric and transducer data described in Reference 27.

The third premise serves to define the mathematical models as a system of parameters describing the occupant, the force field consisting of belts and contact surfaces which acts on the occupant, and the externally applied deceleration forcing function. All these basic parameters must be included in any test validation.

To properly study the field of forces acting on the subject it is necessary to simulate both contact surfaces (such as a seat cushion and seat back) and belts (such as a lap belt and single diagonal shoulder harness). The use of an occupant unrestrained by belts would not provide a test of this section of the analysis. Both frontal and side impacts were carried out to verify the model. In the frontal impact comparisons also can be made with the predictions of a purely planar model such as the HSRI Two-Dimensional Mathematical Crash Victim Simulator.[25] Use of a frontal impact test does not provide a complete test of the operation of the three-dimensional model. Therefore, a lateral impact, which can be carried out on the impact sled, was selected as the most appropriate tool for validating the non-planar properties of the three-dimensional model.

Based on these three premises, two impact sled tests were selected for the validation procedure. Both tests used a 50th percentile male anthropometric dummy and were carried out at speeds of approximately 30 mph. In each case the dummy was restrained by a lap belt and a single diagonal shoulder harness. The first test represented a forward-facing impact and the second a direct side impact. Thus, these two tests represented a complete and economical test of the basic parameters described in the Model - the occupant, the restraint and interior contact forces, and the vehicle deceleration.

3.2 THE EXPERIMENTS

The two validation experiments were carried out on the HSRI impact sled (Figure 17), which is of the acceleration-deceleration type. It is accelerated over a 12-foot distance up to a top speed to 40 mph using a compressed air-actuated puller arm. The deceleration stroke has a maximum length of three feet and a maximum potential of 88 G's. For the purposes of high speed photography a total of 50 kw. of lighting is available. Real time and high speed movies were taken as well as still photos before and after each test.

Triaxial accelerometer packs were located in the head and chest of the 50th percentile Sierra dummy. The accelerometers were Kistler Piezotron 818's. A Statham strain-gage accelerometer was used to record the sled deceleration pulse. Four Lebow seat-belt load transducers were mounted on the seat belt and shoulder harness.

The data was recorded simultaneously on a Honeywell 7600 tape recorder and a Honewell 1612 Visicorder. No filtering was used during the initial recording other than the limitation of the light-beam galvanometers to frequencies under 1000 cps. The following transducer data was recorded:

FIGURE 17. HSRI IMPACT SLED

(a) lower right shoulder belt force; (b) left lap belt force; (c) upper left shoulder belt force; (d) right lap belt force; (e) sled deceleration; (f) head anterior-posterior G-loading; (g) chest anterior-posterior G-loading; (h) head superior-inferior G-loading; (i) chest superior-inferior G-loading; (j) head left-right G-loading; (k) chest left-right G-loading; (l) impact velocity; and, (m) timing signals.

The setup for the frontal impact test is shown in Figure 18. The bucket seat is bolted securely to a framework which is attached to the sled. This framework serves as a mount for attaching belts and other types of restraint systems, and can be rotated to simulate lateral or oblique impact. This has been done for the lateral impact test as is shown in Figure 19. In this setup a series of belts are shown which maintain the initial position of the dummy during the initial acceleration of the sled. These are released before impact and do not interfere with the motions of the dummy.

The test data presented in Figures 20 through 39 were obtained as a result of either detailed analysis of the high speed films using a Vanguard Film Analyzer or by measuring points on the oscillographic recordings. All acceleration and belt transducer data were determined from the oscillographic records and appropriate sums and resultant values computed.

For the front impact test, the excursion and forward motion of the head were determined directly by measurements of the motion of a target placed on the head of the dummy. Likewise the angle of head pitch and the upper leg were obtained by direct measurement (and the subsequent scaling and tabulation by means of specially developed computer programs). The motion of the H-point was very difficult to determine as no direct measurements were possible. However, its location was determinable by trigonometry using data from a thigh target, a lower back target, and the angle of the upper leg with the horizontal. These data, determined on the Vanguard Analyzer, were then processed on

FIGURE 18. FRONTAL IMPACT TEST SETUP

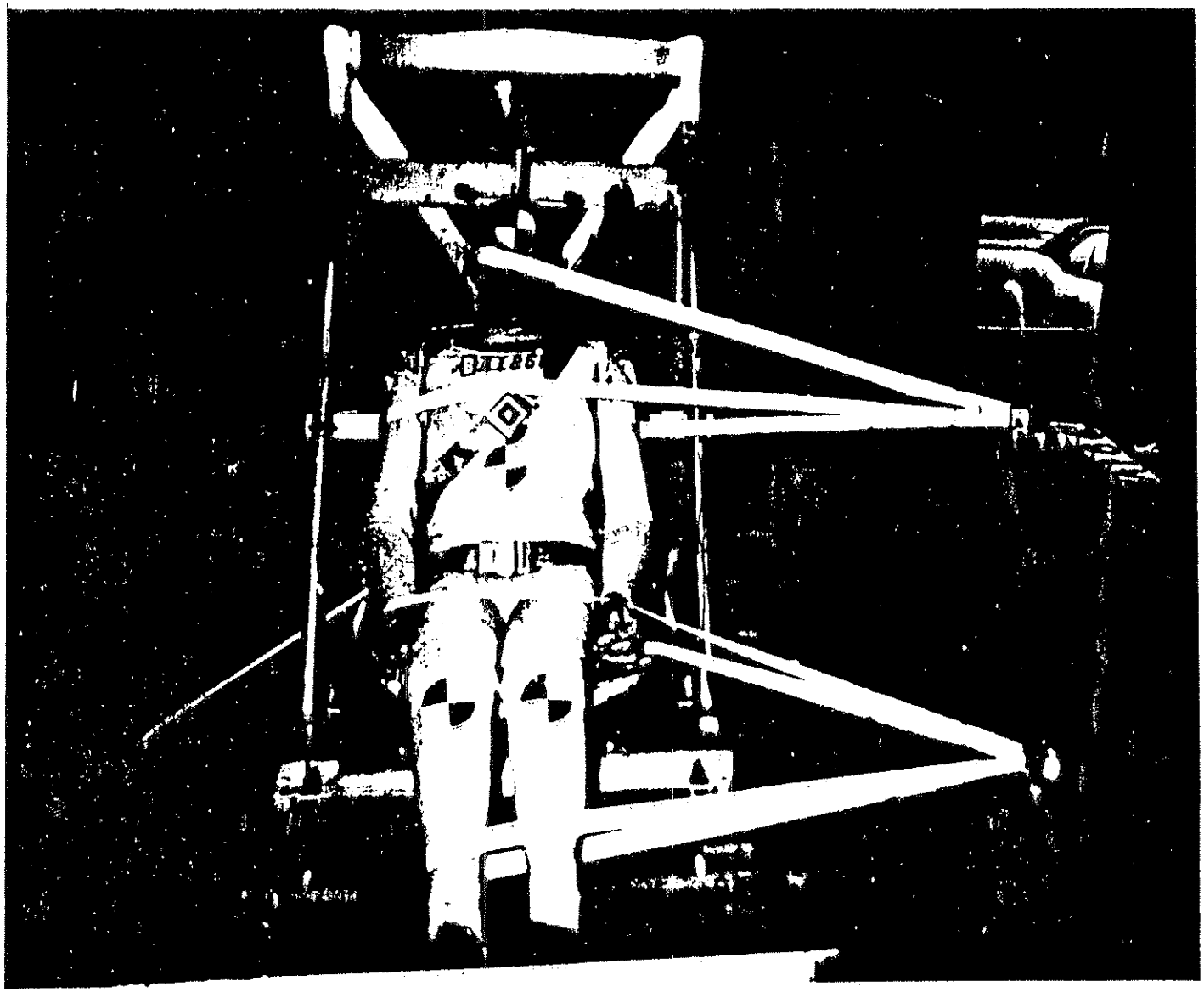

FIGURE 19. LATERAL IMPACT TEST SETUP

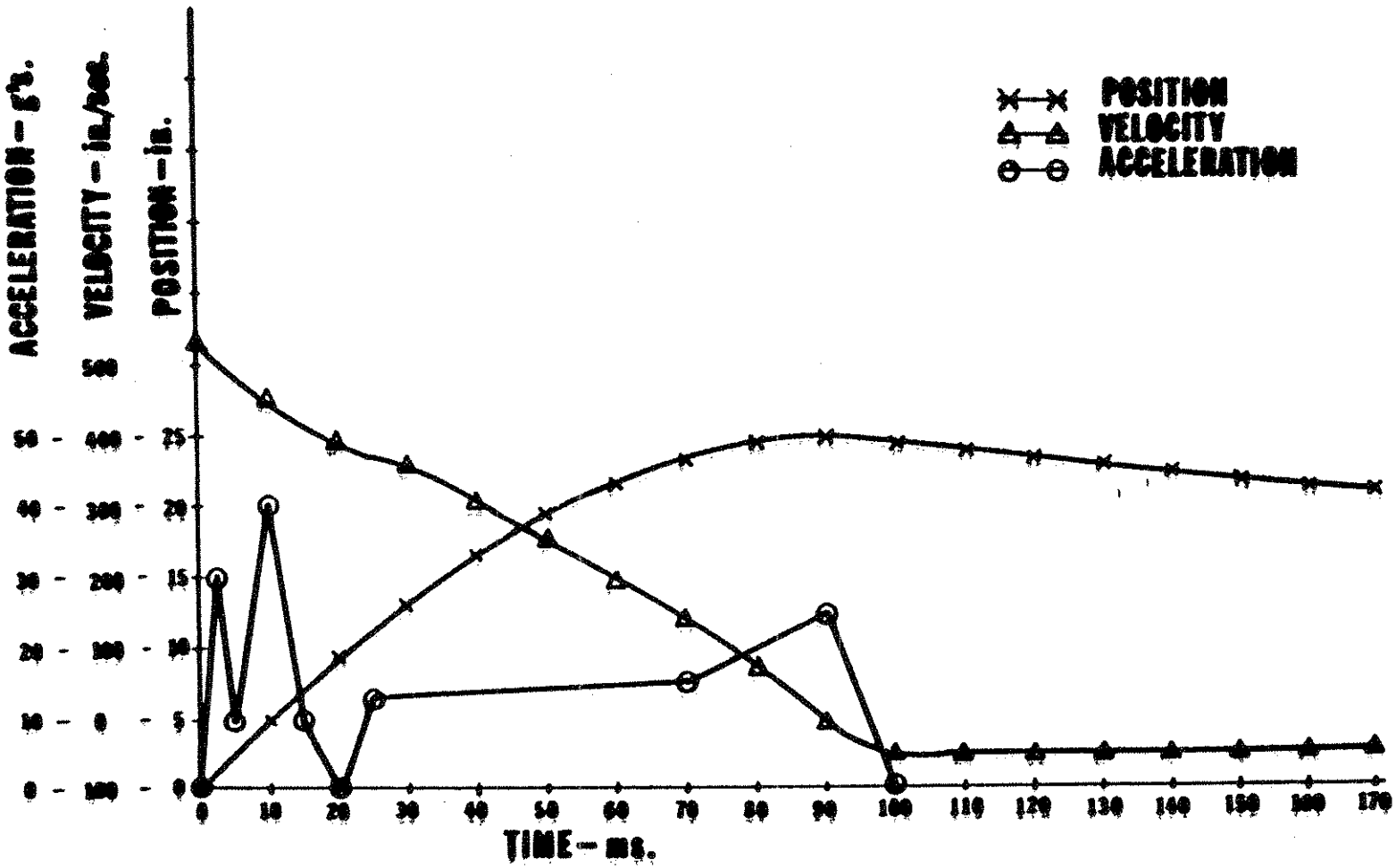

FIGURE 20. VEHICLE KINEMATICS

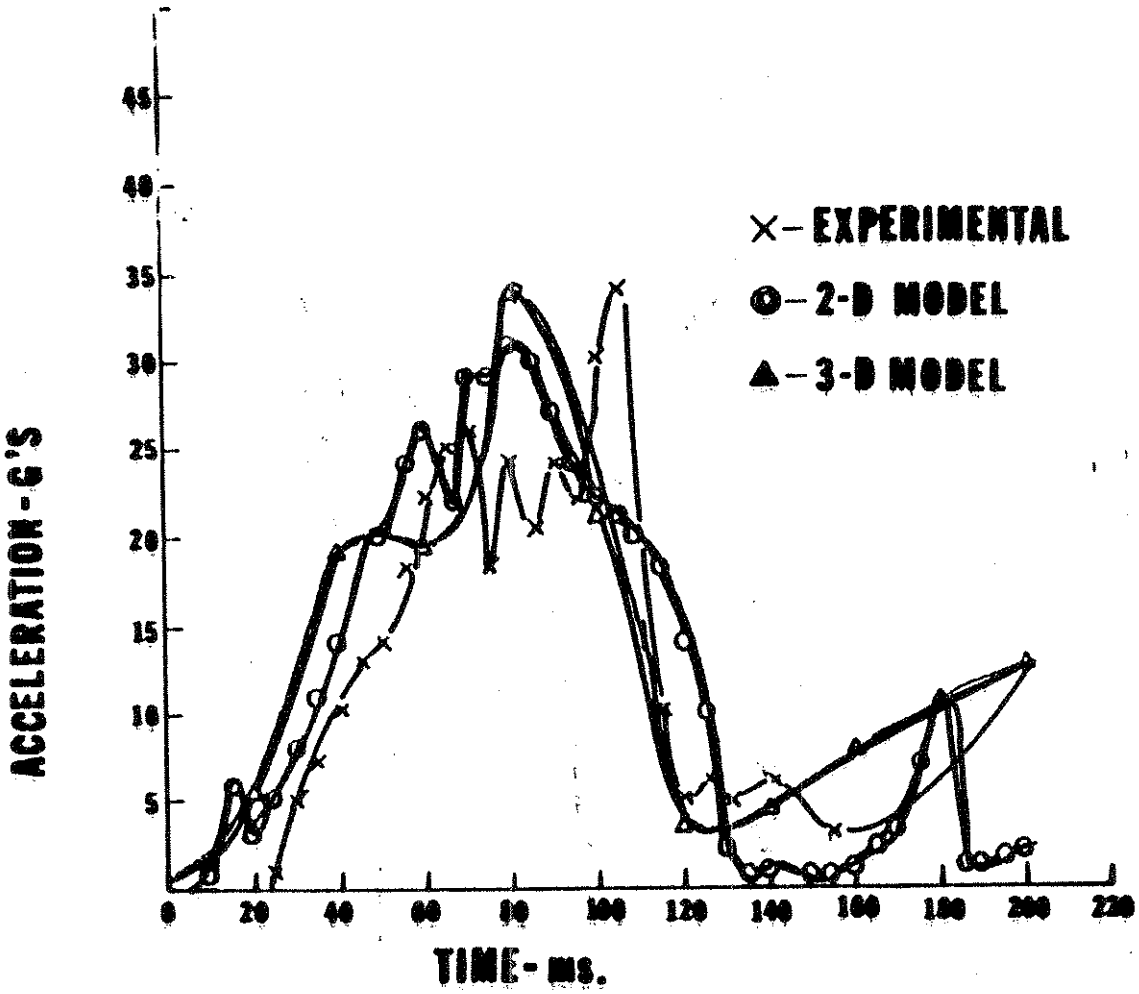

FIGURE 21. RESULTANT CHEST LINEAR ACCELERATION IN G-S

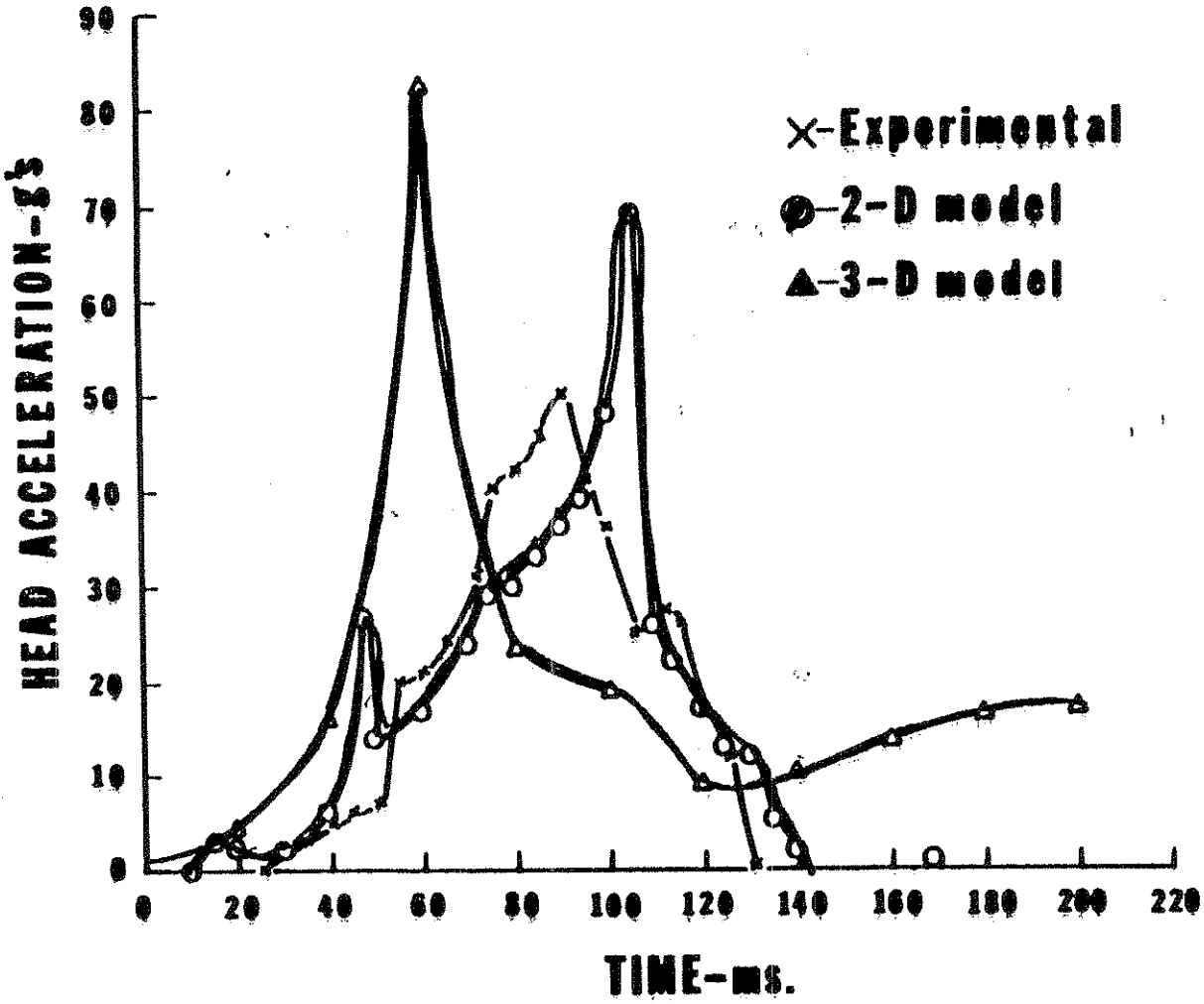

FIGURE 22. RESULTANT HEAD LINEAR ACCELERATION IN G-S

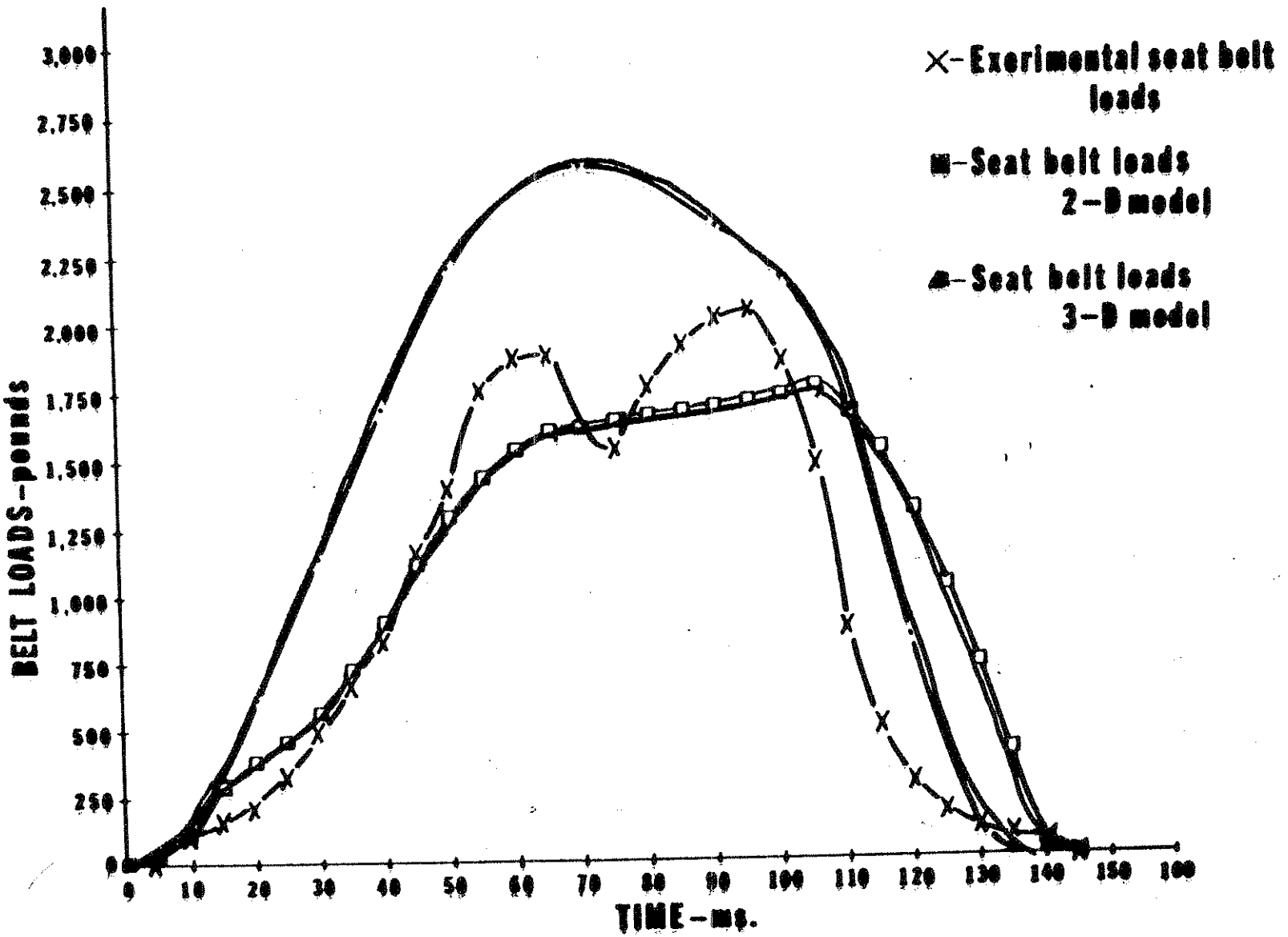

FIGURE 23. SEAT BELT LOADS

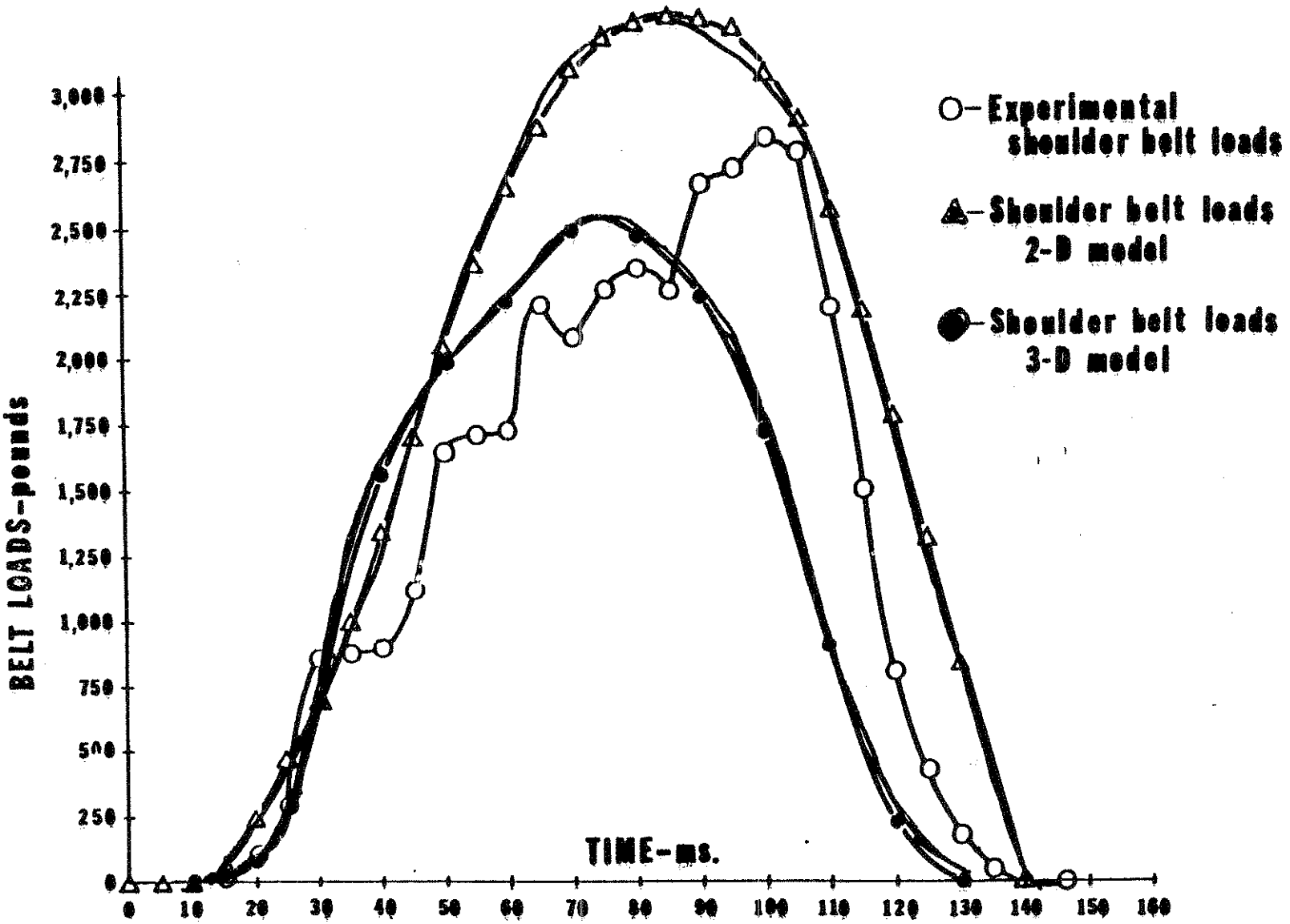

FIGURE 24. SHOULDER HARNESS LOADS

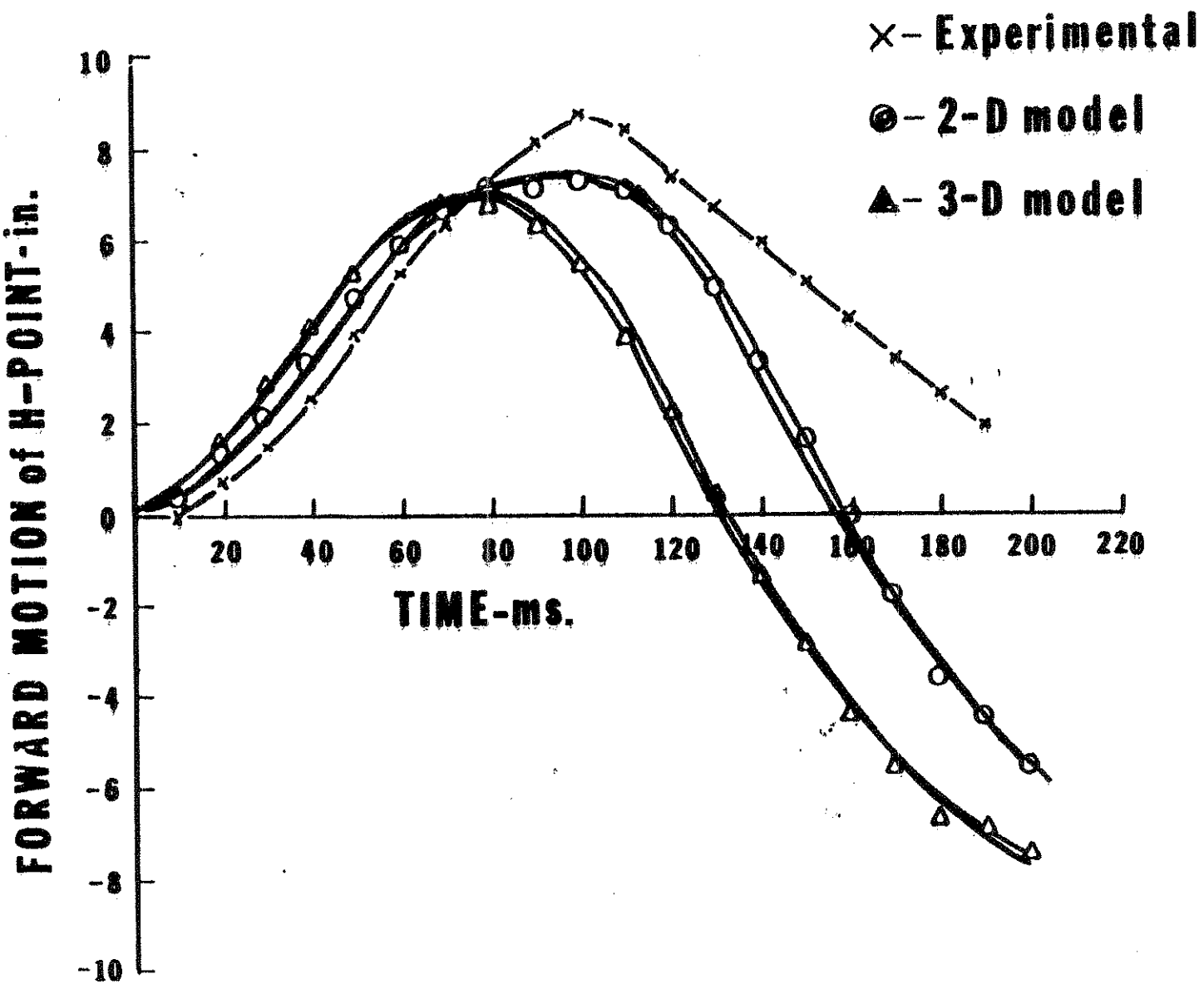

FIGURE 25. FORWARD MOTION OF H-POINT

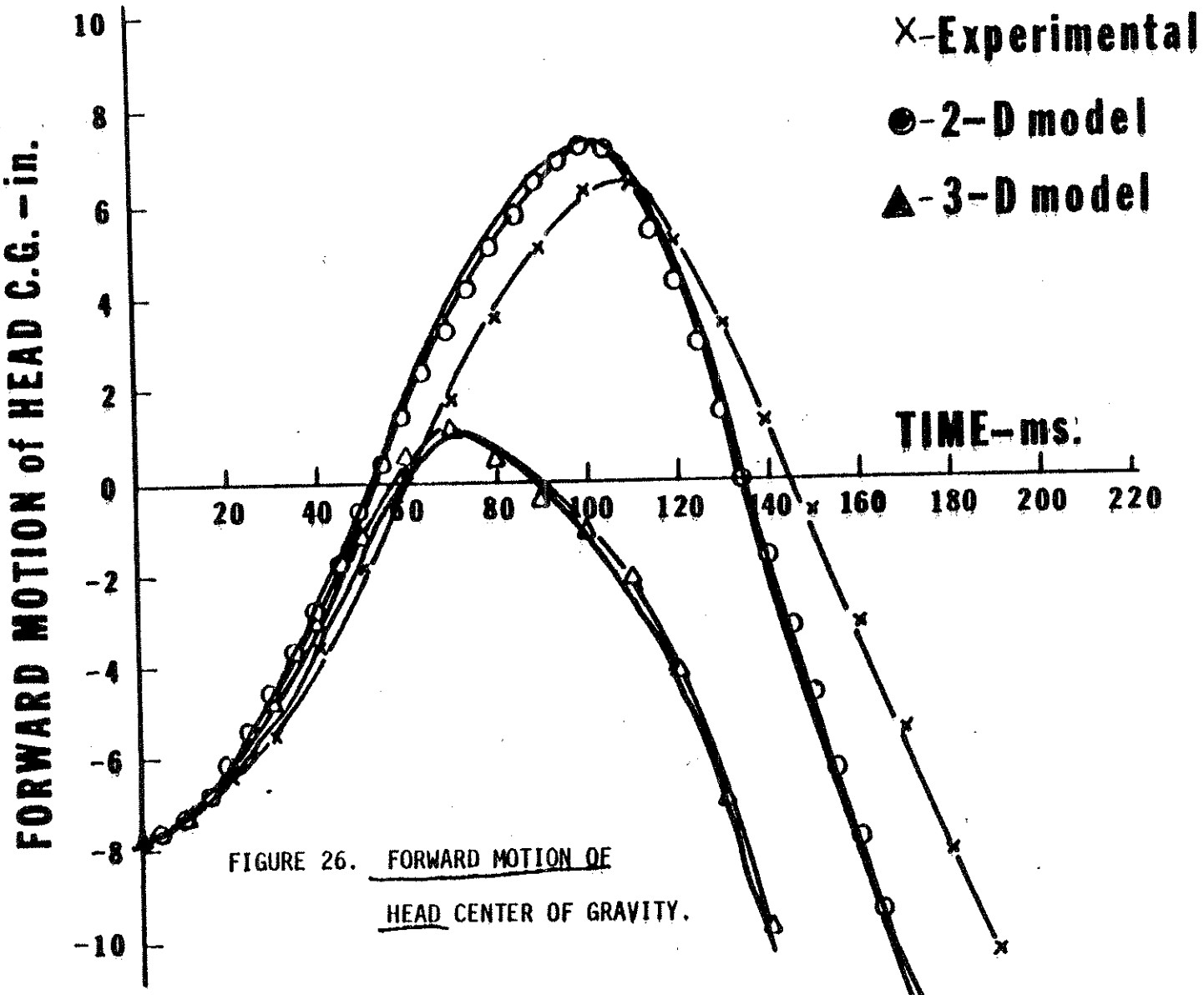

FIGURE 26. FORWARD MOTION OF HEAD CENTER OF GRAVITY.

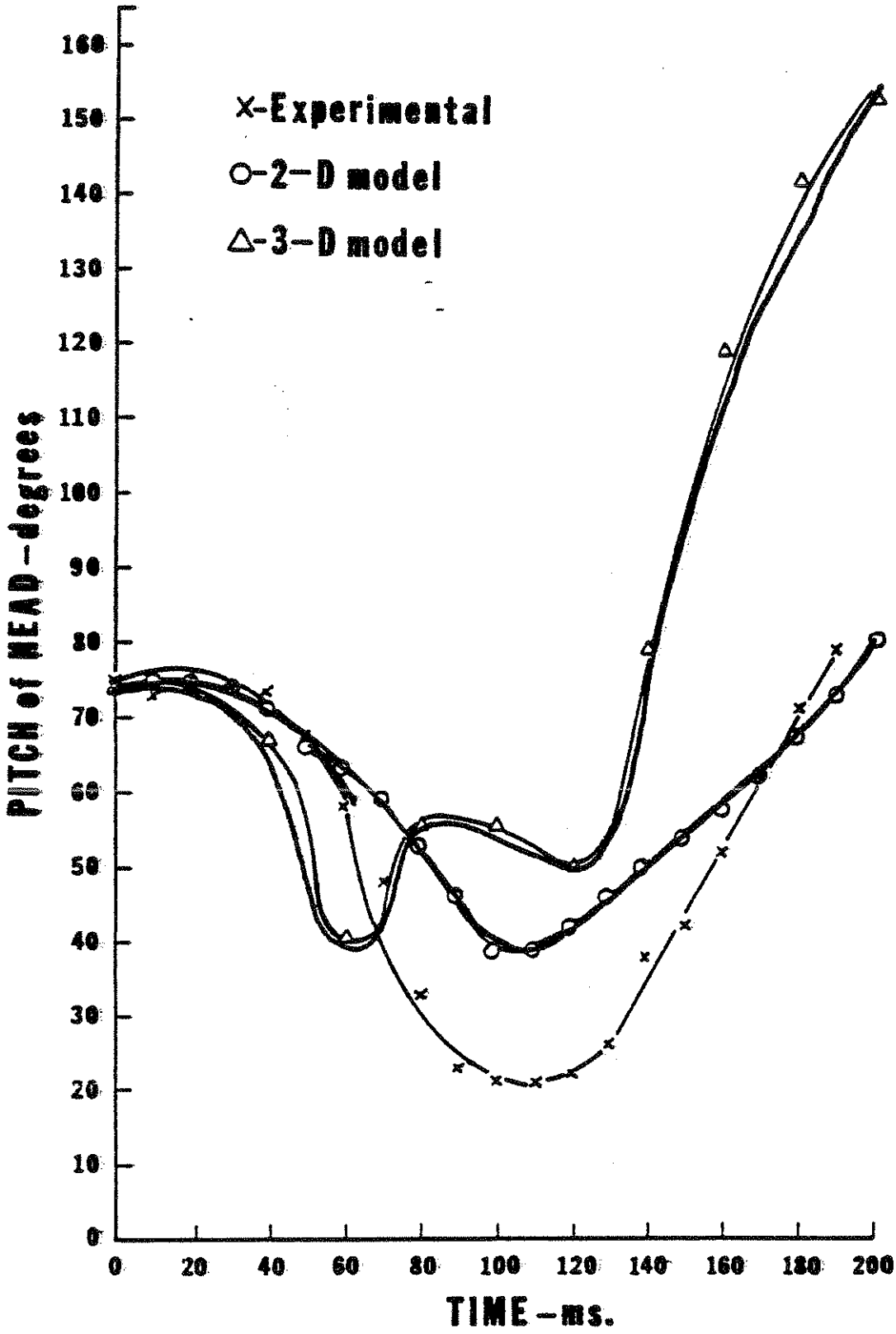

FIGURE 27. PITCH ANGLE OF HEAD

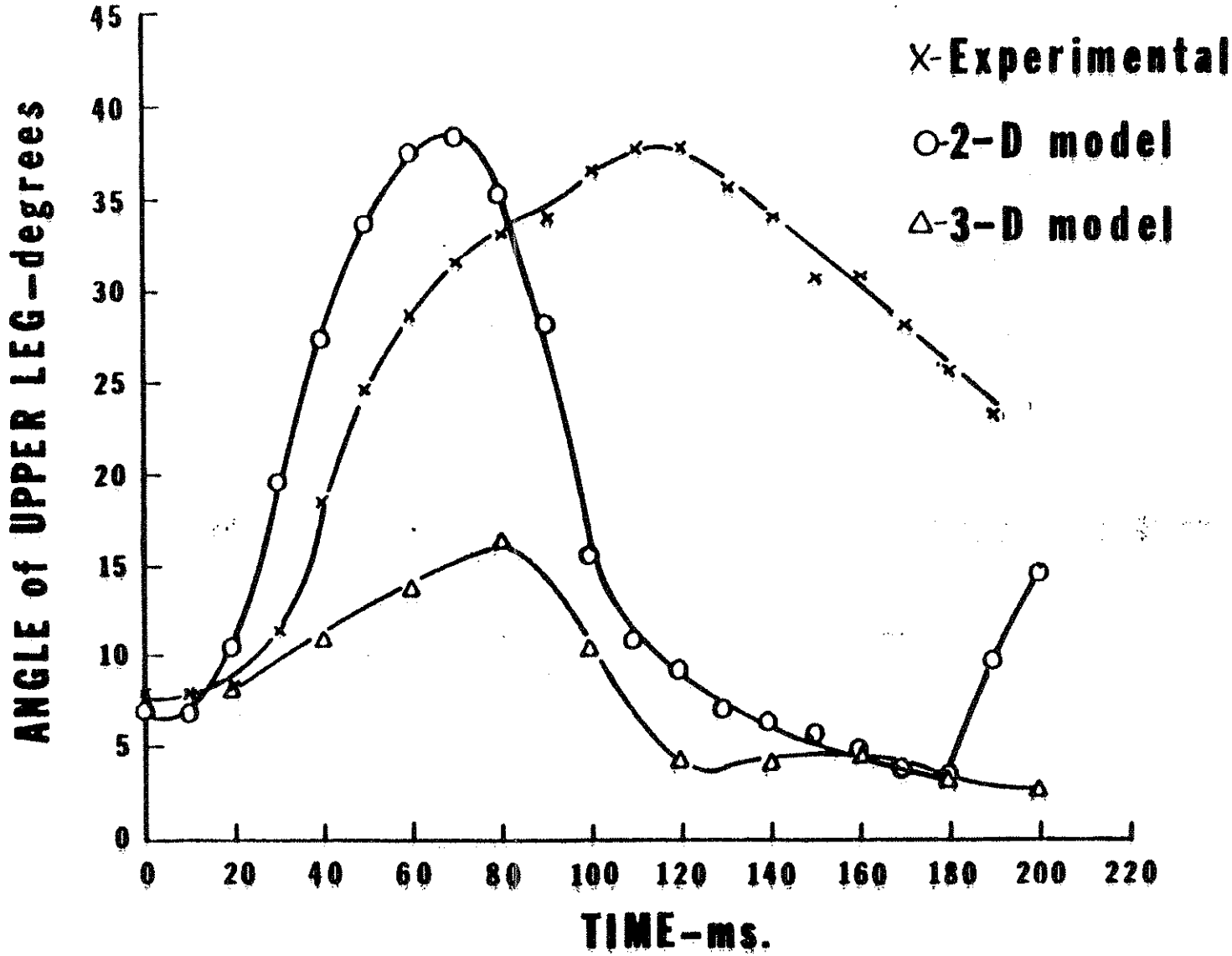

FIGURE 28. PITCH ANGLE OF THE UPPER LEG

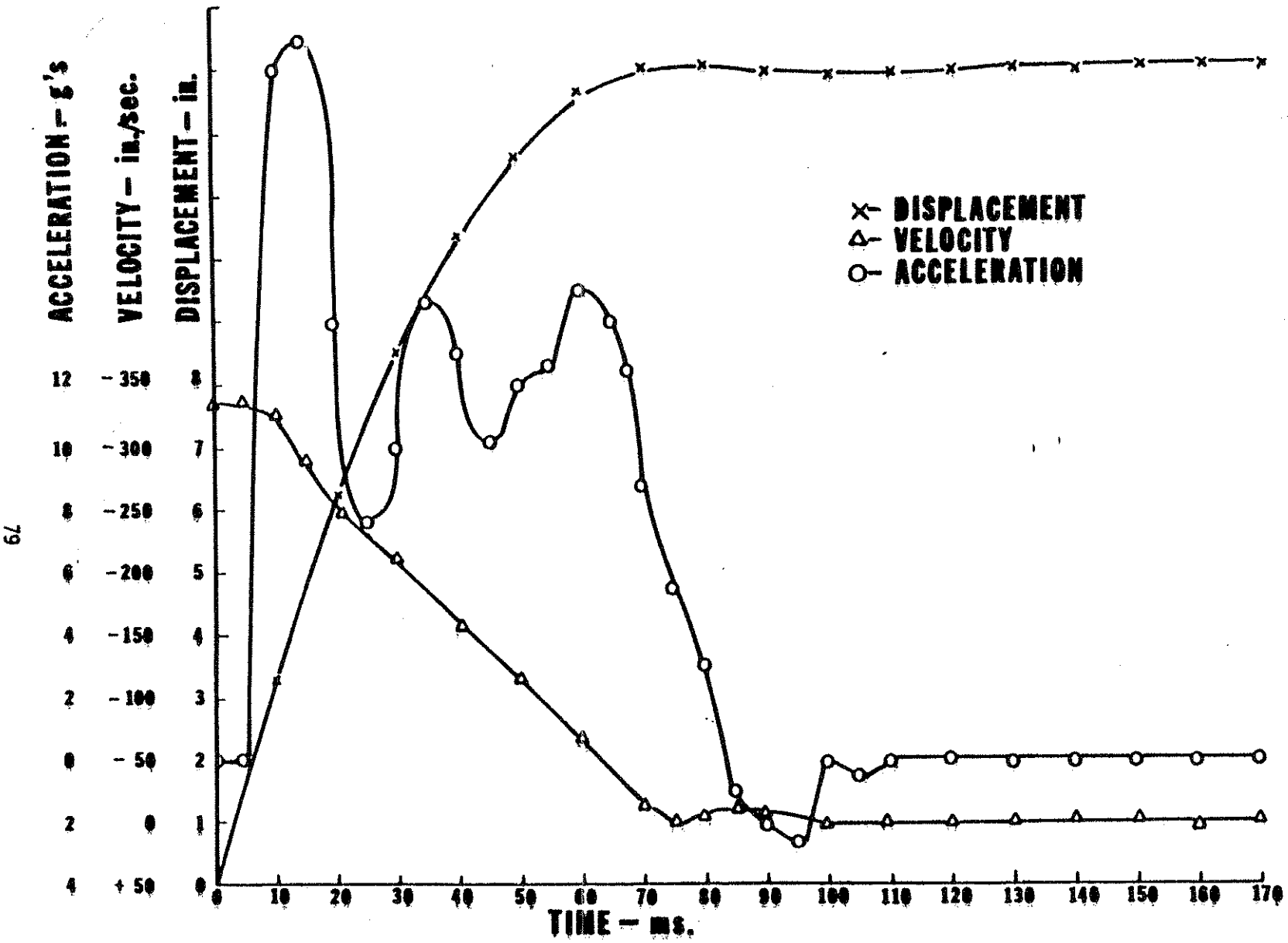

FIGURE 29. VEHICLE KINEMATICS

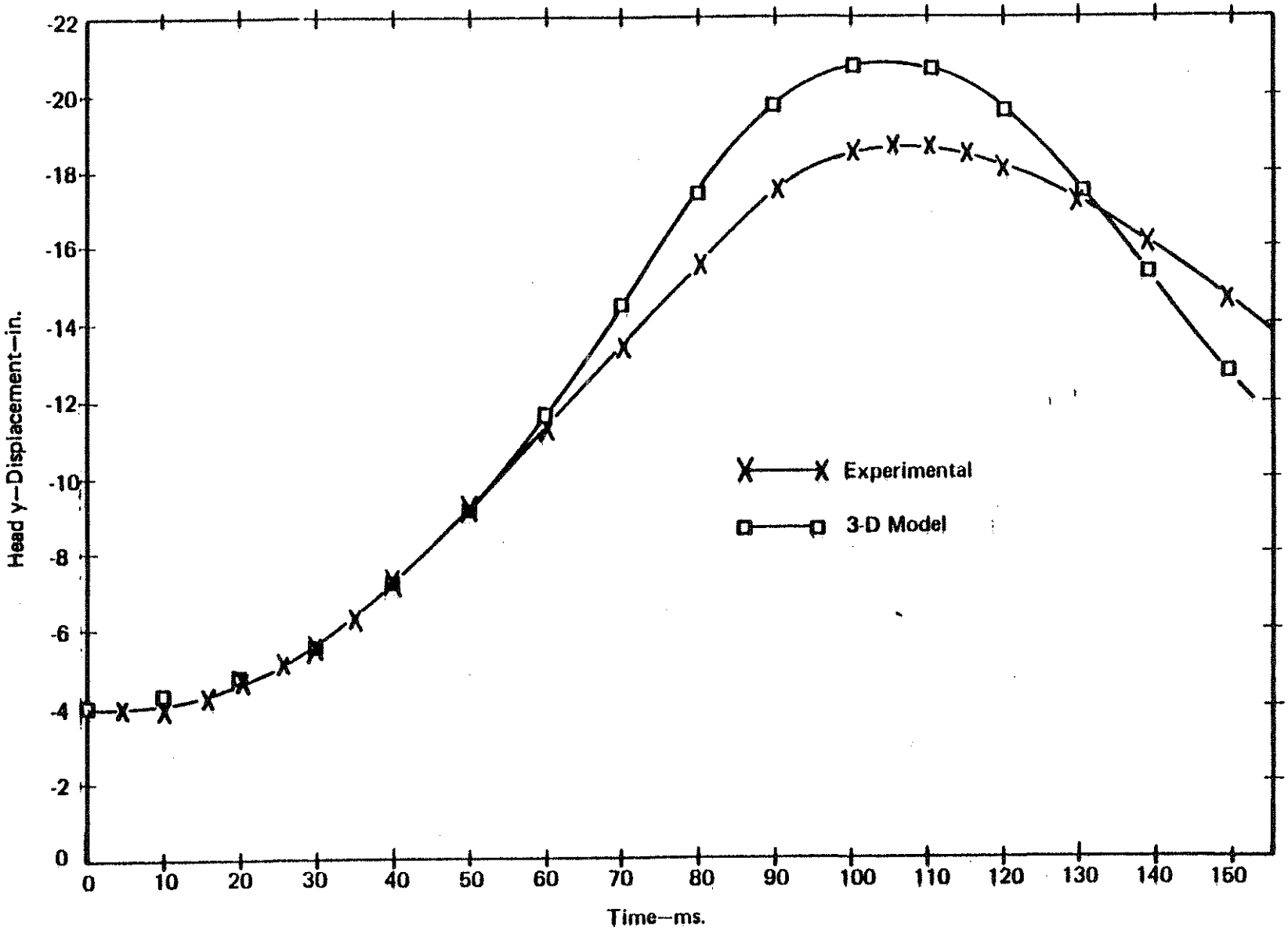

Figure 30. Head Displacement to Side

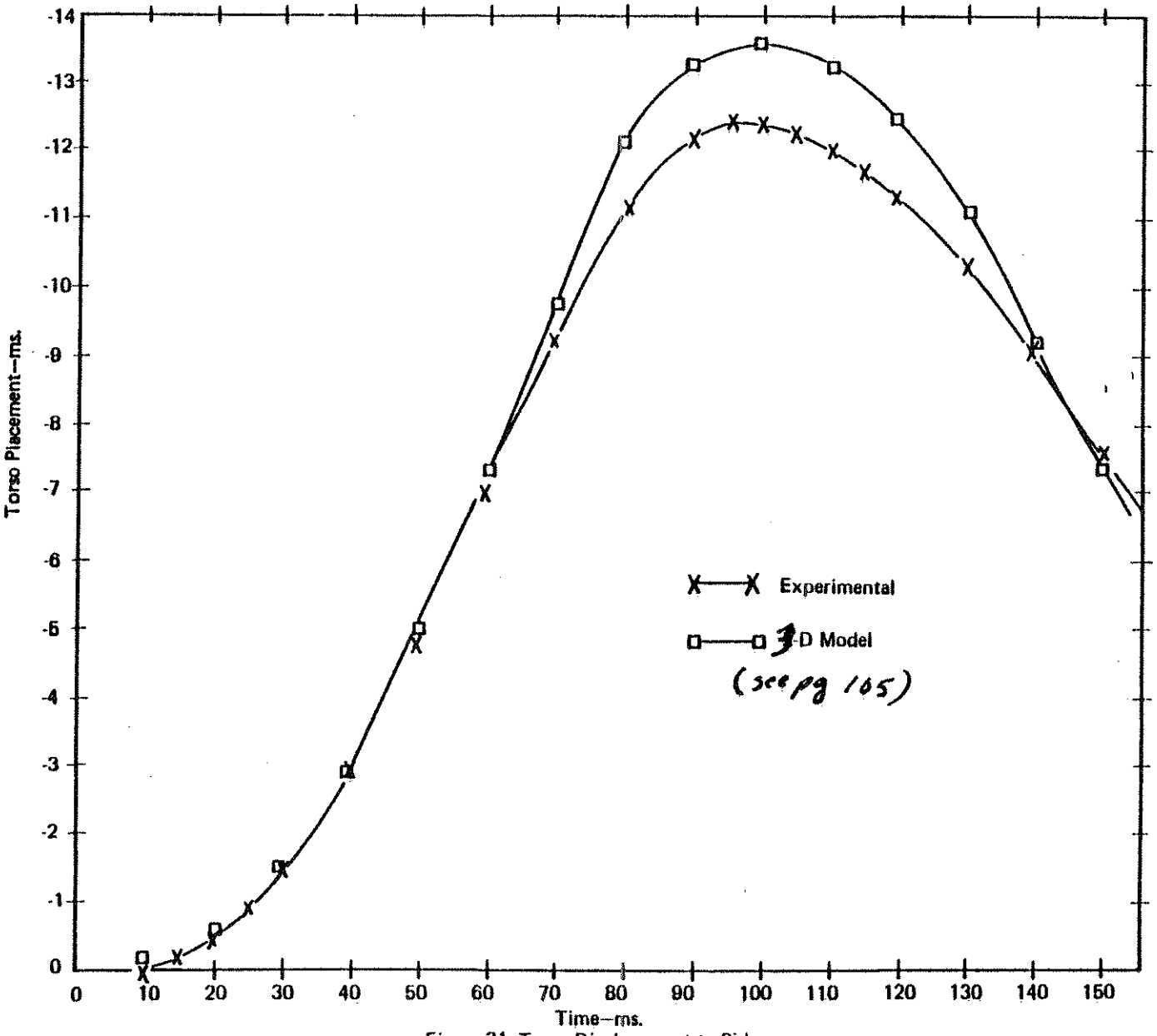

Figure 31. Torso Displacement to Side

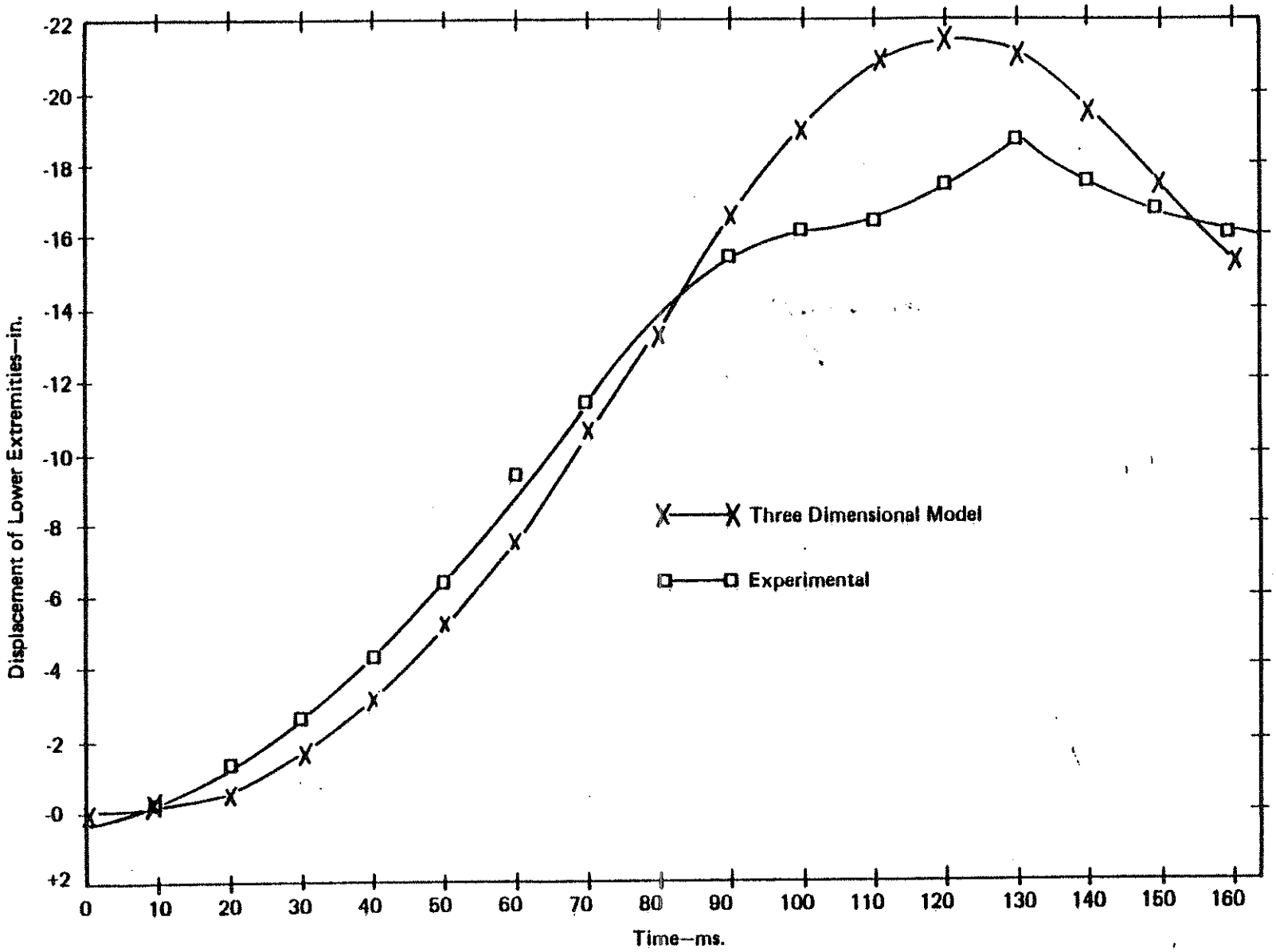

Figure 32. Displacement of Lower Extremities to Side

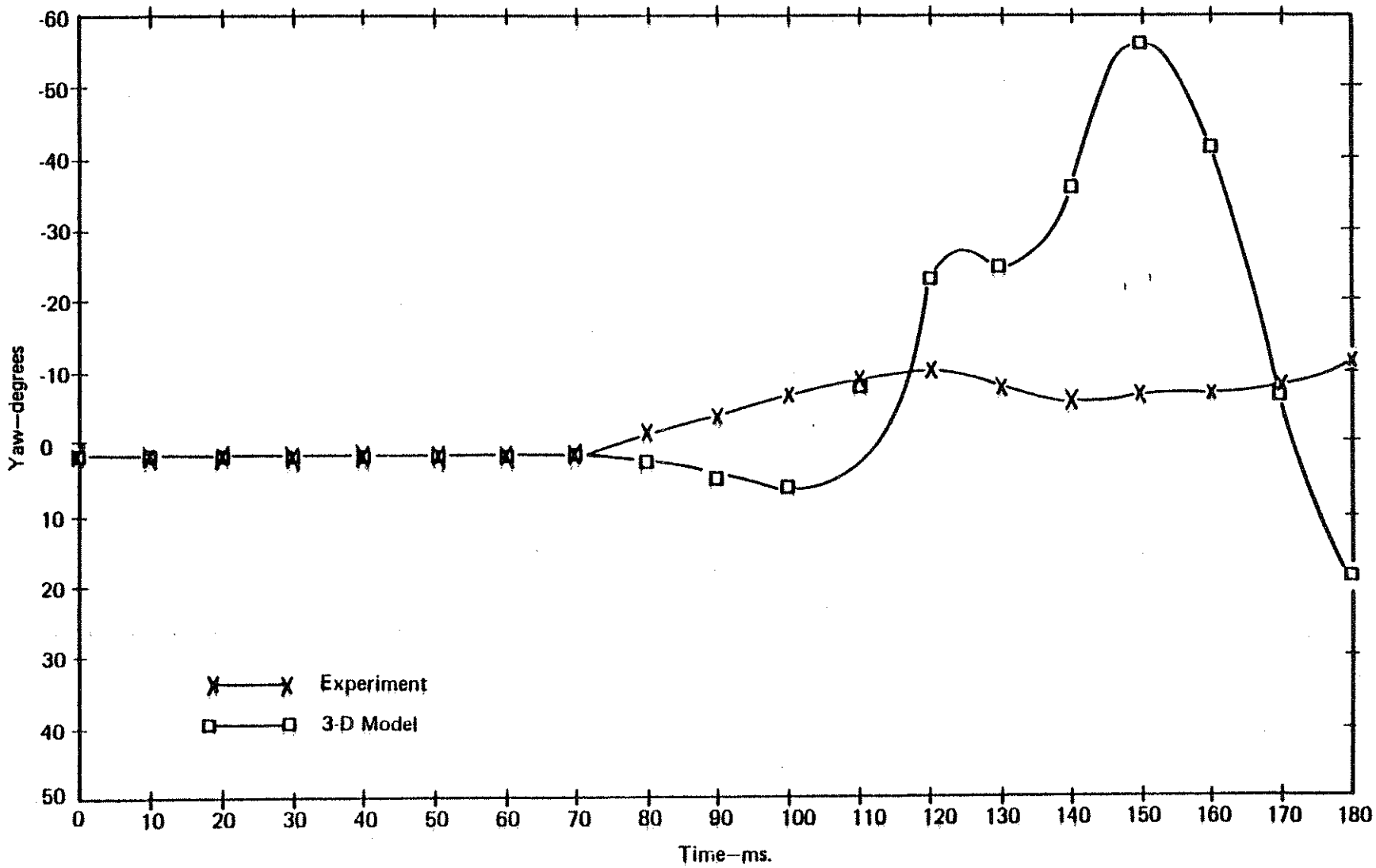

Figure 33. Head Yaw

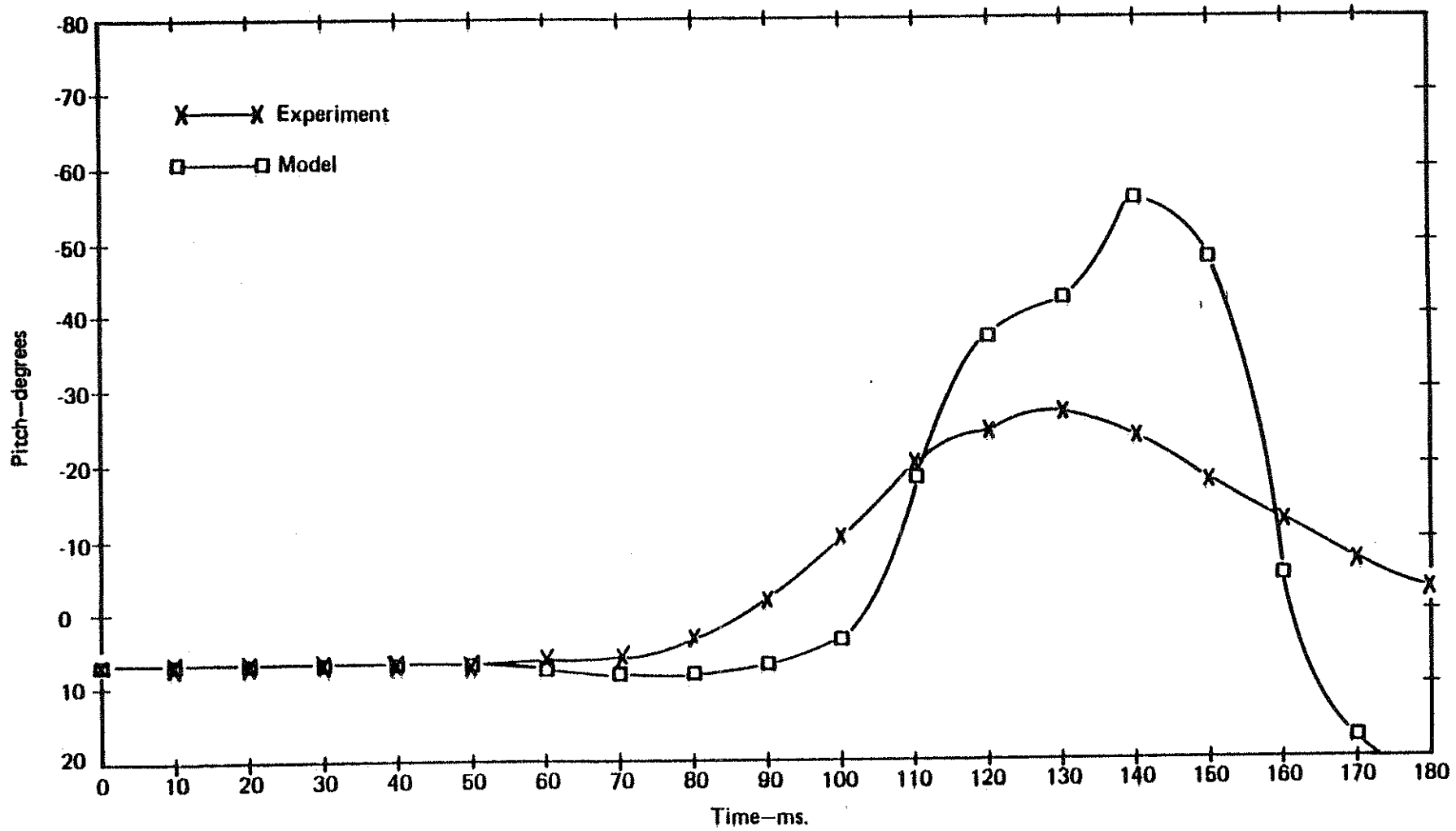

Figure 34. Head Pitch

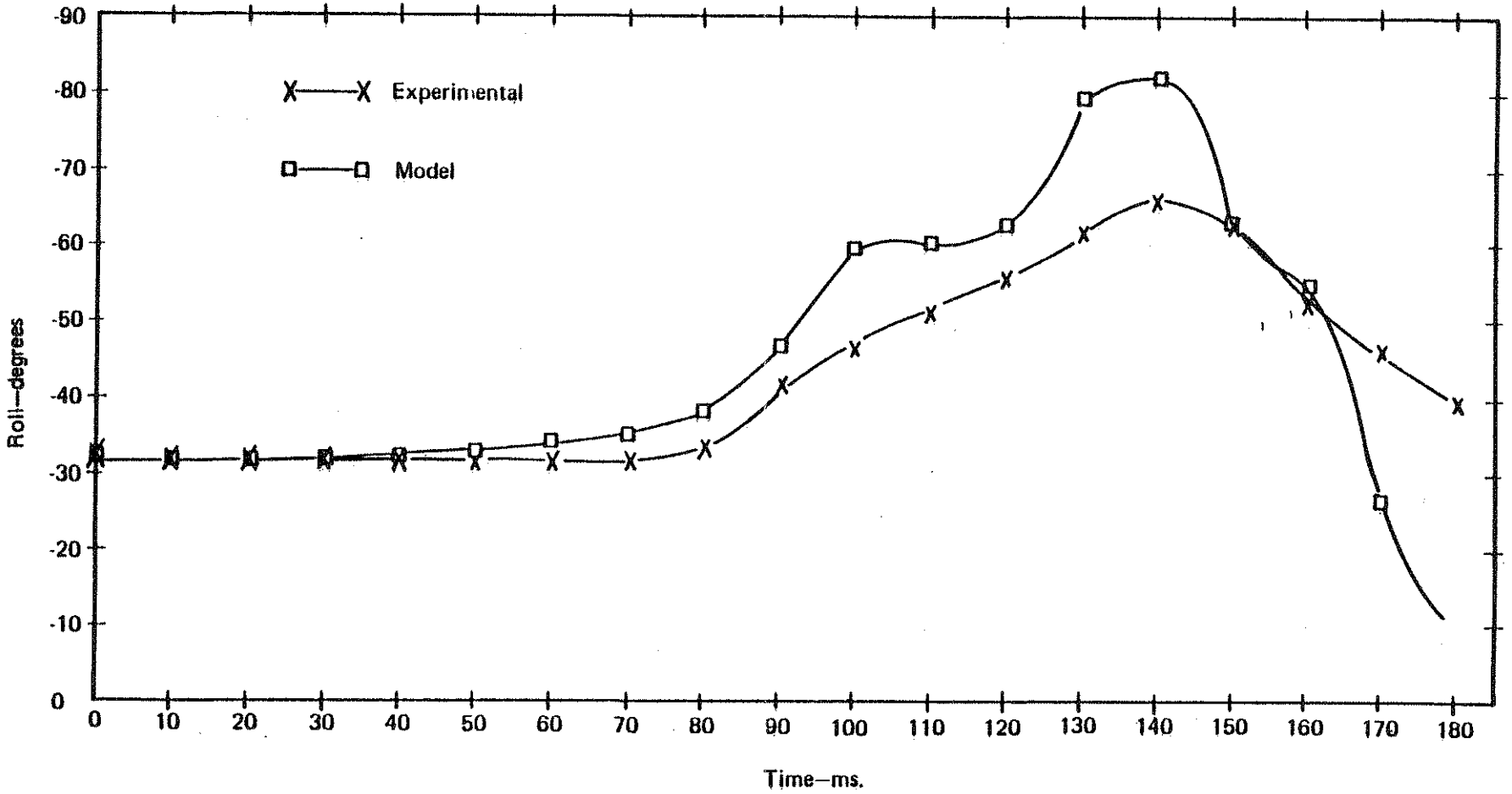

Figure 35. Head Roll

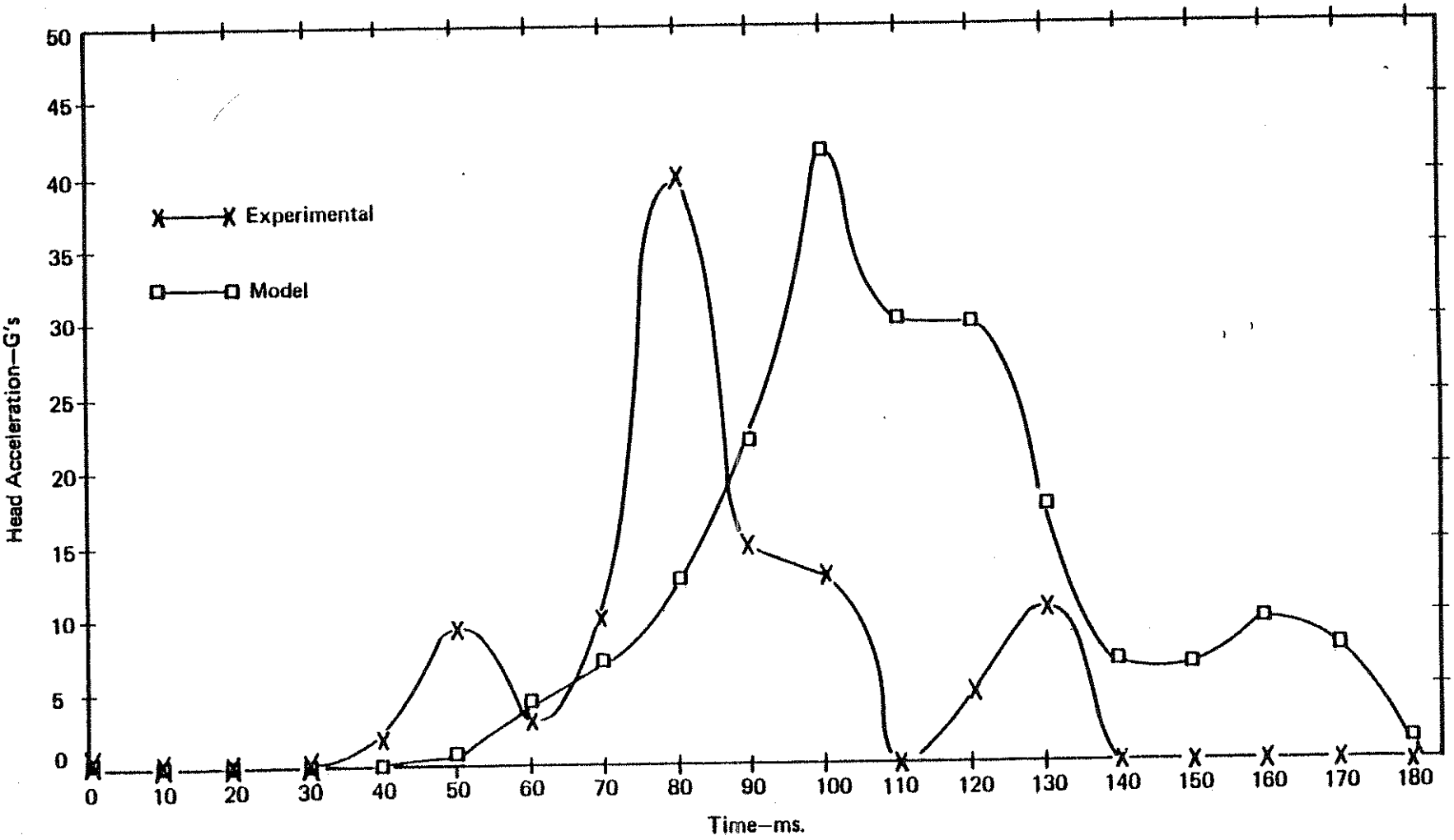

Figure 36. Lateral Head Acceleration

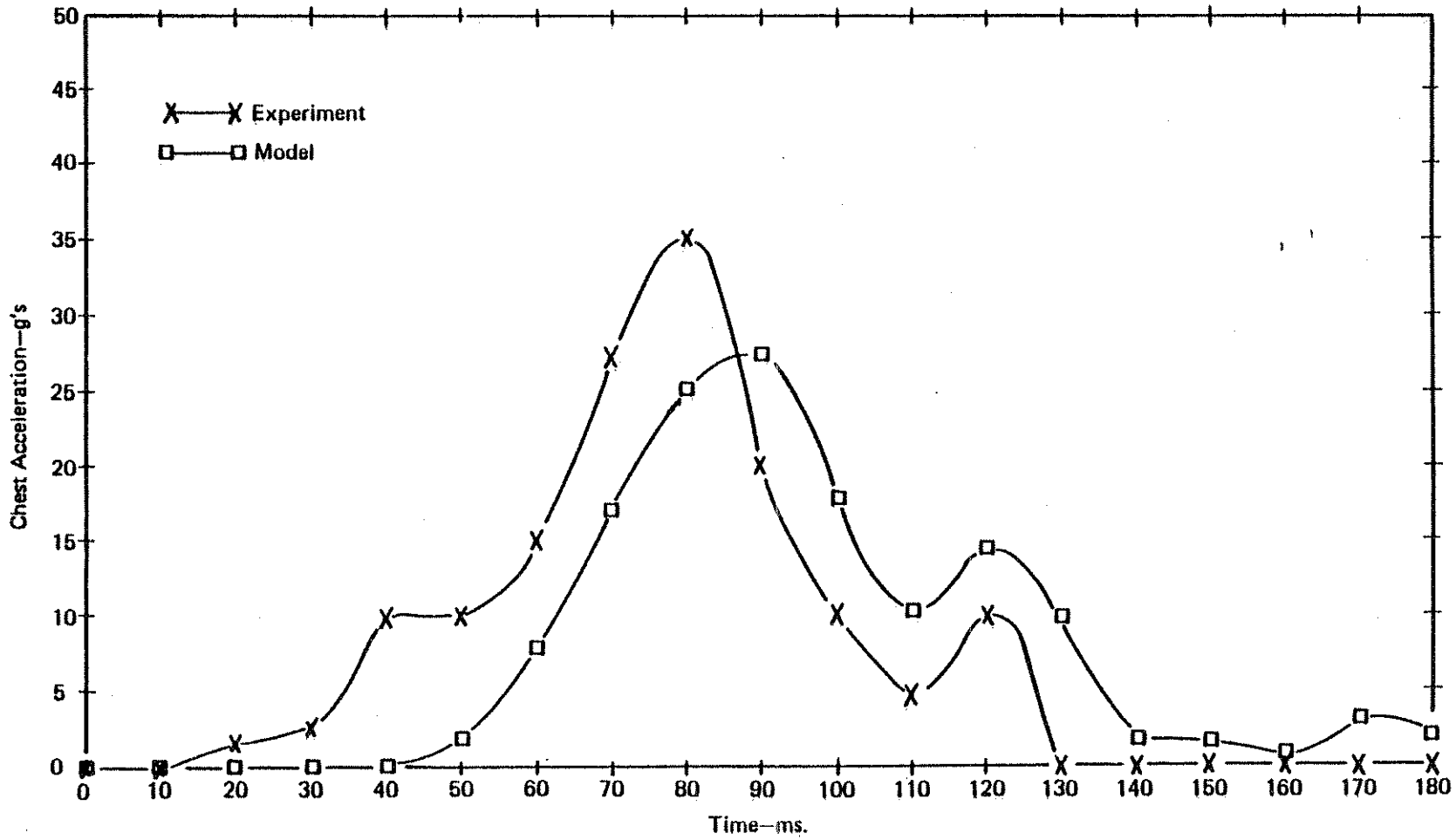

Figure 37. Lateral Torso Acceleration

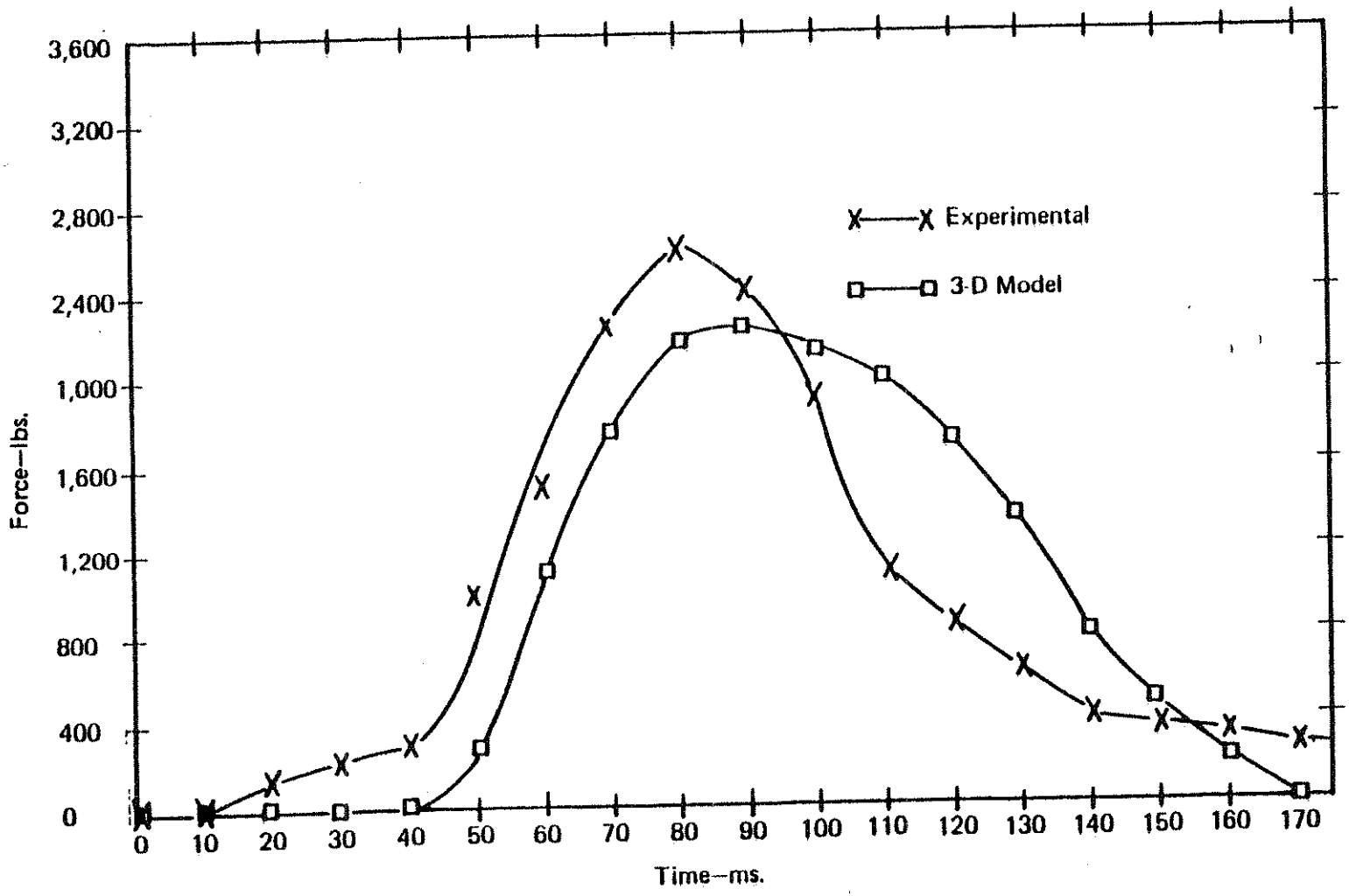

Figure 38. Sum of Seat Belt Loads

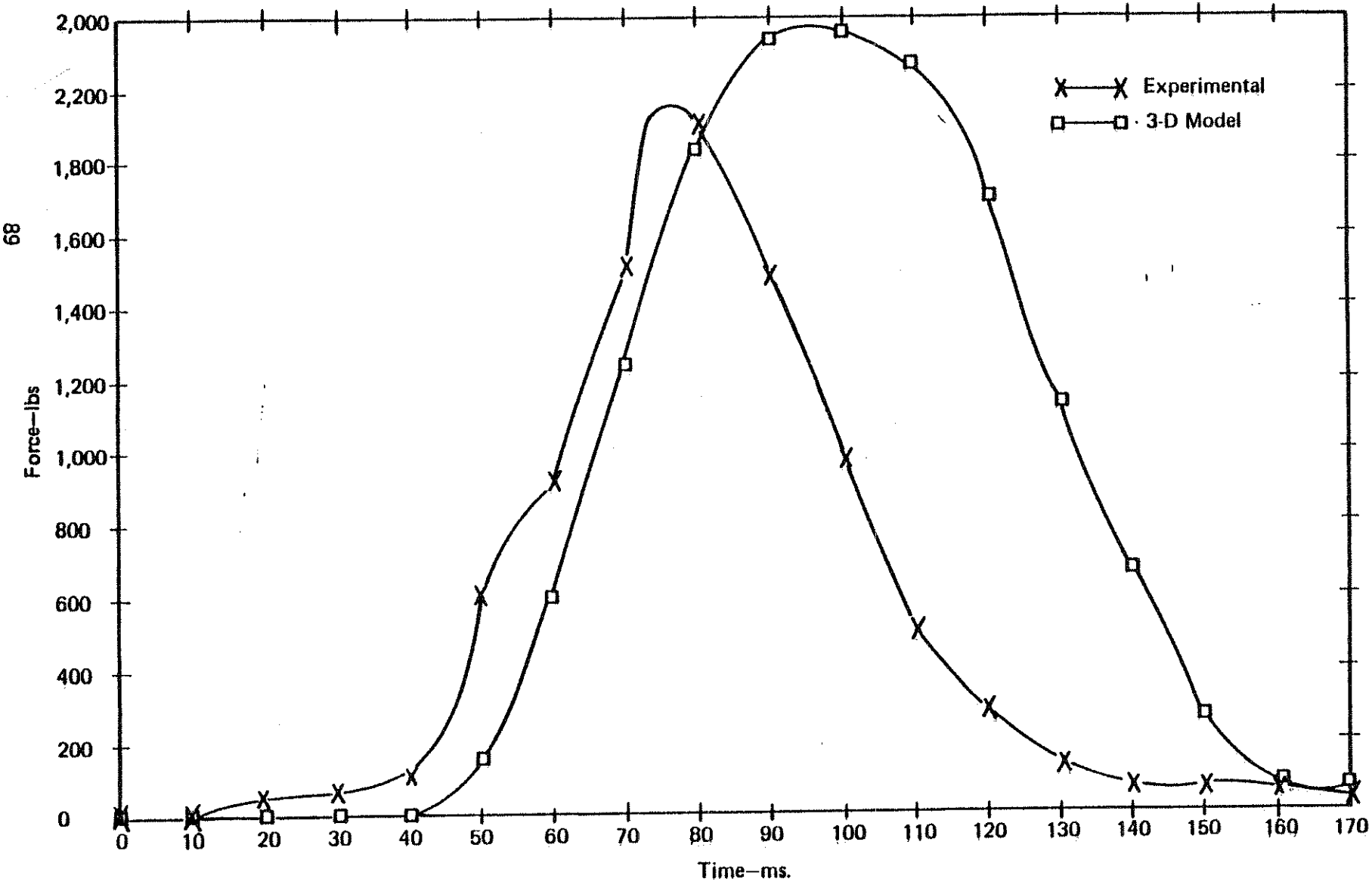

Figure 39. Sum of Shoulder Belt Loads

the HSRI 1130 digital computer using the appropriate trigonometric data handling subroutines.

In the lateral impact test, lateral motion of the three primary body elements was measured directly from the film. However, the pitch, roll and yaw of the head required use of special computer programs capable of processing Vanguard Analyzer data from two films simultaneously. This was necessary in that the views from two cameras are required to define the location of the three angles in space.

3.3 PREPARATION OF DATA SETS FOR THE COMPUTER SIMULATION

The preparation of data sets for the validation exercises of the model involved determination of the mass and inertial properties of the HSRI 50th percentile male Sierra dummy as well as the force-deformation interactions between the dummy and his seat and restraint system. Various other quantities such as the initial impact velocity, the sled deceleration profile, and the positioning of the dummy at the beginning of the deceleration event were determined directly from the test movies or transducer data.

The center of gravity of the various body parts was found by suspending the piece by wires and observing the location of intersecting lines of action. Moments of inertia for eight body parts were found by suspending each piece on a trifilar pendulum. The weights were measured on a precision scale. This data is tabulated in Table 2 and Figure 40. This information is felt to be accurate within 1% as repeated measurements were taken on the various quantities. A correction to the moments of inertia was made based on the weight and distribution of the body skin element.

In determining the moments of inertia for the three-dimensional model, the masses given in Table 2 were combined to describe a three-mass model consisting of head, torso, and lower extremities. The weights of the arms were combined with the torso and the weights of the lower legs with the lower

TABLE 2. WEIGHTS AND MOMENTS OF INERTIA OF HSRI 50th PERCENTILE SIERRA DUMMY (ABOUT LEFT-RIGHT BODY AXIS)

BODY SEGMENT	SEGMENT WEIGHT (lbs.)	SEGMENT MOMENT OF INERTIA (in.lb.sec^2)
right forearm and hand	5.094	0.300
left forearm and hand	5.187	0,309
right upper arm	5.938	0.241
left upper arm	5.656	0.233
lower spine	4.531	0.078
lower torso pelvic area	17.062	1.709
right upper leg	20.125	1.316
left upper leg	20.156	1.307
right lower leg and foot	9.781	1.211
left lower leg and foot	9.813	1.186
upper torso (including shoulder and chest mode, plastic "sub-skin" around rib cage and two lower neck vertebrae clamped tight).	37.438	1.344
head (including two upper neck vertebrae).	15.781	0.436

UPPER TORSO ASSEMBLY

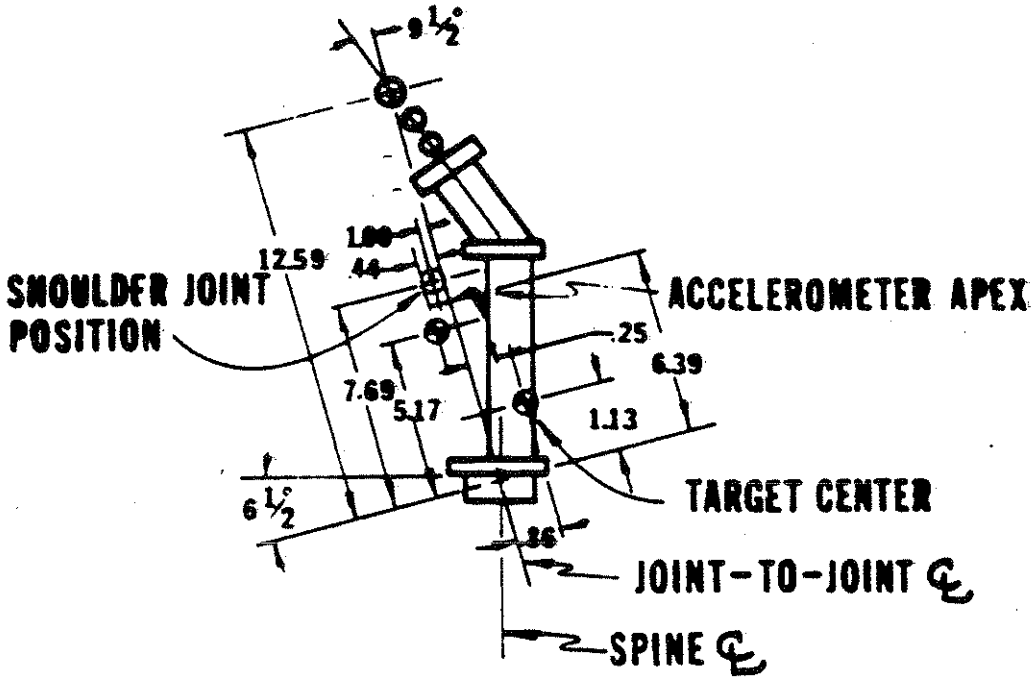

HEAD ASSEMBLY

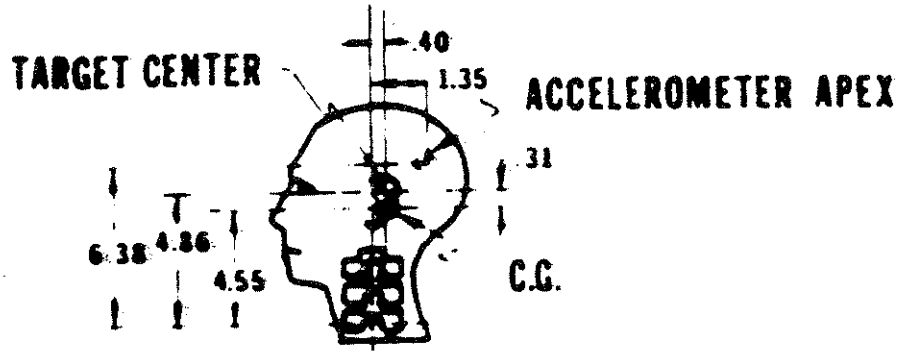

FIGURE 40. CENTERS OF GRAVITY OF BODY SEGMENTS OF HSRI 50TH PERCENTILE SIERRA DUMMY

FOREARM

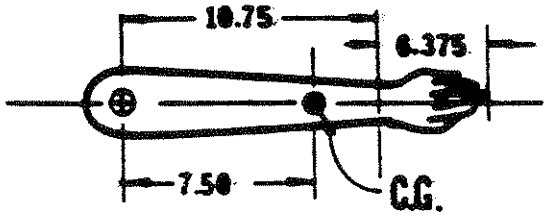

UPPER ARM

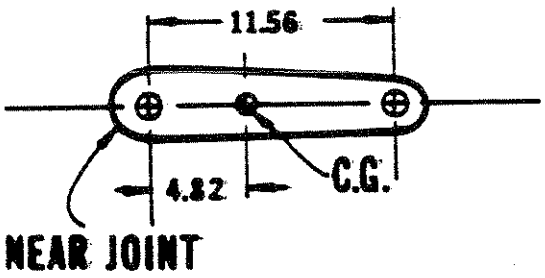

LOWER SPINE

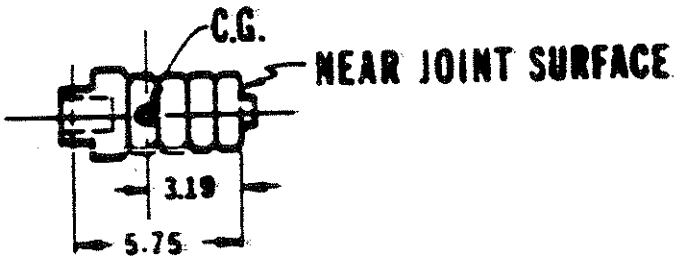

FIGURE 40 (Con.)

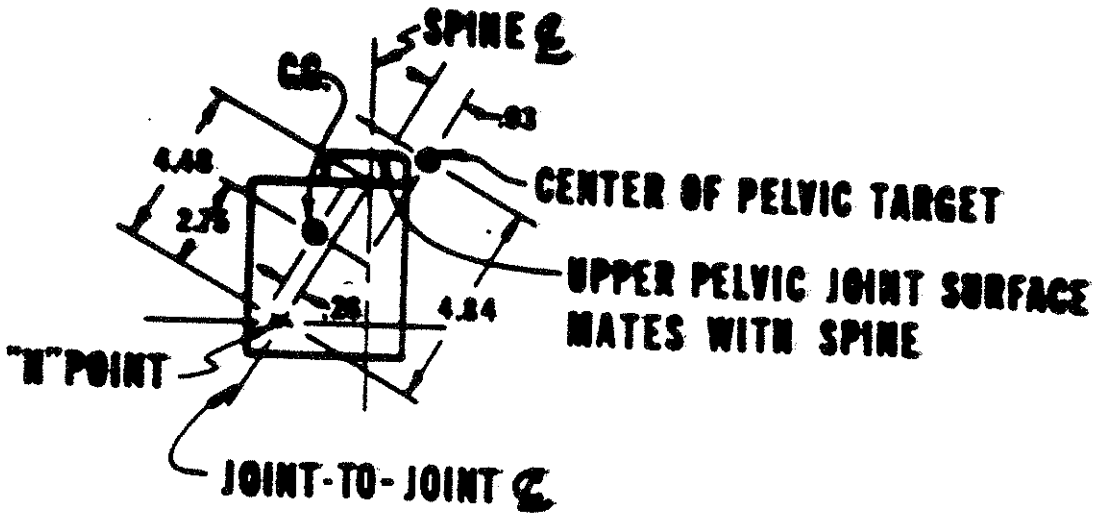

UPPER LEG

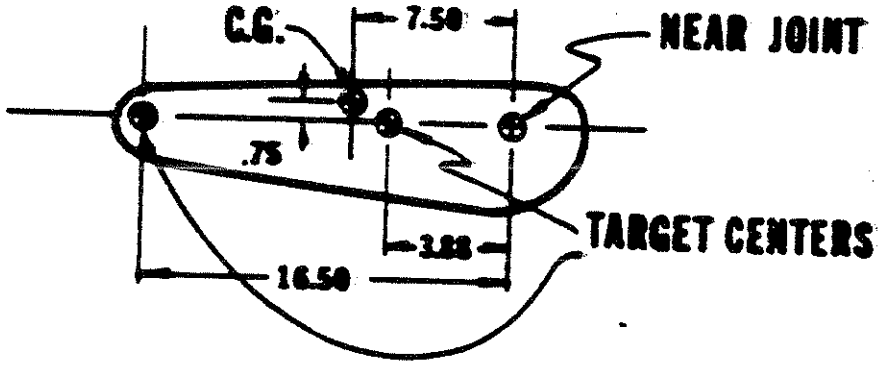

LOWER LEG

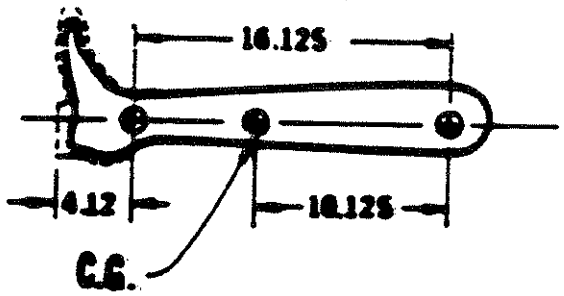

FIGURE 40. (Cont'd.)

extremities. The head was simulated by an ellipsoid and the torso and lower extremities by elliptical cylinders. Front and side views of the resulting composite are shown in Figure 41. The dimensions shown in this figure result from a series of anthropometric measurements taken on the dummy including seated height, seated cervical height, head length, head breadth, chest breadth, maximum chest thickness, buttock-knee length, seated hip breadth, seated knee breadth, and thigh-thickness. A tabulation of the resulting moments of inertia is shown in Table 3. It should be noted that the composite moments of inertia about the y-axis, when computed by this technique, agreed with the values measured and listed in Table 2 with 1%.

Because no data in a form suitable for use as input data to the computer program is available on the load-deformation properties of seats, two static tests were carried out. The test configurations are shown in Figure 42 and the results in Figures 43 and 44. In determining the curve for load-deflection under the buttocks, the deflection was measured by taking height readings "h" at points on the pelvis as shown, as weight was added. For determining the load-deflection curve at the front of the seat, the dummy was hung as shown with the legs up, knees locked, and the buttocks just touching the cushion. The hip joint was loose. The legs were lowered gradually, and load scale readings were taken at progressive points until the scale read zero. At this time the seat front is supporting the legs. Weights were then added until the seat front bottomed out of the seat frame. This test has the disadvantages of being static and only applying the load over part of the seat. However, it does have the advantage of determining a curve which includes deformation properties of both the seat and dummy used in the test.

Another quantity leading to difficulties in measurement was the seat belt load-deflection characteristic. In this case, deformation properties of the belt, buckles, vehicle attachment points, and of the dummy itself must be reflected in the modulus which is used in the model.

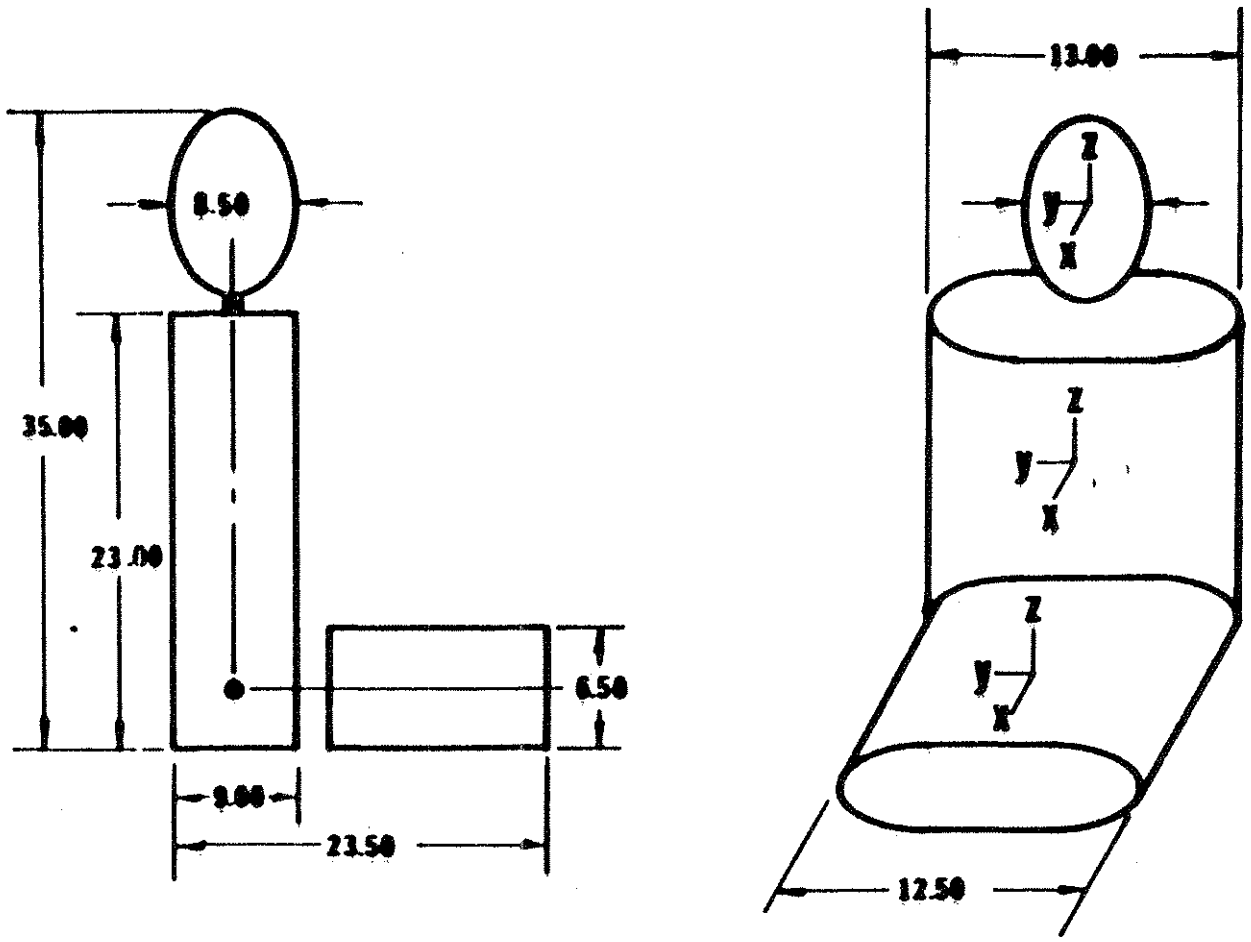

Figure 41. Distribution of Body Mass for Three-Dimensional Model Validation.

BUTTOCK DEFLECTION

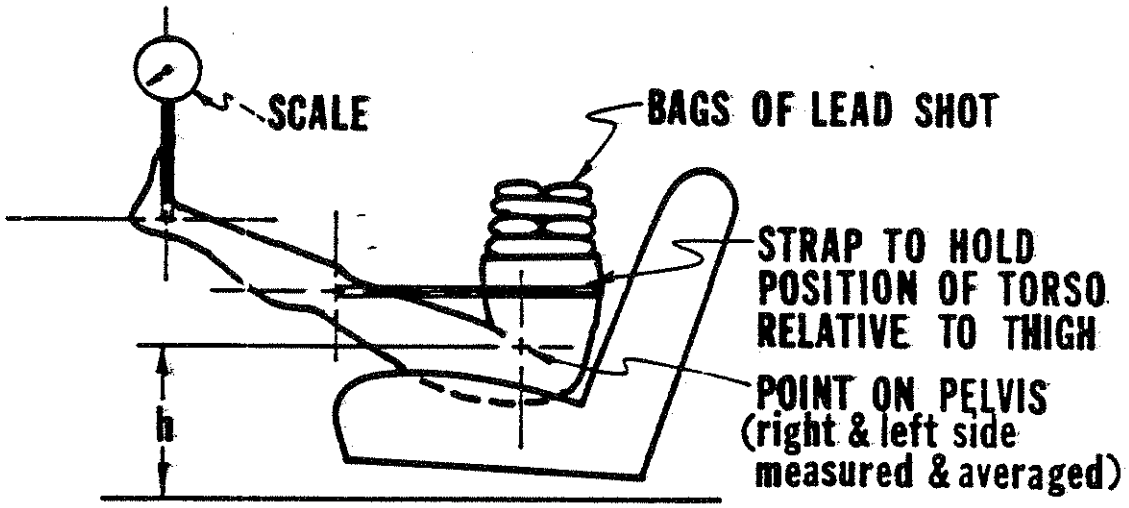

SEAT FRONT DEFLECTION

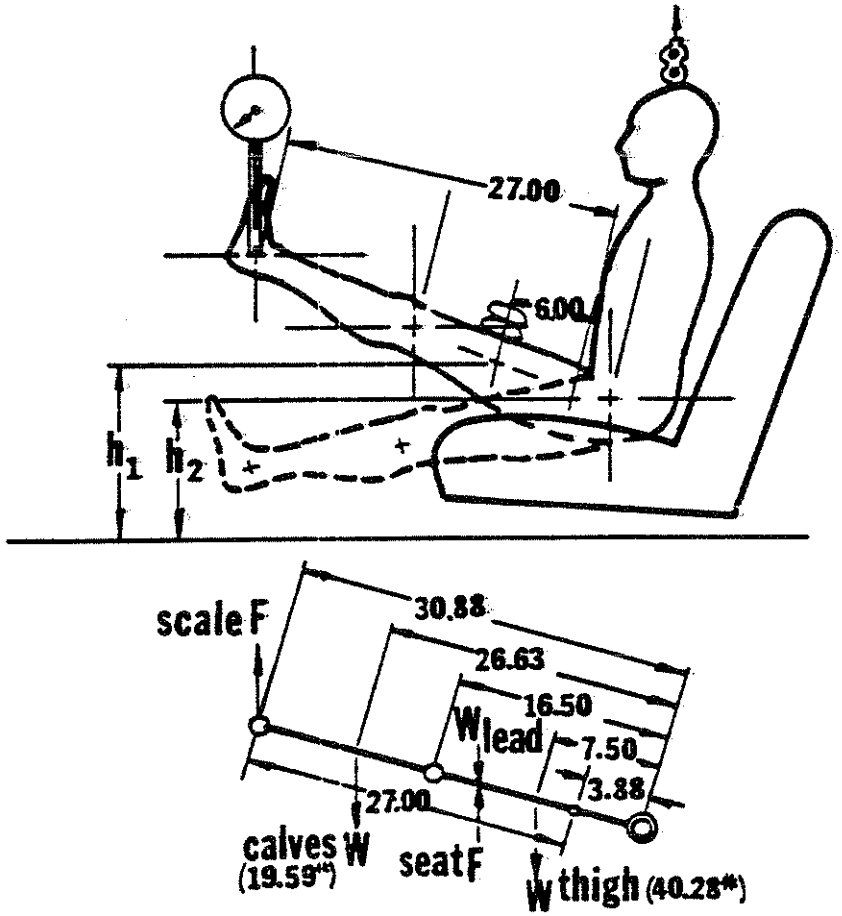

FIGURE 42. TEST CONFIGURATION FOR SEAT PROPERTY TESTS

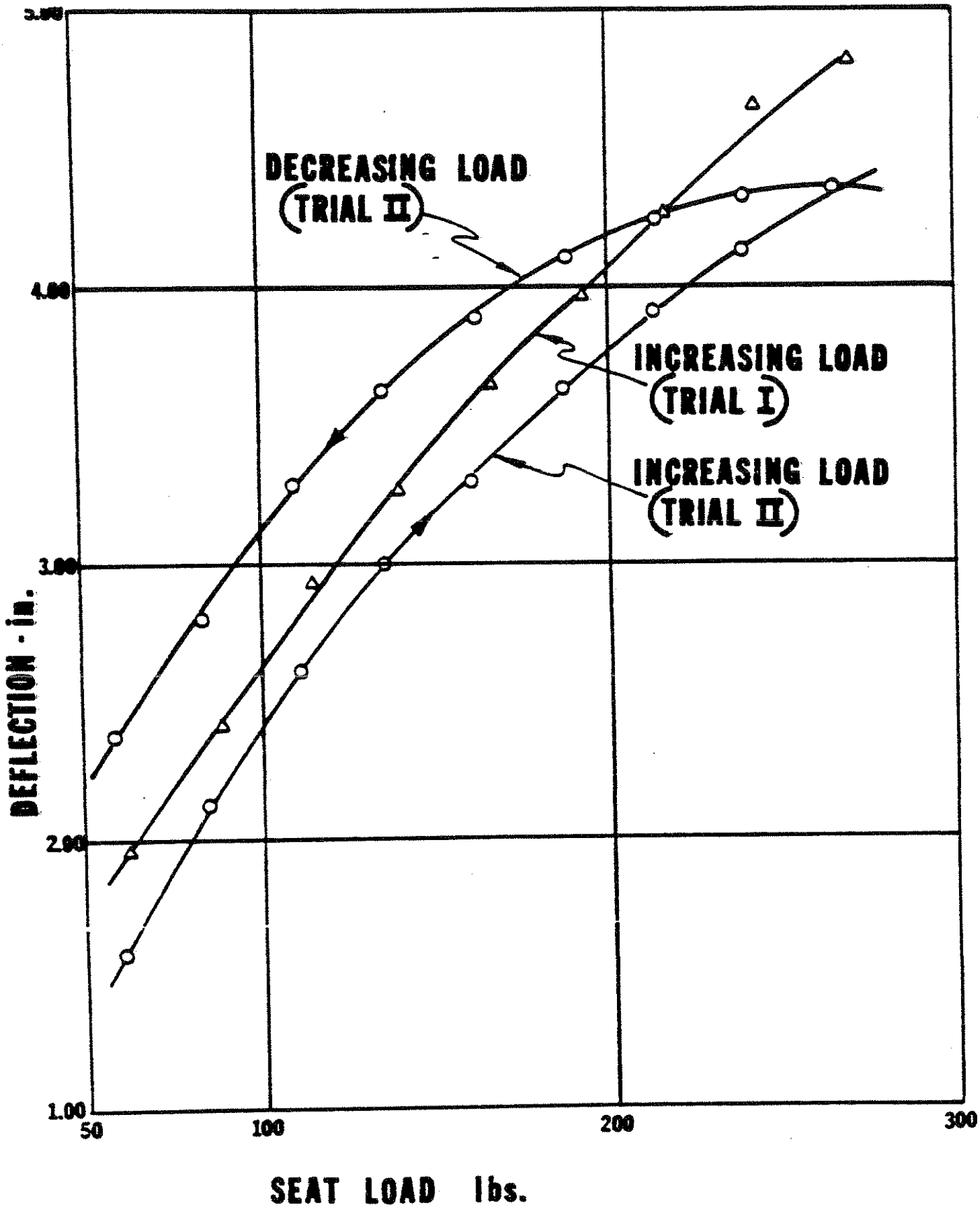

FIGURE 43. SEAT LOAD-DEFLECTION CHARACTERISTICS

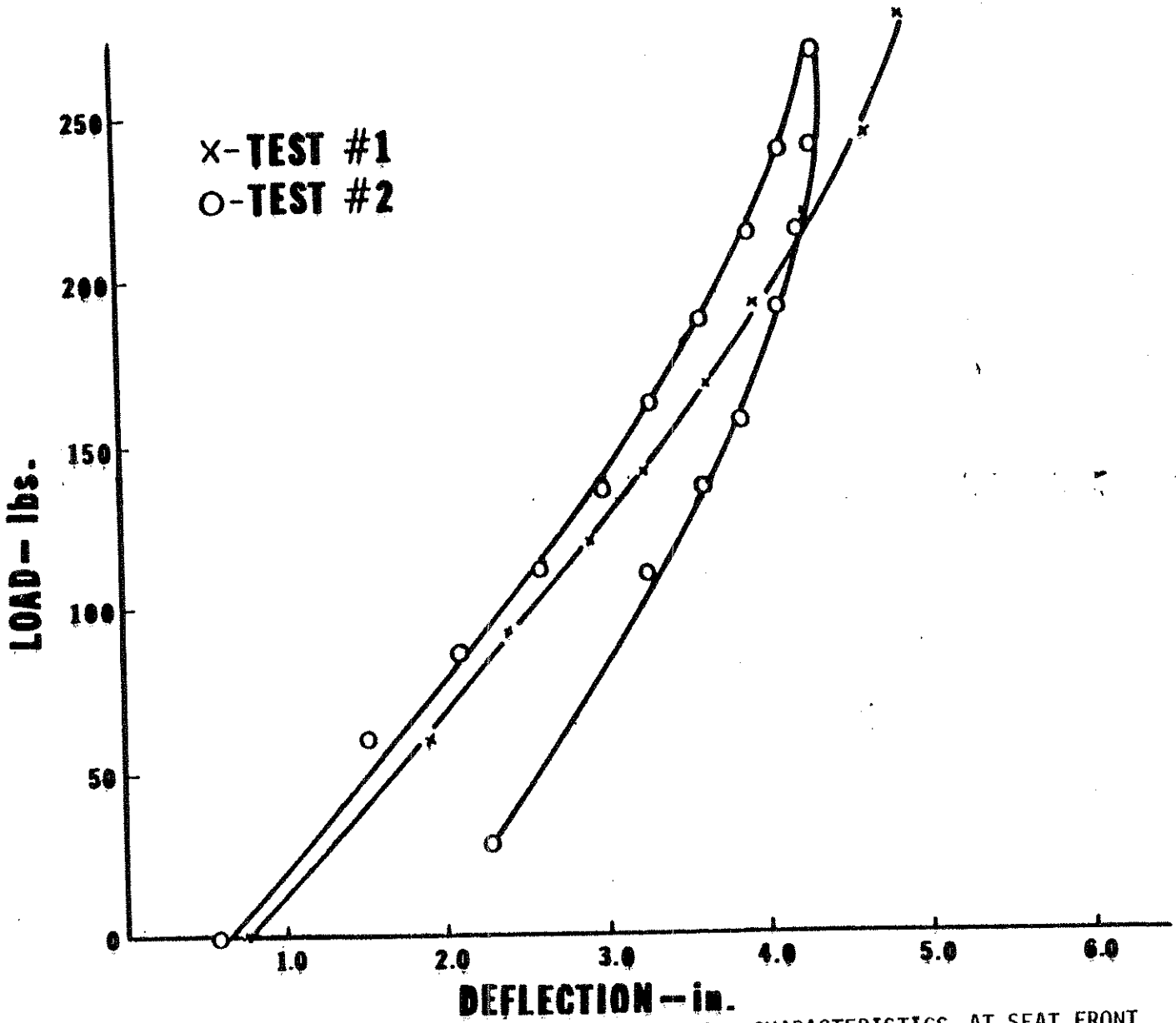

FIGURE 44. SEAT LOAD-DEFLECTION CHARACTERISTICS AT SEAT FRONT

TABLE 3. MOMENTS OF INERTIA FOR THREE-DIMENSIONAL MODEL

BODY SEGMENT	SEGMENT WEIGHT-LBS.	Ix-in.lb.sec^2	Iy-in.lb.sec^2	Iz-in.lb.sec^2
head	15.781	.3672	.442	.221
torso	90.46	12.78	11.5	3.65
lower extremities	50.33	3.54	2.59	1.572

156.571

Thus, the load-deformation characteristics of the seat belts were measured by making use of data gathered during the test itself. Force transducers were used to record the loads in the belts and the high speed movies recorded a view of the action of the belts. It was thus possible, using the known location of the H-point, the belt angle, and the location of the belt attachment point in the vehicle, to construct a table of the seat-belt length as a function of time. This, when combined with the data from the load cells, was used to construct Figure 45. The deformation characteristics for the shoulder harness elements were determined in a similar manner by measuring the deformation from the high speed movies and loads from the force transducers.

3.4 COMPARISONS OF THE PREDICTIONS OF THE HSRI MATHEMATICAL MODELS FOR A FRONT IMPACT TEST

Figures 20-28 show the predictions of both the two- and three-dimensional mathematical models and the results of a frontal impact simulation involving a 50th percentile male dummy restrained by lap belt and single diagonal shoulder harness. Compared are loading forces and accelerations applied to the dummy and the resulting motions.

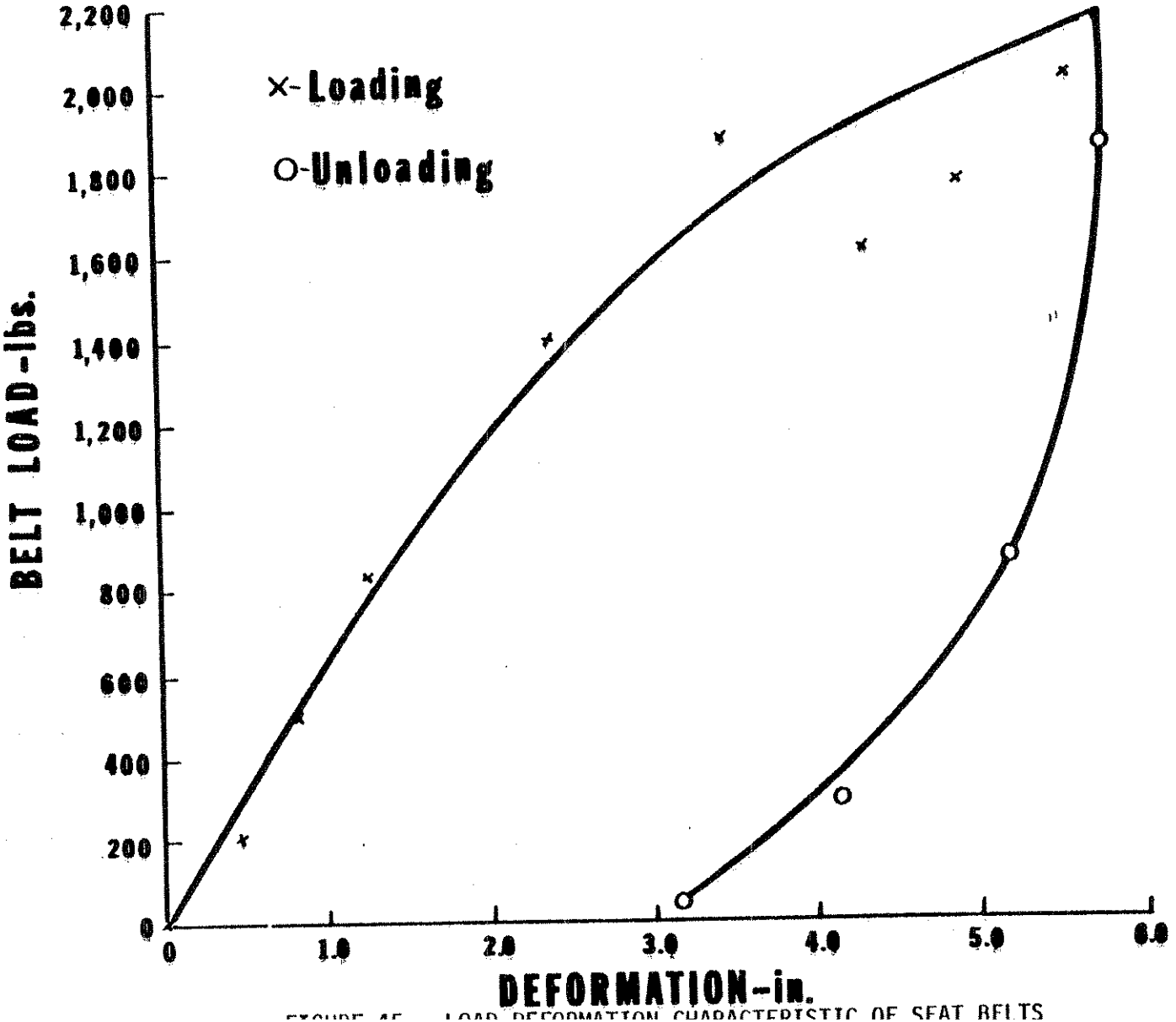

FIGURE 45 LOAD DEFORMATION CHARACTERISTIC OF SEAT BELTS

Figure 21 shows the resultant chest linear accelerations in G's. Agreement between all three curves is remarkably good both in respect to phase and peak G-values. In addition, all three curves show interaction with the seat back during rebound. The predictions of the two-dimensional model are limited to a resultant computed in the forward and vertical plane. However, this does not affect the performance of the model to any great extent as all nonplanar torso accelerations are either measured or predicted by the three-dimensional model to be less than 10 G's.

The agreement between test and analysis as shown in Figure 22 is not as good for resultant head accelerations. Both the two- and three-dimensional models predict an acceleration spike as the head pitches forward to interact with the angular stop located at the neck joint. The three-dimensional model predicts the highest value. In addition, this peak leads the one predicted by the two-dimensional model and the value measured in the test in phase, reflecting the increasing stiffness of the dynamic system as the number of masses are reduced.

Figures 23 and 24 show the comparative seat belt and shoulder harness loads. There is general agreement among the three curves on each graph both in phase and in magnitude. The predictions of both the two- and three-dimensional models are within approximately 15% of the peak values measured in the test.

The forward motion of the H-point and of the head center of gravity is shown in Figures 25 and 26, respectively. Both graphs have similar properties. In each case, rebound from the belts is slowest in the test and fastest in the three-dimensional model. In addition to this, the largest degree of forward motion is observed in the test, whereas the smallest amount of motion occurs for the three-dimensional model. This again reflects the increasing stiffness

of models possessing decreasing numbers of mass elements and is to be expected. The percentage difference between predicted motions and those observed during the tests is approximately 10% with the exception of head forward motion predicted by the three-dimensional model. The error in this case is approximately 36%, indicating again that head motion is limited by the lack of flexibility of the model. This could be a problem in simulations where it is desired to sense contact with vehicle interior elements. However, it is rather easy to compensate for this by sufficiently increasing the size of the head contact-sensing ellipsoid to cancel the error.

The pitch angle of the head is plotted in Figure 27. Both the two- and three-dimensional models predict a peak value which differs from the test value by approximately 32%. It is felt at this time that the greater flexibility of the dummy neck leads to this error in both cases. This phenomenon can be compensated for by increasing the joint stop angles from the values measured in the test, thus providing greater "flexibility."

The final quantity which has been studied is the pitch angle of the upper leg which is shown in Figure 28. A substantial error in magnitude exists between the curve based on the three-dimensional model and the other two curves. A primary reason for the increase of this pitch angle is the force applied at the knee due to the interaction of the foot with the vehicle toeboard. The error in the prediction of the three-dimensional model exists because a contact ellipsoid was not attached to the lower extremity mass to represent the effect of the lower leg. Adding this contact will correct the problem.

3.5 COMPARISON OF THE PREDICTIONS OF THE THREE-DIMENSIONAL MODEL WITH A SIDE IMPACT SLED TEST

Figures 29-39 show predictions of the three-dimensional model and compare them with a side impact sled test involving a 50th percentile male dummy

restrained by a lap belt and single diagonal shoulder harness. Compared are the force, acceleration and motions which are experienced by the dummy.

The seat is modeled by two contact surfaces corresponding to the seat pan and seat back. The corners of these surfaces are specified on the basis of measurements taken of the front two corners of the seat cushion, the ends of the junction between seat cushion and seat back, and the upper two corners of the seat back. The two surfaces extend beyond their junction - the seat back below the seat cushion and the seat cushion behind the seat back. This is done because the belts tend to pull the occupant into the region of this surface junction. It is not desired to have one of the contact sensing ellipsoids slip off the end of the contact surfaces describing the seat. The force-deformation characteristics are assumed to be the same as those used in the front impact simulation.

The belts are defined in terms of two sets of attachment points. Four belt elements are used representing upper and lower shoulder harnesses and left as well as right lap belt segments. The four attachment points on the sled are located easily by direct measurement. The four attachment points on the body are assumed to be those points on the occupant where the belt element first makes contact. They were measured when the dummy was sitting on the sled in the pre-test configuration.

During the test it was observed that the dummy initially slid to the side under the belts about four inches before slack was absorbed. On this basis the model was exercised twice to simulate this test. For the first 40 ms, the dummy was allowed to slide freely to the side on the seat surface until belt slippage was absorbed. At 40 ms, the model was restarted with no slack in the belt elements. This effectively modeled a situation involving slipping belts

although it is a rather awkward and time-consuming procedure. The force-deformation characteristics of the belts (initially assumed to be the same as for the front sled test on the basis that the belts interact with the same structures in the dummy in both tests) were modified to reflect the change in length of the various belt segments. For example, as the dummy slides to the left on the cushion, the right element of the lap belt becomes longer. During the load-carrying phase of the simulation, the left element is stiffer than the right element.

In order to represent body contacts with the seat cushion and seat back, a series of contact sensing spheres were attached to the torso element at strategic locations. After several trials it was found that the key locations were left shoulder, right shoulder, left buttock, and right buttock. This combination has been used successfully in many additional seat and restraint system studies.

The displacement to the side of the three basic elements-head, torso, and lower extremities - is shown in Figures 30-32. In all cases the agreement between theory and test is quite good (less than 10%). The peak values for displacement are in phase in the two cases.

In order to determine the ability of the model to predict orientation in space it was necessary to devise techniques for measuring these quantities photometrically. This was accomplished for the head of the dummy and the results are given in Figures 33-35. Agreement between the predicted and measured values of these quantities is not nearly as good as for the linear motions. However, the reasons for this are fairly clear.

The first possible reason involves a comparison between the mathematical model and human anatomy. In this model and all others which have been developed up to the present time, the mass of the head and neck are assumed to be distributed symmetrically about a line passing through the head-neck joint and

the center of gravity of the head. In reality, this mass is not symmetric about the line of rotation. Although this assumption leads to a major simplification in the equations of motions, it appears to lead to a significant error in the ability of the model to predict head yaw. Whether the performance of the model can be improved by a proper selection of the initial positioning of the occupant and the location of the motion stops is not known at this time.

In all three rotational motions, the predicted values are higher than the measured values. The best agreement is for roll motion (30%). The second possible reason for disagreement involves the selection of joint stops. In anthropometric studies involving human subjects and dummies the limits of voluntary motion (or location of motion-limiting stops) are made on the basis of a single required pitch, roll, or yaw movement. The joint stop locations used in the present exercises of the model used these values. However, it is unknown where stops are located when a combination of the three possible motions are allowed. For example, it is expected in a side impact test that the predominant rotational motion would be roll. The expected roll does occur and agreement between prediction and experiment is fairly good. When the roll stop is on, it can be shown that the limit stops for pitch and yaw are decreased. Thus, the values used in the computer simulation are probably too large and admit the excessive predicted values. Because no known data has been gathered for combinations of rotations, this seemed to be the only logical course.

There are two methods for correcting this problem. The first is a "quick-fix" and involves choosing smaller values for yaw and pitch stops to decrease the predicted motions. The second (and preferred) solution involves a determination of the actual range of motion for the neck joint structure based on a research study of all possible motion combinations. The results of that study would be a recommendation for improving the input data to be used with the model or for possibly altering the mathematical formulation.

The head and chest lateral accelerations are shown in Figures 36 and 37. In the case of the head acceleration, the first peak observed in the prediction of the model occurs at the same time as the motion to the side is arrested and corresponds within 5% of the peak value measured during the test. It should be noted that this value lags the physical event by nearly 20 milliseconds, approximately the same phase shift which was caused by the initial loadings to the torso produced by the belts. The second peak on both traces occurs when the head interacts with the seat back. For the torso, the test value is observed to be 25% higher than the predicted value.

The final two comparisons between theory and test are the belt loadings shown in Figures 38 and 39. The predicted seat belt peak loop loading is low by 10% and the predicted shoulder harness peak loop loading is high by approximately the same amount providing good agreement between theory and test.

4.0 USER'S GUIDE TO THE HSRI THREE-DIMENSIONAL CRASH VICTIM SIMULATOR

The user's guide commences with a detailed description of the input data for the model. This is followed by discussion of normal program output, optional program output, and program error messages.

Methods for running the model from a teletype and obtaining information from the model through that device are treated before the integration techniques employed in the model are presented.

Part 4 concludes with sections describing the physical layout of the program both from a functional and from a procedural point of view.

4.1 DESCRIPTION OF PROGRAM INPUT DATA

Input to the HSRI Three-Dimensional Crash Victim Simulator consists of series of eighty character lines which will be called cards. Almost all of the input cards have a common format which is shown in Table 4.

TABLE 4. THE STANDARD INPUT CARD FORMAT

Field	Card Columns	Description
ID	1	A letter, A through Z, which acts to identify the information being specified on this card.
1	2 - 10	Numeric data in floating point format. The decimal point must be explicitly included except for right-adjusted integers. "D-format" is permissible but must be right-adjusted. Normally left-adjusted "F-format" is used for convenience.
2	11 - 20	Numeric data
3	21 - 30	Numeric data
4	31 - 40	Numeric data

(Table 4. Continued)

Field	Card Columns	Description
5	41 - 50	Numeric data
6	51 - 60	Numeric data
7	61 - 70	Numeric data
8	71 - 80	Numeric data

Seven of the standard input cards trigger special reading sequences for special information which would not easily fit the standard format. These special reading sequences are summarized in Table 5 and presented in detail in Table 7.

TABLE 5. SPECIAL READING SEQUENCES

Standard Card Which Triggers This Sequence	Length of Sequence	Termination of Sequence	Description of Information Contained
B	Fixed length.	Card count of one.	Alpha-numeric title for ellipsoid.
J	Variable length consisting of one card plus one card for each time point.	Card count of (J-card, field two) plus one.	Alpha-numeric title for contact plus corner positions.
L	Switch controlled initiation of sequence. Only if (L-card, field 8) is non-zero.	Card count of one.	Saturation maximum force and unloading slope.
P	Variable length.	Continues to read until a negative time on special card is encountered.	Table of debug code words versus effective times.
S	Fixed length.	Card count of one.	Integration weights.

(Continued on next page)

(Table 5. Continued)

Standard Card Which Triggers This Sequence	Length of Sequence	Termination of Sequence	Description of Deformation Contained
V	Fixed length.	Card count of one.	Alpha-numeric run title.
Y	Fixed length.	Card count of one.	Alpha-numeric event names.

Table 6 contains a typical complete data set for the model. The numbers at the left are line numbers. In line one, the letter "A" represents the position of column one and so on. Note the special reading sequences beginning at lines 5, 7, 9, 11, 13, 15, 26, 29, 32, 35, 38, 41, 45, 47, 49, 77, 83, 87, and 87.6. Note also the omission of the special sequence after line 50. Table 7 contains a detailed explanation of each card type together with all the special reading sequences. The reader is urged to use Table 7 to decode the run specification contained in the data set presented in Table 6 and then check his impressions against Table 9 in Section 4.2 which contains the program's printed summary of what it understood from this same data set. Table 8 summarizes Table 7 in a more usable form.

Order of cards is irrelevant except that the Z-card must always be last and special reading sequences must be together and in proper order. When the program finishes operation using a first data deck, it will look for a second. If it finds more data, it will continue; otherwise, it will sign off. On a second data deck, generally only those cards which contain changes from the first data deck need be specified. Part or all of acceleration tables previously used may be removed by use of the O-card and new N-cards can be read after the O-card to make additions. Calculation of inertial initial conditions is not repeated unless specifically requested (see card T, field 5) but the established initial conditions will persist. The Z-card must be present. The program will continue to look for data sets until it encounters the end of all data.

```
1    A1.       .234        12.78      11.5      3.65       8.375      11.5
2    A2.       .0408       .3672      .442      .221       6.         6.
3    A3.       .13         1.572      2.59      3.54       7.25       11.75
4    B1.       1.          0.         0.        -7.1       4.6        8.5        4.6
5                    CHEST
6    B5.       1.          0.         5.3       0.         4.5        3.5        10.8
7                    RIGHT SIDE
8    B6.       1.          0.         -5.3      0.         4.5        3.5        10.8
9                    LEFT SIDE
10   B2.       1.          0.         0.        7.1        4.6        8.5        4.6
11                   HIP
12   B3.       3.          0.         0.        0.         3.         7.         3.
13                   KNEE
14   B4.       2.          0.         0.        0.         4.25       3.         6.
15                   HEAD
16   C1.       600.        110000.    60.       600.       110000.    50.        2.
17   C2.       800.        110000.    45.       800.       110000.    30.        2.
18   D1.       600.        150000.    70.       150000.   70.         2.         2.
19   D2.       800.        150000.    45.       150000.   35.         2.         2.
20   E19.4     0.          0.         0.        18.        0.         0.         0.
21   F20.      0.          0.         0.        0.         0.         -15.       0.
22   G0.       0.          0.         0.        7.         0.         0.         0.
23   H0.       536.1       0.         0.        0.         0.
24   I0.       0.          0.         0.        0.         0.
25   J1.       1.          -1.        37.21     5.31       1.57       1.         15.
26   BACK SEAT             .455
27   0.      11.        11.    10.     11.       -11.      10.     22.1      11.     39.9
28   J2.       1.          1.         250.      5.31       1.57       1.         15.
29   SEAT CUSHION          .455
30   0.      8.4        11.    32.3    8.4       -11.       32.3   36.       11.     26.
31   J3.       1.          -1.        .1        0.         0.         1.         25.
32   LEFT PAN EDGE         .375
33   0.      36.        -11.   26.     8.4       -11.       32.3   38.3      -11.    35.7
34   J4.       1.          -1.        250.      0.         0.         1.         1.
35   RIGHT PAN EDGE        .375
36   0.      36.        11.    26.     8.4       11.        32.3   38.3      11.     35.7
37   J5.       1.          -1.        .1        0.         0.         1.         25.
38   LEFT BACK EDGE        .46
39   0.      11.        -11.   10.     22.1      -11.       39.0   1.7       -11.    13.8
40   J6.       1.          -1.        250.      0.         0.         1.         1.
41   RIGHT BACK EDGE       .46
42   0.      11.        11.    10.     22.1      11.        39.9   1.7       11.     13.8
43   K1.       2.          1.         3.        5.
44   L1.       0.          -9.5       0.        0.         -2.5       -11.       1.
45   1400.     350.
46   L2.       14.5        11.        36.       0.         5.3        1.7        1.
47   600.      350.
48   L3.       14.5        -11.       36.       0.         -7.1       7.2        1.
49   1500.     312.5
50   L4.       14.5        11.        36.       0.         7.1        7.2
51   M1.       350.        0.         0.        1.         .5
52   M2.       350.        0.         0.        1.         .5
53   M3.       312.5       0.         0.        1.         0.
54   M4.       312.5       0.         0.        1.         0.
55   N1.       0.          0.
56   N1.       .0025       -30.021
57   N1.       .005        -10.
58   N1.       .01         -40.114
59   N1.       .015        -10.
60   N1.       .02         0.
61   N1.       .025        -12.94
62   N1.       .07         -14.959
63   N1.       .09         -22.981
64   N1.       .1          0.
65   N1.       .5          0.
66   N2.       0.          0.
67   N2.       .5          0.
68   N3.       0.          0.
69   N3.       2.          0.
70   N4.       0.          0.
71   N4.       2.          0.
72   N5.       0.          0.
73   N5.       2.          0.
74   N6.       0.          0.
75   N6.       2.          0.
76   O
77             0.          00000000
79             2.          00000000
80             -1.
81   B.0005    .005        1.         1.                   .0000001   0.         1.        5.
82   S.005     .000001     10.        10.
83   1.    1.    1.     100.   100.   100.   100.   100.   100.   100.   100.   100.
84   T.2       32.2        0.         0.        1.         1.
85   U1.       0.          0.         0.        0.         0.
86   V
87             2-D VS. 3-D COMPARISON. TEST NO. A-045, SATURATING TEST
87.3 Y.39      .272        .046
87.4 FRONT COLLISION       RIGHT FRONT PASSENGER        SHOULDER & LAP BELT USE
88
```

TABLE VI
TYPICAL INPUT DATA SET

TABLE 7. INPUT DATA CARDS (3-D MODEL, 12-70)

Cards	Field	Symbol	Figure	Quantity	Units
A	1	n	4,5	Body segment number (1.=torso, 2.=head, 3.=legs) If this number is positive, fields 3, 4, 5 will be moments of inertia. If negative, they will be three measurements of body for computing moments of inertia.	
A	2	m_n	4	Mass of body segment	lb sec^2/in.
A	3	I_{1n} (t_n)	4	Moment of inertia about i-vector (or, 1. anterior-posterior thickness of torso elliptical cylinder 2. anterior-posterior thickness of head ellipsoid 3. inferior-superior thickness of leg elliptical cylinder.)	in lb sec^2 (in.)
A	4	I_{2n} (h_n)	4	Moment of inertia about j-vector (or, 1. length of torso elliptical cylinder 2. inferior-superior length of head ellipsoid 3. length of leg elliptical cylinder.)	in lb sec^2 (in.)
A	5	I_{3n} (w_n)	4	Moment of inertia about k-vector (or, 1. width of torso elliptical cylinder 2. width of head ellipsoid 3. width of leg elliptical cylinder.)	in lb sec^2 (in.)
A	6	ρ_3, ρ_2, or ρ_5	4	Distance from center of gravity to lower joint	in.
A	7	ρ_1, ρ_6, or ρ_4	4	Distance from center of gravity to upper joint	in.

TABLE 7. INPUT DATA CARDS (3-D MODEL, 12-70)

Cards	Field	Symbol	Figure	Quantity	Units
B	1	m	9	Identification number for this ellipsoid must be in range one to ten.	
B	2	n	9	Body segment number to which this ellipsoid is to be attached.	
B	3	x_{em}	9	X coordinate of ellipsoid center relative to body segment system.	in.
B	4	y_{em}	9	Y coordinate of ellipsoid center relative to body segment system.	in.
B	5	z_{em}	9	Z coordinate of ellipsoid center relative to body segment system.	in.
B	6	a_m	9	Ellipsoid semiaxis length parallel to i-vector of body segment.	in.
B	7	b_m	9	Ellipsoid semiaxis length parallel to j-vector of body segment.	in.
B	8	c_m	9	Ellipsoid semiaxis length parallel to k-vector of body segment.	in.
A special card is automatically read after the B card which contacts in columns one through sixteen the alpha-numeric name of this ellipsoid. The name should be centered within these sixteen columns.					
C	1	i	13	Joint index (1=neck, 2=hip)	
C	2	$k_{\psi i}$	13	Torsional elastic constant resisting relative yaw.	in lb/rad.
C	3	$k_{\psi si}$	13	Torsional elastic constant of relative yaw stop.	in lb/rad.

TABLE 7. INPUT DATA CARDS (3-D MODEL, 12-70)

Cards	Field	Symbol	Figure	Quantity	Units
C	4	ψ_{is}	13	Relative yaw angle at which stop is applied	deg.
C	5	$k_{\psi i}$	13	Torsional elastic constant resisting relative roll.	in lb/rad.
C	6	$k\phi_{si}$	13	Torsional elastic constant of relative roll stop.	in lb/rad.
C	7	ϕ_{is}	13	Relative roll angle at which stop is applied.	deg.
C	8	$c_{\psi i}$	13	Relative yaw damping coefficient.	in lb sec/rad.
D	1	i	13	Joint index (1.=neck, 2.=hip)	
D	2	$k_{\theta i}$	13	Torsional elastic constant resisting relative pitch.	in lb/rad.
D	3	$k_{\theta usi}$	13	Torsional elastic constant of upper relative pitch stop. Upper = rearward rotation of head relative to torso. = rearward rotation of legs relative to torso.	in lb/rad.
D	4	θ_{usi}	13	Relative pitch angle at which upper stop is applied.	deg.
D	5	$k_{\theta LSi}$	13	Torsional elastic constant of lower relative pitch stop. lower = forward rotation of head relative to torso. = jacknifing of torso down towards legs.	in lb/rad.

TABLE 7. INPUT DATA CARDS (3-D MODEL, 12-70)

Cards	Field	Symbol	Figure	Quantity	Units
D	6	θ_{LSi}	13	Relative pitch angle at which lower stop is applied.	deg.
D	7	$c_{\theta i}$	13	Relative pitch damping coefficient.	in lb sec/rad.
D	8	$c_{\phi i}$	13	Relative roll damping coefficient.	in lb sec/rad.
E	1	$[x_1]_{t=0}$	5,6	Initial x of torso c.g.*	in.
E	2	$[\dot{x}_1]_{t=0}$	5,6	Initial forward velocity of torso c.g.*	in/sec.
E	3	$[y_1]_{t=0}$	5,6	Initial y of torso c.g.*	in.
E	4	$[\dot{y}_1]_{t=0}$	5,6	Initial right sideways velocity of torso c.g.	in/sec.
E	5	$[z_1]_{t=0}$	5,6	Initial z of torso c.g.*	in.
E	6	$[\dot{z}_1]_{t=0}$	5,6	Initial downward velocity of torso c.g.*	in/sec.
E	7	$[\psi_1]_{t=0}$	5,6	Initial torso yaw*	deg.
E	8	$[\dot{\psi}_1]_{t=0}$	5,6	Initial torso yaw rate.*	deg/sec.
F	1	$[\theta_1]_{t=0}$	5,6	Initial torso pitch.* (may not be exactly ninety degrees in magnitude)	deg.
F	2	$[\dot{\theta}_1]_{t=0}$	5,6	Initial torso pitch rate.*	deg/sec.
F	3	$[\phi_1]_{t=0}$	5,6	Initial torso roll.*	deg.
F	4	$[\dot{\phi}_1]_{t=0}$	5,6	Initial torso roll rate.*	deg/sec.

*These quantities will be interpreted either relative to the inertial system or the vehicle system according to the to the switch in T-card, field five.

TABLE 7. INPUT DATA CARDS (3-D MODEL, 12-70)

Cards	Field	Symbol	Figure	Quantity	Units
F	5	$[\psi_2]_{t=0}$	5,6	Initial head yaw.*	deg.
F	6	$[\dot{\psi}_2]_{t=0}$	5,6	Initial head yaw rate.*	deg/sec.
F	7	$[\theta_2]_{t=0}$	5,6	Initial head pitch.* (May not be exactly ninety degrees in magnitude.)	deg.
F	8	$[\dot{\theta}_2]_{t=0}$	5,6	Initial head pitch rate.*	deg/sec.
G	1	$[\phi_2]_{t=0}$	5,6	Initial head roll.*	deg.
G	2	$[\dot{\phi}_2]_{t=0}$	5,6	Initial head roll rate.*	deg/sec.
G	3	$[\psi_3]_{t=0}$	5,6	Initial legs yaw.*	deg.
G	4	$[\dot{\psi}_3]_{t=0}$	5,6	Initial legs yaw rate.*	deg/sec.
G	5	$[\theta_3]_{t=0}$	5,6	Initial legs pitch.* (May not be exactly ninety degrees in magnitude.)	deg.
G	6	$[\dot{\theta}_3]_{t=0}$	5,6	Initial legs pitch rate.*	deg/sec.
G	7	$[\phi_3]_{t=0}$	5,6	Initial legs roll.*	deg.
G	8	$[\dot{\phi}_3]_{t=0}$	5,6	Initial legs roll rate.*	deg/sec.
H	1	$[x_4]_{t=0}$	5,6	Initial vehicle x,	in.
H	2	$[\dot{x}_4]_{t=0}$	5,6	Initial forward velocity of vehicle.	in/sec.

*These quantities will be interpreted either relative to the inertial system or the vehicle system according to the switch in T-card, field five.

TABLE 7. INPUT DATA CARDS (3-D MODEL, 12-70)

Cards	Field	Symbol	Figure	Quantity	Units
H	3	$[y_4]_{t=0}$	5	Initial vehicle y.	in.
H	4	$[\dot{y}_4]_{t=0}$	5	Initial right sideways velocity of vehicle.	in/sec.
H	5	$[z_4]_{t=0}$	5	Initial vehicle z.	in.
H	6	$[\dot{z}_4]_{t=0}$	5	Initial downward velocity of vehicle.	in/sec.
I	1	$[\psi_4]_{t=0}$	5,6	Initial vehicle yaw.	deg.
I	2	$[\dot{\psi}_4]_{t=0}$	5,6	Initial vehicle yaw rate.	deg/sec.
I	3	$[\theta_4]_{t=0}$	5,6	Initial vehicle pitch. (May not be exactly ninety degrees in magnitude.)	deg.
I	4	$[\dot{\theta}_4]_{t=0}$	5,6	Initial vehicle pitch rate.	deg/sec.
I	5	$[\phi_4]_{t=0}$	5,6	Initial vehicle roll.	deg.
I	6	$[\dot{\phi}_4]_{t=0}$	5,6	Initial vehicle roll rate.	deg/sec.
J	1	k	10	Identification number for this contact surface. This must be in the range from one to twenty-five.	
J	2	-		The number of times at which the position of this contact relative to the vehicle will be specified. The maximum number of times which can be specified for all contact in total is 300. If this field is zero, this contact will be removed from further consideration.	

TABLE 7. INPUT DATA CARDS (3-D MODEL, 12-70)

Cards	Field	Symbol	Figure	Quantity	Units
J	3	-		This field is set to any negative quantity if the origin is in back of this contact, or to any positive quantity if the origin is in front of this contact.	
J	4	k_{1k}		Contact linear elastic coefficient.	lb/in.
J	5	k_{2k}		Contact quadratic elastic coefficient.	lb/in^2
J	6	k_{3k}		Contact cubic elastic coefficient.	lb/in^3
J	7	c_k		Contact linear damping coefficient.	lb sec/in.
J	8	-		Penetration limit.	in.
The J card triggers a special reading sequence, the first card of which has the following special format.					
-	1	-	-	Alpha-numeric title of contact surface. (centered in columns one through sixteen)	-
-	2	λ_k	11	Edge constant. (columns 21 through 30)	-
-	3	$F_{max,k}$	7	Maximum force to be allowed. (columns 31 through 40)	lbs.
-	4	D_k	7	Saturation unloading slope. Must be steep enough to completely unload before load curve zero force deflection. (columns 41 through 50)	lb/in.

TABLE 7. INPUT DATA CARDS (3-D MODEL, 12-70)

Cards	Field	Symbol	Figure	Quantity	Units
The special reading sequence initiated by the J card then concludes by reading one card for each time point specified in field two of the J card. Each of these cards has the following special format.					
-	1	t'	-	Time at which the contact assumes the position and shape specified in the remaining fields on this card. These cards must be in ascending order on time values. (columns 1 through 8)	sec.
-	2	$[\hat{x}_{1k}]_{t=t'}$	10	x coordinate of the middle of the three specified consecutive corner points. (columns 9 through 16)	in.
-	3	$[\hat{y}_{1k}]_{t=t'}$	10	y coordinate of the middle of the three specified consecutive corner points. (columns 17 through 24)	in.
-	4	$[\hat{z}_{1k}]_{t=t'}$	10	z coordinate of the middle of the three specified consecutive corner points. (columns 25 through 32)	in.
-	5	$[\hat{x}_{2k}]_{t=t'}$	10	x coordinate of one endpoint of the three specified consecutive corner points. (columns 33 through 40)	in.
-	6	$[\hat{y}_{2k}]_{t=t'}$	10	y coordinate of one endpoint of the three specified consecutive corner points. (columns 41 through 48)	in.
-	7	$[\hat{z}_{2k}]_{t=t'}$	10	z coordinate of one endpoint of the three specified consecutive corner points. (columns 49 through 56)	in.
-	8	$[\hat{x}_{3k}]_{t=t'}$	10	x coordinate of the other endpoint of the three specified consecutive corner points. (columns 57 through 64)	in.

TABLE 7. INPUT DATA CARDS (3-D MODEL, 12-70)

Cards	Field	Symbol	Figure	Quantity	Units
-	9	$[\hat{y}_{3k}]_{t=t'}$	10	y coordinate of the other endpoint of the three specified consecutive corner points. (columns 65 through 72)	in.
-	10	$[\hat{z}_{3k}]_{t=t'}$	10	z coordinate of the other endpoint of the three specified consecutive corner points. (columns 73 through 80)	
K	1	-	-	The number of the contact to be used for the seat back in movie making and injury predictions. If zero, fields two through eight are numbers of contacts which comprise the forward vehicle structures.	
K	2	-	-	The number of the contact used as seat cushion.	
K	3	-	-	The number of the ellipsoid used as the chest.	
K	4	-	-	The number of the ellipsoid used as the knee.	
K	5-8	-	-	These fields contain the numbers of contacts which comprise the forward vehicle structure. The first zero or blank field encountered from left to right terminates the card.	
L	1	n	-	Belt segment index (1.=left shoulder belt, 2.=right shoulder belt, 3.=left lap belt, 4.=right lap belt)	
L	2	λ_n	14	x coordinate of anchor point in vehicle.	in.

TABLE 7. INPUT DATA CARDS (3-D MODEL, 12-70)

Cards	Field	Symbol	Figure	Quantity	Units
L	3	μ_n	14	y coordinate of anchor point in vehicle.	in.
L	4	υ_n	14	z coordinate of anchor point in vehicle.	in.
L	5	r_n	14	x coordinate of attachment point on torso.	in.
L	6	s_n	14	y coordinate of attachment point on torso.	in.
L	7	t_n	14	z coordinate of attachment point on torso.	in.
L	8	-	-	Switch. If switch=0., no maximum force is to be specified and will be treated as though infinite. If switch=1., maximum force and unloading slope will be specified on the next card.	-
If field 8 of card L is non-zero, a special reading sequence is initiated which will read one card immediately after the L card with the following special format.					
-	1	$F_{max,n}$	7	Maximum force for belt segment n. (columns 1 through 10)	lbs.
-	2	D_n	7	Unloading slope in case of saturation. (columns 11 through 20)	lbs/in.
M	1	n		Belt segment index (See card L, field 1)	
M	2	$b^{k_{1n}}$		Belt linear spring coefficient.	lb/in.
M	3	$b^{k_{2n}}$		Belt quadratic spring coefficient.	lb/in^2

TABLE 7. INPUT DATA CARDS (3-D MODEL, 12-70)

Cards	Field	Symbol	Figure	Quantity	Units
M	4	$_b k_{3n}$		Belt cubic spring coefficient.	lb/in^3
M	5	$_b c_n$		Belt linear damping coefficient.	lb.sec/in.
M	6	Δ_n		Belt slack at t=0. (Make negative for preloading)	in.
M	7			Switch. If switch = 0., belt segment is used. If switch = 1., belt segment is not used.	
M	8			Injury tolerance for body damage from this seat belt segment.	lb.
N	1	n		Acceleration table number.	

n	$\ddot{\sigma}_n$ Special Symbol	Normal Symbol
1.	vehicle forward acceleration.	$\ddot{x}_4$
2.	vehicle side acceleration.	$\ddot{y}_4$
3.	vehicle downward acceleration.	$\ddot{z}_4$
4.	vehicle yaw acceleration.	$\ddot{\psi}_4$
5.	vehicle pitch acceleration.	$\ddot{\theta}_4$
6.	vehicle roll acceleration.	$\ddot{\phi}_4$

See Equation (2.5.24) et seq.

N	2	t'		Time value for acceleration value.	sec.
N	3	$[\ddot{\sigma}_n]_{t=t'}$		Acceleration value.	g's or deg/sec^2
O	1	n		Index of acceleration table to be partially deleted. (See card N field 1)	

TABLE 7. INPUT DATA CARDS (3-D MODEL, 12-70)

Cards	Field	Symbol	Figure	Quantity	Units
0	2	t'_{low}		Lowest value of time for deleting acceleration table values.	sec.
0	3	t'_{high}		Upper value of time for deleting acceleration table values. NOTE: The 0-cards do not need to be included if not needed.	sec.
P				The fields of this card are unused with the exception of the "P" in the first column. This card triggers a special reading sequence of debugging control cards immediately following the P card. The format of these special cards follow.	
-	2			Effective time. (negative value terminates special reading sequence.) (columns 11 through 20)	sec.
-	3			8-digit hexadecimal debugging control word. NOTE: See Part 4.3. These cards must be in ascending order of time values.	
Q	1			Logical I/O Unit Number from which the next input record is to be read. If not 0 to 9, program will read from SCARDS next.	
Q	2			Number of input lines to skip before reading. If negative, will rewind 0 to 9.	
R	1	Δt_{max}		Maximum integration time step.	sec.
R	2	Δt_{prnt}		Print time step which must be an integral multiple of the maximum time step.	sec.

TABLE 7. INPUT DATA CARDS (3-D MODEL, 12-70)

Cards	Field	Symbol	Figure	Quantity	Units
R	3	-		Starting method code: zero is for use of the Euler method, one for modified Runge-Kutta, two for regular Runge-Kutta.	
R	4	-		Predictor-corrector code: zero is use of the Adams-Moulton method, one for Milne-Hamming.	
R	5	$\epsilon_{\ddot{Z}}$		Acceleration minimum magnitude.	
R	6	-		Recording control code: zero is for no recording, one is for movie, two for precautionary summary recording, three for both.	
R	7	ΔV_{lim}		Velocity change limit.	
R	8	$\Delta \ddot{Z}_{lim}$		Extrapolation change limit.	
S	1	ϵ_V		Velocity convergence parameter.	
S	2	ϵ_t		Time epsilon.	sec.
S	3	N_{max}		Maximum number of subdivisions of the maximum time step to be allowed.	
S	4	-		Execution time limit.	min.
A special card is automatically read which contains twelve fields of six columns each. These fields contain the relative weights for the twelve generalized coordinates respectively.					
T	1	T_{max}		Length of simulation in real time.	sec.
T	2	g		Value of gravity. (negative implies 32.2)	ft/sec^2

TABLE 7. INPUT DATA CARDS (3-D MODEL, 12-70)

Cards	Field	Symbol	Figure	Quantity	Units
T	3	-		Switch. If switch = 0., input data is listed. If switch ≠ 0., input data is not listed.	
T	4	-		Switch. If switch = 0., the tabulated summary output is printed. If switch = 1., the belt angle page is left out. If switch = 2., the two pages of vehicle data are left out also. If switch = 3., the three pages of body angles are left out as well. (Higher levels are inclusive of lower levels.)	
T	5			Switch. If switch = 0., the contents of cards C, D, E and F are considered to be relative to the inertial system. If switch is not zero, the contents of these cards are relative to the vehicle, and the program automatically converts to inertial.	
T	6			Switch. If switch = 0., body kinetic energies are not computed. If switch is not zero, body kinetic energies are computed and outputed.	
U	1			Multiplying factor to alter sled X-acceleration table.	
U	2			Multiplying factor to alter sled Y-acceleration table.	
U	3			Multiplying factor to alter sled Z-acceleration table.	
U	4			Multiplying factor to alter sled yaw-acceleration table.	
U	5			Multiplying factor to alter sled pitch-acceleration table.	
U	6			Multiplying factor to alter roll-acceleration table.	
V				Title card. Triggers reading of following BCD card.	

TABLE 7. INPUT DATA CARDS (3-D MODEL, 12-70)

Cards	Field	Symbol	Figure	Quantity	Units
W	1	m	9	Ellipsoid number to be inhibited.	
W	2	k	10	Contact number to be inhibited.	
W	3			Switch. If negative, allow no interaction caused by this ellipsoid infringing on this contact. If zero, remove any previous inhibition. If positive, permit interaction, but do not print the forces generated. A maximum of forty ellipsoid-contact combinations can be reported upon in any run.	
X	1			Tolerance specification index. This controls the interpretation of fields two through seven as shown in the table below. Brackets show default values if quantities is left zero or card is left out. The double bracketed values for angular limits represent default values for stiff and flexible torso respectively.	

Field One Value	0.	1. (all units are deg.)	2. (all units are deg.)
Field 2	Sensitivity index limit [1000.]	Neck yaw lower limit [-70.,-87.]	Neck yaw upper limit [70.,87.]
Field 3	pitch concussion (rad./sec^2) [2000.]	Neck pitch lower limit [-60.,-100.]	Neck pitch upper limit [60.,90.]
Field 4	head side acceleration (g-unit) [46.]	Neck roll lower limit [-40.,-57.]	Neck roll upper limit [40.,57.]
Field 5	chest force (lbs) [1800.]	Hip yaw lower limit [-30.,-47.]	Hip yaw upper limit [30.,47.]
Field 6	knee force (lbs) [1500.]	Hip pitch lower limit [-90.,-120.]	Hip pitch upper limit [30.,50.]
Field 7	forward chest accel. (g-unit) [45.]	Hip roll lower limit [0.,-17.]	Hip roll upper limit [0.,17.]
Field 8	chest s-i g-load [25.]	Switch: 0.=stiff torso, 1.=flexible torso	

TABLE 7. INPUT DATA CARDS (3-D MODEL, 12-70)

Cards	Field	Symbol	Figure	Quantity	Units
Y	1	$P(E_1)$	-	Probability of event one. Must be in range zero to one. (Event one is usually accident type.)	
Y	2	$P(E_2)$	-	Probability of event two. Must be in range zero to one. (Event two is usually occupant position.)	
Y	3	$P(E_3)$	-	Probability of event three. Must be in range zero to one. (Event three is usually restraint system type.)	
The Y card triggers the reading of a card of special format immediately following the Y card.					
-	1	-	-	Alphanumeric description of event one. (centered in columns 1 through 24)	
-	2	-	-	Alphanumeric description of event two. (centered in columns 25 through 48)	
-	3	-	-	Alphanumeric description of event three. (centered in columns 49 through 72)	

TABLE 8. 3-D INPUT FORMATS SUMMARY

BODY PARTS	A	n .gt. 0 n .lt. 0	M_n(mass) same	I_{1n}(around i) t_n	I_{2n}(around j) h_n	I_{3n}(around k) w_n	lower joint to c.g. same		upper joint to c.g. same
	B	m(ell.#)	n(seg.#)	x_{em}	y_{em}	z_{em}	a_m	b_m	c_m
				center relative to e_n			semiaxis lengths along i_n, j_n and k_n		
		if n=0, ell. removed, if a, b, c, = 0, ell. restored.							
		(1-16 alpha ell. name) This card must follow B card.							
JOINTS	C	n n=1 is neck, n=2 is hip	yaw elast	yaw stop	yaw stop angle	roll elast	roll stop	roll stop angle	yaw damping
	D	n	pitch elast	upper pitch stop	upper pitch stop angle	lower pitch stop	lower pitch stop angle	pitch damping	roll damping
INITIAL CONDITIONS (Note: see card T, field 5.)	E	chest x	chest $\dot{x}$	chest y	chest $\dot{y}$	chest z	chest $\dot{z}$	chest yaw	chest yaw dot
	F	chest pitch	chest pitch dot	chest roll	chest roll dot	head yaw	head yaw dot	head pitch	head pitch D
	G	head roll	head roll dot	legs yaw	legs yaw dot	legs pitch	legs pitch dot	legs roll	legs roll dot
	H	cart x	cart x dot	cart y	cart y dot	cart z	cart z dot		
	I	cart yaw	cart yaw dot	cart pitch	cart pitch dot	cart roll	cart roll dot		
		(end of initial conditions)							
CONTACT SPECS	J	contact#	# of times specified if 0, drop	minus=behind plus =front	1st elast constant	2nd elast constant	high elast constant	damping constant	penetration limit
					if all 0, reinstate this contact				
		(1-16) alpha contact name edge constant in (21-30) max force (31-40) unloading scope (41-50). This card must follow J card.							

TABLE 8. 3-D INPUT FORMATS SUMMARY (cont'd.)

CONTACT SPECS (cont'd.)		There must be as many of the following cards as specified in field two of J card.								
		time	middle corner			one end corner			other end corner	
			x	y	z	x	y	z	x	y	z
		(1-8)	(9-16)	(17-24)	(25-32)	(33-40)	(41-48)	(49-56)	(57-64)	(65-72)	(73-80)
DESIGN	K	# of seat top	# of seat bottom	# of chest ellip.	# of knee ellip.	Numbers of forward vehicle structure fill from left to right.					
		if 0, fields three through eight are forward vehicle structure numbers, fill from left to right.									
BELTS	L	n	belt anchor point x y z relative to torso system			belt attachment point x y z relative to cart system			Switch: non-zero causes extra card read with F_{max} and D in columns (1-10) and (11-20) respectively.		
		n=1 is left shoulder, n=2 is right shoulder, n=3 is left lap, n=4 is right lap									
	M	n	linear belt elastic coefficients	quadratic	high	damping constant		slack	if 0, belt tolerance used; if no, not used.		
		n same as for L card.									
TABLES IN	N	table #	time	acceleration							
		table #'s: 1 is cart x, 2 is cart y, 3 is cart z, 4 is cart yaw, 5 is cart pitch, 6 is cart roll									
TABLE DELETE	O	table #	time 1	time 2							
		table #'s same as for card N									
DEBUG	P	(no fields, triggers reading of special cards below)									
		time effective if minus, resume regular input.	hexadecimal debug code word								
READ JUMP	Q	logical # if not 0-9, will be set to SCARDS.	# of lines to skip (if minus, and not SCARDS, will rewind first)								

TABLE 8. 3-D INPUT FORMATS SUMMARY (cont'd.)

INTEGRATION CONTROLS	R	maximum time step	print time step	starting method 0 is Euler 1 is Mod RK 2 is Reg RK	pred-cer method 0 is Adams 1 is Milne	accel. min. magnitude	recording control 0 is none 1 is movie 2 is summary 3 is both	vel. change limit	extrap. change limit
		(field two a multiple of field one)							
	S	velocity convergence parameter	time epsilon	maximum # of subdiv.	execution time limit (min.)				
		(Weight card must follow S card and has 12 fields of 6 columns each containing the relative weights of the 12 generalized coordinates respectively. These weights will be normalized by the program to add to one. All zeroes on this card will cause an error return.)							
SWITCHES	T	maximum time	gravity if minus, 32.2 is used.	0 prints input values, ≠0, inhibits input output.	0 is all 1 no belt ang. 2 no cart var. 3 no body ang. (the summary output inhibitions are inclusive.)	body initial conditions 0 is inertial ≠0 is cart rel.	0 is no energy printout ≠0 is energy printout		
PROFILE MOD.	U	Modifying factors for input cart acceleration table no. 1	2	3	4	5	6		
TITLE	V	(no fields, triggers reading of a special card columns 1-80 which are used for a subtitle. The special alpha card must follow the V card.)							

TABLE 8. 3-D INPUT FORMATS SUMMARY (cont'd.)

CONTACT INHIB.	W	ell. #	contact #	if minus, allow no contact if zero, remove inhibition if plus, allow no printing					
INJURY TOL.	X	n	tol 1	tol 2	tol 3	tol 4	tol 5	tol 6	tol 7
			n = 0				2		
			tol 1 = SI tolerance		low neck yaw		high neck yaw		
			tol 2 = pitch concussion		low neck pitch		high neck pitch		
			tol 3 = head side accel.		low neck roll		high neck roll		
			tol 4 = chest force		low hip yaw		high hip yaw		
			tol 5 = knee force		low hip pitch		high hip pitch		
			tol 6 = forward chest accel.		low hip roll		high hip roll		
			tol 7 = chest S-I g-level		switch 0.=stiff torso, 1.=flexible torso		unused		
PROB.	Y	$P(E_1)$	$P(E_2)$	$P(E_3)$					
	Special Card:								
	Event one name (1-24)		Event two name (25-48)		Event three name (49-72)				
GO!	Z	(no fields, signals start of computation)							

4.2 DESCRIPTION OF NORMAL PROGRAM OUTPUT

The printed output of the HSRI Three-Dimensional Crash Victim Simulator is divided into three general categories. The first category is normal output, that which emerges from a successful run when no special information is required. The second category is auxillary or debugging output, which is extensive information on the inner workings of the program under control of input data. The third category is messages which appear only when certain error conditions arise. This section deals with the first category. Section 4.3 will present the other two categories.

Normal output is divided into three parts. The first part is one or more pages at the beginning, is labeled "Input Data," and presents the problem specified by the input data deck in a somewhat readable form. The second part is the bulk of the normal output, is called "Output Data," and records the simulated model parameters over the time interval of interest. The last four pages comprise the "Injury Data" which contains some estimators for the bodily damage inflected on the victim by the crash.

Each page of normal output begins with a three line heading. The first line identifies the model, the part of normal output in which this page is included, the date of the run, and the page number. The middle line is the descriptive run title supplied by the user. The third line is the statement of policy on units. Thus, velocities are expressed in inches per second or degrees per second.

Table 9 contains the program's presentation of the input data set comprising Table 6. The coordinate positions and Euler angles are the same described in Section 2.3 and illustrated in Figure 6. The initial conditions printed are

THREE DIMENSIONAL CRASH VICTIM SIMULATOR INPUT DATA
2-D VS. 3-D COMPARISON. TEST NO. A-045, SATURATION TEST
UNITS ARE INCHES, DEGREES, POUNDS, AND SECONDS UNLESS NOTED.

INITIAL CONDITIONS

	VEHICLE DISPLACEMENT	VEHICLE VELOCITY	TORSO DISPLACEMENT	TORSO VELOCITY	HEAD DISPLACEMENT	HEAD VELOCITY	LEGS DISPLACEMENT	LEGS VELOCITY
X	0.0	536.	19.40	536.	17.02	536.	33.93	536.
Y	0.0	0.	0.0	0.	-0.0	-0.	0.0	-0.
Z	0.0	0.	18.00	0.	1.40	0.	24.44	-0.
YAA	0.0	0.	0.0	0.	0.0	0.	0.0	0.
PITCH	0.0	0.	20.00	0.	-15.00	0.	7.00	0.
PULL	0.0	0.	0.0	0.	0.0	0.	0.0	0.

BODY PROPERTIES

	MASS	WEIGHT	MOMENTS OF INERTIA ABOUT I	ABOUT J	ABOUT K	DISTANCE FROM C.G. TO LOWER JOINT	C.G. TO UPPER JOINT
TORSO	0.2340	90.4	12.7800	11.5000	3.6500	8.37	11.50
HEAD	0.0408	15.8	0.3672	0.4420	0.2210	6.00	6.00
LEGS	0.1300	50.2	1.5720	2.5900	3.5400	7.25	11.75

BODY CONTACT ELLIPSOIDS

ELLIPSOID NUMBER	FLLIPSOID DESCRIPTION	BODY SEGMENT	CENTER RELATIVE TO SEGMENT C.G. X	Y	Z	SEMIAXIS LENGTHS ALONG SEGMENT SYS. I	J	K
1	CHEST	TORSO	0.0	0.0	-7.10	4.60	8.50	4.60
2	HIP	TORSO	0.0	0.0	7.10	4.60	8.50	4.60
3	KNEE	LEGS	0.0	0.0	0.0	3.00	7.00	3.00
4	HEAD	HEAD	0.0	0.0	0.0	4.25	3.00	6.00
5	RIGHT SIDE	TORSO	0.0	5.30	0.0	4.50	3.50	10.80
6	LEFT SIDE	TORSO	0.0	-5.30	0.0	4.50	3.50	10.80

JOINTS

	ELASTIC CONSTANTS YAW	PITCH	ROLL	STOP CONSTANTS YAW	LOW PITCH	UP	ROLL	DAMPING CONSTANTS YAW	PITCH	ROLL	EFFECTIVE ANGLE YAW	LO PITCH	UP	ROLL
NECK	600.	6	600.	110000.	150000.	150000.	110000.	2.	2.	2.	60.	-70.	70.	50.
HIP	800.	800.	800.	110000.	150000.	150000.	110000.	2.	2.	2.	45.	-35.	45.	30.

VEHICLE INTERIOR INTERACTIVE COMPONENTS

	SLACK	ANCHOR POINT X	Y	Z	BELTS ATTACHMENT POINT X	Y	Z	SPRING CONSTANT 1	2	3	DAMPING CONSTANT	MAXIMUM FORCE	UNLOADING SLOPE
LEFT SHOULDER	0.5	0.0	-9.50	0.0	0.0	-2.50	-11.00	350.00	0.0	0.0	1.00	1400.0	350.0
RIGHT SHOULDER	0.5	14.50	11.00	36.00	0.0	5.30	1.70	350.00	0.0	0.0	1.00	500.00	350.0

CONTACTS

CONTACT NUMBER	CONTACT DESCRIPTION	ELASTIC CONSTANTS 1	2	3	DAMPING CONSTANT	PENETRATION EDGE LIMIT	CONSTANT	MAXIMUM FORCE	UNLOADING SLOPE	DIRECTION
1	SEAT BACK	37.21	5.31	1.57	1.00	15.00	0.455	0.0	0.0	BEHIND
2	SEAT CUSHION	250.00	5.31	1.57	1.00	15.00	0.455	0.0	0.0	FRONT
3	LEFT PAN EDGE	0.10	0.0	0.0	1.00	25.00	0.375	0.0	0.0	BEHIND
4	RIGHT PAN EDGE	250.00	0.0	0.0	1.00	1.00	0.375	0.0	0.0	BEHIND
5	LEFT BACK EDGE	0.10	0.0	0.0	1.00	25.00	0.460	0.0	0.0	BEHIND
6	RIGHT BACK EDGE	250.00	0.0	0.0	1.00	1.00	0.460	0.0	0.0	BEHIND

CONTACT POSITIONS

CONTACT NUMBER	TIME	CORNER X	Y	Z	ADJACENT CORNER X	Y	Z	OTHER ADJACENT CORNER X	Y	Z
1	0.0	11.00	11.00	10.00	11.00	-11.00	10.00	22.10	11.00	39.90
2	0.0	8.40	11.00	32.30	8.40	-11.00	32.30	36.00	11.00	36.00
3	0.0	36.00	-11.00	26.00	8.40	-11.00	32.30	38.30	-11.00	35.70
4	0.0	36.00	11.00	26.00	8.40	11.00	32.30	38.30	11.00	35.70
5	0.0	11.00	-11.00	10.00	22.10	-11.00	39.90	1.70	-11.00	13.80
6	0.0	11.00	11.00	10.00	22.10	11.00	39.90	1.70	11.00	13.80

TABLE IX
NORMAL OUTPUT OF INPUT DATA

PROGRAM CONTROLS

MAXIMUM TIME STOP = 0.00050, FINAL TIME= 0.2000, PRINT TIME STEP= 0.0050, INTEGRATION STARTING= MOD=
RI, PRED.-COR.= MILNE-HAMMING
INTEGRATION WEIGHTS= 0.001 0.001 0.001 0.111 0.111 0.111 0.111 0.111 0.111 0.111 0.111 0.11
VELOCITY CHANGE LIMIT= 0.5000D 01, EXTRAPOLATION CHANGE LIMIT= 0.1000D 01, ACCELERATION MINIMUM
MAGNITUDE= 0.1000D-06
VELOCITY CONVERGENCE PARAMFIER= 0.5000D-02, MAXIMUM TIME SUBDIVISIONS= 10, TIME EPSILON= 0.4883D-07
SUMMARY INHIBITION= OFF, RECORDING CONTROL= NONE, GRAVITY (O-UNITS)= 1.00, INITIAL POSITIONAL
TRANSFORMATION= ON ENERGY PRINT= ON, PROFILE MODIFIERS= 1.000 0.0 0.0 0.0 0.0 0.0
LOCAL EXECUTION TIME LIMIT= 10.000000

TOLERANCES

GADD INDEX = 1.000.0 PITCH CONCUSSION= 2000.0 HEAD G-LOADING= 44.0 CHEST G-LOADING=45.0
CHEST FRACTURE= 1800.0
KNEE FORCE= 1500.0 BELTS= 1800.0 5000.0 -0.0 -0.0

NECK ANGLES	-70.00	30.00	-60.00	60.00	-40.00	40.00
HIP ANGLES	-30.00	30.00	-90.00	30.00	0.0	0.0

DESIGNATIONS

SEAT TOP= 1 SEAT BOTTOM= 2 CHEST= 1 KNEE= 3 FORWARD CONTACTS= 5

VEHICLE ACCELERATION PROFILES

TIME	FORWARD(G-UNITS)	TIME	RIGHT(G-UNITS)	TIME	DOWN	TIME	YAW	TIME	PITCH	TIME	ROLL
0.0	0.0	0.0	0.0	0.0	0.0	0.0	0.	0.0	0.	0.0	0.
0.0025	-30.02	0.5000	0.0	2.0000	0.0	2.0000	0.	2.0000	0.	2.0000	0.
0.0050	-10.00										
0.0060	-40.11										
0.0000	-10.00										
0.0150	0.0										
0.0200	-12.94										
0.0250	-14.96										
0.0700	-22.98										
0.0800	0.0										
0.1000											
0.5000											

TABLE IX
NORMAL OUTPUT OF INPUT DATA (CONT.)

always relative to the inertial frame whether they were specified to the program relative to the vehicle or the inertial frame. For brevity, "Lower Extremities" is shortened to "Legs" throughout the printout output. Initial coordinates and velocities of Head and Legs Centers of Gravity are printed along with the specified values for completeness.

Weight is printed along side of mass for each body segment for convenience. The Moments of Inertia are printed whether they are calculated by the program or put in by the user.

In the section discussing body contact ellipsoids, there is one line for each of the ten possible ellipsoids. The (X, Y, Z) of the printout is (x_{em}, y_{em}, z_{em}) of Section 2.5 and I, J, K columns are a_m, b_m, c_m of the same section.

Under "Joints" the units of the "Elastic Constants" and "Stop Constants" are in.lb./rad. and not degrees as is implied. The unsymmetric pitch values together with the symmetric yaw and roll values are given under "Stop Constants" and "Effective Angle."

One line for each specified belt segment is printed. It should be recalled that the "Anchor Point" is relative to the vehicle whereas the "Attachment Point" is relative to the Torso Body Segment System (see Figure 14).

The information about contacts is summarized in two paragraphs on the printed output. The first paragraph contains one line for each of the contacts used in this run of which there may be up to 25. The "1", "2", and "3" under "Elastic Constants" refer to the subscripts in Equation (2.4.10). All other quantities are as explained in Section 2.5. The second paragraph contains one line for each of the times points up to 300 used in this run. The time points are organized first on the number of the contact to which they apply and then on the time at which they become effective. The first time point for each contact must be

time zero which will hold until another time value is given and so on (see Section 2.5). the corner points are points one, two, and three respectively and are given in vehicle coordinates.

"Program Controls," "Tolerances," and "Designations" are self-explanatory when referred to Sections 4.1 and 4.5.

The six vehicle acceleration profiles are presented in columns under the title, "Vehicle Acceleration Profiles." All the time points actually supplied are shown multiplied by the respective profile modifier so the profile shown here is the actual one which will be used.

The "Output Data" begins with two pages of "Vehicle Kinematics." Values on these pages are relative to the inertial system (see Section 2.3 and Figure 5). The acceleration values are interpolated from the profiles supplied by the user and the velocities and displacements are integrated from these same profiles. Linear accelerations are in g-units. Table 10 contains these two pages from the run produced by the data set in Table 6.

Immediately following these two pages are six pages of similar results for the three body segments. The two pages for the torso values from this same run comprise Table 11 and are typical of any of the body segment outputs. Linear accelerations are inertial and in g-units. Linear displacements are relative to the vehicle system and are in inches. All other quantities are inertial and in the units implied by the policy on units.

The next two pages deal with belt output and make up Table 12. The belt angles reported are the direction angles of each belt segment with respect to the inertial system. For instance, "X" under "RIGHT SHOULDER" is the angle between the vector $\bar{I}$ of the inertial system and the right shoulder belt segment (see Figure 14).

2-D VS. 3-D COMPARISON. TEST NO. A-D45, SATURATION TEST
UNITS ARE INCHES, DEGREES, POUNDS, AND SECONDS UNLESS NOTED.

VEHICLE KINEMATICS

TIME	X-DISP.	X-VEL.	X-ACCEL.	Y-DISP.	Y-VEL.	Y-ACCEL.	Z-DISP.	Z-VEL.	Z-ACCEL.
0.0	0.0	536.10	0.0	0.0	0.0	0.0	0.0	0.0	0.0
0.0050	2.60	502.27	-0.1000E 02	0.0	0.0	0.0	0.0	0.0	0.0
0.0100	5.02	453.86	-0.4011E-02	0.0	0.0	0.0	0.0	0.0	0.0
0.0150	7.14	405.45	-0.1000E 02	0.0	0.0	0.0	0.0	0.0	0.0
0.0200	9.14	395.79	-0.2589E-13	0.0	0.0	0.0	0.0	0.0	0.0
0.0250	11.10	383.29	-0.1294E 02	0.0	0.0	0.0	0.0	0.0	0.0
0.0300	12.95	358.07	-0.1316E 02	0.0	0.0	0.0	0.0	0.0	0.0
0.0350	14.66	332.42	-0.1339E 02	0.0	0.0	0.0	0.0	0.0	0.0
0.0400	16.27	306.34	-0.1361E 02	0.0	0.0	0.0	0.0	0.0	0.0
0.0450	17.74	279.82	-0.1384E 02	0.0	0.0	0.0	0.0	0.0	0.0
0.0500	19.07	252.87	-0.1405E 02	0.0	0.0	0.0	0.0	0.0	0.0
0.0550	20.27	225.49	-0.1429E 02	0.0	0.0	0.0	0.0	0.0	0.0
0.0600	21.32	197.67	-0.1451E 02	0.0	0.0	0.0	0.0	0.0	0.0
0.0650	22.24	169.42	-0.1473E 02	0.0	0.0	0.0	0.0	0.0	0.0
0.0700	23.02	140.74	-0.1498E 02	0.0	0.0	0.0	0.0	0.0	0.0
0.0750	23.65	109.90	-0.1696E 02	0.0	0.0	0.0	0.0	0.0	0.0
0.0800	24.11	75.18	-0.1897E 02	0.0	0.0	0.0	0.0	0.0	0.0
0.0850	24.39	36.60	-0.2098E 02	0.0	0.0	0.0	0.0	0.0	0.0
0.0900	24.47	-5.88	-0.2298E 02	0.0	0.0	0.0	0.0	0.0	0.0
0.0950	24.15	-39.16	-0.1149E 02	0.0	0.0	0.0	0.0	0.0	0.0
0.1000	24.12	-50.26	-0.2825E-11	0.0	0.0	0.0	0.0	0.0	0.0
0.1050	23.60	-50.26	0.0	0.0	0.0	0.0	0.0	0.0	0.0
0.1100	23.61	-50.26	0.0	0.0	0.0	0.0	0.0	0.0	0.0
0.1150	23.36	-50.26	0.0	0.0	0.0	0.0	0.0	0.0	0.0
0.1200	23.11	-50.26	0.0	0.0	0.0	0.0	0.0	0.0	0.0
0.1250	22.86	-50.26	0.0	0.0	0.0	0.0	0.0	0.0	0.0
0.1300	22.61	-50.26	0.0	0.0	0.0	0.0	0.0	0.0	0.0
0.1350	22.36	-50.26	0.0	0.0	0.0	0.0	0.0	0.0	0.0
0.1400	22.10	-50.26	0.0	0.0	0.0	0.0	0.0	0.0	0.0
0.1450	21.85	-50.26	0.0	0.0	0.0	0.0	0.0	0.0	0.0
0.1500	21.60	-50.26	0.0	0.0	0.0	0.0	0.0	0.0	0.0
0.1550	21.35	-50.26	0.0	0.0	0.0	0.0	0.0	0.0	0.0
0.1600	21.10	-50.26	0.0	0.0	0.0	0.0	0.0	0.0	0.0
0.1650	20.85	-50.26	0.0	0.0	0.0	0.0	0.0	0.0	0.0
0.1700	20.60	-50.26	0.0	0.0	0.0	0.0	0.0	0.0	0.0
0.1750	20.35	-50.26	0.0	0.0	0.0	0.0	0.0	0.0	0.0
0.1800	20.09	-50.26	0.0	0.0	0.0	0.0	0.0	0.0	0.0
0.1850	19.84	-50.26	0.0	0.0	0.0	0.0	0.0	0.0	0.0
0.1900	19.59	-50.26	0.0	0.0	0.0	0.0	0.0	0.0	0.0
0.1950	19.34	-50.26	0.0	0.0	0.0	0.0	0.0	0.0	0.0
0.2000	19.09	-50.26	0.0	0.0	0.0	0.0	0.0	0.0	0.0

TABLE 10. NORMAL OUTPUT OF VEHICLE VALUES

VEHICLE KINEMATICS

	YAW			PITCH			ROLL		
TIME	DISP.	VEL.	ACCEL.	DISP.	VEL.	ACCEL.	DISP.	VEL.	ACCEL.
0.0	0.0	0.0	0.0	0.0	0.0	0.0	0.0	0.0	0.0
0.0050	0.0	0.0	0.0	0.0	0.0	0.0	0.0	0.0	0.0
0.0100	0.0	0.0	0.0	0.0	0.0	0.0	0.0	0.0	0.0
0.0150	0.0	0.0	0.0	0.0	0.0	0.0	0.0	0.0	0.0
0.0200	0.0	0.0	0.0	0.0	0.0	0.0	0.0	0.0	0.0
0.0250	0.0	0.0	0.0	0.0	0.0	0.0	0.0	0.0	0.0
0.0300	0.0	0.0	0.0	0.0	0.0	0.0	0.0	0.0	0.0
0.0350	0.0	0.0	0.0	0.0	0.0	0.0	0.0	0.0	0.0
0.0400	0.0	0.0	0.0	0.0	0.0	0.0	0.0	0.0	0.0
0.0450	0.0	0.0	0.0	0.0	0.0	0.0	0.0	0.0	0.0
0.0500	0.0	0.0	0.0	0.0	0.0	0.0	0.0	0.0	0.0
0.0550	0.0	0.0	0.0	0.0	0.0	0.0	0.0	0.0	0.0
0.0600	0.0	0.0	0.0	0.0	0.0	0.0	0.0	0.0	0.0
0.0650	0.0	0.0	0.0	0.0	0.0	0.0	0.0	0.0	0.0
0.0700	0.0	0.0	0.0	0.0	0.0	0.0	0.0	0.0	0.0
0.0750	0.0	0.0	0.0	0.0	0.0	0.0	0.0	0.0	0.0
0.0800	0.0	0.0	0.0	0.0	0.0	0.0	0.0	0.0	0.0
0.0850	0.0	0.0	0.0	0.0	0.0	0.0	0.0	0.0	0.0
0.0900	0.0	0.0	0.0	0.0	0.0	0.0	0.0	0.0	0.0
0.0950	0.0	0.0	0.0	0.0	0.0	0.0	0.0	0.0	0.0
0.1000	0.0	0.0	0.0	0.0	0.0	0.0	0.0	0.0	0.0
0.1050	0.0	0.0	0.0	0.0	0.0	0.0	0.0	0.0	0.0
0.1100	0.0	0.0	0.0	0.0	0.0	0.0	0.0	0.0	0.0
0.1150	0.0	0.0	0.0	0.0	0.0	0.0	0.0	0.0	0.0
0.1200	0.0	0.0	0.0	0.0	0.0	0.0	0.0	0.0	0.0
0.1250	0.0	0.0	0.0	0.0	0.0	0.0	0.0	0.0	0.0
0.1300	0.0	0.0	0.0	0.0	0.0	0.0	0.0	0.0	0.0
0.1350	0.0	0.0	0.0	0.0	0.0	0.0	0.0	0.0	0.0
0.1400	0.0	0.0	0.0	0.0	0.0	0.0	0.0	0.0	0.0
0.1450	0.0	0.0	0.0	0.0	0.0	0.0	0.0	0.0	0.0
0.1500	0.0	0.0	0.0	0.0	0.0	0.0	0.0	0.0	0.0
0.1550	0.0	0.0	0.0	0.0	0.0	0.0	0.0	0.0	0.0
0.1600	0.0	0.0	0.0	0.0	0.0	0.0	0.0	0.0	0.0
0.1650	0.0	0.0	0.0	0.0	0.0	0.0	0.0	0.0	0.0
0.1700	0.0	0.0	0.0	0.0	0.0	0.0	0.0	0.0	0.0
0.1750	0.0	0.0	0.0	0.0	0.0	0.0	0.0	0.0	0.0
0.1800	0.0	0.0	0.0	0.0	0.0	0.0	0.0	0.0	0.0
0.1850	0.0	0.0	0.0	0.0	0.0	0.0	0.0	0.0	0.0
0.1900	0.0	0.0	0.0	0.0	0.0	0.0	0.0	0.0	0.0
0.1950	0.0	0.0	0.0	0.0	0.0	0.0	0.0	0.0	0.0
0.2000	0.0	0.0	0.0	0.0	0.0	0.0	0.0	0.0	0.0

TABLE 10. NORMAL OUTPUT OF VEHICLE VALUES (page 2)

BODY KINEMATICS

TORSO

TIME	X-DISP.	X-VEL.	X-ACCEL.	Y-DISP.	Y-VEL.	Y-ACCEL.	Z-DISP.	Z-VEL.	Z-ACCEL.
0.0	19.40	536.10	-0.2154E 00	0.0	0.0	-0.3771E-03	18.00	0.0	0.5063E 00
0.0050	19.48	535.65	-0.2794E 00	-0.00	-0.00	-0.3763E-03	18.00	1.04	0.6249E 00
0.0100	19.74	534.92	-0.5235E 00	-0.00	-0.00	-0.3779E-03	18.01	2.63	0.1110E 01
0.0150	20.28	532.88	-0.2218E 01	-0.00	-0.20	-0.4374E 00	18.03	5.54	0.1698E 01
0.0200	20.94	525.48	-0.5453E 01	-0.00	-1.93	-0.1322E 01	18.07	8.92	0.1796E 01
0.0250	21.58	512.01	-0.8408E 01	-0.02	-4.88	-0.1640E 01	18.12	12.99	0.2479E 01
0.0300	22.24	492.84	-0.1152E 02	-0.05	-8.17	-0.1740E 01	18.20	18.36	0.2908E 01
0.0350	22.91	467.32	-0.1489E 02	-0.10	-11.54	-0.1736E 01	18.30	23.69	0.2576E 01
0.0400	23.58	435.37	-0.1813E 02	-0.17	-14.83	-0.1665E 01	18.43	28.13	0.1958E 01
0.0450	24.19	397.53	-0.2096E 02	-0.25	-17.97	-0.1579E 01	18.58	31.02	0.1013E 01
0.0500	24.75	354.99	-0.2273E 02	-0.35	-21.00	-0.1486E 01	18.74	31.82	-0.8515E-01
0.0550	25.21	310.46	-0.2334E 02	-0.46	-23.54	-0.1150E 01	18.90	31.07	-0.8708E 00
0.0600	25.60	268.36	-0.1531E 02	-0.58	-25.37	-0.6034E 00	19.05	32.99	0.8551E 01
0.0650	25.96	244.62	-0.1437E 02	-0.71	-26.44	-0.1024E 01	19.28	58.41	0.2421E 01
0.0700	26.31	200.42	-0.2618E 02	-0.85	-27.55	-0.1837E 00	19.58	55.43	-0.5812E 01
0.0750	26.35	148.38	-0.2766E 02	-0.99	-27.57	0.1820E 00	19.82	41.80	-0.8143E 01
0.0800	26.69	93.81	-0.2875E 02	-1.12	-26.80	0.1214E 00	19.99	24.62	-0.4462E 01
0.0850	26.74	37.68	-0.2924E 02	-1.25	-25.18	0.1942E 01	20.07	5.86	-0.4818E 01
0.0900	26.71	-18.69	-0.2896E 02	-1.37	-22.90	001293E 01	20.05	-12.88	-0.4454E 01
0.0950	26.60	-73.88	-0.2739E 02	-1.48	-20.23	0.1458E 01	19.94	-30.08	-0.8197E 01
0.1000	26.34	-123.46	-0.2418E 02	-1.58	-17.24	0.1645E 01	19.75	-43.91	-0.5967E 01
0.1050	25.86	-165.90	-0.1961E 02	-1.63	-13.89	0.1806E 01	19.51	-52.69	-0.3041E 01
0.1100	25.20	-199.02	-0.1468E 02	-1.71	-10.38	0.1789E 01	19.24	-55.57	0.2157E-01
0.1150	24.39	-221.58	-0.5270E 01	-1.76	-6.76	0.2823E 01	18.96	-51.39	0.8816E 01
0.1200	23.53	-222.78	-0.2292E 00	-1.78	-1.98	0.1471E 01	18.77	-26.15	0.9728E 01
0.1250	22.65	-228.77	-0.2677E 01	-1.78	-0.53	0.3683E 00	18.66	-22.48	-0.8930E 00
0.1300	21.75	-231.22	-0.4916E 00	-1.78	-0.19	0.3056E-01	18.54	-25.20	-0.1620E 01
0.1350	20.85	-231.38	0.2453E 00	-1.79	-0.46	-0.2841E 00	18.40	28.88	-0.2164E 01
0.1400	19.84	-230.71	0.7352E 00	-1.79	-1.16	-0.4422E 00	18.55	-32.31	-0.1618E 01
0.1450	19.05	-227.30	0.2568E 01	-1.80	-2.11	-0.5370E 00	18.08	-36.17	-0.2218E 01
0.1500	18.18	-221.75	0.3255E 01	-1.81	-3.22	-0.5921E 00	17.89	-40.47	-0.2434E 01
0.1550	17.34	-214.42	0.4219E 01	-1.83	-4.34	-0.5546E 00	17.67	-45.83	-0.3025E 01
0.1600	16.54	-205.62	0.4931E 01	-1.85	-5.33	-0.4567E 00	17.43	-52.01	-0.3370E 01
0.1650	15.79	-195.08	0.6052E 01	-1.88	-6.06	-0.2899E 00	17.15	-58.90	-0.3788E 01
0.1700	15.09	-182.22	0.7244E 01	-1.91	-6.07	0.3560E 00	16.84	-65.90	-0.3300E 01
0.1750	14.47	-167.28	0.8198E 01	-1.94	-4.61	0.1197E 01	16.49	-71.44	-0.2286E 01
0.1800	13.93	-150.79	0.8783E 01	-1.96	-1.01	0.2505E 01	16.13	-73.51	0.1269E 00
0.1850	13.47	-133.43	0.9153E 01	-1.95	4.73	0.3293E 01	15.76	-71.50	0.1693E 00
0.1900	13.09	-115.66	0.4176E 01	-1.91	11.50	0.3665E 01	15.42	-67.19	0.2719E 01
0.1950	12.81	-98.22	0.8813E 01	-1.83	18.74	0.3792E 01	15.10	-61.06	0.3626E 01
0.2000	12.61	-81.79	0.8162E 01	-1.72	26.02	0.3701E 01	14.31	-53.21	0.4483E 01

TABLE 11. NORMAL OUTPUT OF TORSO VALUES

BODY KINEMATICS

TORSO

	YAW			PITCH			ROLL		
TIME	DISP.	VEL.	ACCEL.	DISP.	VEL.	ACCEL.	DISP.	VEL.	ACCEL.
0.0	0.0	0.0	0.0	20.00	0.0	0.8688E 02	0.0	0.0	0.1210E 01
0.0050	-0.00	0.00	-0.1855E-01	20.00	0.05	-0.1986E 03	0.00	0.01	0.1197E 01
0.0100	-0.00	-0.00	-0.7021E-01	19.99	-3.24	-0.1324E 04	0.00	0.01	0.1170E 01
0.0150	-0.00	-3.90	-0.3249E 04	19.96	-12.30	-0.8619E 03	-0.00	-2.61	-0.2184E 04
0.0200	-0.09	-36.28	-0.9262E 04	19.90	-7.10	0.2903E 04	-0.06	-24.51	-0.6341E 04
0.0250	-0.39	-79.79	-0.6878E 04	19.91	13.60	0.5098E 04	-0.27	-56.79	-0.5857E 04
0.0300	-0.85	-99.51	-0.5584E 03	20.05	43.46	0.6861E 04	-0.61	-79.97	-0.3011E 04
0.0350	-1.32	-83.75	0.6885E 04	20.36	81.75	0.8312E 04	-1.04	-86.20	0.6149E 01
0.0400	-1.63	-32.51	0.1316E 05	20.88	124.82	0.8699E 04	-1.44	-73.62	0.4325E 04
0.0450	-1.61	40.62	0.1550E 05	21.61	166.16	0.7549E 04	-1.75	-45.09	0.6922E 04
0.0500	-1.23	109.45	0.1172E 05	22.52	196.58	0.3785E 04	-1.88	-10.36	0.6845E 04
0.0550	-0.55	157.91	0.7329E 04	23.52	199.99	-0.2380E 04	-1.85	23.25	0.6330E 04
0.0600	0.31	181.52	0.2513E 04	24.45	140.36	-0.3990E 05	-1.66	49.18	0.3564E 04
0.0650	1.22	173.61	-0.7263E 04	24.50	-123.54	-0.4588E 05	-1.41	37.90	-0.1186E 05
0.0700	1.94	106.37	-0.1753E 05	23.61	-196.00	-0.3143E 04	-1.32	11.39	-0.2735E 04
0.0750	2.24	13.99	-0.1828E 05	22.61	-201.54	0.1106E 04	-1.30	-5.88	-0.3590E 04
0.0800	2.10	-65.98	-0.1282E 05	21.64	-184.59	0.5618E 04	-1.37	-20.33	-0.1911E 04
0.0850	1.65	-108.26	-0.3782E 04	20.80	-146.62	0.9377E 04	-1.49	-26.20	0.2889E 03
0.0900	1.09	-105.28	0.4724E 04	20.19	-93.73	0.1132E 05	-1.60	-20.19	0.1029E 04
0.0950	0.66	-61.80	0.1251E 05	19.87	-39.02	0.9987E 04	-1.69	-15.05	0.1018E 04
0.1000	0.54	17.10	0.1857E 05	19.78	0.85	0.5549E 04	-1.75	-8.99	0.1551E 04
0.1050	0.87	115.39	0.1975E 05	19.83	13.83	-0.4534E 03	-1.77	0.42	0.2077E 04
0.1100	1.68	205.16	0.1531E 05	19.87	-2.78	-0.5921E 04	-1.74	9.05	0.9812E 03
0.1150	2.86	261.14	0.6728E 04	19.76	-56.82	-0.3131E 05	-1.69	15.70	0.8642E 04
0.1200	4.20	267.17	-0.4248E 04	18.93	-278.20	-0.3697E 05	-1.55	27.22	-0.5609E 04
0.1250	5.45	228.32	-0.9416E 04	17.29	-352.41	-0.8069E 04	-1.47	6.63	-0.3501E 04
0.1300	6.49	188.55	-0.6359E 04	15.43	-391.03	-0.6813E 04	-1.48	-9.09	-0.2613E 04
0.1350	7.38	163.08	-0.3489E 04	13.41	-417.81	-0.3974E 04	-1.56	-21.86	-0.2590E 04
0.1400	8.13	144.78	-0.5101E 04	11.27	-435.30	-0.2167E 04	-1.70	-18.38	-0.4136E 04
0.1450	8.72	73.98	-0.2281E 05	9.09	-434.61	0.1862E 04	-1.96	-67.12	-0.6929E 04
0.1500	8.78	-49.34	-0.2239E 05	6.95	-418.98	0.4755E 04	-2.38	-98.59	-0.4815E 04
0.1550	8.29	-141.41	-0.1676E 05	4.93	-384.77	0.8761E 04	-2.92	-114.90	-0.2258E 04
0.1600	7.37	-227.03	-0.1722E 05	3.13	-332.50	0.1215E 05	-3.52	-123.54	-0.1249E 04
0.1650	6.02	-310.46	-0.1576E 05	1.63	-264.38	0.1496E 05	-4.15	-128.29	-0.7728E 03
0.1700	4.29	-379.11	-0.1118E 05	0.51	-182.97	0.1759E 05	-4.79	-128.62	0.8365E 03
0.1750	2.28	-417.43	-0.3803E 04	-0.18	-88.79	0.2013E 05	-5.42	-120.36	0.2588E 04
0.1800	0.18	-416.68	0.4228E 04	-0.36	19.09	0.2297E 05	-5.97	-97.23	0.6594E 04
0.1850	-1.81	-374.02	0.1289E 05	0.03	139.56	0.2497E 05	-6.36	-57.38	0.8862E 04
0.1900	-3.49	-289.28	0.2072E 05	1.65	266.54	0.2567E 05	-6.53	-8.97	0.1052E 05
0.1950	-4.65	-170.71	0.2626E 05	2.70	392.31	0.2441E 05	-6.44	49.05	0.1287E 05
0.2000	-5.16	-31.13	0.2915E 05	4.95	507.19	0.2120E 05	-6.02	121.25	0.1614E 05

TABLE 11. NORMAL OUTPUT OF TORSO VALUES (page 2)

BELT LOADS

TIME	LEFT SHOULDER	RIGHT SHOULDER	LEFT SEAT BELT	RIGHT SEAT BELT	SUM OF SHOULDER RESTRAINTS	SUM OF SEAT BELTS
0.0	0.0	0.0	0.0	0.0	0.0	0.0
0.0050	0.0	0.0	12.5	12.5	0.0	25.0
0.0100	0.0	0.0	80.6	60.6	0.0	121.2
0.0150	120.2	0.0	172.9	173.6	120.2	346.5
0.0200	385.6	0.0	301.0	316.3	385.6	617.3
0.0250	568.8	79.2	410.7	459.9	672.0	870.6
0.0300	788.2	186.8	516.6	699.3	975.0	1125.9
0.0350	977.8	301.9	632.0	764.2	1279.7	1396.2
0.0400	1153.1	409.7	758.8	913.0	1562.8	1671.7
0.0450	1387.1	488.3	885.5	1045.3	1795.4	1940.8
0.0500	1400.0	500.0	1035.1	1155.7	1900.0	2100.8
0.0550	1400.0	500.0	1165.5	1242.0	1900.0	2408.5
0.0600	1400.0	500.0	1273.8	1292.5	1900.0	2572.3
0.0650	1400.0	488.3	1307.5	1287.3	1898.3	2594.8
0.0700	1400.0	485.5	1302.3	1264.5	1885.5	2566.8
0.0750	1400.0	476.2	1269.1	1249.6	1876.2	2518.7
0.0800	1470.0	479.6	1215.4	1243.1	1879.6	2458.4
0.0850	1480.0	495.3	1156.1	1244.1	1896.3	2400.1
0.0900	1395.2	500.0	1107.4	1251.2	1895.2	2358.6
0.0950	1349.2	500.0	1066.4	1247.4	1849.2	2313.8
0.1000	1287.7	493.2	1006.4	1195.6	1735.9	2202.1
0.1050	1030.4	466.1	919.0	1083.3	1516.9	2002.3
0.1100	807.6	398.7	810.9	923.9	1206.3	1734.8
0.1150	533.0	396.1	678.7	730.3	839.1	1409.1
0.1200	265.2	186.0	484.5	484.2	476.1	968.7
0.1250	80.5	53.6	270.5	247.2	150.2	517.7
0.1300	0.0	0.0	111.5	100.6	0.0	212.2
0.1350	0.0	0.0	0.0	0.0	0.0	0.0
0.1400	0.0	0.0	0.0	0.0	0.0	0.0
0.1450	0.0	0.0	0.0	0.0	0.0	0.0
0.1500	0.0	0.0	0.0	0.0	0.0	0.0
0.1550	0.0	0.0	0.0	0.0	0.0	0.0
0.1600	0.0	0.0	0.0	0.0	0.0	0.0
0.1650	0.0	0.0	0.0	0.0	0.0	0.0
0.1700	0.0	119.9	0.0	0.0	119.9	0.0
0.1750	0.0	282.2	0.0	10.8	282.2	10.8
0.1800	0.0	446.7	0.0	167.1	446.7	167.1
0.1850	0.0	500.0	0.0	310.3	500.0	310.3
0.1900	0.0	500.0	0.0	419.5	500.0	419.5
0.1950	0.0	500.0	0.0	495.3	500.0	495.3
0.2000	0.0	500.0	0.0	548.9	500.0	548.9

TABLE 12. NORMAL OUTPUT OF BELT VALUES

BELT ANGLES

TIME	LEFT SHOULDER			RIGHT SHOULDER			LEFT SEAT BELT			RIGHT SEAT BELT		
	X	Y	Z	X	Y	Z	X	Y	Z	X	Y	Z
0.0	33.6	68.1	65.9	72.5	108.2	154.3	58.2	73.8	143.4	58.2	106.2	143.4
0.0050	33.5	68.2	66.0	72.3	108.2	154.1	58.0	73.9	143.2	58.0	106.1	143.2
0.0100	33.0	68.4	66.3	71.5	108.1	153.6	57.1	74.0	142.4	57.1	106.0	142.4
0.0150	32.2	69.0	66.8	69.8	108.0	152.4	55.2	74.3	140.9	55.2	105.7	140.9
0.0200	31.2	69.7	67.4	67.8	107.4	151.0	53.1	74.7	139.0	53.1	105.3	139.0
0.0250	34.6	70.3	67.8	66.0	107.5	149.6	51.1	75.0	137.2	51.0	104.9	137.2
0.0300	26.8	71.1	68.1	64.1	107.4	148.0	49.0	75.4	135.3	48.9	104.5	135.3
0.0350	28.8	71.8	68.2	62.1	107.3	146.3	46.8	75.8	133.3	46.8	104.1	133.4
0.0400	28.4	72.6	68.3	60.3	107.2	146.7	44.6	75.2	131.3	44.8	103.8	131.5
0.0450	28.6	73.3	68.2	58.6	107.2	143.2	42.5	76.8	129.4	43.0	103.6	129.8
0.0500	27.7	74.0	68.0	57.2	107.3	141.8	40.5	77.3	127.7	41.5	103.5	128.3
0.0550	27.6	74.6	67.8	56.0	107.5	140.6	38.7	77.9	126.1	40.3	103.4	127.1
0.0600	27.8	75.2	67.5	55.0	107.8	139.5	37.3	78.5	124.9	39.3	103.7	126.0
0.0650	27.2	75.8	67.3	54.1	108.1	138.4	35.8	79.1	123.6	38.3	104.0	124.8
0.0700	26.8	76.6	67.2	53.1	108.5	137.2	34.8	79.5	122.2	37.3	104.4	123.5
0.0750	26.6	77.1	67.2	52.5	109.8	136.7	31.2	79.8	121.2	36.6	104.9	122.5
0.0800	26.3	77.6	67.2	51.9	109.4	135.5	32.5	80.2	120.6	35.2	105.4	121.8
0.0850	26.0	77.9	67.3	51.7	109.7	135.1	32.2	80.6	120.5	36.1	105.8	121.5
0.0900	25.8	78.1	67.4	51.9	110.0	135.1	32.3	80.9	120.7	36.3	106.2	121.5
0.0950	25.5	78.3	67.6	52.3	110.3	135.3	32.8	81.2	121.3	36.9	106.6	121.8
0.1000	25.4	78.4	67.8	53.2	110.6	136.0	33.7	81.5	122.3	37.9	107.0	122.7
0.1050	25.1	78.4	67.9	54.8	110.9	137.3	35.1	81.6	123.8	39.6	107.5	124.2
0.1100	25.1	78.8	67.9	56.9	111.1	139.1	37.0	81.5	125.7	41.8	108.0	126.2
0.1150	25.4	78.2	67.9	59.5	111.7	141.2	39.2	81.3	127.8	44.7	108.6	128.8
0.1200	25.5	77.9	67.9	62.3	112.1	143.3	41.5	80.9	110.0	47.8	109.5	131.4
0.1250	25.6	77.7	67.9	65.1	112.0	145.3	44.0	80.4	132.4	51.8	110.5	134.3
0.1300	25.7	77.5	67.9	68.1	113.1	147.3	46.9	79.9	135.1	55.3	111.5	137.4
0.1350	25.9	77.2	68.0	71.2	113.4	149.2	50.2	79.3	138.2	59.7	112.6	140.7
0.1400	25.9	76.8	68.2	74.4	113.7	151.1	54.0	78.8	141.7	64.6	113.5	144.2
0.1450	25.9	74.5	68.3	77.6	113.8	152.7	58.2	78.2	145.6	69.8	114.2	147.6
0.1500	25.9	76.3	68.4	80.6	113.9	154.1	69.0	77.8	149.9	74.9	114.6	150.6
0.1550	26.0	76.1	68.6	83.3	113.7	155.2	68.2	77.4	154.5	79.6	114.5	153.1
0.1600	26.0	76.9	68.7	85.7	113.5	156.1	73.7	77.2	159.0	83.7	114.1	154.9
0.1650	25.9	75.8	68.8	87.7	113.1	156.7	74.2	77.0	163.0	87.1	113.5	156.3
0.1700	25.8	75.7	69.0	89.4	112.7	157.3	84.4	77.0	165.8	89.7	112.7	157.3
0.1750	25.7	75.6	69.2	90.7	112.9	157.7	89.0	77.1	167.1	91.5	111.8	158.2
0.1800	25.6	75.4	69.5	91.7	111.8	158.1	92.8	77.2	166.8	92.5	110.9	158.9
0.1850	25.6	74.9	69.8	92.4	111.4	158.5	95.6	77.2	166.0	93.0	110.2	159.6
0.1900	25.9	74.0	70.2	92.9	110.9	158.9	97.2	77.3	165.4	93.1	109.5	160.2
0.1950	26.5	72.6	70.6	93.2	110.4	159.3	97.8	77.5	165.2	92.8	109.0	160.8
0.2000	27.6	70.7	71.0	93.5	110.0	159.7	97.4	77.7	165.5	92.3	108.6	161.2

TABLE 12. NORMAL OUTPUT OF BELT VALUES (page 2)

The next two pages are concerned with joint values. The first page is the torques actually produced in each of the joints against motion in the relative Euler angles (see Section 2.7). The second page lists the values of the relative angles together with the position of the hip with respect to the vehicle system. Table 13 shows the output for joints.

Then there usually follow several pages of contact output. Up to forty ellipsoid-contact interactions which actually produce force are reported over the time span of interest, four interactions per page. If more than forty interactions occur, only the first forty uninhibited for printing are reported although any additional are computed and their effects on the motion taken into account. If this occurs and the information on the addition interactions is necessary, it can be obtained by repeating the run after adding W-cards to inhibig the printing of some or all of the interactions reported in the current run (see Table 7, W-card). Table 14 is a typical page on contact output showing four interactions. The force is given rounded to the closest pound so forces less than a half pound are reported as zero. Deflection Value and Rate is the point of maximum impringement. Impact X and Y is the modified contact surface coordinates of the point of maximum impringement as explained in Section 2.5 and are in inches.

The optional kinetic energy printout and the "Injury Data" part of the output are self-explanatory and are included as Table 15. The reader who wises to learn more of the injury prediction features of this simulator is directed to reference 28.

If the Print Time Step is such that more than forty-one time points occur during the interval of interest, the complete normal output occurs for the first forty-one time points and then complete normal output is printed for the second forty-one time points where that last time point of the first printing becomes the first point of the second forty-one for sake of continuity.

2-D VS. 3-D COMPARISON. TEST NO. A-045, SATURATION TEST
UNITS ARE INCHES, DEGREES, POUNDS, and SECONDS UNLESS NOTED.

JOINT FORCES

	MOMENTS DUE TO JOINT ELASTICITY						MOMENTS DUE TO JOINT STOP					
	NECK			HIP			NECK			HIP		
TIME	YAW	PITCH	ROLL	YAW	PITCH	ROLL	YAW	PITCH	ROLL	YAW	PITCH	ROLL
0.0	0.0	0.0	0.0	0.0	0.0	0.0	0.0	0.0	0.0	0.0	0.0	0.0
0.0050	-0.0	0.1	0.0	0.0	-0.7	-0.0	0.0	0.0	0.0	0.0	0.0	0.0
0.0100	-0.0	0.4	0.0	0.0	-3.0	-0.0	0.0	0.0	0.0	0.0	0.0	0.0
0.0150	-0.0	0.3	-0.0	-0.0	-7.6	-0.0	0.0	0.0	0.0	0.0	0.0	0.0
0.0200	-0.7	1.3	-1.3	-1.1	-14.6	-0.4	0.0	0.0	0.0	0.0	0.0	0.0
0.0250	-2.8	7.6	-5.6	-4.8	-22.5	-1.9	0.0	0.0	0.0	0.0	0.0	0.0
0.0300	-5.7	22.6	-13.7	-16.6	-30.4	-4.5	0.0	0.0	0.0	0.0	0.0	0.0
0.0350	-7.7	49.2	-25.1	-16.9	-37.4	-7.9	0.0	0.0	0.0	0.0	0.0	0.0
0.0400	-6.8	98.0	-39.1	-21.4	-42.4	-11.5	0.0	0.0	0.0	0.0	0.0	0.0
0.0450	-1.6	146.6	-54.2	-22.7	-44.6	-14.8	0.0	0.0	0.0	0.0	0.0	0.0
0.0500	6.2	219.5	-68.2	-20.2	-43.3	-17.3	0.0	0.0	0.0	0.0	0.0	0.0
0.0550	10.4	297.8	-74.1	-15.0	-39.1	-18.8	0.0	0.0	0.0	0.0	0.0	0.0
0.0600	-7.9	418.1	-67.8	-8.7	-34.0	-19.0	0.0	9180.8	0.0	0.0	0.0	0.0
0.0650	112.6	415.7	-162.5	-2.7	-45.6	-18.7	0.0	12251.1	0.0	0.0	0.0	0.0
0.0700	325.6	376.9	-351.9	1.8	-74.5	-19.4	0.0	0.0	0.0	0.0	0.0	0.0
0.0750	344.1	215.1	-349.6	-0.9	-99.3	-18.8	0.0	0.0	0.0	0.0	0.0	0.0
0.0800	233.7	171.6	-290.7	-8.7	-116.1	-17.2	0.0	0.0	0.0	0.0	0.0	0.0
0.0850	157.8	168.9	-209.8	-19.9	-122.4	-15.1	0.0	0.0	0.0	0.0	0.0	0.0
0.0900	64.7	171.2	-91.7	-31.0	-117.1	-12.9	0.0	0.0	0.0	0.0	0.0	0.0
0.0950	-90.3	189.5	41.7	-38.6	-100.3	-11.3	0.0	0.0	0.0	0.0	0.0	0.0
0.1000	-235.6	211.0	176.3	-39.6	-74.3	-11.4	0.0	0.0	0.0	0.0	0.0	0.0
0.1050	-332.2	242.9	287.9	-31.5	-42.8	-13.9	0.0	0.0	0.0	0.0	0.0	0.0
0.1100	-343.4	302.1	332.3	-14.0	-11.2	-19.2	0.0	0.0	0.0	0.0	0.0	0.0
0.1150	-165.3	392.1	291.6	11.4	15.6	-26.9	0.0	6417.5	0.0	0.0	0.0	0.0
0.1200	69.1	397.2	4.8	39.3	22.6	-33.9	0.0	7653.8	0.0	0.0	0.0	0.0
0.1250	147.5	320.5	-34.3	65.0	8.3	-39.8	0.0	0.0	0.0	0.0	0.0	0.0
0.1300	146.1	233.2	2.4	68.3	-12.6	-43.8	0.0	0.0	0.0	0.0	0.0	0.0
0.1350	121.2	158.3	56.3	107.8	-38.3	-45.9	0.0	0.0	0.0	0.0	0.0	0.0
0.1400	95.9	58.7	109.5	125.2	-67.4	-46.3	0.0	0.0	0.0	0.0	0.0	0.0
0.1450	75.3	-44.0	137.2	139.7	-98.5	-45.8	0.0	0.0	0.0	0.0	0.0	0.0
0.1500	56.0	-145.2	156.6	146.9	-129.4	-45.0	0.0	0.0	0.0	0.0	0.0	0.0
0.1550	36.8	-244.2	163.4	146.6	-157.9	-44.5	0.0	0.0	0.0	0.0	0.0	0.0
0.1600	15.0	-377.0	159.9	140.9	-181.7	-44.6	0.0	0.0	0.0	0.0	0.0	0.0
0.1650	-7.8	-428.0	148.5	130.2	-198.9	-45.5	0.0	0.0	0.0	0.0	0.0	0.0
0.1700	-31.5	-498.7	131.3	115.5	-207.7	-47.3	0.0	0.0	0.0	0.0	0.0	0.0
0.1750	-53.7	-550.6	114.0	98.8	-207.3	49.7	0.0	0.0	0.0	0.0	0.0	0.0
0.1800	-70.3	-590.6	100.4	82.8	-197.8	-51.6	0.0	0.0	0.0	0.0	0.0	0.0
0.1850	-76.1	-628.7	97.8	70.2	-178.5	-51.5	0.0	0.0	0.0	0.0	0.0	0.0
0.1900	-66.9	-646.4	110.5	63.8	-152.9	-48.2	0.0	0.0	0.0	0.0	0.0	0.0
0.1950	-40.6	-647.3	139.4	65.7	-118.6	-41.3	0.0	0.0	0.0	0.0	0.0	0.0
0.2000	1.2	-629.4	181.4	77.2	-77.0	-31.0	0.0	0.0	0.0	0.0	0.0	0.0

TABLE 13. NORMAL OUTPUT OF JOINT VALUES.

2-D VS. 3-D COMPARISON. TEST NO. A-045, SATURATION TEST
UNITS ARE INCHES, DEGREES, POUNDS, AND SECONDS UNLESS NOTED.

	RELATIVE EULER ANGLES						RELATIVE HIP POSITION		
	HEAD			LEGS					
TIME	YAW	PITCH	ROLL	YAW	PITCH	ROLL	X	Y	Z
0.0	0.0	-35.0	0.0	0.0	-13.0	0.0	22.26	0.0	25.87
0.0050	0.0	-35.0	-0.0	-0.0	-13.0	0.0	22.34	-0.00	25.87
0.0100	0.0	-35.0	-0.0	-0.0	-12.8	0.0	22.60	-0.00	25.88
0.0150	0.0	-35.0	0.0	0.0	-12.5	0.0	23.14	-0.00	25.90
0.0200	0.1	-35.1	0.1	0.1	-12.0	0.0	23.79	-0.00	25.94
0.0250	0.3	-35.7	0.5	0.3	-11.4	0.1	24.43	-0.00	26.00
0.0300	0.5	-37.2	1.3	0.8	-10.8	0.3	25.11	-0.01	26.07
0.0350	0.7	-39.7	2.4	1.2	-10.3	0.6	25.83	-0.02	26.16
0.0400	0.6	-43.6	3.7	1.5	-10.0	0.8	26.56	-0.04	26.26
0.0450	0.2	-49.0	5.2	1.6	-9.8	1.1	27.28	-0.08	26.37
0.0500	-0.6	-56.0	6.6	1.4	-9.9	1.2	27.96	-0.14	26.47
0.0550	-1.8	-64.3	7.1	1.1	-10.2	1.3	28.96	-0.22	26.57
0.0600	0.6	-78.5	6.0	0.6	-10.6	1.4	29.00	-0.32	26.67
0.0650	-10.7	-74.7	15.5	0.2	-9.7	1.3	29.43	-0.43	26.90
0.0700	-31.1	-63.7	33.6	-0.1	-7.7	1.4	29.65	-0.54	27.25
0.0750	-32.9	-55.5	33.3	0.1	-5.9	1.3	29.76	-0.67	27.55
0.0800	-28.0	-51.4	27.8	0.6	-4.7	1.2	29.77	-0.81	27.77
0.0850	-16.9	-50.4	19.5	1.4	-4.2	1.1	29.71	-0.95	27.89
0.0900	-5.2	-51.3	8.8	2.2	-4.6	0.9	29.60	-1.08	27.90
0.0950	8.0	-50.1	-4.0	2.8	-5.8	0.8	29.44	-1.20	27.81
0.1000	2.5	-56.2	-17.0	2.8	-7.7	0.8	29.17	-1.29	27.63
0.1050	31.7	-58.2	-27.5	2.3	-9.9	1.0	28.70	-1.35	27.38
0.1100	32.8	-66.8	-31.7	1.0	-12.2	1.4	28.04	-1.38	27.11
0.1150	16.1	-72.4	-19.2	-0.8	-14.1	1.9	27.21	-1.37	26.84
0.1200	-6.6	-72.9	-0.5	-2.8	-14.6	2.4	26.22	-1.35	26.69
0.1250	-14.1	-65.6	3.3	-4.7	-13.6	2.8	25.11	-1.33	26.65
0.1300	-14.0	-57.8	-0.2	-6.3	-12.1	3.1	23.94	-1.32	26.61
0.1350	-11.6	-49.4	-5.4	-7.7	-10.3	3.3	22.74	-1.31	26.55
0.1400	-9.2	-49.3	-9.9	-9.0	-8.2	3.3	21.53	-1.31	26.46
0.1450	-7.2	-30.8	-13.1	-10.0	-5.9	3.3	20.31	-1.31	26.34
0.1500	-5.4	-21.1	-15.0	-10.5	-3.7	3.2	19.12	-1.31	26.19
0.1550	-3.4	-11.7	-15.6	-10.5	-1.7	3.2	17.99	-1.30	26.00
0.1600	-1.4	-2.8	-15.3	-10.1	0.0	3.2	16.52	-1.29	25.77
0.1650	0.7	6.1	-14.2	-9.3	1.2	3.3	15.96	-1.26	25.50
0.1700	3.0	12.0	-12.6	-8.3	1.9	3.4	15.11	-1.21	25.18
0.1750	5.1	17.6	-10.9	-7.1	1.8	3.6	14.41	-1.15	24.83
0.1800	6.7	22.0	-9.6	-5.9	1.2	3.7	13.87	-1.09	24.46
0.1850	7.3	25.1	-9.3	-5.0	-0.1	3.7	13.50	-1.02	24.09
0.1900	6.4	26.7	-10.6	-4.6	-2.0	3.4	13.30	-0.97	23.74
0.1950	3.9	26.8	-13.3	-4.7	-4.5	3.0	13.28	-0.93	23.41
0.2000	-0.1	25.1	-17.3	-5.5	-7.5	2.2	13.41	-0.91	23.11

TABLE 13. NORMAL OUTPUT OF JOINT VALUES (page 2)

	HIP AT SEAT CUSHION					KNEE AT SEAT CUSHION					KNEE AT LEFT PAN EDGE					RIGHT SIDE AT SEAT CUSHION				
TIME	FORCE	DEFLECTION VALUE	DEFLECTION RATE	IMPACT X	IMPACT Y	FORCE	DEFLECTION VALUE	DEFLECTION RATE	IMPACT X	IMPACT Y	FORCE	DEFLECTION VALUE	DEFLECTION RATE	IMPACT X	IMPACT Y	FORCE	DEFLECTION VALUE	DEFLECTION RATE	IMPACT X	IMPACT Y
0.0	38.	0.15	0.	11.0	14.8	147.	1.02	0.	11.0	26.6	0.	18.00	-0.	1.7	-2.0	0.	0.0	0.	0.0	0.0
0.0050	44.	0.17	8.	11.0	14.9	150.	1.02	4.	11.0	26.7	0.	18.00	-0.	1.6	-2.0	0.	0.0	0.	0.0	0.0
0.0100	65.	0.24	21.	11.0	15.1	157.	1.06	12.	11.0	27.0	0.	18.00	-0.	1.3	-1.9	0.	0.0	0.	0.0	0.0
0.0150	108.	0.38	34.	11.0	15.0	167.	1.14	19.	11.0	27.5	0.	18.00	-0.	0.8	-1.9	0.	0.0	0.	0.0	0.0
0.0200	158.	0.56	38.	11.0	16.3	170.	1.23	17.	11.0	28.1	0.	18.00	-0.	0.2	-1.8	0.	0.0	0.	0.0	0.0
0.0250	211.	0.76	41.	11.0	16.9	171.	1.31	15.	11.0	28.7	0.	18.00	-0.	-0.4	-1.7	0.	0.0	0.	0.0	0.0
0.0300	278.	0.98	47.	11.1	17.5	172.	1.38	15.	11.0	29.4	0.	18.00	-0.	-1.1	-1.6	5.	0.02	42.	5.7	17.8
0.0350	329.	1.23	52.	11.2	18.2	171.	1.46	16.	11.0	30.1	0.	18.00	-1.	-1.8	-1.5	49.	0.24	45.	5.7	18.5
0.0400	385.	1.49	54.	11.3	18.9	170.	1.54	16.	11.0	30.8	0.	17.99	-1.	-2.5	-1.5	95.	0.47	47.	5.7	19.3
0.0450	436.	1.76	53.	11.4	19.5	167.	1.63	17.	11.0	31.5	0.	0.0	0.	0.0	0.0	139.	0.71	47.	5.8	19.9
0.0500	461.	2.02	60.	11.5	20.1	165.	1.71	17.	11.1	32.1	0.	0.0	0.	0.0	0.0	180.	0.94	45.	5.8	20.5
0.0550	520.	2.26	45.	11.6	20.7	164.	1.80	18.	11.1	32.7	0.	0.0	0.	0.0	0.0	213.	1.16	42.	5.9	21.0
0.0600	559.	2.47	44.	11.7	21.1	164.	1.90	21.	11.1	33.1	0.	0.0	0.	0.0	0.0	245.	1.37	44.	6.0	21.4
0.0650	646.	2.77	77.	11.3	21.5	171.	2.02	23.	11.2	33.4	0.	0.0	0.	0.0	0.0	314.	1.67	77.	6.1	21.7
0.0700	732.	3.16	72.	11.9	21.6	182.	2.17	31.	11.2	33.6	0.	0.0	0.	0.0	0.0	381.	2.06	72.	6.2	21.7
0.0750	794.	3.47	54.	12.1	21.7	196.	2.33	33.	11.3	33.6	0.	0.0	0.	0.0	0.0	431.	2.38	54.	6.3	21.7
0.0800	824.	3.69	32.	12.2	21.7	212.	2.50	35.	11.4	33.6	0.	0.0	0.	0.0	0.0	462.	2.59	32.	6.5	21.7
0.0850	835.	3,79	8.	12.4	21.6	232.	2.68	36.	11.4	33.5	0.	0.0	0.	0.0	0.0	473.	2.69	9.	6.6	21.7
0.0900	813.	3.77	-14.	12.5	21.5	253.	2.86	38.	11.5	33.4	0.	0.0	0.	0.0	0.0	462.	2.68	-13.	6.7	21.6
0.0950	763.	3.65	-36.	12.6	21.4	275.	3.05	36.	11.6	33.2	0.	0.0	0.	0.0	0.0	428.	2.56	-36.	6.9	21.5
0.1000	689.	3.41	-59.	12.7	21.1	297.	3.21	28.	11.7	33.0	0.	0.0	0.	0.0	0.0	371.	2.32	-60.	7.0	21.3
0.1050	598.	3.07	-77.	12.8	20.7	320.	3.32	16.	11.8	32.6	0.	0.0	0.	0.0	0.0	288.	1.96	-80.	7.0	20.9
0.1100	502.	2.65	-87.	12.8	20.2	344.	3.36	3.	11.9	32.0	0.	0.0	0.	0.0	0.0	216.	1.53	-91.	7.0	20.2
0.1150	418.	2.21	-67.	12.9	19.4	385.	3.34	-11.	12.0	31.2	0.	0.0	0.	0.0	0.0	133.	1.07	-91.	7.0	19.3
0.1200	359.	1.84	-60.	12.9	18.5	382.	3.26	-23.	12.1	30.2	0.	0.0	0.	0.0	0.0	99.	0.69	-63.	7.0	18.3
0.1250	306.	1.55	-58.	12.9	17.5	390.	3.11	-36.	12.1	29.1	0.	0.0	0.	0.0	0.0	58.	0.38	-62.	7.0	17.1
0.1300	239.	1.25	-62.	12.9	16.4	384.	2.90	-49.	12.2	28.0	0.	0.0	0.	0.0	0.0	8.	0.06	-67.	7.0	15.8
0.1350	166.	0.93	-68.	13.0	15.3	363.	2.63	-61.	12.3	26.8	0.	0.0	0.	0.0	0.0	0.	0.0	0.	0.0	0.0
0.1400	58.	0.57	-73.	13.1	14.2	325.	2.30	-71.	12.4	25.7	0.	0.0	0.	0.0	0.0	0.	0.0	0.	0.0	0.0
0.1450	32.	0.20	-78.	13.1	13.1	272.	1.92	-79.	12.5	24.5	0.	0.0	0.	0.0	0.0	0.	0.0	0.	0.0	0.0
0.1500	0.	0.0	0.	0.0	0.0	208.	1.51	-85.	12.6	23.4	0.	0.0	0.	0.0	0.0	0.	0.0	0.	0.0	0.0
0.1550	0.	0.0	0.	0.0	0.0	135.	1.08	-87.	12.8	22.3	0.	0.0	0.	0.0	0.0	0.	0.0	0.	0.0	0.0
0.1600	0.	0.0	0.	0.0	0.0	80.	0.65	-86.	12.9	21.3	0.	0.0	0.	0.0	0.0	0.	0.0	0.	0.0	0.0
0.1650	0.	0.0	0.	0.0	0.0	29.	0.23	-83.	13.0	20.4	0.	0.0	0.	0.0	0.0	0.	0.0	0.	0.0	0.0
0.1700	0.	0.0	0.	0.0	0.0	0.	0.0	0.	0.0	0.0	0.	0.0	0.	0.0	0.0	0.	0.0	0.	0.0	0.0
0.1750	0.	0.0	0.	0.0	0.0	0.	0.0	0.	0.0	0.0	0.	0.0	0.	0.0	0.0	0.	0.0	0.	0.0	0.0
0.1800	0.	0.0	0.	0.0	0.0	0.	0.0	0.	0.0	0.0	0.	0.0	0.	0.0	0.0	0.	0.0	0.	0.0	0.0
0.1850	0.	0.0	0.	0.0	0.0	0.	0.0	0.	0.0	0.0	0.	0.0	0.	0.0	0.0	0.	0.0	0.	0.0	0.0
0.1900	0.	0.0	0.	0.0	0.0	0.	0.0	0.	0.0	0.0	0.	0.0	0.	0.0	0.0	0.	0.0	0.	0.0	0.0
0.1950	0.	0.0	0.	0.0	0.0	0.	0.0	0.	0.0	0.0	0.	0.0	0.	0.0	0.0	0.	0.0	0.	0.0	0.0
0.2000	0.	0.0	0.	0.0	0.0	0.	0.0	0.	0.0	0.0	0.	0.0	0.	0.0	0.0	0.	0.0	0.	0.0	0.0

TABLE 14. NORMAL OUTPUT OF CONTACT FORCES

2-D VS. 3-D COMPARISON. TEST NO. A-045, SATURATION TEST
UNITS ARE INCHES, DEGREES, POUNDS, and SECONDS UNLESS NOTED.

	BODY KINETIC ENERGY											
	TRANSLATIONAL				ROTATIONAL				TOTAL			
TIME	TORSO	HEAD	LEGS	ALL	TORSO	HEAD	LEGS	ALL	TORSO	HEAD	LEGS	ALL
0.0	33526.	5863.	18681.	59170.	0.	0.	0.	0.	33626.	5863.	18681.	58170.
0.0050	33570.	5864.	18615.	58049.	0.	0.	0.	0.	33570.	5864.	18616.	58049.
0.0100	33479.	5866.	18492.	57837.	0.	0.	1.	1.	33479.	5866.	18493.	57837.
0.0150	33226.	5862.	18208.	57296.	0.	0.	2.	2.	33226.	5862.	18210.	57299.
0.0200	32317.	5804.	17592.	55813.	1.	0.	4.	6.	32318.	5804.	17697.	55819.
0.0250	30695.	5684.	16922.	53300.	5.	3.	7.	14.	30700.	5686.	16928.	53314.
0.0300	28466.	5507.	15874.	49840.	12.	9.	9.	31.	28478.	5516.	15883.	49877.
0.0350	25633.	5271.	14537.	45441.	22.	22.	12.	56.	25655.	5293.	14549.	45497.
0.0400	22296.	4973.	12923.	40192.	36.	45.	13.	94.	22331.	5018.	12937.	40286.
0.0450	18640.	4511.	11083.	34335.	56.	79.	13.	148.	18696.	4690.	11096.	34482.
0.0500	14916.	4189.	9107.	28212.	77.	123.	11.	211.	14993.	4312.	9118.	28423.
0.0550	11455.	3731.	7105.	22291.	83.	170.	8.	261.	11537.	3901.	7114.	22552.
0.0600	9628.	2894.	5115.	16637.	49.	140.	8.	198.	8678.	3034.	5123.	16835.
0.0650	7482.	934.	3018.	11434.	44.	149.	26.	219.	7526.	1083.	3043.	11653.
0.0700	5148.	505.	1753.	7405.	75.	187.	19.	282.	5223.	692.	1772.	7688.
0.0750	2869.	277.	925.	4071.	72.	74.	8.	153.	2941.	351.	933.	4225.
0.0800	1185.	144.	408.	1736.	61.	43.	3.	107.	1246.	187.	411.	1844.
0.0850	244.	75.	158.	477.	43.	64.	9.	116.	287.	138.	167.	593.
0.0900	122.	45.	148.	315.	21.	104.	26.	151.	142.	150.	174.	466.
0.0950	784.	46.	375.	1205.	4.	125.	49.	179.	788.	172.	424.	1384.
0.1000	2044.	87.	846.	2977.	1.	109.	71.	180.	2044.	196.	917.	3157.
0.1050	3568.	183.	1541.	5292.	10.	90.	83.	182.	3577.	273.	1624.	5474.
0.1100	5008.	334.	2386.	7728.	28.	129.	81.	238.	5036.	463.	2467.	7966.
0.1150	6059.	516.	3295.	9869.	51.	206.	64.	320.	6109.	722.	3359.	10190.
0.1200	5887.	1315.	4437.	11630.	182.	73.	22.	277.	6070.	1388.	4459.	11916.
0.1250	6182.	1637.	5052.	12871.	256.	106.	13.	375.	6438.	1743.	5065.	13246.
0.1300	6329.	1701.	5373.	13404.	297.	117.	10.	423.	6627.	1818.	5383.	13827.
0.1350	6361.	1739.	5564.	13664.	331.	132.	7.	470.	6692.	1871.	5571.	14134.
0.1400	6340.	1752.	5691.	13791.	356.	143.	6.	505.	6705.	1895.	5697.	14296.
0.1450	6198.	1741.	5610.	13549.	348.	147.	6.	501.	6546.	1888.	5616.	14050.
0.1500	5947.	1708.	5352.	13006.	323.	144.	7.	474.	6270.	1852.	5358.	13480.
0.1550	5627.	1658.	4923.	12208.	284.	135.	8.	426.	5911.	1792.	4930.	12634.
0.1600	5266.	1596.	4354.	11216.	235.	119.	10.	364.	5501.	1715.	4364.	11580.
0.1650	4863.	1529.	3679.	10071.	190.	100.	14.	304.	5053.	1629.	3693.	10374.
0.1700	4397.	1458.	2938.	8793.	150.	82.	20.	258.	4553.	1540.	2957.	9051.
0.1750	3872.	1382.	2197.	7451.	133.	65.	27.	225.	4004.	1447.	2224.	7676.
0.1800	3293.	1293.	1521.	6107.	121.	50.	32.	203.	3413.	1343.	1553.	6310.
0.1850	2684.	1188.	957.	4829.	134.	37.	35.	205.	2818.	1225.	992.	5034.
0.1900	2109.	1066.	543.	3717.	192.	28.	36.	256.	2301.	1094.	579.	3973.
0.1950	1606.	937.	287.	2830.	308.	26.	36.	370.	1914.	963.	323.	3201.
0.2000	1193.	805.	172.	2171.	482.	30.	36.	548.	1675.	835.	209.	2718.

TABLE 15. OPTIONAL NORMAL OUTPUT

2-D VS. 3-D COMPARISON. TEST NO. A-045, SATURATION TEST
UNITS ARE INCHES, DEGREES, POUNDS, AND SECONDS UNLESS NOTED.

SUMMARY OF TOLERANCE DATA USED IN INJURY CRITERIA

QUANTITY	MAXIMUM ACCEPTABLE VALUE	NATURE OF INJURY OR DATA	WEIGHTING CODE
1. SEVERITY INDEX	1. 1000	1. INTERNAL HEAD INJURY. DANGEROUS TO LIFE.	1. 22/26
2. HEAD PITCH ACCELERATION	2. 2000 RAD/SEC/SEC	2. 50% CHANCE OF CEREBRAL CONCUSSION.	2. 12/26
3. HEAD LATERAL G-LEVEL	3. 46 G PEAK	3. HUMAN VOLUNTEER SUBJECT EXPERIENCED HEADACHE AND SORE NECK FOR 3 DAYS.	3. 1/26
4. CHEST LOAD	4. 1600 LB	4. RIB FRACTURE OF CADAVER.	4. 13/26
5. SHOULDER BELT LOAD	5. 1800 LB COMBINED	5. PREDICTED TOLERANCE LEVEL WITHOUT INJURY.	5. 1/26
6. PELVIC BELT LOAD	6. 5000 LB	6. MAXIMUM VOLUNTARY LOAD.	6. 1/26
7. KNEE LOAD (EACH)	7. 1500 LB	7. COMMINUTED PATELLA FRACTURE.	7. 12/26
8. CHEST A-P G-LOAD	8. 45 G PEAK	8. VOLUNTEER DATA WITH NO INJURY. (DURATION= .09 SEC, RISE TIME = 500 G/SEC) HIGHER RISE TIMES OR LONGER DURATIONS CAN DECREASE THIS VALUE SIGNIFICANTLY.	8. 4/26
9. CHEST S-I G-LOAD	9. 25 G PEAK	9. VOLUNTEER DATA. FRACTURED VERTEBRAE OBSERVED AT THIS LEVEL.	9. 16/26

LIST OF REFERENCES

1. GADD, C.W., ''USE OF A WEIGHTED-IMPULSE CRITERION FOR ESTIMATING INJURY HAZARD'', PROC. 10TH. STAPP CAR CRASH CONF., NOV. 1966, P. 95-100.
2. OMMAYA, A.K. ET AL, ''COMPARATIVE TOLERANCES FOR CEREBRAL CONCUSSION BY HEAD IMPACT AND WHIPLASH INJURY IN PRIMATES'', 1970 INTERNATIONAL AUTOMOBILE SAFETY CONFERENCE COMPENDIUM, SAE PUB. NO. P-30, P. 808-817.
3. ZABORONSKI, A.B., ''HUMAN TOLERANCE TO LATERAL IMPACT WITH LAP BELT ONLY'', PROC. 8TH. STAPP CAR CRASH CONF., OCT. 1964, P. 34-71.
4. GADD, C.W. AND PATRICK, L.M., ''SYSTEM VERSUS LABORATORY IMPACT TESTS FOR ESTIMATING INJURY HAZARD'', SAE PAPER NO. 680053, JAN. 1968.
5. -, ESTIMATED PROBABLE THRESHOLD OF INJURY BY BIOMECHANICS TASK FORCE OF SAE OCCUPANT RESTRAINT SYSTEMS SUBCOMMITTEE.
6. STAPP, J.P. AND ENFIELD, D.L., ''EVALUATION OF THE LAP-TYPE AUTOMOBILE SAFETY BELT WITH REFERENCE TO HUMAN TOLERANCE'', SAE PAPER NO. 62A, 1958.
7. SNYDER, R.G.,''HUMAN IMPACT TOLERANCE'', 1970 INTERNATIONAL AUTOMOBILE SAFETY CONFERENCE COMPENDIUM, SAE PUB. NO. P-30, P. 712-782.
8. IBID.
9. IBID.

NOTE: THE WEIGHTING CODE IS BASED ON VAN KIRK, D.J. AND LANGE, W.A., ''A DETAILED INJURY SCALE FOR ACCIDENT INVESTIGATION'', PROC. OF THE 12TH. STAPP CAR CRASH CONFERENCE, OCT. 1968, P. 240-259. MINOR INJURY = 1-4/26, MODERATE INJURY = 8-10/26, MODERATELY SEVERE INJURY = 12-14/26, SEVERE INJURY = 16-18/26, CRITICAL INJURY = 20-22/26, FATAL INJURY = 24-26/26.

SUMMARY OF ANGULAR MOTION LIMITS USED IN INJURY CRITERIA

JOINT	MOTION	DIRECTION	STIFF TORSO
1. NECK	PITCH	HYPEREXTENSION	60 DEG
	PITCH	FLEXION	60 DEG
	ROLL	LATERAL FLEXION	40 DEG
	YAW	ROTATION	70 DEG
2. HIP	PITCH	HYPEREXTENSION	0 DEG
	PITCH	FLEXION	120 DEG
	ROLL	LATERAL FLEXION	0 DEG
	YAW	LEG SPREAD	30 DEG

NOTE: ALL QUANTITIES MEASURED FROM AN ERECT STANDING POSITION EXCEPT LEG SPREAD

NOTE: THESE DATA ARE DERIVED FROM SAE 1963 AND REPRESENT VOLUNTARY MOTION RANGES.

TABLE 15. OPTIONAL NORMAL OUTPUT (page 3)

SUMMARY OF QUANTITIES EXCEEDING TOLERANCES

QUANTITY	PEAK	TIME OF OCCURRENCE	DURATION	TIME START	TIME END	WEIGHTING CODE
SEVERITY INDEX	89297.2	0.2000	0.1506	0.0494	0.2000	22
NECK PITCH ANGLE	-74.7	0.0650	0.0199	0.0524	0.0723	0
NECK PITCH ANGLE	-72.9	0.1800	0.0220	0.1066	0.1286	0
HIP PULL ANGLE	3.7	0.1880	0.2000	0.0	0.2000	0
HEAD PITCH ACCELERATION	510210.7	0.0650	0.0123	0.0560	0.0683	12
HEAD PITCH ACCELERATION	-116386.1	0.0750	0.0018	0.0746	0.0756	12
HEAD SIDE ACCELERATION	339683.1	0.1150	0.0124	0.1103	0.1232	12
HEAD SIDE ACCELERATION	1055.5	0.0050	0.0903	0.0513	0.1416	1
CHEST FORWARD ACCELERATION	59.1	0.1700	0.0193	0.1590	0.1783	1
CHEST FORWARD ACCELERATION	61.1	0.0650	0.0060	0.0600	0.0661	4
	1900.0	0.0500	0.0520	0.0452	0.0972	1
CHEST S-1 ACCELERATION	-75.7	0.0050	0.0134	0.0565	0.0899	16
CHEST S-1 ACCELERATION	-52.3	0.1250	0.0121	0.1112	0.1234	16
CHEST S-1 ACCELERATION	35.4	0.1850	0.0349	0.1636	0.1985	16

TABLE 15. OPTIONAL NORMAL OUTPUT (page 4)

PROBABILITY OF OCCURRENCE

THE PROBABILITY OF OCCURRENCE IS BASED ON:

1. PROBABILITY OF FRONT COLLISION - 0.3900
2. PROBABILITY OF RIGHT FRONT PASSENGER - 0.2920
3. PROBABILITY OF SHOULDER & LAP BELT USE - 0.0460

PROBABILITY OF OCCURRENCE - 0.0052

TABLE 15. OPTIONAL NORMAL OUTPUT (page 5)

4.3 DESCRIPTION OF AUXILLARY PROGRAM OUTPUT.

Auxillary or debugging printout for this program is organized in terms of sixteen four-level switches. Each switch corresponds to a particular section of the program. The levels of a particular switch control the depth of detail of the debugging printout from the section of the program which the switch covers. Higher levels of a switch include all the printout from lower levels from the switch.

The four levels are represented by intergers zero through three. Zero represents no debugging printout, and high levels are represented by larger integers as described in Table 16.

TABLE 16. DEBUG SWITCH DEFINITION

0 = summary output only

1 = primary debugging information such as forces

2 = secondary debugging information such as the contributions to the generalized force vector of each force component.

3 = tertiary debugging information to allow a detailed inspection of the inner workings of the program.

To avoid needless volume of printing, each of the sixteen switches is allowed to vary its level as a function of simulated time during a run of the program. In order to avoid inputing sixteen separate tables of debug level versus effective time, advantage is taken of the binary characteristics of the IBM 360/67 computer. The four levels of a debugging switch can be represented by two binary bits. The possibilities for all sixteen switches can then be represented by thirty-two bits. Eight hexadecimal digits also represent thirty-two bits. Hence debugging control is achieved by use of a table of eight hexadecimal digit control words versus effective time. When any or all of the switches

change levels, a new control word in the table is needed. The switches correspond to groups of two bits from the left of the word, i.e., switch one is controlled by the left-most two bits, switch two by the next two, and so on. The switch will take on the specified level at the first time step in simulated time beyond the effective time specified.

As an example setup of the hexadecimal debugging control word, consider the case where printout of the quantity "QJ," the joint generalized force vector, is desired. This is specified under debug switch 4, debug level 2. As each digit of the hexadecimal word covers two debug switches, this printout will be covered by the second two bits of the second digit. Because no special printout is desired from debug switch 3, the first two bits describing the second hexadecimal digit must be "00." Because the desired debug level is 2, the last two bits of the second digit must be "10." Therefore the second digit takes on the value "0010" or "2." Thus, the hexadecimal word will be "02000000" at the effective time.

The table of effective times and control words is specified to the program by means of the P-card described in Table 7. The total span of simulated time for the run should be covered by effective times of control words if the P-card is used at all. Removals from control word tables can be made by use of the O-card with a table number of seven and new additions by the P-card again.

The user is warned that the volume of printout is startlingly huge and hence utmost discretion must be exercised in the use of this feature.

Table 17 contains a detailed list of the sixteen debug switches and the quantities which will be printed for each debug level of each switch. Table 17 should be used in conjunction with the Symbol Dictionary (see Section 4.8), Table 26, and (in some cases) a listing of the program. Each line in Table 17 corresponds to one line in the printed output so this table can be used to identify individual quantities. In some cases, it has been necessary because

TABLE 17. DEBUG FORMATS

Debug Switch	Debug Level	Quantity	SUBROUTINE
1	1	1 BXA(1) BYA(1) BZA(1) BXA(2) BYA(2) BZA(2)	BELT
1	2	1 BX BY BZ BXD BYD BZD	BELT
1	3	1 BC(1) BC(2) BC(3) BC(4) BC(5) BC(6) BC(7) BC(8) BC(9) BC(10) BC(11) BC(12)	BELT
2	1	2 J DELB(J) DELD(J) FB(J) (inside a 4-deep loop on J)	BELT
2	2	2 QB(1) QB(2) QB(3) QB(4) QB(5) QB(6) QB(7) QB(8) QB(9) QB(10) QB(11) QB(12)	BELT
2	3	2 J PDB(J,1) PDB(J,2) PDB(J,3) PDB(J,4) PDB(J,5) PDB(J,6) (inside a 4-deep loop on J)	BELT
3	1	3 T KNTOT KNTACC KNTDUB	STASH
3	2	11 values of ICOUNT(I) for I=1,11 10 values of ICOUNT(I) for I=12,21	STASH
4	1	4 DA(1,1) DD(1,1) EJ(1,1) SJ(1,1) DA(1,2) DD(1,2) EJ(1,2) SJ(1,2) DA(1,3) DD(1,3) EJ(1,3) SJ(1,3) DA(2,1) DD(2,1) EJ(2,1) SJ(2,1) DA(2,2) DD(2,2) EJ(2,2) SJ(2,2) DA(2,3) DD(2,3) EJ(2,3) SJ(2,3)	JOINT
4	2	4 QJ(1) QJ(2) QJ(3) QJ(4) QJ(5) QJ(6) QJ(7) QJ(8) QJ(9) QJ(10) QJ(11) QJ(12)	JOINT
4	3	4 ATHA ENPSI DPSI ENPHI DPHI These quantities are inside a 2-deep loop.	JOINT

TABLE 17. DEBUG FORMATS (page 2)

Debug Switch	Debug Level	Quantity	SUBROUTINE
4	3	4 PDA(1,1,1) PDA(1,1,2) PDA(1,1,3) PDA(1,1,4) PDA(1,1,5) PDA(1,1,6) PDA(1,2,1) PDA(1,2,2) PDA(1,2,3) PDA(1,2,4) PDA(1,2,5) PDA(1,2,6) PDA(1,3,1) PDA(1,3,2) PDA(1,3,3) PDA(1,3,4) PDA(1,3,5) PDA(1,3,6)	JOINT
4	3	PDA(2,1,1) PDA(2,1,2) PDA(2,1,3) PDA(2,1,4) PDA(2,1,5) PDA(2,1,6) PDA(2,2,1) PDA(2,2,2) PDA(2,2,3) PDA(2,2,4) PDA(2,2,5) PDA(2,2,6) PDA(2,3,1) PDA(2,3,2) PDA(2,3,3) PDA(2,3,4) PDA(2,3,5) PDA(2,3,6)	JOINT
5	1	5 1 BC(29,I) BC(30,I) BC(31,I) BC(32,I) These quantities are inside an up to 25-deep loop on I.	CONTAC
5	1	5 1 XHAT(1) XHAT(2) XHAT(3) XHAT(4) XHAT(5) XHAT(6) XHAT(7) XHAT(8) XHAT(9) DHAT(1) DHAT(2) DAHT(3) DHAT(4) DHAT(5) DHAT(6) DHAT(7) DHAT(8) DHAT(9) These quantities are inside an up to 25-deep loop on I.	CONTAC
5	1	5 1 I BC(4,I) BC(5,I) BC(6,I) BC(7,I) BC(8,I) BC(9,I) BC(10,I) BC(11,I) BC(12,I) *BC(41,I) These quantities are inside an up to 25-deep loop on I.	CONTAC
5	2	5 2 I BB(1,I) BB(2,I) BB(3,I) BB(4,I) BB(5,I) BB(6,I) BB(7,I) BB(8,I) *BB(9,I) BB(10,I) BB(11,I) BB(12,I) BC(14,I) BC(15,I) BC(16,I) BC(17,I) BC(18,I) *BC(19,I) BC(20,I) BC(21,I) BC(22,I) BC(23,I)	CONTAC

TABLE 17. DEBUG FORMATS (page 3)

Debug Switch	Debug Level	Quantity	SUBROUTINE
5	3	5 3 DDC(I) DMC(1,I) DMC(2,I) DMC(3,I) DDS(I) These quantities are inside an up to 25-deep loop on I.	CONTAC
5	3	5 3 BC(33,I) BC(34,I) BC(35,I) BC(36,I) BC(37,I) BC(38,I) These quantities are inside an up to 25-deep loop on I.	CONTAC
6	1	6 1 I AL(8,I) AL(9,I) AL(10,I) These quantities are inside an up to 10-deep loop on I.	CONTAC
6	2	6 2 I J AL(21,I) AL(22,I) AL(23,I) AL(24,I) AL(25,I) AL(26,I) AL(27,I) AL(28,I) *AL(29,I) These quantities are inside an up to 10-deep loop on I.	CONTAC
6	3	6 3 ALC(1) ALC(2) ALC(3) ALC(4) ALC(5) ALC(6) ALC(7) ALC(8) ALC(9) ALC(10)	CONTAC
7	1	7 1 I J ETA ETAD FT TSQ SFAC TSR RFAC These quantities are inside nested loops on I=1,10 and J=1,25.	CONTAC
7	2	QS(1) QS(2) QS(3) QS(4) QS(5) QS(6) QS(7) QS(8) QS(9) QS(10) QS(11) QS(12)	CONTAC
7	3	7 3 XZ YZ ZZ ETA XZA YZA ZZA TSP XZB YZB ZZB TSQ These quantities are inside nested loops on I=1,10 and J=1,25.	CONTAC
7	3	7 3 DD(1) DD(2) DD(3) DD(4) DD(5) DD(6) DD(7) DD(8) DD(9) DD(10) DD(11) DD(12) These quantities are inside nested loops on I=1,10 and J=1,25.	CONTAC
7	3	QS(1) QS(2) QS(3) QS(4) QS(5) QS(6) QS(7) QS(8) QS(9) QS(10) QS(11) QS(12) These quantities are inside nested loop on I=1,10 and J=1,25. This printout shows the build up of the vector reported in its final form at level two.	CONTAC

TABLE 17. DEBUG FORMATS (page 4)

Debug Switch	Debug Level	Quantity	SUBROUTINE
8	1	CARTIN CARTV(1,1) CARTV(2,1) CARTV(3,1) CARTV(1,2) CARTV(2,2) CARTV(3,2) CARTV(1,3) CARTV(2,3) CARTV(3,3) CARTV(1,4) CARTV(2,4) CARTV(3,4) CARTV(1,5) CARTV(2,5) CARTV(3,5) CARTV(1,6) CARTV(2,6) CARTV(3,6)	CARTIN
9	1	9 MT IT ILIM TT(1) MILL	MAIN
9	2	1 XXX(1,1,1) XXX(1,1,2) XXX(1,1,3) PCV(1) PCX(1) 2 XXX(1,2,1) XXX(1,2,2) XXX(1,2,3) PCV(2) PCX(2) 3 XXX(1,3,1) XXX(1,3,2) XXX(1,3,3) PCV(3) PCX(3) 4 XXX(1,4,1) XXX(1,4,2) XXX(1,4,3) PCV(4) PCX(4) 5 XXX(1,5,1) XXX(1,5,2) XXX(1,5,3) PCV(5) PCX(5) 6 XXX(1,6,1) XXX(1,6,2) XXX(1,6,3) PCV(6) PCX(6) 7 XXX(1,7,1) XXX(1,7,2) XXX(1,7,3) PCV(7) PCX(7) 8 XXX(1,8,1) XXX(1,8,2) XXX(1,8,3) PCV(8) PCX(8) 9 XXX(1,9,1) XXX(1,9,2) XXX(1,9,3) PCV(9) PCX(9) 10 XXX(1,10,1) XXX(1,10,2) XXX(1,10,3) PCV(10) PCX(10) 11 XXX(1,11,1) XXX(1,11,2) XXX(1,11,3) PCV(11) PCX(11) 12 XXX(1,12,1) XXX(1,12,2) XXX(1,12,3) PCV(12) PCX(12)	MAIN

TABLE 17. DEBUG FORMATS (page 5)

Debug Switch	Debug Level	Quantity	SUBROUTINE
9	3	J TT(J) XXX(J,1,1) XXX(J,1,2) XXX(J,1,3) XXX(J,2,1) XXX(J,2,2) XXX(J,2,3) XXX(J,3,1) XXX(J,3,2) XXX(J,3,3) XXX(J,4,1) XXX(J,4,2) XXX(J,4,3) XXX(J,5,1) XXX(J,5,2) XXX(J,5,3) XXX(J,6,1) XXX(J,6,2) XXX(J,6,3) XXX(J,7,1) XXX(J,7,2) XXX(J,7,3) XXX(J,8,1) XXX(J,8,2) XXX(J,8,3) XXX(J,9,1) XXX(J,9,2) XXX(J,9,3) XXX(J,10,1) XXX(J,10,2) XXX(J,10,3) XXX(J,11,1) XXX(J,11,2) XXX(J,11,3) XXX(J,12,1) XXX(J,12,2) XXX(J,12,3) for J=2,10	MAIN
10	1	10 J I ITST(I,J) D DD F TEPS(I,J) OMT(I,J)	NEWLOF
11	1	11 UX(1) UV(1) Q(1) UA(1) UX(2) UV(2) Q(2) UA(2) UX(3) UV(3) Q(3) UA(3) UX(4) UV(4) Q(4) UA(4) UX(5) UV(5) Q(5) UA(5) UX(6) UV(6) Q(6) UA(6) UX(7) UV(7) Q(7) UA(7) UX(8) UV(8) Q(8) UA(8) UX(9) UV(9) Q(9) UA(9) UX(10) UV(10) Q(10) UA(10) UX(11) UV(11) Q(11) UA(11) UX(12) UV(12) Q(12) UA(12)	ACCEL
11	2	11 EM(1,1) EM(1,2) EM(1,3) EM(1,4) EM(1,5) EM(1,6) EM(1,7) EM(1,8) EM(1,9) EM(1,10) EM(1,11) EM(1,12) EM(2,1) EM(2,2) EM(2,3) EM(2,4) EM(2,5) EM(2,6) EM(2,7) EM(2,8) EM(2,9) EM(2,10) EM(2,11) EM(2,12)	ACCEL

TABLE 17. DEBUG FORMATS (page 6)

Debug Switch	Debug Level		Quantity						SUBROUTINE
			(Continued from previous page)						
11	2	11	EM(3,1)	EM(3,2)	EM(3,3)	EM(3,4)	EM(3,5)	EM(3,6)	ACCEL
			EM(3,7)	EM(3,8)	EM(3,9)	EM(3,10)	EM(3,11)	EM(3,12)	
			EM(4,1)	EM(4,2)	EM(4,3)	EM(4,4)	EM(4,5)	EM(4,6)	
			EM(4,7)	EM(4,8)	EM(4,9)	EM(4,10)	EM(4,11)	EM(4,12)	
			EM(5,1)	EM(5,2)	EM(5,3)	EM(5,4)	EM(5,5)	EM(5,6)	
			EM(5,7)	EM(5,8)	EM(5,9)	EM(5,10)	EM(5,11)	EM(5,12)	
			EM(6,1)	EM(6,2)	EM(6,3)	EM(6,4)	EM(6,5)	EM(6,6)	
			EM(6,7)	EM(6,8)	EM(6,9)	EM(6,10)	EM(6,11)	EM(6,12)	
			EM(7,1)	EM(7,2)	EM(7,3)	EM(7,4)	EM(7,5)	EM(7,6)	
			EM(7,7)	EM(7,8)	EM(7,9)	EM(7,10)	EM(7,11)	EM(7,12)	
			EM(8,1)	EM(8,2)	EM(8,3)	EM(8,4)	EM(8,5)	EM(8,6)	
			EM(8,7)	EM(8,8)	EM(8,9)	EM(8,10)	EM(8,11)	EM(8,12)	
			EM(9,1)	EM(9,2)	EM(9,3)	EM(9,4)	EM(9,5)	EM(9,6)	
			EM(9,7)	EM(9,8)	EM(9,9)	EM(9,10)	EM(9,11)	EM(9,12)	
			EM(10,1)	EM(10,2)	EM(10,3)	EM(10,4)	EM(10,5)	EM(10,6)	
			EM(10,7)	EM(10,8)	EM(10,9)	EM(10,10)	EM(10,11)	EM(10,12)	
			EM(11,1)	EM(11,2)	EM(11,3)	EM(11,4)	EM(11,5)	EM(11,6)	
			EM(11,7)	EM(11,8)	EM(11,9)	EM(11,10)	EM(11,11)	EM(11,12)	
			EM(12,1)	EM(12,2)	EM(12,3)	EM(12,4)	EM(12,5)	EM(12,6)	
			EM(12,7)	EM(12,8)	EM(12,9)	EM(12,10)	EM(12,11)	EM(12,12)	

TABLE 17. DEBUG FORMATS (page 7)

Debug Switch	Debug Level	Quantity	SUBROUTINE
11	3	11 U(1,1) U(1,2) U(1,3) U(1,4) UP(1,1) UP(1,2) UP(1,3) UP(1,4) U(2,1) U(2,2) U(2,3) U(2,4) UP(2,1) UP(2,2) UP(2,3) UP(2,4) U(3,1) U(3,2) U(3,3) U(3,4) UP(3,1) UP(3,2) UP(3,3) UP(3,4) U(4,1) U(4,2) U(4,3) U(4,4) UP(4,1) UP(4,2) UP(4,3) UP(4,4)	ACCEL
11	3	11 V(1,1) V(1,2) V(1,3) V(1,4) V(2,1) V(2,2) V(2,3) V(2,4) V(3,1) V(3,2) V(3,3) V(3,4) V(4,1) V(4,2) V(4,3) V(4,4) W(1,1) W(1,2) W(1,3) W(1,4) W(2,1) W(2,2) W(2,3) W(2,4) W(3,1) W(3,2) W(3,3) W(3,4) W(4,1) W(4,2) W(4,3) W(4,4) W(5,1) W(5,2) W(5,3) W(5,4) W(6,1) W(6,2) W(6,3) W(6,4)	ACCEL
12	1	12 QG(1) QG(2) QB(3) QG(4) QG(5) QG(6) QG(7) QG(8) QG(9) QG(10) QG(11) QG(12) QT(1) QT(2) QT(3) QT(4) QT(5) QT(6) QT(7) QT(8) QT(9) QT(10) QT(11) QT(12)	ACCEL
12	3	12 TA(1) TB(1) TC(1,1) TC(2,1) TC(3,1) TD(1,1) TD(2,1) TD(3,1) TD(4,1) TD(5,1) TD(6,1) TD(7,1) TD(8,1) QTD(1,1) QTD(2,1) QTD(3,1) TA(2) TB(2) TC(1,2) TC(2,2) TC(3,2) TD(1,2) TD(2,2) TD(3,2) TD(4,2) TD(5,2) TD(6,2) TD(7,2) TD(8,2) QTD(1,2) QTD(2,2) QTD(3,2) TA(3) TD(3) TC(1,3) TC(2,3) TC(3,3) TD(1,3) TD(2,3) TD(3,3) TD(4,3) TD(5,3) TD(6,3) TD(7,3) TD(8,3) QTD(1,3) QTD(2,3) QTD(3,3)	ACCEL
13	1	13 IT DEL TS TSA TSB	LIMIT

TABLE 17. DEBUG FORMATS (page 8)

Debug Switch	Debug Level	Quantity	SUBROUTINE
13	2	13 1 UA(1) DUM(1) 2 UA(2) DUM(2) 3 UA(3) DUM(3) 4 UA(4) DUM(4) 5 UA(5) DUM(5) 6 UA(6) DUM(6) 7 UA(7) DUM(7) 8 UA(8) DUM(8) 9 UA(9) DUM(9) 10 UA(10) DUM(10) 11 UA(11) DUM(11) 12 UA(12) DUM(12) DUM here contains the extrapolated accelerations $\ddot{q}'_k$	LIMIT
14	1	14 T TDCUR XHPP SII ACN(1) ACN(2) ACN(3) ACN(4) ACN(5) ACN(6) ACN(7) ACN(8) ACN(9)	STASH
14	2	14 2 YHPP(IMAX) XCPP(IMAX) YCPP(IMAX)	STASH
15	1	15 XCN(1) XCN(2) XCN(3) XCN(4) XCN(5) XCN(6) XCN(7) XCN(8) XCN(9) VCN(1) VCN(2) VCN(3) VCN(4) VCN(5) VCN(6) VCN(7) VCN(8) VCN(9)	CONTAC
15	1	15 ST(1,6) ST(2,6) ST(3,6) ST(1,1) ST(2,1) ST(3,1) ST(1,5) ST(2,5) ST(3,5) ST(1,2) ST(2,2) ST(3,2) ST(1,4) ST(2,4) ST(3,4) ST(1,3) ST(2,3) ST(3,3) IST(1) IST(2)	CONTAC
15	2	15 2 I CE(1,I) CE(2,I) CE(3,I) CE(4,I) CE(5,I) CE(6,I) CE(7,I) CE(8,I) CE(9,I) CH(1,I) CH(2,I) CH(3,I) These quantities are inside a 3-deep loop on I.	CONTAC
15	2	15 2 CD(1,1) CD(2,1) CD(3,1) CD(4,1) CD(5,1) CD(6,1) CD(1,2) CD(2,2) CD(3,2) CD(4,2) CD(5,2) CD(6,2) CD(1,3) CD(2,3) CD(3,3) CD(4,3) CD(5,3) CD(6,3)	CONTAC

TABLE 17. DEBUG FORMATS (page 9)

Debug Switch	Debug Level	Quantity	SUBROUTINE
15	3	15 DUM(1) DUM(2) DUM(3) DUM(4) DUM(5) DUM(6) DUM(7) DUM(8) DUM(9) DUM(10) DUM(11) DUM(12) DUM(13) DUM(14) DUM(15) DUM(16) DUM(17) DUM(18) DUM(19) DUM(20) DUM(21) DUM(22) DUM(23) DUM(24) DUM(25) DUM(26) DUM(27) DUM(28) DUM(29) DUM(30) DUM(31) DUM(32) DUM(33) Here DUM contains corner determination temp. storage.	CONTAC
15	3	15 3 DT(1,I) DT(2,I) DT(3,I) DT(4,I) DT(5,I) DT(6,I) DT(7,I) DT(8,I) DT(9,I) DT(10,I) DT(11,I) DT(12,I) DT(13,I) DT(14,I) DT(15,I) DT(16,I) DT(17,I) DT(18,I) DT(19,I) DT(20,I) DT(21,I) DT(22,I) DT(23,I) DT(24,I) DT(25,I) DT(26,I) DT(27,I) DT(28,I) DT(29,I) DT(30,I) DT(31,I) DT(32,I) DT(33,I) DT(34,I) DT(35,I) DT(36,I) DT(37,I) DT(38,I) DT(39,I) DT(40,I) DT(41,I) DT(42,I) DT(43,I) DT(44,I) DT(45,I) DT(46,I) DT(47,I) DT(48,I) DT(49,I) DT(50,I) DT(51,I) DT(52,I) DT(53,I) DT(54,I) CC(1,I) CC(2,I) CC(3,I) CC(4,I) CC(5,I) CC(6,I) CC(7,I) CC(8,I) CC(9,I)	CONTAC
16	1	16 1 T XHPP	SPX
16	1	16 1 T XCPP ZCPP YHPP	SPY
16	2	16 2 IQT IE TOL F 1 TIM(1) QT(1) 2 TIM(2) QT(2) 3 TIM(3) QT(3) 4 TIM(4) QT(4) 5 TIM(5) QT(5) 6 TIM(6) QT(6) . . . . 40 TIM(40) QT(40) 41 TIM(41) QT(41)	EXCES

TABLE 17. DEBUG FORMATS (page 10)

Debug Switch	Debug Level	Quantity	SUBROUTINE
16	3	16 3 UX(1) UX(2) UX(3) UX(4) UX(5) UX(6) UX(7) UX(8) UX(9) *UX(10) UX(11) UX(12) UV(1) UV(2) UV(3) UV(4) UV(5) UV(6) UV(7) UV(8) UV(9) *UV(10) UV(11) UV(12) UA(1) UA(2) UA(3) UA(4) UA(5) UA(6) UA(7) UA(8) UA(9) *UA(10) UA(11) UA(12) XCN(1) XCN(2) XCN(3) XCN(4) XCN(5) XCN(6) XCN(7) XCN(8) XCN(9) VCN(1) VCN(2) VCN(3) VCN(4) VCN(5) VCN(6) VCN(7) VCN(8) VCN(9) ACN(1) ACN(2) ACN(3) ACN(4) ACN(5) ACN(6) ACN(7) ACN(8) ACN(9) C(1,1) C(2,1) C(3,1) C(1,2) C(2,2) C(3,2) C(1,3) C(2,3) C(3,3) C(1,4) C(2,4) C(3,4) S(1,1) S(2,1) S(3,1) S(1,2) S(2,2) S(3,2) S(1,3) S(2,3) S(3,3) S(1,4) S(2,4) S(3,4) U(1,1) U(2,1) U(3,1) U(4,1) U(1,2) U(2,2) U(3,2) U(4,2) U(1,3) U(2,3) U(3,3) U(4,3) U(1,4) U(2,4) U(3,4) U(4,4) UP(1,1) UP(2,1) UP(3,1) UP(4,1) UP(1,2) UP(2,2) UP(3,2) UP(4,2) UP(1,3) UP(2,3) UP(3,3) UP(4,3) UP(1,4) UP(2,4) UP(3,4) UP(4,4) V(1,1) V(2,1) V(3,1) V(4,1) V(1,2) V(2,2) V(3,2) V(4,2) V(1,3) V(2,3) V(3,3) V(4,3) V(1,4) V(2,4) V(3,4) V(4,4) W(1,1) W(2,1) W(3,1) W(4,1) W(5,1) W(6,1) W(1,2) W(2,2) W(3,2) W(4,2) W(5,2) W(6,2) W(1,3) W(2,3) W(3,3) W(4,3) W(5,3) W(6,3) W(1,4) W(2,4) W(3,4) W(4,4) W(5,4) W(6,4)	SPX
16	3	16 4 Exactly the same quantities as preceding printout but this with current values at the time SPY is called.	SPY

of space to enter more than one line for a single printed line in the output. Such "continuation" lines are marked with a *.

Under the column entitled "Quantity" there appears a facsimile of each output line including the line indentification and showing the Fortram name of each printed quantity. The name of the subroutine from which this print-out is made is given in the column labelled "Subroutine."

These printouts are organized on debug switch and debug level and not on the order in which they appear.

Table 18 contains a summary of the material presented in Table 17 for the convenience of the user. A short description of each set of quantities is given instead of the explicit format.

Error messages produced by this simulator are shown in Table 19 which is self-explanatory.

4.4 INTEGRATION TECHNIQUES AND PROGRAM CONTROLS

The equations of motion arising in the simulation of the three-dimensional crash victim are, in form, a system of twelve simultaneous, nonlinear, second-order, ordinary differential equations in twelve unknowns. In this system the second derivatives of the twelve unknowns appear only linearly, so that it is possible to solve for them in terms of the first derivatives, the unknowns, and various constants.

Hence this system of equations is integrated by employing predictor-corrector techniques for an initial value problem, together with a starting method for initializing the required history of established values. Two separate predictor-corrector methods are available in the HSRI Three-Dimensional Crash Victim Simulator. The one most commonly used is the classical Milne method as modified by Hamming for faster convergence. With the Milne-Hamming method, and much of the

TABLE 18. SUMMARY OF DEBUG FORMATS

Debug Switch	Debug Level	Description
1	1	Belt Anchors and attachment positions for current belt segment.
1	2	Components of belt length and derivatives.
1	3	Partials of attachment positions
2	1	Belt deflection, rate, and force.
2	2	Belt generalized force contributions.
2	3	Belt lever arms (for current belt segment).
3	1	Integration step and evaluation summary
3	2	Number of steps at each step size
4	1	Joint deflections, rates, elastic and stop forces.
4	2	Joint generalized forces.
4	3	Relative angle components and lever arms
5	1	Contact plane coefficients, corner positions, and derivatives
5	2, 3	Contact plane contributions to lever arms
6	1	Ellipsoid center position

TABLE 18. SUMMARY OF DEBUG FORMATS (Page 2)

Debug Switch	Debug Level	Description
6	2, 3	Ellipsoid contributions to lever arms
7	1	Contact plane - ellipsoid interaction deflections, rate, force, impact position and "effectiveness" contributions.
7	2	Total generalized force for all contact interactions
7	3	Tangent points to parallel plane, lever arms, and build up of generalized force.
8	1	Vehicle integration values
9	1	Current integration step level, last established time, execution time
9	2	Last integrated values and corrections
9	3	Time history of integrated values
10	1	Load-deflection parameter summary for each force determination
11	1	Current generalized values, derivative, and forces
11	2	Current mass matrix
11	3	Current labelled coordinate combinations
12	1	Gravitational and kinetic energy generalized forces
12	3	Intermediate building blocks for QT

TABLE 18. SUMMARY OF DEBUG FORMATS (Page 3)

Debug Switch	Debug Level	Description
13	1, 2	Summary of limits parameters
14	1, 2	Recorded body segment relative accelerations
15	1	Body segment c.g. positions and velocities and seat corner positions
15	2, 3	Building blocks for contact lever arms, rates, and corner positions
16	1	Computed body segment relative accelerations
16	2	Time history of tolerance-related quantity
16	3	All quantities necessary to body segment relative acceleration computation

TABLE 19. ERROR MESSAGES

Message	Condition and Action Required	Subroutine
AT TIME = [time / XX.XXXX] RUN TIME LIMIT EXCEED [msec of execution / XXXXXX] [limit in msec / XXXXXX]	The user's specified execution time limit has been exceeded. Execution will be stopped. If not deliberate, recheck input for bad control values.	MAIN
AT TIME = [time / XX.XXXX] FATAL ERROR, MAXIMUM NUMBER OF INTERVAL SUBDIVISION EXCEEDED.	Recheck input data looking for parameters that would cause unusually large forces such as misplaced contact planes, ellipsoids, belt anchors, or initial body positions.	MAIN
AT TIME [time / XX.XXXX] FATAL ERROR, ANGLE FOR INDEX [generalized coordinate subscript / XXX] EXCEEDS TEN RADIANS	Integration is running away, look for large force producers such as listed in the last box.	MAIN
ILLEGAL CARD SKIPPED [contents of card]	A mispunched input card has been encountered. This card is skipped and execution is not interrupted.	READAT
TABLE NO. [Table Index / XX] LAST TIME SEGMENT EXTENDED TO TMAX.	Time interval specified for this table does not reach tmax. The interval is extended by changing the last abcissa to tmax.	INTAB
NEGATIVE PERMANENT DEFORMATION PREDICTED. CHECK INPUT FOR INDEX [ellipsoid # / XXXXX / # of belt segment if next is 26] [contact # / XXXXX / belts if 26]	Saturation unloading slope is too small for rise time of force.	NEWLOF

logic which surrounds its use, we have followed the approach taken in the SSP subroutines, HPCG and DHPCG.[29] The Milne-Hamming method can be summarized by Equation (4.4.1).

For k = 1,12:

$$
\begin{aligned}
\dot{P}_{k,1} &= \dot{Z}_{k,-3} + \frac{4\Delta t}{3}(2\ddot{Z}_{k,0} - \ddot{Z}_{k,1} + 2\ddot{Z}_{k,-2}) \\
P_{k,1} &= Z_{k,-3} + \frac{4\Delta t}{3}(2\dot{Z}_{k,0} - \dot{Z}_{k,-1} + 2\dot{Z}_{k,-2}) \\
\dot{H}_{k,1} &= \dot{P}_{k,1} - \frac{112}{121}(\dot{P}_{k,0} - \dot{C}_{k,0}) \\
H_{k,1} &= P_{k,1} - \frac{112}{121}(P_{k,0} - C_{k,0}) \\
\dot{C}_{k,1} &= \frac{1}{8}[9\ddot{Z}_{k,0} - \dot{Z}_{k,-2} + 3\Delta t(\ddot{H}_{k,1} + 2\ddot{Z}_{k,0} - \ddot{Z}_{k,-1})] \\
C_{k,1} &= \frac{1}{8}[9Z_{k,0} - Z_{k,-2} + 3\Delta t(\dot{C}_{k,1} + 2\dot{Z}_{k,0} - \dot{Z}_{k,-1})] \\
\dot{Z}_{k,} &= \frac{1}{121}(112\dot{C}_{k,1} + 9\dot{P}_{k,1}) \\
Z_{k,1} &= \frac{1}{121}(112C_{k,1} + 9P_{k,1})
\end{aligned}
\qquad (4.4.1)
$$

where

$Z_{k,j}$ is the value of the k-th generalized coordinate in the recorded history of established values which corresponds to time t - jΔt where t is the last recorded established time and Δt is the current integration time step. Note: where k appears as a subscript in a formula, that formula is evaluated for values of k from one to twelve before anything else is done.

$\dot{Z}_{k,j}, \ddot{Z}_{k,j}$ are respectively first and second derivatives of the corresponding generalized coordinates.

$P_{k,j}, \dot{P}_{k,j}$ are the results of the Milne predictor for the corresponding generalized coordinates and velocities.

$H_{k,1}, \dot{H}_{k,1}$ are the predictions for the corresponding generalized coordinates and velocities used including the Hamming modification.

$\ddot{H}_{k,1}$ are computed by evaluation of Equation (2.2.3) using the values $H_{k,1}$ and $\dot{H}_{k,1}$ as generalized coordinates and velocities.

$C_{k,j}, \dot{C}_{k,j}$ are the results of the Milne corrector for the generalized coordinates and velocities. Note: the k implies that $\ddot{H}_{1,1}, \ddot{H}_{2,1}, \ldots, \ddot{H}_{12,1}$ are all being referred to here.

$Z_{k,1}, \dot{Z}_{k,1}$ are the corrected values of the generalized coordinates and velocities after the Hamming modification has been applied. These are the values tested for convergence. If convergence fails with the single correction, the integration time step is halved immediately.

The alternate predictor-corrector is the classical Adams-Moulton method which exhibits much greater stability. When this option is employed, up to ten corrections are permitted to obtain convergence before the time step is halved. The Adams-Moulton method is used both in four-point and five-point forms based on how many established prints are available in the time history. The two forms are presented in Equation (4.4.2).

Four-point, for k = 1,12:

$$\dot{P}_{k,1} = \dot{Z}_{k,0} + \Delta t(c_8\ddot{Z}_{k,0} + c_9\ddot{Z}_{k,-1} + c_{10}\ddot{Z}_{k,-2} - c_{11}\ddot{Z}_{k,-3})$$

$$P_{k,1} = Z_{k,0} + \Delta t(c_{19}\dot{P}_{k,1} + c_{20}\dot{Z}_{k,0} + c_{21}\dot{Z}_{k,-1} + c_{22}\dot{Z}_{k,-2} + c_{23}\dot{Z}_{k,-3}) \qquad (4.4.2)$$

$$\dot{C}_{k,1} = \dot{Z}_{k,0} + \Delta t(c_{19}\ddot{P}_{k,1} + c_{20}\ddot{Z}_{k,0} + c_{21}\ddot{Z}_{k,-1} + c_{22}\ddot{Z}_{k,-2} + c_{23}\ddot{Z}_{k,-3})$$

(Continued on next page)

$$C_{k,1} = Z_{k,0} + \Delta t(c_{19}\dot{C}_{k,1} + c_{20}\dot{Z}_{k,0} + c_{21}\dot{Z}_{k,-1} + c_{22}\dot{Z}_{k,-2} + c_{23}\dot{Z}_{k,-3})$$

(4.4.2 continued)

Five-point, for k = 1,12:

$$\dot{P}_{k,1} = \dot{Z}_{k,0} + \Delta t(c_{15}\ddot{Z}_{k,0} + c_{16}\ddot{Z}_{k,-1} + c_{17}\ddot{Z}_{k,-2} + c_{18}\ddot{Z}_{k,-3} + c_{19}\ddot{Z}_{k,-4})$$

$$P_{k,1} = Z_{k,0} + \Delta t(c_{24}\dot{P}_{k,1} + c_{25}\dot{Z}_{k,0} + c_{26}\dot{Z}_{k,-1} + c_{27}\dot{Z}_{k,-2} + c_{28}\dot{Z}_{k,-3} + c_{29}\dot{Z}_{k,-4})$$

$$\dot{C}_{k,1} = \dot{Z}_{k,0} + \Delta t(c_{24}\ddot{P}_{k,1} + c_{25}\ddot{Z}_{k,0} + c_{26}\ddot{Z}_{k,-1} + c_{27}\ddot{Z}_{k,-2} + c_{28}\ddot{Z}_{k,-3} + c_{29}\ddot{Z}_{k,-4})$$

$$C_{k,1} = Z_{k,0} + \Delta t(c_{24}\dot{C}_{k,1} + c_{25}\dot{Z}_{k,0} + c_{26}\dot{Z}_{k,-1} + c_{27}\dot{Z}_{k,-2} + c_{28}\dot{Z}_{k,-3} + c_{29}\dot{Z}_{k,-4})$$

where

$P_{k,1}, \dot{P}_{k,1}, C_{k,1}, \dot{C}_{k,1}, Z_{k,j}, \dot{Z}_{k,j}$, and $\ddot{Z}_{k,j}$ have corresponding definitions as in Equation (4.4.1).

$\ddot{P}_{k,1}$ are computed by evaluation of Equation (2.2.3) using the values $P_{k,1}$ and $\dot{P}_{k,1}$ as coordinates and velocities.

c_i are the constants presented in Table 20.

Actual experience with the computer program indicates that the Milne-Hamming method failed only once to achieve good results. A corresponding run using the Adams-Moulton method did produce good results but at considerable expense. On straightforward runs, the two methods are approximately equivalent in efficiency with a slight advantage to the Milne-Hamming. On runs of moderate difficulty, the Milne-Hamming method is much better.

Three starting methods are available. The normal method is a Runge-Kutta procedure as specially modified by Ralston[30] to gain maximum convergence. This method is highly unstable, but with a partial second iteration for improvement of results, it has never failed in our actual experience. The second integration starting method offered is a classical Runge-Kutta method

TABLE 20. INTEGRATION RULE COEFFICIENTS

i	c_i	Ralston Version
1	1.5	
2	0.5	
3	1.9166666666666667	
4	- 1.3333333333333333	
5	0.41666666666666667	
6	0.66666666666666667	
7	- 0.083333333333333333	
8	2.2916666666666667	
9	- 2.4583333333333333	
10	1.5416666666666667	
11	0.375	
12	0.79166666666666667	
13	- 0.20833333333333333	Independent of choice of Runge-Kutta method.
14	0.041666666666666667	
15	2.6402777777777778	
16	- 3.8527777777777778	
17	3.6333333333333333	
18	- 1.7694444444444444	
19	0.34861111111111111	
20	0.8972222222222222	
21	- 0.3666666666666667	
22	0.1472222222222222	
23	- 0.02638888888888889	
24	0.3465277777777778	
25	0.9076388888888889	
26	- 0.3875	
27	0.1680555555555556	
28	- 0.36805555555555556	
29	0.0020833333333333333	
30	0.5	0.4
31	0.5	0.45573725421878943
32	0.0	0.29697760924775360
33	0.5	0.15875964497103583
34	1.0	1.0
35	0.0	0.21810038822592047
36	0.0	- 3.0509651486929308
37	1.0	3.8328647604670103
38	0.16666666666666667	0.17476028226269037
39	0.33333333333333333	- 0.55148066287873294
40	0.33333333333333333	1.2055355993965235
41	0.16666666666666667	0.17118478121951903
42	$c_{32} + c_{33}$	
43	$c_{30}c_{31}$	
44	$c_{35} + c_{36} + c_{37}$	
45	$c_{30}c_{36} + c_{32}c_{37}$	These are computed after the appropriate values are assigned c_{30} through c_{41}.
46	$c_{33}c_{37}$	
47	$c_{38} + c_{39} + c_{40} + c_{41}$	
48	$c_{30}c_{39} + c_{32}c_{40} + c_{35}c_{41}$	
49	$c_{33}c_{40} + c_{36}c_{41}$	
50	$c_{37}c_{41}$	

with greater stability and less accuracy. Equation (4.4.3) presents a general four-point Runge-Kutta method for second-order equations. Specific Runge-Kutta methods are obtained by an appropriate set of constants c_{30} through c_{41} and the computed constants c_{42} through c_{51}. The constants needed for the normal Runge-Kutta are presented in Table 20 in the left column and those needed for the Ralston modification are in the right column.

For k = 1,12:

$$t_1 = t$$

$$K_{k,1} = Z_{k,0}$$

$$\dot{K}_{k,1} = \dot{Z}_{k,0}$$

$$t_2 = t + c_{30}\Delta t$$

$$K_{k,2} = Z_{k,0} + c_{30}\Delta t\dot{Z}_{k,0}$$

$$\dot{K}_{k,2} = \dot{Z}_{k,0} + c_{30}\ddot{K}_{k,1}\Delta t$$

$$t_3 = t + c_{31}\Delta t \qquad (4.4.3)$$

$$K_{k,3} = Z_{k,0} + c_{42}\Delta t\dot{Z}_{k,0} + c_{43}(\Delta t)^2\ddot{K}_{k,1}$$

$$\dot{K}_{k,3} = \dot{Z}_{k,0} + c_{32}\Delta t\ddot{K}_{k,1} + c_{33}\Delta t\ddot{K}_{k,2}$$

$$t_4 = t + c_{34}\Delta t$$

$$K_{k,4} = Z_{k,0} + \Delta t c_{44}\dot{Z}_{k,0} + c_{45}(\Delta t)^2\ddot{K}_{k,1} + c_{46}(\Delta t)^2\ddot{K}_{k,2}$$

$$\dot{K}_{k,4} = \dot{Z}_{k,0} + \Delta t c_{35}\ddot{K}_{k,1} + c_{36}\Delta t\ddot{K}_{k,2} + c_{37}\Delta t\ddot{K}_{k,3}$$

$$Z_{k,1} = Z_{k,0} + \Delta t c_{47}\dot{Z}_{k,0} + (\Delta t)^2(c_{48}\ddot{K}_{k,1} + c_{49}\ddot{K}_{k,2} + c_{50}\ddot{K}_{k,3})$$

$$\dot{Z}_{k,1} = \dot{Z}_{k,0} + \Delta t(c_{38}\ddot{K}_{k,1} + c_{39}\ddot{K}_{k,2} + c_{40}\ddot{K}_{k,3} + c_{41}\ddot{K}_{k,4})$$

where

$Z_{k,0}, \dot{Z}_{k,0}, t, \Delta t, c_m, Z_{k,1}$, and $\dot{Z}_{k,1}$ are as defined with Equations (4.4.1) and (4.4.2), and $\ddot{K}_{k,1}, \ddot{K}_{k,2}, \ddot{K}_{k,3}$, and $\ddot{K}_{k,4}$ are all computed by evaluations of Equation (2.2.3) using the corresponding $t_m, \dot{K}_{k,m}, K_{k,m}$ given above as coordinates and velocities.

The third starting method uses the Euler method to establish the second point, the trapezoidal rule to establish the third point, and Simpson's rule to establish the fourth point. This third option uses a regular predictor-corrector type iteration to establish convergence at each of the levels. Equation (4.4.4) shows the formulas used.

Modified Euler Method (one point)

$$\dot{P}_{k,1} = \dot{Z}_{k,0} + \Delta t \ddot{Z}_{k,0}$$

$$P_{k,1} = Z_{k,0} + c_2 \Delta t(\dot{Z}_{k,0} + \dot{P}_{k,1})$$

$$\dot{C}_{k,1} = \dot{Z}_{k,0} + c_2 \Delta t(\ddot{P}_{k,1} + \ddot{Z}_{k,0})$$

$$C_{k,1} = Z_{k,0} + c_2 \Delta t(\dot{C}_{k,1} + \dot{Z}_{k,0})$$

Modified Trapezoidal Rule (two points)

$$\dot{P}_{k,1} = \dot{Z}_{k,0} + \Delta t(c_1 \ddot{Z}_{k,0} - c_2 \ddot{Z}_{k,-1}) \qquad (4.4.4)$$

$$P_{k,1} = Z_{k,0} + \Delta t(c_5 \dot{P}_{k,1} + c_6 \dot{Z}_{k,0} + c_7 \dot{Z}_{k,-1})$$

$$\dot{C}_{k,1} = \dot{Z}_{k,0} + \Delta t(c_5 \ddot{P}_{k,1} + c_6 \ddot{Z}_{k,0} + c_7 \ddot{Z}_{k,-1})$$

$$C_{k,1} = Z_{k,0} + \Delta t(c_5 \dot{C}_{k,1} + c_6 \dot{Z}_{k,0} + c_7 \dot{Z}_{k,-1})$$

Modified Simpson's Rule (three points)

$$\dot{P}_{k,1} = \dot{Z}_{k,0} + \Delta t(c_3 \ddot{Z}_{k,0} + c_4 \ddot{Z}_{k,-1} + c_5 \ddot{Z}_{k,-2})$$

$$P_{k,1} = Z_{k,0} + \Delta t(c_{11} \dot{P}_{k,1} + c_{12} \dot{Z}_{k,0} + c_{13} \dot{Z}_{k,-1} + c_{14} \dot{Z}_{k,-2})$$

$$\dot{C}_{k,1} = \dot{Z}_{k,0} + \Delta t(c_{11}\ddot{P}_{k,1} + c_{12}\ddot{Z}_{k,0} + c_{13}\ddot{Z}_{k,-1} + c_{14}\ddot{Z}_{k,-2})$$

$$C_{k,1} = Z_{k,0} + \Delta t(c_{11}\dot{C}_{k,1} + c_{12}\dot{Z}_{k,0} + c_{13}\dot{Z}_{k,-1} + c_{14}\dot{Z}_{k,-2}) \qquad \text{(4.4.4 Concluded)}$$

where definitions are similar to those in Equation (4.4.2).

Determinationof convergence is uniform among all the various methods employed. The absolute error of the weighted averages of first derivatives obtained by two seperate calculations of the solution to the system of equations at a particular time is required to have less magnitude than a specified value. The convergence test can be expressed by the following inequality.

$$\hat{N} \sum_{k=1}^{12} \bar{u}_k \left| \dot{Z}_{k,1}^{(n)} - \dot{Z}_{k,1}^{(n-1)} \right| \leq \epsilon_v \qquad (4.4.5)$$

where $\hat{N}$ is a method scaling constant.

$\bar{u}_k$ are the absolute integration weights. These are the relative integration weights read in the S-card sequence after they have been normalized to add to one

$\dot{Z}_{k,1}^{(n)}$ are defined as the current trial values of generalized velocities at the new time

$\dot{Z}_{k,1}^{(n-1)}$ are defined as the previous trial values of generalized velocities at the new time

If the Milne-Hamming method is being employed, $\hat{N}$=1, $\dot{Z}_{k,1}^{(n)} = \dot{Z}_{k,1}$ and $\dot{Z}_{k,1}^{(n-1)} = \dot{H}_{k,1}$ (see Equation (4.4.1)). If the test fails, the integration time step is immediately halved.

If either Runge-Kutta method is being employed, $N = \frac{1}{15}$, $\dot{Z}_{k,1}^{(n)} = \dot{Z}_{k,1}$ determined at the original time step and $\dot{Z}_{k,1}^{(n)} = \dot{Z}_{k,1}$ determined by two applications of the rule at half the original time step. If the test fails, the time step is halved, the $\dot{Z}_{k,1}^{(n-1}$ are set to the $\dot{Z}_{k,1}^{(n)}$, and the new $\dot{Z}_{k,1}^{(n)}$ are determined by two applications of the rule at half the current time step. This iteration is continued until convergence is attained or until the allowed number of halvings is exceeded. Once convergence has been achieved, three points of the required four points in the time history have been established. The fourth point is calculated by one more application of the rule at the half integration step. A single iteration is then taken to improve the four established values by using four-point interpolation formulas for the displacements and velocities and a revaluation of the accelerations for the second, third, and fourth points of the history, each in turn. If the current time is considered to be that of the last of the four established points, and Δt is the half time step, then the equations used in order of application in the iteration are those presented in Equation (4.4.6).

For k = 1,12,

$$\dot{Z}_{k,-2} = \dot{Z}_{k,-3} + \frac{\Delta t}{24}(9\,\ddot{Z}_{k,-3} + 19\,\ddot{Z}_{k,-2} - 5\,\ddot{Z}_{k,-1} + \ddot{Z}_{k,0})$$

$$Z_{k,-2} = Z_{k,-3} + \frac{\Delta t}{24}(9\,\dot{Z}_{k,-3} + 19\,\dot{Z}_{k,-2} - 5\,\dot{Z}_{k,-1} + \dot{Z}_{k,0})$$

$$\dot{Z}_{k,-1} = \dot{Z}_{k,-3} + \frac{\Delta t}{3}(\ddot{Z}_{k,-3} + 4\,\ddot{Z}_{k,-2} + \ddot{Z}_{k,-1})$$

$$Z_{k,-1} = Z_{k,-3} + \frac{\Delta t}{3}(\dot{Z}_{k,-3} + 4\,\dot{Z}_{k,-2} + \dot{Z}_{k,-1})$$

$$\dot{Z}_{k,0} = \dot{Z}_{k,-3} + \frac{3}{8}\Delta t\,(\ddot{Z}_{k,-3} + 3\,\ddot{Z}_{k,-2} + 3\,\ddot{Z}_{k,-1} + \ddot{Z}_{k,0})$$

$$Z_{k,0} = Z_{k,-3} + \frac{3}{8}\Delta t\,(\dot{Z}_{k,-3} + 3\,\dot{Z}_{k,-2} + 3\,\dot{Z}_{k,-1} + \dot{Z}_{k,0}) \qquad (4.4.6)$$

where $\ddot{Z}_{k,-2}$ are recomputed after the first two equations and the new values are throughout the rest of the equations. $\ddot{Z}_{k,-1}$ are recomputed after the fourth equation, and $\ddot{Z}_{k,0}$ are recomputed after the sixth equation.

If any of the methods set forth in Equations (4.4.2) and (4.4.4) is being employed, $\hat{N} = 1$, $\dot{Z}_{k,1}^{(n-1)} = \dot{P}_{k,1}$, and $\dot{Z}_{k,1}^{(n)} = \dot{C}_{k,1}$. If the test fails, the $P_{k,1}$, $\dot{P}_{k,1}$ are set to the $C_{k,1}$, $\dot{C}_{k,1}$, and the corresponding corrector equations are used again. This iteration is tried ten times to obtain convergence before the time step is halved.

In all cases, when convergence fails and the time step interval is halved, the missing points in the time history are supplied by use of sixth-order Bessel central difference interpolation formulas[31] and a single iteration. The number of halvings is incremented and checked against the limit. Then the following iteration is employed.

$$\Delta t = \frac{\Delta t}{2}$$

for k = 1,12,

$$\dot{Z}_{k,-\frac{1}{2}} = \frac{1}{256}\left(80\dot{Z}_{k,0} + 135\dot{Z}_{k,-1} + 40\dot{Z}_{k,-2} + \dot{Z}_{k,-3}\right) + \frac{15}{128}\Delta t\left(\ddot{Z}_{k,-2} + 6\ddot{Z}_{k,-1} - \ddot{Z}_{k,0}\right)$$

$$Z_{k,-\frac{1}{2}} = \frac{1}{256}\left(80Z_{k,0} + 135Z_{k,-1} + 40Z_{k,-2} + Z_{k,-3}\right) + \frac{15}{128}\Delta t\left(\dot{Z}_{k,-2} + 6\dot{Z}_{k,-1} - \dot{Z}_{k,0}\right) \qquad (4.4.7)$$

$$\dot{Z}_{k,-\frac{3}{2}} = \frac{1}{256}\left(12\dot{Z}_{k,0} + 135\dot{Z}_{k,-1} + 108\dot{Z}_{k,-2} + \dot{Z}_{k,-3}\right) + \frac{3}{128}\Delta t\left(9\ddot{Z}_{k,-2} - 18\ddot{Z}_{k,-1} - \ddot{Z}_{k,0}\right)$$

(Continued on Next Page)

$$Z_{k,-\frac{3}{2}} = \frac{1}{256}\left(12Z_{k,0} + 135Z_{k,-1} + 108Z_{k,-2} + Z_{k,-3}\right)$$
$$+ \frac{3}{128}\Delta t\left(9\ddot{Z}_{k,-2} - 18\ddot{Z}_{k,-1} - \ddot{Z}_{k,0}\right)$$

$$\ddot{Z}_{k,-4} = \ddot{Z}_{k,-2}$$

$$\dot{Z}_{k,-4} = \dot{Z}_{k,-2}$$

$$Z_{k,-4} = Z_{k,-2}$$

$$\ddot{Z}_{k,-2} = \ddot{Z}_{k,-1}$$

$$\dot{Z}_{k,-2} = \dot{Z}_{k,-1}$$

$$Z_{k,-2} = Z_{k,-1}$$

$$\ddot{Z}_{k,-1} = \ddot{Z}_{k,-\frac{1}{2}}\text{ , etc.}$$

$$\ddot{Z}_{k,-3} = \ddot{Z}_{k,-\frac{3}{2}}\text{ , etc.}$$

$$\dot{P}_{k,0} - \dot{C}_{k,0} = \frac{242}{27}\left(\dot{Z}_{k,0} - \dot{Z}_{k,-3}\right) - \frac{121}{36}\Delta t\left(\ddot{Z}_{k,0} + 3\ddot{Z}_{k,-1} + 3\ddot{Z}_{k,-2} + \ddot{Z}_{k,-3}\right)$$

$$P_{k,0} - C_{k,0} = \frac{242}{27}\left(Z_{k,0} - Z_{k,-3}\right) - \frac{121}{36}\Delta t\left(\dot{Z}_{k,0} + 3\dot{Z}_{k,-1} + 3\dot{Z}_{k,-2} + \dot{Z}_{k,-3}\right)$$

(4.4.7 Concluded)

If convergence succeeds by a factor of fifty better than required, the time step is doubled if other conditions are met. These conditions are that the current integration time step size is smaller than Δt_{max}, that the time history contains at least seven good points, and that the new larger step will not jump over the next increment of Δt_{prnt}. If these conditions are all met, the following reshuffling and calculation takes place.

$$\Delta t = 2\Delta t$$

for k = 1,12,

$$\ddot{Z}_{k,-1} = \ddot{Z}_{k,-2}$$

$$\dot{Z}_{k,-1} = \dot{Z}_{k,-2}$$

$$Z_{k,-1} = Z_{k,-2}$$

$$\ddot{Z}_{k,-2} = \ddot{Z}_{k,-4} \text{ , etc.} \qquad (4.4.8)$$

$$\ddot{Z}_{k,-3} = \ddot{Z}_{k,-6} \text{ , etc.}$$

$$\ddot{Z}_{k,-4} = \ddot{Z}_{k,-8} \text{ , etc.}$$

$$\dot{P}_{k,0} - \dot{C}_{k,0} = \frac{242}{27}(\dot{Z}_{k,0} - \dot{Z}_{k,-3}) - \frac{121}{36}\Delta t\,(\ddot{Z}_{k,0} + 3\ddot{Z}_{k,-1} + 3\ddot{Z}_{k,-2} + \ddot{Z}_{k,-3}$$

$$P_{k,0} - C_{k,0} = \frac{242}{27}(Z_{k,0} - Z_{k,-3}) - \frac{121}{36}\Delta t\,(\dot{Z}_{k,0} + 3\dot{Z}_{k,-1} + 3\dot{Z}_{k,-2} + \dot{Z}_{k,-3}$$

Experience dictates that convergence by itself is not sufficient to guarantee good results in all impact situations. Since initial value procedures seldom are capable of regaining any lost accuracy, it is of utmost importance to prevent the solution from deviating from the true solution. During a time interval in which impact occurs, the solution is smooth both before and during the impact, but changes shape abruptly shortly after the moment of impact. Calculation of a good solution often requires decreasing the integration time step before the convergence test is violated. This situation is recognized by extrapolating the value of second derivatives at a particular time, based on the time history of their established values, and comparing these against their predicted values. If the disagreement is too great, the time step is halved. This test is formalized in Equation (4.4.9).

For k = 1,12,

$$E\ddot{Z}_{k,1} = 4\ddot{Z}_{k,0} - 6\ddot{Z}_{k,-1} + 4\ddot{Z}_{k,-2} - \ddot{Z}_{k,-3}$$

$$\tilde{\varepsilon} = \sum_{k=1}^{12} \bar{\mu}_k \left| E\ddot{Z}_{k,1} - \ddot{Z}_{k,1}^{(n-1)} \right| \leq \Delta\ddot{\bar{Z}}_{lim}$$

or failing that

$$\hat{\varepsilon} = \sum_{k=1}^{12} \bar{\mu}_k \left| \ddot{Z}_{k,1}^{(n-1)} \right| \neq 0 \quad \text{and} \quad \frac{\tilde{\varepsilon}}{\hat{\varepsilon}} \leq \Delta\ddot{\bar{Z}}_{lim}$$

$$\text{or} \quad \hat{\varepsilon} = 0 \quad \text{and} \quad \frac{\tilde{\varepsilon}}{\sum_{k=1}^{12} \bar{\mu}_k \left| E\ddot{Z}_{k,1} \right|} \leq \Delta\ddot{\bar{Z}}_{lim} \tag{4.4.9}$$

where $\ddot{Z}_{k,1}^{(n-1)}$ is defined as it was for Equation (4.4.5) except this test is used only when the Milne-Hamming method or the Adams-Moulton method is being employed and $\Delta\ddot{\bar{Z}}_{lim}$ is the extrapolation change limit.

Further, it has been noted that occasionally the level of activity can become too great for computation of good results at a particular time step without convergence failing. A test has been incorporated to limit the value of the weighted average of the second derivatives multiplied by the integration step. This weighted average velocity change has been taken as a measure of the "activity load" during the time step. If the activity load is too great, the time step is halved.

$$\Delta t \sum_{k=1}^{12} \bar{\mu}_k \left| \ddot{Z}_{k,1}^{(n-1)} \right| \leq \Delta V_{lim} \tag{4.4.10}$$

where ΔV_{lim} is the velocity change limit

$\ddot{Z}_{k,1}^{(n-1)}$ is defined here as in Equation (4.4.9)

Both these tests are applied only after prediction in the two predictor-corrector methods and must be passed before correction is begun. Either of these tests will be skipped if the corresponding limit is specified as zero.

The least important feature of the integration scheme used in the computer solution is intended mainly to keep out the introduction of small errors in the solutions and normal printout. The computed values of the second derivatives are scanned and set at zero if they are smaller in magnitude than a specified value. If this option is not desired, the acceleration minimum magnitude parameter is set at zero. This option helps the accuracy in some extreme cases, but mostly it acts to remove irrelevant detail from the regular printout.

The basic integration control parameter is the maximum integration time step. Under certain conditions, which already have been discussed in this section, the program will cut down the size of the integration time step by halving it up to a specified number of times. Regular printout occurs at multiples of the print time step parameter which itself must be an integral multiple of the maximum time step.

The time epsilon parameter is the absolute difference between two computed times which must be exceeded for them to be treated as distinct by the program. When the execution time limit parameter is non-zero, it causes the program to keep track of how much central processing unit (C.P.U.) time it has used and sign off when this limit is exceeded.

This program has built-in tests against body injury tolerances which lead to supplementary pages of printed output describing the violations of these tolerances and the probable injuries resulting. The reader who is interested in more details beyond the X-card in Table 7 and the self-explanatory output shown in Table 15 is directed to Reference 28. An excellent overall treatment of the topics considered in this section will be found in Reference 32.

4.5 USE OF THE PROGRAM IN THE MICHIGAN TERMINAL SYSTEM

This program is designed to be used normally in batch mode. It is also possible to exercise this model from terminals with the use of a companion program, TALK3. The bulk of this section constitutes a user's guide for TALK3. Pictorial output can be provided by use of another companion program 3DP which is discussed in Part 5.

Normal batch mode execution of the program has input coming in on SCARDS, normal output coming out on SPRINT, and debugging output coming out on logical unit number six. By use of the Q-card in the data, the input stream can be changed to any of the logical unit numbers zero through nine wherever in the data deck that course of action might be useful. This option is thought to aid in the organization of data, but has never been used in the Michigan Terminal System (MTS).

Two other optional outputs are available to provide "conversation" between the program and the two companion programs. These two options are controlled by a switch in the R-card, sixth field. The special output for the pictorial program comes out on logical unit number one and that for TALK3 on logical unit number two.

The full run statement for the program in MTS is

```
$RUN SP78:THREED SCARDS=DATA 1=PICTORIAL 2=SUMMARY 6=DEBUG SPRINT=PRINTOUT
```

where

DATA is a file containing the input data deck

PICTORIAL is an empty file to hold the special output for 3DP

SUMMARY is an empty file to hold the special binary output for TALK3

DEBUG is an empty file to hold the auxillary output

PRINTOUT is an empty file to hold the normal output

Normal batch operation calls for the run statement:

$RUN SP78:THREED SCARDS=DATA

Here both 6 and SPRINT default to *SINK* (the normal print stream) and 1 and 2 are unused by an appropriate value in the controlling switch. Running the program over a terminal usually requires a run statement:

$RUN SP78:THREED SCARDS=DATA 2=SUMMARY SPRINT=*DUMMY* (or a file) with 1 and 6 unused.

4.5.1 GENERAL DESCRIPTION OF TALK3. The program TALK3 presents a way of extracting pieces of the normal printout information. It is designed to be used in conversational mode, with the user being prompted for instructions. However, once the user is familiar with the program it would be easier to put the instructions in a file which would decrease printing and time spent on the terminal.

TALK3 is called using:

$RUN SP78:TALK3 1=SUMMARY

where SUMMARY is the file containing the special output from the 3-D model. The program begins with the statement

'ENTER 6 IF CONVERSATIONAL, 7 IF NOT'

For normal usage the user will type 6. If the user wants to bypass conversation with the program, a 7 should be entered. In this case the $RUN statement should be:

```
$RUN SP78:TALK3  1=SUMMARY  4=INSTS  7=*DUMMY*
```

where INSTS is the file containing the instructions which would otherwise be given by the user from terminal. These instructions must conform to the required format. Consequently, in the following sections, whenever instructions must be entered, the format will be given.

```
'ENTER 1 IF GENERAL, 2 IF CONTACT, 3 IF COMPLEX, 4 IF LIST, 5 IF DONE'
 Format:  (I1)
```

Enter 1, 2, 3 or 4, depending on the type of information desired (see Sections 4.5.2, 4.5.3, 4.5.4, or 4.5.5, respectively), or a 5 if you are through using the program.

4.5.2 THE GENERAL TYPE OF INFORMATION REQUEST. The results of 115 different variables are stored by the 3-D model. (See Tables 21 and 22 for listings of these variables.) This type of information request will list from one to five variables against time in a specified time period. The "conversation" is as follows:

```
'HOW MANY VARIABLES'
 Format:  (I1)
```

Enter a number from 1 to 5 indicating the number of variables to be listed.

```
'ENTER VARIABLE NUMBERS'
'(     ) (     ) (     ) (     ) (     )'
 Format:  (5(IX, I3, IX))
```

Enter the specified number of variable numbers (see Table 21) so that they appear under but within the sets of parenthesis.

```
'ENTER TIME INTERVAL'
'FROM (      ) to (      )
 Format:  (5X, F7.5, 4X, F7.5)
```

Enter the time interval in the appropriate places.

At this point the specified information will be printed and the program will return to the information type question.

4.5.3 THE CONTACT TYPE OF INFORMATION REQUEST. There is a maximum of 40 contact interactions for which information is stored. This type of information request enables the user to ask about any or all of this data. The communications are:

'ENTER CONTACT NUMBER'

Format: (I2)

'ENTER ELLIPSOID NUMBER'

Format: (I2)

The numbers entered here correspond to the numbers used in the 3-D model, with one exception. If a zero is entered for either the contact number or the ellipsoid number, then all possible combinations are investigated. For example, if ellipsoid 1 is the head, and 0 and 1 are entered, then the results of any contact with the head would be printed. Note: Both the contact number and the ellipsoid number cannot be 0 at the same time.

'ENTER TIME INTERVAL'

'FROM ( ) to ( ) - ( ) = MAX. NO OF LINES TO BE PRINTED'

Format: (5X, F7.5, 4X, F7.5, 5X, I3)

In the first two spaces enter the time interval. Since any line containing all zeros will not be printed, for any time interval there is an uncertain number of lines to be printed. The third entry enables the user to limit this printing. For example, if the user is interested only in when contact first occurs, he would only want to print two or three time steps.

If the specified contact did not occur during the given time interval nothing will be printed and the program will prompt an information type. If the user does not possess the required knowledge of the contact and ellipsoid numbers used in the crash victim simulator run, he is referred to Section 4.5.5.

4.5.4 THE COMPLEX TYPE OF INFORMATION REQUEST. This type of information request answers such questions as what was the head's roll when it hit the door. The "conversation" is:

'ENTER DECISION VARIABLE'

Format: (I10)

The decision variable will be tested against a comparison value in order to determine the time which will be printed. In the example above, the contact force of the head against the door is the decision variable, and we become interested in seeing head roll when that force becomes positive. If the decision variable is one of the 115 variables from Section 4.5.2, its number is simply entered. If the variable is a CONTACT quantity, a code should be entered which is made up as follows:

Digit 1:	1 (To indicate a contact)
Digits 2 & 3:	Contact Number
Digits 4 & 5:	Ellipsoid Number
Digit 6:	A number from 1 to 5 representing the quantity of interest in the contact that was specified
	1 = Force
	2 = Deflection Value

3 = Deflection Rate

4 = X - Impact

5 = Y - Impact

For example: 105043 represents the deflection rate of the contact interaction between surface 5 and ellipsoid 4. A zero cannot be entered here for contacts or ellipsoids.

'ENTER COMPARISON VALUE'

Format: (F15.8)

This is the value with which the decision variable will be compared.

'ENTER COMPARISON MODE - 1 if GT, 2 if LT'

Format: (I1)

Enter 1 if the period of interest is when the decision variable surpasses the comparison value.

Enter 2 if it is to be surpassed by the comparison value.

'HOW MANY VARIABLES'

Format: (I1)

Enter the number of variables that will be printed when the decision variable reaches its critical value. (Maximum = 4)

'ENTER VARIABLE NUMBERS'

( ) ( ) ( ) ( )

Format: (4(1X, I6, 1X)

TABLE 21. VARIABLES (in numerical order)

1	Vehicle	X-Disp
2	Head	X-Disp
3	Torso	X-Disp
4	Legs	X-Disp
5	Vehicle	X-Vel
6	Head	X-Vel
7	Torso	X-Vel
8	Legs	X-Vel
9	Vehicle	X-Accel
10	Head	X-Accel
11	Torso	X-Accel
12	Legs	X-Accel
13	Vehicle	Y-Disp
14	Head	Y-Disp
15	Torso	Y-Disp
16	Legs	Y-Disp
17	Head	Y-Vel
18	Head	Y-Vel
19	Torso	Y-Vel
20	Legs	Y-Vel
21	Vehicle	Y-Accel
22	Head	Y-Accel
23	Torso	Y-Accel
24	Legs	Y-Accel
25	Vehicle	Z-Disp

TABLE 21. VARIABLES (page 2)

26	Head	Z-Disp
27	Torso	Z-Disp
28	Legs	Z-Disp
29	Vehicle	Z-Vel
30	Head	Z-Vel
31	Torso	Z-Vel
32	Legs	Z-Vel
33	Vehicle	Z-Accel
34	Head	Z-Accel
35	Torso	Z-Accel
36	Legs	Z-Accel
37	Vehicle	Yaw-Disp
38	Head	Yaw-Disp
39	Torso	Yaw-Disp
40	Legs	Yaw-Disp
41	Vehicle	Yaw-Vel
42	Head	Yaw-Vel
43	Torso	Yaw-Vel
44	Legs	Yaw-Vel
45	Vehicle	Yaw-Accel
46	Head	Yaw-Accel
47	Torso	Yaw-Accel
48	Legs	Yaw-Accel
49	Vehicle	Pitch-Disp
50	Head	Pitch-Disp

TABLE 21. VARIABLES (page 3)

51	Head	Pitch-Disp
52	Legs	Pitch-Disp
53	Vehicle	Pitch-Vel
54	Head	Pitch-Vel
55	Torso	Pitch-Vel
56	Legs	Pitch-Vel
57	Vehicle	Pitch-Accel
58	Head	Pitch-Accel
59	Torso	Pitch-Accel
60	Legs	Pitch-Accel
61	Vehicle	Roll-Disp
62	Head	Roll-Disp
63	Torso	Roll-Disp
64	Legs	Roll-Disp
65	Vehicle	Roll-Vel
66	Vehicle	Roll-Vel
67	Torso	Roll-Vel
68	Legs	Roll-Vel
69	Vehicle	Roll-Accel
70	Head	Roll-Accel
71	Torso	Roll-Accel
72	Legs	Roll-Accel
73	Belt Load	L. Shoulder
74	Belt Load	R. Shoulder
75	Belt Load	Left Seat

TABLE 21. VARIABLES (page 4)

76	Belt Load	Right Seat
77	Belt Angles	L. Shoulder-X
78	Joint Elast.	Neck Yaw
79	Belt Angles	L. Shoulder-Y
80	Joint Elast.	Neck Pitch
81	Belt Angles	L. Shoulder-Z
82	Joint Elast.	Neck Roll
83	Belt Angles	R. Shoulder-X
84	Joint Elast.	Hip Yaw
85	Belt Angles	R. Shoulder-Y
86	Joint Elast.	Hip Pitch
87	Belt Angles	R. Shoulder-Z
88	Joint Elast.	Hip Roll
89	Belt Angles	Left Seat-X
90	Joint Stop	Neck Yaw
91	Belt Angles	Left Seat-Y
92	Joint Stop	Neck Pitch
93	Belt Angles	Left Seat-Z
94	Joint Stop	Neck Roll
95	Belt Angles	Right Seat-X
96	Joint Stop	Hip Yaw
97	Belt Angles	Right Seat-Y
98	Joint Stop	Hip Pitch
99	Belt Angles	Right Seat-Z
100	Joint Stop	Hip Roll

TABLE 21. VARIABLES (page 5)

I01	Euler Angle	Head Yaw
I02	Euler Angle	Head Pitch
I03	Euler Angle	Head Roll
I04	Euler Angle	Legs Yaw
I05	Euler Angle	Legs Pitch
I06	Euler Angle	Legs Roll
I07	Hip Position	X
I08	Hip Position	Y
I09	Hip Position	Z

TABLE 22. VARIABLES (in alphabetical order)

89	Belt Angles	Left Seat-X
91	Belt Angles	Left Seat-Y
93	Belt Angles	Left Seat-Z
77	Belt Angles	Left Shoulder-X
79	Belt Angles	Left Shoulder-Y
81	Belt Angles	Left Shoulder-Z
95	Belt Angles	Right Seat-X
97	Belt Angles	Right Seat-Y
99	Belt Angles	Right Seat-Z
83	Belt Angles	Right Shoulder-X
85	Belt Angles	Right Shoulder-Y
87	Belt Angles	Right Shoulder-Z
75	Belt Load	Left Seat
73	Belt Load	Left Shoulder
76	Belt Load	Right Seat
74	Belt Load	Right Shoulder
102	Euler Angle	Head-Pitch
103	Euler Angle	Head-Roll
101	Euler Angle	Head-Yaw
105	Euler Angle	Legs-Pitch
106	Euler Angle	Legs-Roll
104	Euler Angle	Legs-Yaw
58	Head	Pitch-Accel
50	Head	Pitch-Disp
54	Head	Pitch-Vel

TABLE 22. VARIABLES (page 2)

70	Head	Roll-Accel
62	Head	Roll-Disp
66	Head	Roll-Vel
10	Head	X-Accel
2	Head	X-Disp
6	Head	X-Vel
22	Head	Y-Accel
14	Head	Y-Disp
18	Head	Y-Vel
46	Head	Yaw-Accel
38	Head	Yaw-Disp
42	Head	Yaw-Vel
34	Head	Z-Accel
26	Head	Z-Disp
30	Head	Z-Vel
107	Hip Position	X
108	Hip Position	Y
109	Hip Position	Z
86	Joint Elasticity	Hip Pitch
88	Joint Elasticity	Hip Roll
84	Joint Elasticity	Hip Yaw
80	Joint Elasticity	Neck Pitch
82	Joint Elasticity	Neck Roll
78	Joint Elasticity	Neck Yaw
98	Joint Stop	Hip Pitch

TABLE 22. VARIABLES (page 3)

100	Joint Stop	Hip Roll
96	Joint Stop	Hip Yaw
92	Joint Stop	Neck Pitch
94	Joint Stop	Neck Roll
90	Joint Stop	Neck Yaw
60	Legs	Pitch-Accel
52	Legs	Pitch-Disp
56	Legs	Pitch-Vel
72	Legs	Roll-Accel
64	Legs	Roll-Disp
68	Legs	Roll-Vel
12	Legs	X-Accel
4	Legs	X-Disp
8	Legs	X-Vel
24	Legs	Y-Accel
16	Legs	Y-Disp
20	Legs	Y-Vel
48	Legs	Yaw-Accel
40	Legs	Yaw-Disp
44	Legs	Yaw-Vel
36	Legs	Z-Accel
28	Legs	Z-Disp
32	Legs	Z-Vel
59	Torso	Pitch-Accel
51	Torso	Pitch-Disp

TABLE 22. VARIABLES (page 4)

55	Torso	Pitch-Vel
71	Torso	Roll-Accel
63	Torso	Roll-Disp
67	Torso	Roll-Vel
11	Torso	X-Accel
3	Torso	X-Disp
7	Torso	X-Vel
23	Torso	Y-Accel
15	Torso	Y-Disp
19	Torso	Y-Vel
47	Torso	Yaw-Accel
39	Torso	Yaw-Disp
43	Torso	Yaw-Vel
35	Torso	Z-Accel
27	Torso	Z-Disp
31	Torso	Z-Vel
57	Vehicle	Pitch-Accel
49	Vehicle	Pitch-Disp
53	Vehicle	Pitch-Vel
69	Vehicle	Roll-Accel
61	Vehicle	Roll-Disp
65	Vehicle	Roll-Vel
9	Vehicle	X-Accel
1	Vehicle	X-Disp
5	Vehicle	X-Vel

TABLE 22. VARIABLES (page 5)

21	Vehicle	Y-Accel
13	Vehicle	Y-Disp
17	Vehicle	Y-Vel
45	Vehicle	Yaw-Accel
37	Vehicle	Yaw-Disp
41	Vehicle	Yaw-Vel
33	Vehicle	Z-Accel
25	Vehicle	Z-Disp
29	Vehicle	Z-Vel

Enter the specified number of variable numbers. Again, any or all of these variables may be coded as mentioned above.

'ENTER TIME INTERVAL'

'FROM ( ) TO ( )'

Format: (5X, F7.5, 4X, F7.5)

Enter the time interval for which the search should be made.

The output of this section consists of:

1. The time at which the critical value was reached.
2. The value of the decision variable.
3. The values of the variables at that time (in the order that they were given, if there is more than one).

4.5.5 THE LIST TYPE OF INFORMATION REQUEST. This type of information request will simply list both all the contact surfaces which were used in the simulator run together with their numbers and all the ellipsoids used.

Two tables follow which contain listings of the variable numbers with the variables first in numerical order then in alphabetical order.

4.6 OVERALL PROGRAM ORGANIZATION AND FLOW

The overall functional layout of the program is implied by the integration techniques employed (see Section 4.4). The program is segmented so that the solution of Equation (2.2.3) for the generalized accelerations is accomplished by providing subroutine ACCEL with the current time, generalized coordinates, and generalized velocities. CARTIN is a subroutine which given time produces the vehicle coordinates, velocities, and accelerations. Figure 46 shows the overall flow of the program in terms of calls to these two subroutines.

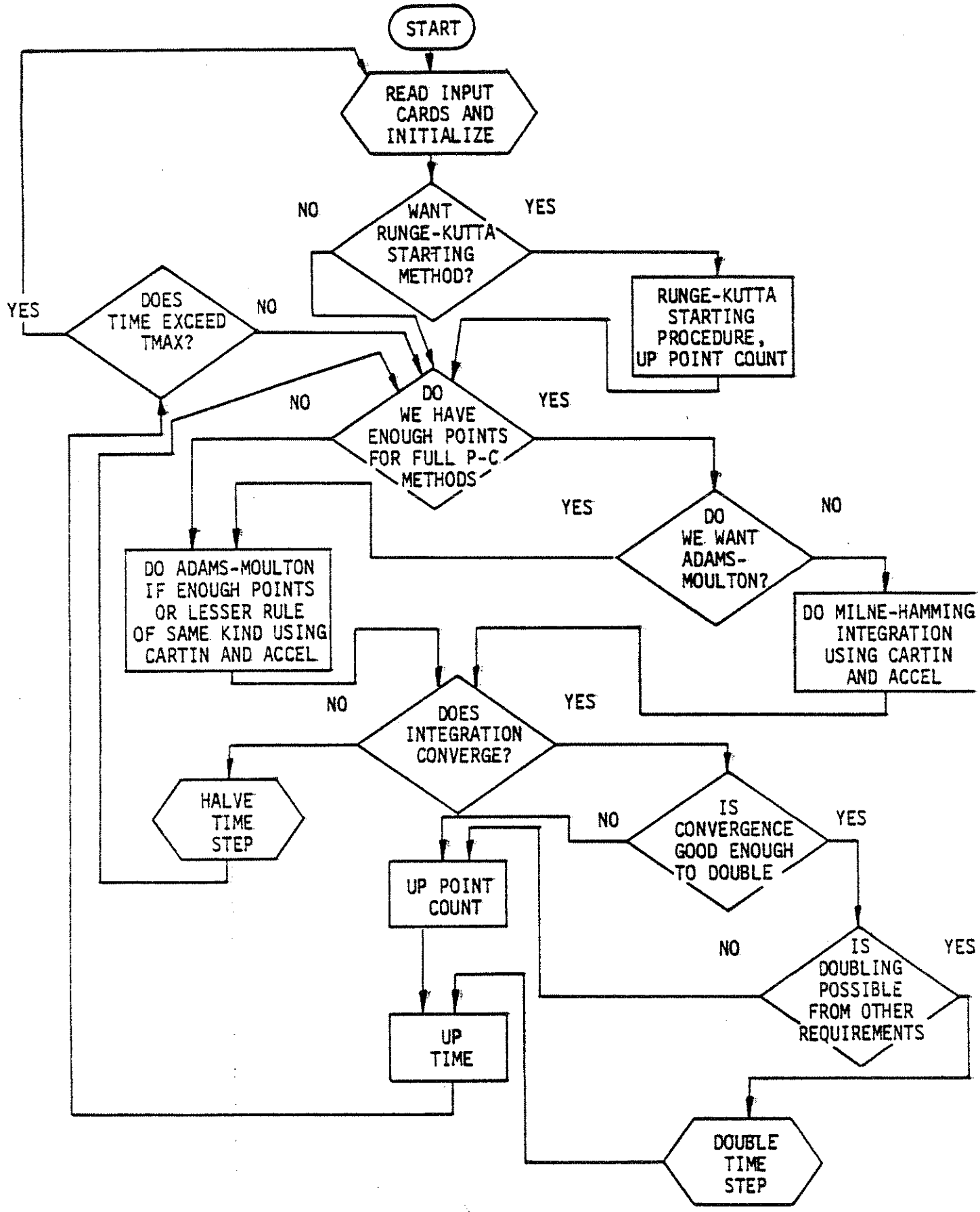

Figure 46. Flow Diagram for Three-Dimensional Victim Simulator

All variables are first initialized and accelerations are computed at time zero. A time step is then chosen and new accelerations computed. Based on this predicted value, a corrected value is obtained using a different mathematical forward prediction rule. This iterative predictor-corrector method is used until a convergence test is passed. An additional procedure which is applied is the limiting procedures discussed in Section 4.4. These tests occur in the flow diagram within the boxes which state that one or the other integrations should be done. After acceptable accelerations are determined, the equations are integrated to give final values for velocities, displacements, and other quantities as required and the information stored for later output.

4.7 SUBPROGRAM DESCRIPTIONS AND FLOW

The physical organization of the program consists of a main program, thirty-two subprograms, and twenty-one Fortran and MTS utility routines. In what follows, the main program will be treated as a subprogram which is named MAIN and is simply called first.

Table 23 contains a short description of each of the thirty-three subprograms together with four columns of information about interactions and communication between them. The Flow Sequence is a series of statements about parts of a program which indicate the steps that are taken and in what order and can be considered a flow diagram that has been written out. A flow sequence can be as elaborate as the whole program given step by step in English or as simple as a general description of purpose. In order to facilitate identification of which parts of the program code which correspond to each of the flow sequence statements, a "Statement Location" column has been provided. The statement location consists of a range of Fortran

Number	Subprogram Name	Statement Location	Flow Sequence or Description	Commons	Subprograms Called	Subprograms Calling	Special Output
1	ACCEL	120-160B	Initialize parameters if time is zero.	AC,BUG, CART,CNT, EP,QV,T, TC,TG,U	BELT CONTAC JOINT DABS DCOS DSIN SLE1	MAIN	DB11 DB12
		160-165	Check for run abort if angles running away.				
		165F-300B	Compute Equations (2.3.11), (2.3.12), and (2.3.13).				
		300-310F	Obtain generalized force contributions due to contact interactions, belts, and joints.				
		310	Sum up contributions to obtain total generalized force vector.				
		313B-END	Solve Equation (2.2.2) for generalized accelerations numerically.				
2	BELT	110F-150	Main loop which treats an individual belt segment. This loop is executed for each of the belt segments present.	BC,BUG, BV,CART, QV,T,TG,U	NEWLOF DARCOS DMIN1 DSQRT	ACCEL	DB1 DB2
		110F-120	Compute attachment and anchor points for current segment using Equations (2.6.3) and (2.6.4).				
		120F-130B	Compute attachment and anchor difference components and elongation using Equation (2.6.5).				
		130-135B	Compute lever arms using Equations (2.6.6) through (2.6.9), elongation rate using Equations (2.6.10) through (2.6.14), and force using NEWLOF.				
		160	Sum up all generalized force contributions for belts.				
3	CARTIN		Integrate the piece-wise linear acceleration profile segment by segment up to the current time using the exact solution. Certain tables are used which are computed in READAT for efficiency sake.	BUG, CART, TAB, DUM, PERD,T	GETY	MAIN RK	DB8
4	CMIL		Compute Milne corrector with Hamming's modification using the last four formulas in Equation (4.4.1).	C,T,U, XX	NONE	MAIN	NONE

TABLE 23. SUBPROGRAM SPECIFICATIONS AND APPEARANCES

Number	Subprogram Name	Statement Location	Flow Sequence or Description	Commons	Subprograms Called	Subprograms Calling	Special Output
5	CONTAC	9996F-550B	Initialize if time zero.	AC,BUG, CART,CON, DUM,IC MI,QV,T, TC,TG,U, XCN	NEWLOF DSQRT DMIN1 DSIGN	ACCEL	DB5 DB6 DB7 DB15
		550-110	Compute preliminary quantities which depend only on the contacts.				
		550F-70B	Interpolate corner point positions and velocities.				
		70-80B	Compute contact plane coefficients and rates in vehicle coordinates using Equation (2.5.8).				
		8095F-9911B	Compute contact plane coefficients and rates in inertial coordinates using Equation (2.5.7) and parts of lever arm expressions.				
		110F-111B	Compute junction points for seat back and seat cushion if pictorial ouput switch is on.				
		111-125	Compute body segment center of gravity locations using Equations (2.3.10), their velocities, and parts of the lever arm expressions dependent upon the coordinate matrix derivatives.				
		125F-130	Compute the parts of the lever arms dependent upon the ellipsoids using Equations (2.5.9) and (2.5.6).				
		140F-320	Compute forces, lever arms, impact positions for all combinations of ellipsoids and contact surfaces				
		140F-160B	Compute point of maximum deflection when there is contact using Equations (2.5.5) and (2.5.4).				
		160-230B	Compute contact surface coordinates and effectiveness factor using Equation (2.5.2).				
		230-790B	Compute lever arms, deflection, and deflection-rate using Equations (2.5.3) and (2.5.10) through (2.5.35).				
		798	Determine force by calling NEWLOF.				
		798F-END	Adjust force by effectiveness factor, store for printing, accumulate generalized force vector.				

TABLE 23. SUBPROGRAM SPECIFICATIONS AND APPEARANCES (continued)

Number	Subprogram Name	Statement Location	Flow Sequence or Description	Commons	Subprograms Called	Subprograms Calling	Special Output
6	CONTRL		Check to see if there are seven good points and that the doubled time step will not skip over next print time. If not all so, set switch which will prevent doubling.	DUM, EP,T	DABS DMOD	MAIN	NONE
7	CORK		Compute Moulton corrector using the second or the fourth pair of formulas in Equation (4.4.2) or if fewer points, the second, fourth, or sixth pair of formulas in Equation (4.4.4) depending on the number of points.	C,T,U, XX	NONE	MAIN	NONE
8	DEBUG		Obtain hexadecimal control word from table seven using GETY, extract the 16 two bit fields and shift to become integers and store in debug switch array.	BUG,T	GETY LAND SHFTR	MAIN READAT	NONE
9	DESCPT		Prints the two pages of normal printout summarizing injury data shown on pages two and three of Table 14.	MC,TOL	TITLE DABS	SUMRY	NONE
10	DETAB		Copy one of the deceleration tables back on itself leaving out any prints which fall in the specified closed time interval.	PERD,TAB	DABS DMAX1 DMIN1	READAT	NONE
11	ENTAB		Enter a new point in one of the deceleration tables.	PERD,TAB	MINO	READAT	NONE
12	ENTER		Enter a newly established set of generalized coordinates, velocities and accelerations together with the current time in the time history. If a normal entry, push down the values currently in the time history before entering the new ones.	T,U,XX	NONE	MAIN	NONE
13	EXCES		Check injury prediction quantities for violations. Report same in normal printout on "Summary of Quantities Exceeding Tolerances" page shown as page four of Table 15.	BUG	ABS DABS	SUMRY	DB16
14	GETY		Determine correct piecewise interval for current time and deceleration table and interpolate to current time. Don't interpolate if debug control word	PERD,TAB	DMOD MAXO	CARTIN DEBUG	NONE

TABLE 23. SUBPROGRAM SPECIFICATIONS AND APPEARANCES (continued)

Number	Subprogram Name	Statement Location	Flow Sequence or Description	Commons	Subprograms Called	Subprograms Calling	Special Output
15	INTAB		Sort deceleration tables into order and then compute slope and intercept for each of the linear segments of each table.	PERD,T, TAB	NONE	READAT	E5
16	JOINT	ENT-100B	Compute derivatives of rotation matrix for torso.	BUG,DUM, JC,JV, MC,QV, T,TG,U	DABS DARSIN DATAN2 DMIN1 DSIGN DSQRT	ACCEL	DB4
		100-180	For each of neck and hip joints, compute relative angles using Equations (2.7.7) through (2.7.12), compute torques controling joint motion using Equations (2.7.13) and (2.7.14), and apply to generalized force vector using lever arms computed using Equations (2.7.15), (2.7.16), and (2.7.17).				
17	LIMIT		Check to see if the activity load is too great for this time step using Equation (4.4.10). Then check to see if extrapolation change is too much using Equation (4.4.9).	BUG,DUM, EP,T,U, XX	DABS	MAIN	DB13
18	MAIN		Flow in the main program is shown by Figure 46.	BUG, CNT,EP T,TC,U, ULP,ULT, XX	ACCEL CARTIN CMIL CONTRL CORK DEBUG ENTER LIMIT PMIL PRED READAT RK STASH SUMRY UPDATE DABS MINO TIME	NONE	DB9 E1 E2 E3
		30-100B	Compute starting values with a Runge-Kutta method using subroutine RK and Equation (4.4.6).				
		100-END	Compute continuing time steps using a predictor-corrector method.				
		160-210B	Halve the time step using Equation (4.4.7).				
		265-285B	Double the time step using Equation (4.4.8).				
		285-END	Print error messages if corresponding conditions have arisen.				

TABLE 23. SUBPROGRAM SPECIFICATIONS AND APPEARANCES (continued)

Number	Subprogram Name	Statement Location	Flow Sequence or Description	Commons	Subprograms Called	Subprograms Calling	Special Output
19	NEWLOF		Compute force given deflection and deflection-rate using Equation (2.4.11).	BUG,LD, ULP, ULT	STASH SUMRY EMIN1 ERROR	BELT CONTAC	DB10 E6
20	NUPAGE		Check to see if output page is full and insert page eject and title if so.	NONE	TITLE	READAT	NONE
21	PAGE4		Print probability of occurrence page shown as page five of Table 15.	PP	NONE	SUMRY	NONE
22	PMIL		Compute Milne predictor with Hamming's modification using the first four formulas in Equation (4.4.1).	C,T, U,XX	NONE	MAIN	NONE
23	PRED		Compute Adams predictor using the first or third pair of formulas in Equation (4.4.2) or if fewer points, the first, third, or fifth pair of formulas in Equation (4.4.4) depending on the number of points.	C,T,XX	NONE	MAIN	NONE
24	READAT	ENT-1B	Do initialization of all basic quantities for run.	AC,BC, BV,CART, CON,DUM, EP,IC, JC,LD, MC,PP, T,TAB, TC,TL, TOL,U, XX	DEBUG DETAB ENTAB INTAB NUPAGE REDTAB RELCLE TITLE DABS DCOS DFLOAT DMAX1 DSIN DSQRT IDINT MAXO TIME	MAIN	E4
		1-2600B	For each card identification letter A through Y go to corresponding section of code which converts units and stores the quantities present on the card in the proper common. Then go back and read another card. This process is terminated normally by a Z-card.				
		2600-END	For a Z-card, do data checking, conversion, and immediate initializations in final preparation for executing the simulator. Print the normal printout containing input quantities shown as Table 9.				

TABLE 23. SUBPROGRAM SPECIFICATIONS AND APPEARANCES (Continued)

Number	Subprogram Name	Statement Location	Flow Sequence or Description	Commons	Subprograms Called	Subprograms Calling	Special Output
25	REDTAB		Initialize all deacceleration tables to zero and set size parameters.	PERD, TAB	NONE	READAT	NONE
26	RELCLE		Convert initial conditions with respect to vehicle system into equivalent values with respect to inertial system.	DUM	DARSIN DATAN2 DCOS DSIN	READAT	NONE
27	RK		Set up constants for desired Runge-Kutta method and and integrate a starting point using Equation (4.4.3).	EP,T, U,XX	ACCEL CARTIN	MAIN	NONE
28	SPX		Compute the head anterior-posterior acceleration component and return as argument XHPP.	BUG, DUM,T, TG,U, XCN	NONE	STASH	DBIG
29	SPY		Compute the head lateral acceleration component, the chest anterior-posterior acceleration component, and the chest superior-inferior acceleration component and return as arguments YHPP, XCPP, ZCPP respectively.	BUG, DUM,T, TG,U,	NONE	STASH	DBIG
30	STASH		Store one time point in accumulating arrays for a page of normal printout. If this time point completes a full page, call SUMRY to print page. If either or both of the special outputs for TALK3 and 3DP respectively are desired, add the information from the current time in the form of an additional record, accumulate the severity index integration.	AC,BC, BUG,BV, CART, CNT,CON, DUM,EP, IC,JV, MC,SS, SW,SZ, T,TC, TG,TL, TOL,U, XCN	SPX SPY SUMRY DABS	NEWLOF MAIN	DB3 DB14

TABLE 23. SUBPROGRAM SPECIFICATIONS AND APPEARANCES (Continued)

Number	Subprogram Name	Statement Location	Flow Sequence or Description	Common	Subprograms Called	Subprograms Calling	Special Output
31	SUMRY		Print one page of bulk of normal printout shown as Tables 10, 11, 12, 13, 14 and page one of 15. Then call routines which produce the supplementary injury printout.	BC,CON, PP,SS, SW,SZ, TL,TOL	DESCPT EXCES PAGE4 TITLE	NEWLOF MAIN STASH	NONE
32	TITLE		Increment page count, insert page eject, and print the three-line title for the new page of normal printout.	TL	NONE	DESCPT NUPAGE READAT SUMRY	NONE
33	UPDATE		Update special arrays which contain the values of certain quantities at the last established time point in final preparation for accepting the current time point as established.	JV,TC	NONE	MAIN	NONE

TABLE 23. SUBPROGRAM SPECIFICATIONS AND APPEARANCES (Concluded)

TABLE 24. LIBRARY FUNCTION DESCRIPTIONS

1.	ABS	Integer absolute value of an integer argument.
2.	DABS	Double precision absolute value of a double precision argument.
3.	DARCOS	Double precision arccosine of a double precision argument.
4.	DARSIN	Double precision arcsine of a double precision argument.
5.	DATAN2	Double precision arctangent of two double precision arguments.
6.	DCOS	Double precision cosine of a double precision argument.
7.	DFLOAT	Convert integer argument to double precision.
8.	DMAX1	Obtain maximum of two or more double precision arguments.
9.	DMIN1	Obtain minimum of two or more double precision arguments.
10.	DMOD	Obtain double precision argument one modulo double precision argument two.
11.	DSIGN	Obtain sign of double precision argument two times the magnitude of double precision argument one.
12.	DSIN	Double precision sine of a double precision argument.
13.	DSQRT	Double precision square root of a double precision argument (which must be positive).
14.	ERROR	Return control to MTS to terminate execution and trigger a hexadecimal memory dump if that has been permitted by the user.[33]
15.	IDINT	Obtain the largest integer (in magnitude) in a double precision argument.
16.	LAND	Obtain a bitwise logical "and" of two full word arguments (i.e., the result has bits on only if the corresponding bits of both arguments are on).[33]
17.	MAXO	Integer maximum of two or more integer arguments.
18.	MINO	Integer minimum of two or more integer arguments.
19.	SHFTR	The first full word argument is shifted right by the number of bits specified by the second integer argument.
20.	SLE1	Solve the set of simultaneous linear equations AX=B by Gaussian elimination (see MTS Vol. 3, page 235).[33]
21.	TIME	Allow the user easy access to the elapsed time, CPU time used, time of day, and the date in convenient units (see MTS Vol. 3, page 257).[33]

TABLE 25. LABELED COMMON DESCRIPTIONS

Number	Common Name	Subprograms Which Use	Description
1	AC	ACCEL,CONTAC,READAT,STASH	Physical properties of body segments.
2	BC	BELT,READAT,STASH,SUMRY	Physical properties of belts.
3	BUG	ACCEL,BELT,CARTIN,CONTAC, DEBUG,EXCES,JOINT,LIMIT, MAIN,NEWLOF,SPX,SPY,STASH	Debug printout control switches.
4	BV	BELT,READAT,STASH	Belt forces and subsidiaries.
5	C	CMIL,CORK,PMIL,PRED	Integration rule constants.
6	CART	ACCEL,BELT,CARTIN,CONTAC, READAT,STASH	Vehicle quantities and derived integration constants.
7	CNT	ACCEL,MAIN,STASH	Integration step counters.
8	CON	CONTAC,READAT,STASH,SUMRY	Contact and ellipsoid input parameters.
9	DUM	CARTIN,CONTAC,CONTRL, JOINT,LIMIT,READAT,RELCLE, SPX,SPY,STASH	Temporary storage and profile modifiers.
10	EP	ACCEL,CONTRL,LIMIT,MAIN, READAT,RK,STASH	Program control input parameters.
11	IC	CONTAC,READAT,STASH	Contact forces and subsidiaries.
12	JC	JOINT,READAT	Joint input parameters.
13	JV	JOINT,STASH,UPDATE	Joint forces and subsidiaries.
14	LD	NEWLOF,READAT	Force saturation parameters.
15	MC	CONTAC,DESCPT,JOINT, READAT,STASH	Numerical constants
16	PERD	CARTIN,DETAB,ENTAB,GETY, INTAB, REDTAB	Deceleration table size parameters.
17	PP	PAGE4,READAT,SUMRY	Probability printout parameters.
18	QV	ACCEL,BELT,CONTAC,JOINT	Generalized force contributions.
19	SS	STASH,SUMRY	Storage for one printed page of vehicle and body kinematics.
20	SW	STASH,SUMRY	One printed page storage for belts, relative quantities, joints and kinetic energies.
21	SZ	STASH,SUMRY	One printed page storage for severity index, contact forces and injury parameters.
22	T	ACCEL,BELT,CARTIN,CMIL, CONTAC,CONTRL,CORK,DEBUG, ENTER,INTAB,JOINT,LIMIT, MAIN,PMIL,PRED,READAT,RK, SPX,SPY,STASH	Time control parameters.

TABLE 25. LABELED COMMON DESCRIPTIONS
(continued)

Number	Common Name	Subprogram Which Use	Description
23	TAB	DETAB,ENTAB,GETY,INTAB, READAT,REDTAB	Deceleration and debug tables and subsidiaries.
24	TC	ACCEL,CONTAC,MAIN,READAT, STASH,UPDATE	Reoccurring combinations of body angles and velocities.
25	TG	ACCEL,BELT,CONTAC,JOINT, SPX,SPY,STASH	Trigonometric combinations presented in Equation (2.3.12)
26	TL	READAT,STASH,TITLE	Printout page title and print controls.
27	TOL	DESCPT,READAT,STASH,SUMRY	Injury tolerance input parameters.
28	U	ACCEL,BELT,CMIL,CONTAC, CORK,ENTER,JOINT,LIMIT, MAIN,PMIL,READAT,RK,SPX, SPY,STASH	Current values of generalized coordinates and derivatives.
29	ULP	MAIN,NEWLOF	Last established values of load-deflection variables.
30	ULT	MAIN,NEWLOF	Current values of load-deflection variables.
31	XCN	CONTAC,SPX,SPY,STASH	Body segment center of gravity coordinates and derivatives.
32	XX	CMIL,CORK,ENTER,LIMIT, MAIN,PMIL,PRED,READAT,RK	Time history of established values of generalized coordinates,velocities, and accelerations.

statement numbers which includes the code which is being talked about. Often there will be no statement number on the ends of the code to be discussed. This problem is handled by appending a suffix of "B" or "F" (which means "before" or "after" respectively) to a nearby statement number. "END" designates the physical last statement of the subprogram (and "ENT" the first).

The "Commons" column lists in alphabetical order all the labeled commons used for communication between this subprogram and others. The "Subprograms Called" column lists all the other subprograms in alphabetical order which this one uses followed by a list of all the library functions used. "Subprograms Calling" lists all the subprograms which use this one. "Special Output" lists all the auxillary output which eminates from this subprogram. A prefix of "DB" indicates the debug switch number found in Tables 17 and 18. A prefix of "E" indicates the number of the error message in the order found in Table 19.

Table 24 lists each of the library functions used and gives a brief description of each. Table 25 presents all the labeled commons, the subprograms which share each one, and an indication about the type of information each contains.

4.8 SYMBOL DICTIONARY

This section consists of three tables which offer an aid to a more detailed examination of the program code and its correspondence to the analysis behind the code.

Table 26 is the main symbol dictionary which is ordered on the Fortran name given to each quantity. The "Symbol" column contains the analytical symbol used in Part 2 and/or 4.1. The third column gives either the label of the common in which this variable resides or the name of the subprogram in which it is used if it is not shared between subprograms. Columns four and

five are used together to detail quantities which have been stored in arrays instead of individual variables. If a number appears in column five, it refers to the corresponding value in the first column of Table 28 which defines the quantity or type of information for each value of the subscript up to the number in the "Dimension" column.

Table 27 is provided to ease getting from the analysis to the program code and is ordered on symbol. Table 28 specifies the meanings of most of the subscripts used in arrays.

TABLE 26. SYMBOL DICTIONARY

Fortran Name	Symbol	Subprogram or Common	Dimension	Units or Subscript Reference	Definition
A	δ	NEWLOF	1	in.	Argument, total deflection, Figure 7.
AC	-	CON	300 10	32 1	Storage for corner point coordinates of contact surfaces.
ACCM	$\Delta\bar{Z}_{lim}$	EP	1	-	Extrapolation change limit.
ACN	-	XCN	9	2 in/sec^2	Accelerations of body segment centers of gravity.
AF	$\Delta t\bar{K}_{k,l}$	RK	12	3	First Runge-Kutta acceleration evaluation times the time step.
AKE	-	SUMRY	1	in.lb	Total linear kinetic energy.
AL	-	CON	34 10	4 33	Ellipsoid information storage array.
ALC	-	CONTAC	10	33	Ellipsoid intermediate result used in contact lever arms.
ANG	-	JC	2 3	5 6	Joint relative angle stop angles.
ANGTOL	-	TOL	6 2	7 deg. 8	Joint relative angle tolerance limits.
ANJ	-	JC	2	5 rad	Joint relative angle upper pitch stop angle.
ATHA	$A\theta_{ij}$	JOINT	1	-	Sine of relative pitch angle in a joint.
BA	-	BC	2 3 4	9 in. 10 11	Belt endpoint coordinates.
BANG	-	BV	4	11	Belt projected angles.
BASTOL	-	READAT	6 2 2	7 8 12	Default values of relative angle tolerance limits.
BB	-	CONTAC	12 25	- 34	Contact surface intermediate results.
BC	-	BELT	12	in.	Belt intermediate results in rate calculation.
BC	-	CON	41 25	13 34	Contact surface information array.
BEA	-	SW	41 12	35 14	Belt angle printout storage.

TABLE 26. SYMBOL DICTIONARY
(Continued)

Fortran Name	Symbol	Subprogram or Common	Dimension	Units or Subscript Reference	Definition
BEL	-	BEL	41 4	35 11	Belt force printout storage.
BELTOL	-	TOL	4	15	Combined belt force tolerance limits.
BF	$\Delta t\ddot{K}_{k,2}$	RK	12	3	Second Runge-Kutta acceleration evaluation times the time step.
BJOF	-	SW	41 12	35 16	Joint torque printout storage.
BKE	-	SUMRY	1	in.lb.	Total rotational kinetic energy.
BL	$\ell_n(t)$	BELT	4	11	Belt segment lengths.
BLEK	-	SS	41 18	35 17	Leg kinematics printout storage.
BLZ	$\ell_n(o)$	BELT	4	11	Initial belt segment lengths.
BX	-	BELT	1	in.	X-component of belt length.
BXA	$\hat{x}_n, \hat{\underline{X}}_n$	BELT	2	9	Inertial X-coordinate of belt endpoints.
BXD	-	BELT	1	in/sec	Rate of change of belt length X-component.
BY	-	BELT	1	in.	Y-component of belt length.
BYA	$\hat{y}_n, \hat{\underline{Y}}_n$	BELT	2	9	Inertial Y-coordinate of belt endpoints.
BYD	-	BELT	1	in/sec	Rate of change of belt length Y-component.
BZ	-	BELT	1	in.	Y-component of belt length.
BZA	$\hat{z}_n, \hat{\underline{Z}}_n$	BELT	2	9	Inertial Z-coordinate of belt endpoints.
BZD	-	BELT	1	in/sec	Rate of change of belt length Z-component.
C	c_i	C	29	-	Integration rule coefficients for predictor-correctors, Table 20, lines one through twenty-nine.
C	c_i+29	RK	21	-	Integration rule coefficients for Runge-Kutta methods, Table 20, lines thirty through fifty.

TABLE 26. SYMBOL DICTIONARY
(Continued)

	Symbol	Subprogram or Common		Units or Subscript Reference	Definition
C	-	TG	3 4	6 18	Cosines of generalized angles.
CARD	-	READAT	8	-	Temporary storage for numerical fields of input data cards.
CARTV	-	CART	3 6	19 20	Vehicle kinematics.
CC	-	CONTAC	9 3	- 21	Intermediate results from body segments in contact surface lever arms.
CD	-	CONTAC	6 3	- 21	Intermediate results from body segments in contact surface lever arms.
CE	-	CONTAC	9 3	- 21	Intermediate results from body segments in contact surface lever arms.
CEPT	-	ULP	26 10	39 33	Computed deflection at which force will go zero during saturation unloading.
CF	$\Delta t\ddot{K}_{k,3}$	RK	12	3	Third Runge-Kutta acceleration evaluation times the time step.
CH	-	CONTAC	3 3	10 21	Body segment center of gravity coordinates.
CI	-	READAT,RELCLE	36	22	Initial conditions which end up inertial.
CK	-	SZ	41 5 40	35 23 36	Contact force printout storage.
CKE	-	SUMRY	1	in.lb.	Total kinetic energy for the torso.
CMOTOL	-	TOL	1	g-units	Tolerance limit for chest anterior-posterior acceleration.
CNST	-	TAB	100 6 2	37 20 40	Storage for deceleration table computed slopes and intercepts.
CONTOL	-	TOL	1	rad/sec^2	Tolerance limit for pitch concussion.
CORTOL	-	TOL	1	lbs	Tolerance limit for chest force.
CSITOL	-	TOL	1	g-units	Tolerance limit for chest superior-inferior acceleration.

TABLE 26. SYMBOL DICTIONARY
(Continued)

Fortran Name	Symbol	Subprogram or Common	Dimension	Units or Subscript Reference	Definition
CT	-	IC	5 40	23 36	Contact output storage between CONTAC and STASH.
CUR	-	CART	100 6 2	37 20 41	Storage for deceleration table computed velocities and displacements for each linear segment.
CUT	-	BELT,CONTAC,JOINT	1	-	Factor to make damping forces continuous at zero deflection (see Figure 7).
D	-	C	4	-	Milne integration coefficients.
D	δ'	NEWLOF	1	in.	Effective deflection into a load-deflection curve.
D	t_n	READAT	1	in.	Thickness along i-axis inputted for moment of inertia calculation.
DA	-	JV	2 3	5 6	Joint relative angles.
DAMPJ	-	JC	2 3	5 6	Joint relative angle damping coefficients.
DAZ	-	JOINT	2 3	5 6	Initial joint relative angles.
DD	-	CONTAC	13	42	Lever arms and deflection rate for contacts.
DD	$\dot{\delta}$	NEWLOF	1	in/sec	Deflection rate for load-deflection curve.
DDC	-	CONTAC	25	34	Vehicle contribution to contact deflection rate.
DDS	-	CONTAC	25	34	Contact surface contribution to contact deflection rate.
DEL	-	LIMIT,MAIN	1	-	Weighted averages of various test quantities.
DELB	δ_n	BV	4	11	Belt elongations.
DELD	$\dot{\delta}_n$	BV	4	11	Belt elongation rates.
DELTAT	Δt_{max}	T	1	sec	Maximum time step.
DF	$\Delta t\ddot{K}_{k,4}$	RK	12	3	Fourth Runge-Kutta acceleration evaluation times the time step.
DFAC	-	DUM	6	20	Factor to change the amplitude of a deceleration table.

TABLE 26. SYMBOL DICTIONARY
(Continued)

Fortran Name	Symbol	Subprogram or Common	Dimension	Units or Subscript Reference	Definition
DHAT	-	CONTAC	9	1 in/sec	Contact surface corner coordinate rates.
DK	-	CONTACT	1	-	Part of the contact normalizing factor.
DKE	-	SUMRY	1	in.lb.	Total kinetic energy for the head.
DLJ	ρ_i	READAT	3	21	Distance from body segment center of gravity to lower joints.
DMAX	-	EXCES	1	-	Maximum value of variable above its tolerance level
DMC	-	CONTAC	3 25	- 34	Intermediate results in computing DDC.
DONTOL	-	READAT	1	deg/sec^2	CONTOL in degrees.
DPHI	$D\phi_{ij}$	JOINT	1	-	Proportional to cosine of relative roll.
DPSI	$D\psi_{ij}$	JOINT	1	-	Proportional to cosine of relative yaw.
DR	$\pi/180$	MC	1	rad/deg	Angular conversion factor from degrees to radians.
DT	-	CONTAC	54 3	- 21	Intermediate results for contacts.
DTMIN	ϵ_t	EP	1	sec	Inputted time epsilon.
DTPRNT	Δt_{prnt}	T	1	sec	Inputted print time interval.
DUJ	ρ_i	READAT	3	21	Distance from body segment center of gravity to upper joints.
DUM	-	DUM	48	-	Temporary storage array.
DUR	-	EXCES	1	sec	Duration of tolerance violation.
EDEPS	$\epsilon_{\ddot{Z}}$	EP	1	-	Inputted acceleration minimum magnitude.
EJ	-	JV	2 3	5 6	Joint elasticity torque.
EKE	-	SUMRY	1	in.lb.	Total kinetic energy for legs.
ELAS	-	JC	2 3	5 6	Symmetric joint elasticity coefficients.
EM	m	ACCEL	12 12	3 3	Generalized mass matrix.

TABLE 26. SYMBOL DICTIONARY
(Continued)

Fortran Name	Symbol	Subprogram or Common	Dimension	Units or Subscript Reference	Definition
EMM	m_i	AC	3	21	Body segment mass.
ENPHI	$N\phi_{ij}$	JOINT	1	-	Proportional to sine of relative roll.
ENPSI	$N\psi_{ij}$	JOINT	1	-	Proportional to sine of relative yaw.
ENRG	-	SW	41 6	35 20	Kinetic energy printout storage.
EPS	ϵ	CONTAC	1	sec	Parameter for linearizing contact surface corner point velocities.
EPSLN	Ω	ULP	26 10	39 33	Accumulated permanent deformation.
EPZA	ΔV_{lim}	EP	1	-	Inputted velocity change limit.
EPZV	ϵ_v	EP	1	-	Inputted velocity convergence parameter.
ESG	g	MC	1	in/sec^2	Earth standard gravity (386.4 in/sec^2).
ETA	δ	CONTAC	1	in.	Deflection of contact surface by body ellipsoid
EYE	I_{in}	AC	3 3	10 21	Body segment principle axis moments of inertia.
F	-	EXCES	1	-	Argument specifying if tolerance test is to be below limit, above in magnitude, or above limit by comparing to zero.
F	$\lvert F_F \rvert$	NEWLOF	1	lb.	Argument returning computed force.
FARB	F_{max}	LD	29	43	Inputted maximum force for saturation.
FB	-	BV	4	11	Belt force.
FDK	-	CONTAC	1	-	Intermediate result in deflection rate and lever arm calculations.
FED	-	JOINT	1	-	Intermediate result in joint lever arm for roll calculation.
FK	k	CONTAC	1	-	Normalization factor in contact calculations for deflection.
FKE	-	SUMRY	1	in.lb.	Total kinetic energy.
FT	-	CONTAC	1	lb.	Total contact force.

TABLE 26. SYMBOL DICTIONARY
(Continued)

Fortran Name	Symbol	Subprogram or Common	Dimension	Units or Subscript Reference	Definition
GNETOL	-	TOL	1	lb.	Tolerance limit for knee force.
GRAV	g	MC	1	in/sec^2	Local gravity constant.
H	h_n	READAT	1	in.	Height of body segment used in calculation of moments of inertia.
HEK	-	SS	41	35	Head kinematics printout storage.
HP	-	STASH	3	10	Relative hip coordinates.
I	i	MANY	1	-	General index.
IA	-	CONTAC	1	-	General index.
IA	-	DESCPT	4 2	- -	Angular tolerance printout label storage.
IACCEL	-	TC	1	-	Fatal flag that an angle has exceeded ten radians, when non-zero the contents is the index of the first offending angle.
IACMAX	-	READAT	1	-	Total number of points in AC, maximum is 300.
IALPH	-	READAT	26	-	Input card identification letter storage.
IBLANK	-	READAT	1	-	EBCD for blanks used in making formats.
IBUG	-	BUG	16	-	Debug output control switch array.
IC	-	NUPAGE	1	-	Argument which is set non-zero if new page was required.
IC	-	DEBUG	16	-	Shift control array in debug unpacking.
IC	-	CON	9 25	24 34	Contact surface information.
ICF	-	TOL	16	-	Indices of contacts comprising frontal structure of vehicle interior.
ICHEST	-	TOL	1	-	Index of ellipsoid simulating chest.
ICK	-	READAT	1	-	New page switch, non-zero for new page.
ICOUNT	-	CNT	21	-	Number of time steps at each of the possible halving levels.

TABLE 26. SYMBOL DICTIONARY
(Continued)

Fortran Name	Symbol	Subprogram or Common -	Dimension	Units or Subscript Reference	Definition
ICT	-	IC	2	25	Storage for indices of ellipsoids and contacts interacting to produce force.
ID	-	READAT	1	-	Input card identification letter.
IDATE	-	TL	3	-	Date label storage.
IDESP	-	EXCES	7 15	- -	Tolerance label printout storage.
IDUM	-	DUM	96	-	Equivalenced to DUM, used in READAT to hold English versions of inputted switches.
IDUM	-	SUMRY	32	-	Used to formulate contact page headings.
IE	-	EXCES	1	-	Injury weighting code value as argument.
IE	-	SUMRY	21	-	Weighting code storage for injuries.
IENRG	-	TL	1	-	Inputted energy printout switch.
IFM	-	READAT	25	-	Used to construct the appropriate format for the current line of deceleration profile printout.
IFRMT	-	READAT	12	-	EBCD format components needed for IFM.
IFRMTA	-	SUMRY	108	-	Used to construct a format for the current heading in the contact printout pages.
IFRMTB	-	SUMRY	28	-	Used to construct a format for the current numerical line of contact information for the contact printout pages.
IHIB	-	IC	10 25	33 34	Inputted inhibitions of contact interactions.
IHIBRD	-	READAT	1	-	Inputted switch to inhibit printout of inputted values.
IHIBSM	-	TL	1	-	Inputted switch to inhibit parts of normal printout from SUMRY.

TABLE 26. SYMBOL DICTIONARY
(Continued)

Fortran Name	Symbol	Subprogram or Common	Dimension	Units or Subscript Reference	Definition
II	-	MANY	1	-	General index.
II	-	LIMIT	1	-	Argument which is switch when non-zero means to halve current time step.
III	-	INTAB	1	-	General index.
IK	-	SZ	2 40	25 36	Ellipsoid and contact indices for each interaction which is to be reported on this "page" of printout.
IKNEE	-	TOL	1	-	Index of ellipsoid simulating knee.
IL	-	CON	6 10	26 33	Ellipsoid information.
ILIM	-	CNT	1	-	Current time step halving level.
IM	-	STASH	1	-	General index.
IMAX	-	EXCES	1	-	Time point index of peak tolerance violation.
IMAX	-	GETY,INTAB	1	-	Number of points in current deceleration profile table.
IMAX	-	SZ	1	-	Number of time points on current printout page.
IMIN	-	GETY	1	-	Index of deceleration profile table point which will serve as the start of the search for the current time interval.
IN	-	TITLE	3 3	- -	EBCD of printout part subtitle labels.
INTCI	-	READAT	1	-	Inputted switch controlling the conversion of initial conditions.
INZ	-	PMIL,PRED	1	-	Switch to recognize the first time through these routines after loading to initialize constants.
IOVER	-	STASH	1	-	Argument which is non-zero causes by-passing of the normal print time test in order to record data for printing.
IP	-	PP	3 6	- -	Probability event label storage.

TABLE 26. SYMBOL DICTIONARY
(Continued)

Fortran Name	Symbol	Subprogram or Common	Dimension	Units or Subscript Reference	Definition
IPAGE	-	TL	1	-	Printout page counter.
IPC	-	EP	1	-	Inputted predictor-corrector selection switch.
IPENG	-	TC	10 25	33 34	Switch for every interaction which records if that interaction produced force or was approached from behind.
IPERM	-	ACCEL	24	-	Temporary storaged required by SLE1.
IQT	-	EXCES	1	-	Argument which is index of tolerance printout label.
IRK	-	EP	1	-	Inputted integration starting method selection switch.
ISA	-	ACCEL,BELT,JOINT	1	-	Index of first debug level switch.
ISB	-	ACCEL,BELT,JOINT	1	-	Index of second debug level switch.
ISB	-	CONTAC	1	-	Index of seat back corner point furthest from seat cushion.
ISB	-	READAT	1	-	Lower limit index for deceleration profile printout.
ISBB	-	CONTAC	1	-	Index of seat back corner point next furthest from seat cushion (see ISB).
ISC	-	CONTAC	1	-	Index of seat cushion corner point furthest from seat back.
ISCC	-	CONTAC	1	-	Index of seat cushion corner point next furthest from seat back (see ISC).
ISEB	-	IC	1	-	Index of contact surface simulating the seat back.
ISET	-	IC	1	-	Index of contact surface simulating the seat cushion.
IST	-	CONTAC	2	-	(ISB,ISBB) ordered by Y-value.

TABLE 26. SYMBOL DICTIONARY
(Continued)

Fortran Name	Symbol	Subprogram or Common	Dimension	Units or Subscript Reference	Definition
ISTIFF	-	TOL	1	-	Inputted switch specifying stiff or flexible torso for purpose of angular tolerance default limits.
ISWT	-	GETY	1	-	Switch which causes table interpolation to be suspended, invoked only for debug control word table (number seven).
ISWT	-	ULP	26 10	39 33	Switch which records last status of each interaction of possibilities shown in Figure 7.
IT	-	MAIN	1	-	Correction number index in the Adams-Moulton type of predictor-corrector.
ITAB	-	PERD	1	-	Number of deceleration profile type of tables (six).
ITHRU	-	READAT	1	-	Similar to INZ but for READAT.
ITITLE	-	TL	1	-	Inputted subtitle storage.
ITOL	-	DESCPT	8	-	Temporary storage for tolerance limit values to be printed as integers.
ITOR	-	READAT	2 5	- -	EBCD of body segment names and directions used in printout of inputted values.
ITST	-	ULT	26 10	39 33	Temporary value of ISWT.
J	j	MANY	1	-	Equivalenced to double precision table value to enable access to last 32 bits.
JA	-	CONTAC	1	-	General index.
JJ	-	MANY	1	-	General index.
K	k	MANY	1	-	General index.
KA	-	SUMRY	1	-	General index.
KB	-	SUMRY	1	-	General index.
KK	-	READAT	1	-	General index.
KNTACC	-	CNT	1	-	Number of times ACCEL has been called.

TABLE 26. SYMBOL DICTIONARY
(Continued)

Fortran Name	Symbol	Subprogram or Common	Dimension	Units or Subscript Reference	Definition
KNTDUB	-	CNT	1	-	Number of times convergence has been good enough to double the time step but other requirements were not met.
KNTOT	-	CNT	1	-	Total number of time steps of all sizes.
KT	-	ENTER	1	-	General index.
KTA	-	ENTER	1	-	General index.
L	1	MANY	1	-	General index.
LA	-	SUMRY	1	-	General index.
LB	-	SUMRY	1	-	General index.
LC	-	SUMRY	1	-	General index.
LD	-	SUMRY	1	-	General index.
LIMENT	-	PERD	1	-	Maximum number of entries allowed per deceleration table (100).
LIMTAB	-	PERD	1	-	Maximum number of input tables both deceleration and others (7).
LINE	-	READAT	1	-	Printout line counter.
LL	-	RELCLE	1	-	General index.
LN	-	READAT	1	-	Logical device number to be read from next.
LS	-	READAT	1	-	Number of lines to skip before reading.
LSWT	-	LD	29	43	Switch which is set non-zero if saturation is to be checked for.
M	m	MANY	1	-	General index.
MASK	-	DEBUG	16	-	Two bit masks for extracting each switch value from the total control word.
MILL	-	MAIN	1	msec	Total CPU time of execution so far.
MK	-	SZ	1	-	Number of contact forces to be printed.
ML	-	CONTAC	1	-	General index.
ML	-	SUMRY	1	-	Number of contact forces per page.
MLIM	N_{max}	EP	1	-	Inputted maximum number of halvings which will be permitted.

TABLE 26. SYMBOL DICTIONARY
(Continued)

Fortran Name	Symbol	Subprogram or Common	Dimension	Units or Subscript Reference	Definition
QTD	-	ACCEL	3 3	- -	Intermediate results used in centifugal force terms.
RFAC	R	CONTAC	1	-	Contact surface edge effect factor.
RHO	ρ_i	AC	6	29	Body segment center of gravity to joint distance.
RHOST	-	CONTAC	2	in.	Directed distance from torso center of gravity to neck and hip.
RHP	-	SW	41 9	35 30	Relative angle and hip position printout storage.
S	-	TG	3 4	6 18	Sines of generalized angles.
SA	k_1	NEWLOF	1	lb/in.	Linear spring constant as argument.
SAVE	-	MAIN	12	3	Temporary storage for first attempt with Runge-Kutta.
SB	k_2	NEWLOF	1	lb/in^2	Quadradtic spring constant as argument.
SBEL	-	SUMRY	41 2	35 15	Total belt forces, sum for shoulder belts and lap belts.
SC	k_3	NEWLOF	1	lb/in^3	Cubic spring constant as argument.
SD	c	NEWLOF	1	lb.sec/in.	Damping constant as argument.
SFAC	S	CONTAC	1	-	Contact surface edge effect factor.
SI	-	SZ	41	35	Severity index storage.
SIDTOL	-	TOL	1	g-units	Head lateral acceleration tolerance limit.
SIGMB	-	BC	3 4	46 11	Belt elastic coefficient.
SIGZB	-	BC	4	11	Belt damping coefficients.
SII	-	STASH	1	-	Accumulation of severity index.
SITOL	-	TOL	1	-	Severity index tolerance limit.
SJ	-	JV	2 3	5 6	Joint stop torque.
SLAK	Δ_n	BC	4	11	Belt segment slack

TABLE 26. SYMBOL DICTIONARY
(Continued)

Fortran Name	Symbol	Subprogram or Common	Dimension	Units or Subscript Reference	Definition
SLOPE	D	LD	29	43	Unloading slope in case of saturation.
ST	-	IC	3 6	10 31	Seat corner point coordinates.
STOP	-	JC	2 3	5 6	Joint stop coefficients, symmetric yaw and roll and lower pitch.
STOR	-	TAB	100 7 2	37 44 -	Storage for input table time points.
STP	-	JC	2	5	Upper pitch stop coefficients.
T	t	T	1	sec	Simulated time.
T	-	EXCES	1	-	Argument containing tolerance level.
TA	-	TC	3	$(rad/sec)^2$	Factor in centrifugal force terms.
TB	-	ACCEL	3	in.lb.	Factor in centrifugal force terms.
TC	-	TC	3 2	$(rad/sec)^2$	Factor in centrifugal force terms.
TCEP	-	ULT	26 10	39 33	Temporary value of CEPT.
TD	-	ACCEL	8 3	$(rad/sec)^2$	Factor in centrifugal force terms.
TDCUR	Δt	T	1	sec	Current integration time step.
TE	-	CONTAC	3 3	rad/sec 21	Factor in body segment center of gravity velocities.
TEPS	-	ULT	26 10	39 33	Temporary value of EPSLN.
TG	-	STASH	3 3	rad/sec^2 21	Factor in body segment center of gravity accelerations.
THD	-	JOINT	1	-	Factor in joint pitch lever arms.
TIM	-	SS	41	35	Time printout storage.
TJ	-	JOINT	2 3	5 6	Total joint torque.
TMAX	T_{max}	T	1	sec	Program run simulated time duration.

TABLE 26. SYMBOL DICTIONARY
(Continued)

Fortran Name	Symbol	Subprogram or Common	Dimension	Units or Subscript Reference	Definition
TMAX	-	EXCES	1	sec	Time of peak value of tolerance violation.
TOK	-	SS	41 18	35 17	Torso kinematics printout storage.
TOL	-	EXCES	1	-	Argument for tolerance level.
TOLF	-	ULT	26 10	39 33	Temporary value of OLDF.
TOLG	-	READAT	4	11	Belt segment force tolerance level.
TPC	-	CONTAC	1	-	Fraction of next time segment during which the contact surface corner point velocity is to be linearized.
TPRINT	-	T	1	sec	Computed next print time.
TQ	-	CARTIN,READAT	1	sec^2	Factor used in vehicle integration.
TS	-	EXCES,LIMIT,READAT	1	-	Temporary storage.
TS	-	ACCEL	8	-	Temporary storage.
TS	-	BELT	6	-	Temporary storage.
TSA	-	MANY	1	-	Temporary storage.
TSB	-	MANY	1	-	Temporary storage.
TSC	-	MANY	1	-	Temporary storage.
TSD	-	CONTAC	1	-	Temporary storage.
TSE	-	CONTAC	1	-	Temporary storage.
TSED	-	EXCES	1	sec	Time at which tolerance violation ceases.
TSF	-	CONTAC	1	-	Temporary storage.
TSG	-	CONTAC	1	-	Temporary storage.
TSH	-	CONTAC	1	-	Temporary storage.
TSI	-	CONTAC	1	-	Temporary storage.
TSN	-	CONTAC	1	-	Temporary storage.
TSP	-	CONTAC	1	-	Temporary storage.
TSQ	-	CONTAC	1	-	Temporary storage.
TSR	-	CONTAC	1	-	Temporary storage.
TSS	-	CONTAC	1	-	Temporary storage.
TSTR	-	EXCES	1	sec	Time at which tolerance violation begins.
TSXZ	-	CONTAC	1	in.	Factor in contact calculations.
TSYZ	-	CONTAC	1	in.	Factor in contact calculations.

TABLE 26. SYMBOL DICTIONARY
(Continued)

Fortran Name	Symbol	Subprogram or Common	Dimension	Units or Subscript Reference	Definition
TSZ	-	READAT	4 2	- -	Temporary storage.
TSZZ	-	CONTAC	1	in.	Factor in contact calculations.
TT	-	CARTIN	1	sec	Time on current deceleration table segment.
TT	-	SUMRY	1	lb.	Current force tolerance level.
TT	-	XX	10	38	Time history time storage.
TTT	-	READAT	1	sec	Length of current deceleration table segment.
U	u_{mk}	TG	4 4	- 18	Trigonometric combination, see Equation (2.3.12).
UA	$\ddot{Z}_k$	U	12	3	Generalized accelerations.
UDFE	-	JOINT	1	rad/sec	Factor in joint roll velocity.
UDPS	-	JOINT	1	rad/sec	Factor in joint yaw velocity.
UP	u'_{mk}	TG	4 4	- 18	Trigonometric combination, see Equation (2.3.12).
UP1JD	-	JOINT	1	rad/sec	Trigonometric combination rate.
UP1TD	-	JOINT	1	rad/sec	Trigonometric combination rate.
UP3JD	-	JOINT	1	rad/sec	Trigonometric combination rate.
UP3TD	-	JOINT	1	rad/sec	Trigonometric combination rate.
UV	$\dot{Z}_k$	U	12	3	Generalized velocities.
UX	Z_k	U	12	3	Generalized coordinates.
U2JD	-	JOINT	1	rad/sec	Trigonometric combination rate.
U2TD	-	JOINT	1	rad/sec	Trigonometric combination rate.
U3JD	-	JOINT	1	rad/sec	Trigonometric combination rate.
U3TD	-	JOINT	1	rad/sec	Trigonometric combination rate.
V	V_{mk}	TG	4	-	Trigonometric combination, see Equation (2.3.12).
VCN	-	XCN	9	2 in/sec	Body segment center of gravity velocities.

TABLE 26. SYMBOL DICTIONARY
(Continued)

Fortran Name	Symbol	Subprogram or Common	Dimension	Units or Subscript Reference	Definition
VDFE	-	JOINT	1	rad/sec	Factor in joint roll velocity.
VDPS	-	JOINT	1	rad/sec	Factor in joint yaw velocity.
VEK	-	SS	41	35	Vehicle kinematics printout storage.
V1JD	-	JOINT	1	rad/sec	Trigonometric combination rate.
V11D	-	JOINT	1	rad/sec	Trigonometric combination rate.
V2JD	-	JOINT	1	rad/sec	Trigonometric combination rate.
V21D	-	JOINT	1	rad/sec	Trigonometric combination rate.
V3JD	-	JOINT	1	rad/sec	Trigonometric combination rate.
V31D	-	JOINT	1	rad/sec	Trigonometric combination rate.
V4JD	-	JOINT	1	rad/sec	Trigonometric combination rate.
V41D	-	JOINT	1	rad/sec	Trigonometric combination rate.
W	w_n	READAT	1	in.	Width of body segment used in calculation of moments of inertia.
W	W_{mk}	TG	6	-	Trigonometric combination, see Equation (2.3.12).
WGT	$\overline{\mu}_k$	EP	12	3	Weighting factors.
WS	X	CONTAC	1	-	X-coordinate of special contact surface system, see Equation (2.5.2).
WT	Y	CONTAC	1	-	Y-coordinate of special contact surface system, see Equation (2.5.2).
X	-	ENTAB,GETY,INTAB	1	sec	Abcissa of input table.
XA	-	DETAB	1	sec	Lower endpoint of time range to be deleted.
XAT	-	DETAB	1	sec	Temporary storage for interchanging XA and XB.
XB	-	DETAB	1	sec	Upper endpoind of time range to be deleted.
XCN	-	XCN	9	2	Body segment center of gravity coordinates.

TABLE 26. SYMBOL DICTIONARY
(Continued)

Fortran Name	Symbol	Subprogram or Common -	Dimension	Units or Subscript Reference	Definition
XCDD	-	STASH	1	in/sec^2	Chest anterior-posterior acceleration.
XCPP	-	SPY	1	in/sec^2	Chest anterior-posterior acceleration as argument.
XCPP	-	SZ	41	35	Chest anterior-posterior acceleration tolerance testing storage.
XDTH	-	JOINT	1	rad/sec	Factor in joint pitch velocity.
XHAT	-	CONTAC	9	1	Contact surface corner point coordinates.
XHPP	-	SPX,STASH	1	in/sec^2	Head anterior-posterior acceleration.
XX	-	GETY	1	sec	Abcissa of input table.
XXX	-	XX	10 12 3	38 3 19	Time history of body kinematics.
XZ	x_o	CONTAC	1	in.	X-coordinate of actual contact point.
XZA	-	CONTAC	1	in.	X-coordinate of first possible contact point.
XZB	-	CONTAC	1	in.	X-coordinate of second possible contact point.
Y	-	DEBUG,ENTAB,GETY, INTAB	1	-	Ordinate of input table.
YCDD	-	STASH	1	in/sec^2	Chest superior-inferior acceleration.
YCPP	-	SZ	41	38	Chest superior-inferior acceleration.
YHDD	-	STASH	1	in/sec^2	Head lateral acceleration.
YHPP	-	SPY	1	in/sec^2	Head lateral acceleration as argument.
YHPP	-	SZ	41	35	Head lateral acceleration tolerance testing storage.
YZ	y_o	CONTAC	1	in.	Y-coordinate of actual contact point.
YZA	-	CONTAC	1	in.	Y-coordinate of first possible contact point.
YZB	-	CONTAC	1	in.	Y-coordinate of second possible contact point.
ZCPP	-	SPY	1	in/sec^2	Chest superior-inferior acceleration as argument.
ZZ	z_o	CONTAC	1	in.	Z-coordinate of actual contact point.

TABLE 26. SYMBOL DICTIONARY
(Concluded)

Fortran Name	Symbol	Subprogram or Common	Dimension	Units or Subscript Reference	Definition
ZZA	-	CONTAC	1	in.	Z-coordinate of first possible contact point.
ZZB	-	CONTAC	1	in.	Z-coordinate of second possible contact point.

Symbol	Fortran Name	Symbol	Fortran Name	Symbol	Fortran Name	Symbol	Fortran Name
$A_{\theta ij}$	ATHA	$K_{k,4}\Delta t$	DF	T_{max}	TMAX	δ_n	DELB
c	SD	ℓ	L	U_{mk}	U	δ'	D
c_i	C	$\ell_n(o)$	BLZ	U'_{mk}	UP	δ	DD
D	SLOPE	$\ell_n(t)$	BL	V_{mk}	V	$\dot{\delta}_n$	DELD
$D_{\psi ij}$	DPSI	m	EM,M	w_n	W	Δ_n	SLAK
$D_{\phi ij}$	DPHI	m_i	EMM	W_{mk}	W	Δt	TDUR
$\vec{F}$	F,OLDF	n	N	X	WS	Δt_{max}	DELTAT
F_{max}	FARD	N_{max}	MLIM	x_o	XZ	Δt_{prnt}	DTPRNT
g	ESG,GRAV	$N_{\psi ij}$	ENPSI	$\hat{x}_n$	BXA	ΔV_{lim}	EPZA
h_n	H	$N_{\phi ij}$	ENPHI	$\hat{\underline{x}}_n$	BXA	$\Delta\ddot{\bar{Z}}_{lim}$	ACCM
I_{in}	EYE	$P_{k,1}$	PX	Y	WT	ϵ	EPS,OM
i	I	$P_{k,1}$	PV	y_o	YZ	ϵ_t	DTMIN
j	J	$\vec{Q}$	Q	$\hat{y}_n$	BYA	ϵ_v	EPZV
k	FK,K	$\vec{Q}_B$	QB	$\hat{\underline{Y}}_n$	BYA	$\epsilon_{\ddot{z}}$	EDEPS
k_1	SA	$\vec{Q}_C$	QS	z_o	ZZ	$\bar{\mu}_k$	WGT
k_2	SB	$\vec{Q}_G$	QG	$\hat{z}_n$	BZA	π	PI
k_3	SC	$\vec{Q}_J$	QJ	Z_k	UX	$\pi/2$	PITWO
$K_{k,1}\Delta t$	AF	$\vec{Q}_T$	QT	$\dot{Z}_k$	UV	$\pi/180$	DR
$K_{k,2}\Delta t$	BF	R	RFAC	$\ddot{Z}_k$	UA	ρ_i	RHO,DUJ,DLJ
$K_{k,3}\Delta t$	CF	S	SFAC	δ	A,ETA	Ω	EPSLN
		t	T				
		t_n	D				

TABLE 27. SYMBOL AND FORTRAN NAME CORRESPONDENCE

TABLE 28. SUBSCRIPT REFERENCE EXPLANATIONS

Subscript Reference Number	Subscript Values	Subscript Explanation	Units	Symbol
1	1	X-coordinate of first corner point of contact surface.	in.	$\hat{x}_1$
	2	Y-coordinate of first corner point of contact surface.	in.	$\hat{y}_1$
	3	Z-coordinate of first corner point	in.	$\hat{z}_1$
	4	X-coordinate of one adjacent corner point.	in.	$\hat{x}_2$
	5	Y-coordinate of one adjacent corner point.	in.	$\hat{y}_2$
	6	Z-coordinate of one adjacent corner point.	in.	$\hat{z}_2$
	7	X-coordinate of other adjacent corner point.	in.	$\hat{x}_3$
	8	Y-coordinate of other adjacent corner point.	in.	$\hat{y}_3$
	9	Z-coordinate of other adjacent corner point.	in.	$\hat{z}_3$
	10	Time at which contact surface assumes this position. If the dimension is nine, this one is omitted.	sec	t'
2	1	Inertial X-coordinate for torso center of gravity.	in.	x_1
	2	Inertial Y-coordinate for torso center of gravity.	in.	y_1
	3	Inertial Z-coordinate for torso center of gravity.	in.	z_1
	4	Inertial X-coordinate for head center of gravity.	in.	x_2
	5	Inertial Y-coordinate for head center of gravity.	in.	y_2
	6	Inertial Z-coordinate for head center of gravity.	in.	z_2
	7	Inertial X-coordinate for legs center of gravity.	in.	x_3
	8	Inertial Y-coordinate for legs center of gravity.	in.	y_3
	9	Inertial Z-coordinate for legs center of gravity.	in.	z_3
3	1	Inertial X-coordinate for torso center of gravity.	in. or lb.	x_1
	2	Inertial Y-coordinate for torso center of gravity.	in. or lb.	y_1
	3	Inertial Z-coordinate for torso center of gravity.	in. or lb	z_1
	4	Inertial torso yaw angle.	rad or in.lb	ψ_1
	5	Inertial torso pitch angle.	rad or in.lb	θ_1

TABLE 28. SUBSCRIPT REFERENCE EXPLANATIONS
(Continued)

Subscript Reference Number	Subscript Values	Subscript Explanation	Units	Symbol
3 (Cont'd)	6	Inertial torso roll angle.	rad or in.lb	ϕ_1
	7	Inertial head yaw angle.	rad or in.lb	ψ_2
	8	Inertial head pitch angle.	rad or in.lb	θ_2
	9	Inertial head roll angle.	rad or in.lb	ϕ_2
	10	Inertial legs yaw angle.	rad or in.lb	ψ_3
	11	Inertial legs pitch angle.	rad or in.lb	θ_3
	12	Inertial legs roll angle.	rad or in.lb	ϕ_3
4	1	Square of semimajor axis length in i-direction.	in^2	a_m^2
	2	Square of semimajor axis length in j-direction.	in^2	b_m^2
	3	Square of semimajor axis length in k-direction.	in^2	c_m^2
	4	Coordinate of ellipsoid center relative to body segment center of gravity in i-direction.	in.	x_{em}
	5	Coordinate of ellipsoid center relative to body segment center of gravity in j-direction.	in.	y_{em}
	6	Coordinate of ellipsoid center relative to body segment center of gravity in k-direction.	in.	z_{em}
	7	Maximum of semimajor axis lengths.	in.	-
	8	Inertial x-coordinate of ellipsoid center.	in.	-
	9	Inertial y-coordinate of ellipsoid center.	in.	-
	10	Inertial z-coordinate of ellipsoid center.	in.	-
	11-20	Vestigial.	-	-
	21-26	Coefficients of extreme point equations.	in^2	-
	27-29	Coefficients of extreme point equations.	in.	-
	30-34	Vestigial.	-	-
5	1	Neck	-	-
	2	Hip	-	-
6	1	Yaw	-	-
	2	Pitch	-	-
	3	Roll	-	-
7	1	Neck yaw	-	-
	2	Neck pitch	-	-
	3	Neck roll	-	-

TABLE 28. SUBSCRIPT REFERENCE EXPLANATIONS
(Continued)

Subscript Reference Number	Subscript Values	Subscript Explanation	Units	Symbol
7 (Cont'd)	4	Hip yaw	-	-
	5	Hip pitch	-	-
	6	Hip roll	-	-
8	1	Upper	-	-
	2	Lower	-	-
9	1	Attachment point	-	-
	2	Anchor point	-	-
10	1	x,i-direction	-	-
	2	y,j-direction	-	-
	3	z,k-direction	-	-
11	1	Left shoulder belt segment.	-	-
	2	Right shoulder belt segment.	-	-
	3	Left lap belt segment.	-	-
	4	Right lap belt segment.	-	-
12	1	Stiff torso	-	-
	2	Flexible torso	-	-
13	1	First elastic coefficient.	lb/in.	k_{1k}
	2	Second elastic coefficient.	lb/in^2	k_{2k}
	3	Third elastic coefficient.	lb/in^3	k_{3k}
	4	Coefficients of surface relative to vehicle.	in^2	p
	5	Coefficients of surface relative to vehicle.	in^2	q
	6	Coefficients of surface relative to vehicle.	in^2	r
	7	Coefficients of surface relative to vehicle.	in^3	s
	8	Coefficients of surface relative to inertial space.	in^2	A
	9	Coefficients of surface relative to inertial space.	in^2	B
	10	Coefficients of surface relative to inertial space.	in^2	C
	11	Coefficients of surface relative to inertial space.	in^3	D
	12	Direction factor	-	-
	13	Input direction factor.	-	-
	14	These are intermediate results.	in^4	-
	15-17	These are intermediate results.	in^3	-
	18	These are intermediate results.	in^4	-
	19-21	These are intermediate results.	in^3	-
	22-23	Surface side lengths.	in.	-
	24-25	Vestigial	-	-
	26	Depth parameter	in.	-

TABLE 28. SUBSCRIPT REFERENCE EXPLANATIONS
(Continued)

Subscript Reference Number	Subscript Values	Subscript Explanation	Units	Symbol
13 (Cont'd)	27	Edge parameter	in.	λ_k
	28	Damping coefficient.	lb.sec/in.	c_k
	29	Coefficient rates of surface relative to vehicle.	in^2/sec	$\dot{p}$
	30	Coefficient rates of surface relative to vehicle.	in^2/sec	$\dot{q}$
	31	Coefficient rates of surface relative to vehicle.	in^2/sec	$\dot{r}$
	32	Coefficient rates of surface relative to vehicle.	in^3/sec	$\dot{s}$
	33-38	Combinations of (8,9,10) taken in pairs.	in^4	-
	39	Vestigial	-	-
	40	Square of (41).	in^4	-
	41	Normalizing factor.	in^2	-
14	1	Left shoulder belt in x-direction.	deg	-
	2	Left shoulder belt in y-direction.	deg	-
	3	Left shoulder belt in z-direction.	deg	-
	4	Right shoulder belt in x-direction.	deg	-
	5	Right shoulder belt in y-direction.	deg	-
	6	Right shoulder belt in z-direction.	deg	-
	7	Left lap belt in x-direction.	deg	-
	8	Left lap belt in y-direction.	deg	-
	9	Left lap belt in z-direction.	deg	-
	10	Right lap belt in x-direction.	deg	-
	11	Right lap belt in y-direction.	deg	-
	12	Right lap belt in z-direction.	deg	-
15	1	Shoulder	-	-
	2	Lap	-	-
16	1	Neck yaw elastic torque.	in.lb	-
	2	Neck pitch elastic torque.	in.lb	-
	3	Neck roll elastic torque.	in.lb	-
	4	Hip yaw elastic torque.	in.lb	-
	5	Hip pitch elastic torque.	in.lb	-
	6	Hip roll elastic torque.	in.lb	-
	7	Neck yaw stop torque.	in.lb	-
	8	Neck pitch stop torque.	in.lb	-
	9	Neck roll stop torque.	in.lb	-
	10	Hip yaw stop torque.	in.lb	-
	11	Hip pitch stop torque.	in.lb	-
	12	Hip roll stop torque.	in.lb	-
17	1	Center of gravity x-coordinate.	in.	-
	2	Center of gravity x-velocity.	in./sec	-
	3	Center of gravity x-acceleration.	g-units	-
	4	Center of gravity y-coordinate.	in.	-
	5	Center of gravity y-velocity.	in./sec	-

TABLE 28. SUBSCRIPT REFERENCE EXPLANATIONS
(Continued)

Subscript Reference Number	Subscript Values	Subscript Explanation	Units	Symbol
17 (Cont'd)	6	Center of gravity y-acceleration.	g-units	-
	7	Center of gravity z-coordinate.	in.	-
	8	Center of gravity z-velocity	in./sec^2	-
	9	Center of gravity z-acceleration.	g-units	-
	10	Yaw angle	deg	ψ_n
	11	Yaw velocity	deg/sec	$\dot{\psi}_n$
	12	Yaw acceleration	deg/sec^2	$\ddot{\psi}_n$
	13	Pitch angle	deg	θ_n
	14	Pitch velocity	deg/sec	$\dot{\theta}_n$
	15	Pitch acceleration	deg/sec^2	$\ddot{\theta}_n$
	16	Roll angle	deg	ϕ_n
	17	Roll velocity	deg/sec	$\dot{\phi}_n$
	18	Roll acceleration	deg/sec^2	$\ddot{\phi}_n$
18	1	Torso	-	-
	2	Head	-	-
	3	Legs	-	-
	4	Vehicle	-	-
19	1	Coordinate	-	-
	2	Velocity	-/sec	-
	3	Acceleration	-/sec^2	-
20	1	x-direction	in.	-
	2	y-direction	in.	-
	3	z-direction	in.	-
	4	Yaw	rad	-
	5	Pitch	rad	-
	6	Roll	rad	-
21	1	Torso	-	-
	2	Head	-	-
	3	Legs	-	-
22	1	Torso center of gravity x-coordinate.	in.	-
	2	Torso center of gravity x-velocity.	in./sec	-
	3	Torso center of gravity y-coordin coordinate.	in.	-
	4	Torso center of gravity y-velocity.	in./sec	-
	5	Torso center of gravity z-coordinate.	in.	-
	6	Torso center of gravity z-velocity.	in./sec	-
	7	Torso yaw angle.	deg	-
	8	Torso yaw velocity.	deg/sec	-
	9	Torso pitch angle.	deg	-
	10	Torso pitch velocity.	deg/sec	-

TABLE 28. SUBSCRIPT REFERENCE EXPLANATIONS
(Continued)

Subscript Reference Number	Subscript Values	Subscript Explanation	Units	Symbol
22 (Cont'd)	11	Torso roll angle.	deg	-
	12	Torso roll velocity.	deg/sec	-
	13	Head yaw angle.	deg	-
	14	Head yaw velocity.	deg/sec	-
	15	Head pitch angle.	deg	-
	16	Head pitch velocity.	deg/sec	-
	17	Head roll angle.	deg	-
	18	Head roll velocity.	deg/sec	-
	19	Legs yaw angle.	deg	-
	20	Legs yaw velocity.	deg/sec	-
	21	Legs pitch angle.	deg	-
	22	Legs pitch velocity.	deg/sec	-
	23	Legs roll angle.	deg	-
	24	Legs roll velocity.	deg/sec	-
	25	Vehicle point "0" x-coordinate.	in.	-
	26	Vehicle point "0" x-velocity.	in./sec	-
	27	Vehicle point "0" y-coordinate.	in.	-
	28	Vehicle point "0" y-velocity.	in./sec	-
	29	Vehicle point "0" z-coordinate.	in.	-
	30	Vehicle point "0" z-velocity.	in./sec	-
	31	Vehicle yaw angle.	deg	-
	32	Vehicle yaw velocity.	deg/sec	-
	33	Vehicle pitch angle.	deg	-
	34	Vehicle pitch velocity.	deg/sec	-
	35	Vehicle roll angle.	deg	-
	36	Vehicle roll velocity.	deg/sec	-
23	1	Force	lb	$\lvert F_F \rvert$
	2	Deflection	in.	δ
	3	Deflection rate	in./sec	$\dot{\delta}$
	4	First location of force on surface.	in.	-
	5	Second location of force on surface.	in.	-
24	1	Moving contact switch.	-	-
	2	AC starting index.	-	-
	3	AC ending index.	-	-
	4	AC pointer.	-	-
	5-8	EBCD contact subtitle storage.	-	-
	9	Use switch.	-	-
25	1	Ellipsoid index for contact.	-	-
	2	Surface index for contact.	-	-
26	1	Body segment index.	-	-
	2-5	EBCD ellipsoid subtitle storage.	-	-
	6	Use switch.	-	-
27	1	Torso yaw direction.	-	-
	2	Torso pitch direction.	-	-
	3	Torso roll direction.	-	-

TABLE 28. SUBSCRIPT REFERENCE EXPLANATIONS
(Continued)

Subscript Reference Number	Subscript Values	Subscript Explanation	Units	Symbol
27 (Cont'd)	4	Yaw direction for body segment across the joint.	-	-
	5	Pitch direction for body segment across the joint.	-	-
	6	Roll direction for body segment across the joint.	-	-
28	1	Accident type.	-	-
	2	Occupant position.	-	-
	3	Restraint type.	-	-
29	1	Torso center of gravity to neck.	-	-
	2	Head center of gravity to neck.	-	-
	3	Torso center of gravity to hip.	-	-
	4	Legs center of gravity to hip.	-	-
	5	Legs center of gravity to knees.	-	-
	6	Head center of gravity to top of skull.	-	-
30	1	Relative neck yaw angle.	deg	$\Delta\psi_{21}$
	2	Relative neck pitch angle.	deg	$\Delta\theta_{21}$
	3	Relative neck roll angle.	deg	$\Delta\phi_{21}$
	4	Relative hip yaw angle.	deg	$\Delta\psi_{31}$
	5	Relative hip pitch angle.	deg	$\Delta\theta_{31}$
	6	Relative hip roll angle.	deg	$\Delta\phi_{31}$
	7	Relative hip position x-coordinate.	in.	-
	8	Relative hip position y-coordinate.	in.	-
	9	Relative hip position z-coordinate.	in.	-
31	1	Left back corner.	in.	-
	2	Left intersection.	in.	-
	3	Left cushion corner.	in.	-
	4	Right cushion corner.	in.	-
	5	Right intersection.	in.	-
	6	Right back corner.	in.	-
32	1-300	One for each of the different possible contact surface corner time points. This storage is shared by all contacts moving or not.	-	-
33	1-10	One for each of the possible ellipsoid numbers.	-	-
34	1-25	One for each of the possible contact surface numbers.	-	-
35	1-41	One for each of the possible time points per printed page.	-	-

TABLE 28. SUBSCRIPT REFERENCE EXPLANATIONS
(Continued)

Subscript Reference Number	Subscript Values	Subscript Explanation	Units	Symbol
36	1-40	One for each of the possible contact interactions producing force at one time. Any over 40 are used but unrecorded.	-	-
37	1-100	One for each of the possible time points in each of input tables.	-	-
38	1-10	One for each of the established sets of body kinematics stored backward in time.	-	-
39	1-25	One for each of the contacts for all possible interactions.	-	-
	26	Special value causes first four "ellipsoids" to mean four belt segments according to subscript reference 11.	-	-
40	1	Slope	in./sec	-
	2	Intercept	in.	-
41	1	Velocity at beginning of segment.	in./sec	-
	2	Displacement at beginning of segment.	in.	-
42	1-12	One for each lever arm.	-	$\frac{\partial \delta}{\partial Z_k}$
	13	Deflection rate.	-/sec	$\dot{\delta}$
43	1-25	One for each contact.	-	-
	26-29	One for each belt segment ordered as in subscript reference 11.	-	-
44	1-6	As in subscript reference 20 for vehicle accelerations.	$in./sec^2$	σ_k
	7	Debug hexadecimal control word.	-	-
45	1	Number of points in table.	-	-
	2	Change switch.	-	-
	3	Scan type switch.	-	-
	4	Last scan pointer.	-	-
46	1	Linear elastic coefficient.	lb/in.	$b^{k}{}_{1n}$
	2	Quadratic elastic coefficient.	lb/in^2	$b^{k}{}_{2n}$
	3	Cubic elastic coefficient.	lb/in^3	$b^{k}{}_{3n}$

5.0. THREE DIMENSIONAL CRASH VICTIM SIMULATOR PICTORIAL OUTPUT PROGRAM

One of the major difficulties in using the Three-Dimensional Crash Victim Simulator is the problem of visualizing the chain of physical events tabulated in the printed output of the simulator. The current pictorial output of the simulator is a first attempt to fulfill this need. Since the state-of-the-art in display techniques does not include a completely workable hidden line removal algorithm, a modified stick figure is used for the basic component of the pictorial output.

The modified stick figure shows the body segment coordinate axes imbedded in the centerline of each of the three body segments. The four belt segments are shown as straight lines from the vehicle anchor points to the body attachment points if the corresponding belt segment is present in the simulation. The seat back and seat cushion are illustrated by outlines of their front and top edges respectively. This modified stick figure does enable the motion of the body to be visualized adequately.

The pictorial output is the product of a simulated camera taking pictures of the modified stick figure. The camera's position relative to the vehicle or relative to the inertial system, the camera's focal length either finite or infinite, and the point at which the camera is aiming are specified as parts of the input to the pictorial program.

The pictorial program also allows a choice of four pictorial output devices which may be used in any combination on a particular run. The four devices are a cathode ray tube display, a sixteen millimeter movie, an off-line twenty-eight-inch digital incremental plotter, and an on-line ten-inch digital incremental plotter.

The next section describes how to use the pictorial output program in conjunction with the HSRI Crash Victim Simulator on the Michigan Terminal System. This part concludes with technical descriptions of the two major components of the pictorial output program: the display control section and the stick figure display section. These descriptions are necessary for full utilization of the pictorial output program.

5.1. USE OF THE PICTORIAL OUTPUT PROGRAM IN MTS

Due to the complexity of usage of the pictorial output program in MTS, a step by step procedure is presented here with explanation interspersed as needed.

The pictorial output program is run separately from the crash victim simulator. Communication from the crash victim simulator to the pictorial output program is accomplished by means of one of the special output options of the simulator. This optional output is controlled by field six on card R of the simulator input data and consists of a formated "movie" file output via logical unit number one. The values of field six on card R which will instruct the simulator to produce this file are one or three (the latter will trigger another special output option as well). The format of the movie file is detailed in Table 30. It is possible to synthesize the file for purposes of displaying empirical or other data.

The first step in the procedure is to run the crash victim simulator to produce the movie file. The movie file will contain information for exactly those times which appear in the normal simulator output. It is then necessary for the user to so set field two of the card R that all the times he wishes to display are included in the printed output. This step is accomplished by the following MTS command (see also Section 4.5):

```
$RUN SP78:THREED  SCARDS=INPUTFILE 1=FILENAME
```

where INPUTFILE is the name of the file which contains the simulator input cards and FILENAME is the name of the movie file.

The second step is to use the MTS program *PERMIT to make this file be what is called "read only." This permit status prohibits any changes from

being made in the movie file by any user of MTS, but allows any user on any user number to read the contents of that file. Conversely, it is necessary that once a movie file is finished with, *PERMIT must be used to set the permit code to NONE before it can be emptied and used to hold another movie or something else. This step is carried out by issuing the MTS command:

$RUN *PERMIT PAR=FILENAME RO or conversely, $RUN *PERMIT PAR=FILENAME NONE where FILENAME is the name of the file in question.

The following manipulations fall into three classes, those which are preparatory for the run of the pictorial output program, those which are in response to the prompting of the program itself, and those which involve processing of the pictorial output. Manipulations of class one revolve around the proper setting up of the RUN statement for the pictorial output program. Since the RUN statement is long and complicated, as a practical matter it is stored in a file. The file containing the pictorial run statement will be referred to as the command file. Typical contents of the command file are shown in Table 29. The following steps will discuss changes in the command file and preparation for those changes in terms of the options of the pictorial output program.

Step three concerns line four of the command file as shown in Table 29. This particular line states that the file CELL was the last movie file used from SXXX. This line must be modified to specify the name of the movie file on SXXX. This is done by carrying out the following MTS commands: Let U be the name of the command file and FILENAME be the name of the movie file on SXXX .

```
$GET U
4,5=SXXX:FILENAME --
No character line
```

This procedure will seem less arbitrary if it is explained that a minus sign terminating a MTS input line carries the significance of telling MTS to treat the next input line as a continuation of the current input line. Each line of the command file except the last terminates with a minus sign. Hence, when the command file is given to MTS as input in a later step, MTS will treat the whole file as shown in Table 29 as a single command line.

TABLE 29. THE COMMAND FILE LAYOUT

Line Number	Contents
1	$RUN SP78:3DP 0=-P 2=-M -
2	6=*DUMMY* -
3	7=*PIBTAPE* -
4	5=SXXX:CELL -
5	3=SXXX:S -
6	4=SXXX:EX -
7	8=PLOTFILE(LAST+1000)

Making changes in the command file requires using MTS to manipulate lines which will later command MTS, so an extra minus sign is necessary on the change followed by a no character line. The last minus sign will be interpreted as a continuation of the line which contains the change. The next-to-last minus sign will go in as part of the change plus any characters on the

next input line. The no character line will cause the minus sign to be the last character of the changed line in the command file. This manipulation must be done on a teletype.

Step four concerns whether or not off-line twenty-eight inch CALCOMP plots are among the choices for output. Line seven of the command file specifies the name of the file in which the plotter commands will be stored. In Table 29, this file's name is PLOTFILE. If no plotting is desired, line seven can specify any file name.

Step five has to do with movie making. If there is to be no movie making as one of the output options employed in this run, line three as shown in Table 29 should be modified by the MTS commands below.

```
$GET U
3,7=-T --
No character line
```

If movies are desired, line three must be left as shown and the following MTS commands must be completed before the run begins.

```
 $CRE  -P  TYPE=SEQ
 $RUN *MOUNT PAR=(Rack number of movie tape)
ON 7TP *PIBTAPE* SIZE=3024, MODE=8CV,
RING=IN '  I.D.  name of movie tape '
```

Movie generation requires writing a tape which will be ultimately sent to a SC4020 installation for processing to produce film. The tape must be capable of recording 800 bytes per inch of seven track information which the film producing equipment expects.

All of the input parameters which control the pictorial output program are normally supplied in answer to prompting by the program itself. Certain of these parameters may become repetitious from run to run, so two special

files can be optionally read in lieu of responding to prompting. The file S on SXXX specified in line five of the command file as shown in Table 29. would be expected to contain the point of interest, the vantage point, and focal length together with a simulated time to be explained shortly if the pictorial output program is instructed to use the file. The simulated time comes about from an interest in simulating a moving camera. This is done by using a particular set of camera parameters until a specific time in the simulated crash, and reading a different set. This process may be carried out again and again. The simulated time provided in each entry of a set of camera data is the time in the crash at which the next camera data entry is to be read.

Likewise file EX on SXXX of line six in Table 29 if used would contain picture boundary information. The formats of both these files is presented in Section 5.2 (Tables 31 and 32). If either or both of these files are used, the files themselves and the corresponding lines of the command file need to be set up. This completes the preparation for a run of the pictorial output program.

Step six invokes the RUN command which has been built up in the command file by commanding MTS:

```
$SOURCE U+*MSOURCE*
```

The program is very large and usually takes several minutes to load. When execution begins, the program will print:

```
0 FOR INTERTIAL, 1 FOR RELATIVE
?
```

This is asking if the corresponding prompting is to be used in place of the file specified in line five of Table 29. An answer of YES or NO is expected. PEEK is the name given in Section 5.3 to the array which brings the camera data to the stick figure display section and is adopted as a shorthand for asking this question. Note that the PEEK array (Table 32) contains the information from both the PEEK file (Table 31) and the picture boundary file (Table 32) after conversion to the coordinate system specified in Section 5.3.

The program will next inquire:

```
PICTURE PLACEMENT TO BE ENTERED?
?
```

This is the corresponding question about the other file (line six of Table 29) and likewise is answered YES or NO. If this query has been refused, the next four promptings do not occur and the corresponding information is read from the file.

The four optional promptings are as follows:

```
X-MINIMUM=  ?
?
X-MAXIMUM=  ?
?
Y-MINIMUM=  ?
?
Y-MAXIMUM=  ?
?
```

Each request is met with a single number. The four numbers define the boundaries of the film in the camera.

This information is used together with the camera data as follows. First, the stick figure in three-dimensional space is translated so that the point of interest is at the origin. Second, the object is rotated first around

the X-axis and then around the Y-axis until the vantage point lies on the positive Z-axis. The figure is then translated in the Z-direction until the distance from the vantage point to the X-Y plane is the focal length. Perspective and a translation are applied to move the point (X-MINIMUM, Y-MINIMUM) to the origin. The resulting picture in the first quadrant of the X-Y plane is scaled so that the point (X-MAXIMUM, Y-MAXIMUM) fits inside a square 9.375 inches on a side. The contents of this square are output to the various pictorial devices. Hence, these four numbers act as a crude specification of the film size except that the "film" is always a square and the larger side of a rectangular film size is scaled to fit one side of this square.

The program will then prompt:

```
OMEGA =?
?
```

This is the length in inches used as cross bar length (see Section 5.3 of this report). The positive X-axis cross bar length will be twice the other two in the case of the torso and head, likewise with the negative Z-axis on the legs.

```
IAC =?
?
```

This is the output option switch as explained in Section 5.3. The program will inquire about the simulated times in the crash victim simulator output for which pictorial output is desired with the following three questions.

```
BEGINNING TIME =?
?
TIME INCREMENT =?
?
FINAL TIME =?
?
```

Proper response is three times in seconds, one to each question, which will be used to start at the BEGINNING TIME and taking every TIME INCREMENT thereafter until FINAL TIME is exceeded.

If the ENTER PEEK? question was answered NO, the program will go to work at this point. Otherwise, the program will ask:

```
     TIMEB=?
?
```

This is the simulated time in seconds at which new camera data entry is to be read that was explained earlier. Next, the following requirement is made.

```
     ENTER POINT OF INTEREST
?
```

The expected reply is three numbers with decimal points and separated by commas. These numbers represent the coordinates of the point of interest in inches. If inertial was specified above, these coordinates are taken with respect to the simulator inertial system. If relative was specified above, these coordinates are taken with respect to the simulator vehicle system. Similar response is sought by the next prompting except that the coordinates of the vantage point are desired.

```
     ENTER VANTAGE POINT
?
```

The focal length in inches is requested by:

```
     ENTER FOCAL LENGTH
?
```

The convention is followed that if focal length is entered as a negative number, orthographic projection (infinite focal length) is assumed. Further entries of camera data (the last four requirements) are asked for as needed. The program will now proceed to produce the pictorial output. If the CRT option is employed, the program will come back to the teletype on every frame. When the user wants to see the next frame, he presses the carriage return key. If he wants to start over, he types a one and then the carriage return. Some of the pictorial device routines which are used by the program will cause some printing that is merely for the user's information. When the pictorial output is completed, the program will prompt:

0 TO BEGIN OVER, 1 TO REPEAT RUN

If a zero is specified, the program simply begins again at the first prompting and all the options are again open with the lone exception that at most one movie can be generated on one loading of the program. If one is specified as the answer, the same run is repeated except that if inertial was specified, relative is now used. This procedure works only if input was from files in lines five and six of Table 29. The third response is an end of file given by the MTS command:

$ENDFILE

This causes termination of the program. If more than one movie is desired to be generated, the following procedure is employed. The first movie is made according to the instructions above. The resulting movie tape (which is known as *PIBTAPE* to MTS) is copied into a file, the tape is rewound, and a second movie is generated by following the instructions already

given starting at step six. Assuming that steps one through five have been carried out, that two movies are desired, and the file T is a sequential file of sufficient capacity, the following MTS commands will illustrate this procedure.

```
$SOURCE U+*MSOURCE*
```

(Reply to prompting on the teletype.)

```
$ENDFILE        (after 0 TO BEGIN OVER line.)
$COPY *PIBTAPE* TO T
$COPY *SOURCE* TO *PIBTAPE*@CC
REW
$ENDFILE
$SOURCE U+*MSOURCE*
```

(Reply to cause the next movie to be generated.)

```
$ENDFILE
$COPY *PIBTAPE* TO T
$COPY *SOURCE* TO *PIBTAPE*@CC
REW
$ENDFILE
$COPY T TO *PIBTAPE*
$COPY *SOURCE* TO *PIBTAPE*@CC
WEF
WEF
WEF
WEF
WEF
REW
$ENDFILE
```

The procedure generalizes easily to more movies. It is a considerable investment in time and money to send away a movie tape for processing on a SC4020 to produce film or 35mm slides. A facility has been developed on MTS for simulating a SC4020 using the CALCOMP plotter or the printer as an output device. For one or more movies on tape, the following MTS will invoke the SC4020 simulation to produce a CALCOMP plot from every tenth frame on the tape (excepting leader).

```
$RUN *FLIKPLT 7=*PIBTAPE* 9=PLOTFILE PAR=CCPLT=1, NPRT=10
```

This will cause the CALCOMP commands to be written in the file PLOTFILE. The commands resident in this file or perhaps other CALCOMP files produced by the CALCOMP section of the pictorial output program itself need to be communicated to the CALCOMP for plots to result. The files must be given a ready only permit code via *PERMIT then the following MTS command will put that file in the waiting line for CALCOMP processing.

```
$RUN *CCQUEUE PAR=PLOTFILE
```

This routine will issue a receipt which can be turned in at the Computing Center to get the completed plot after processing.

Figure 47 shows a series of eleven slides taken off a CRT display produced by this program. These slides are presented as an enlarged proof sheet which has been labelled according to simulated time of occurrence. These represent a back view of a side collision.

Figure 48 shows a CALCOMP plot of a top view of another, but similar, side collision. Figure 49 shows the same collision at approximately the same time as seen from about the right rear wheel. Figure 50 is a CALCOMP reconstruction of a movie frame.

Figures 50 and 51 contrast a high-resolution CALCOMP plot with a low-resolution printer plot of this same side collision. Figures 52 and 53 illustrate the effects of varying film boundaries in a front view at about this same time.

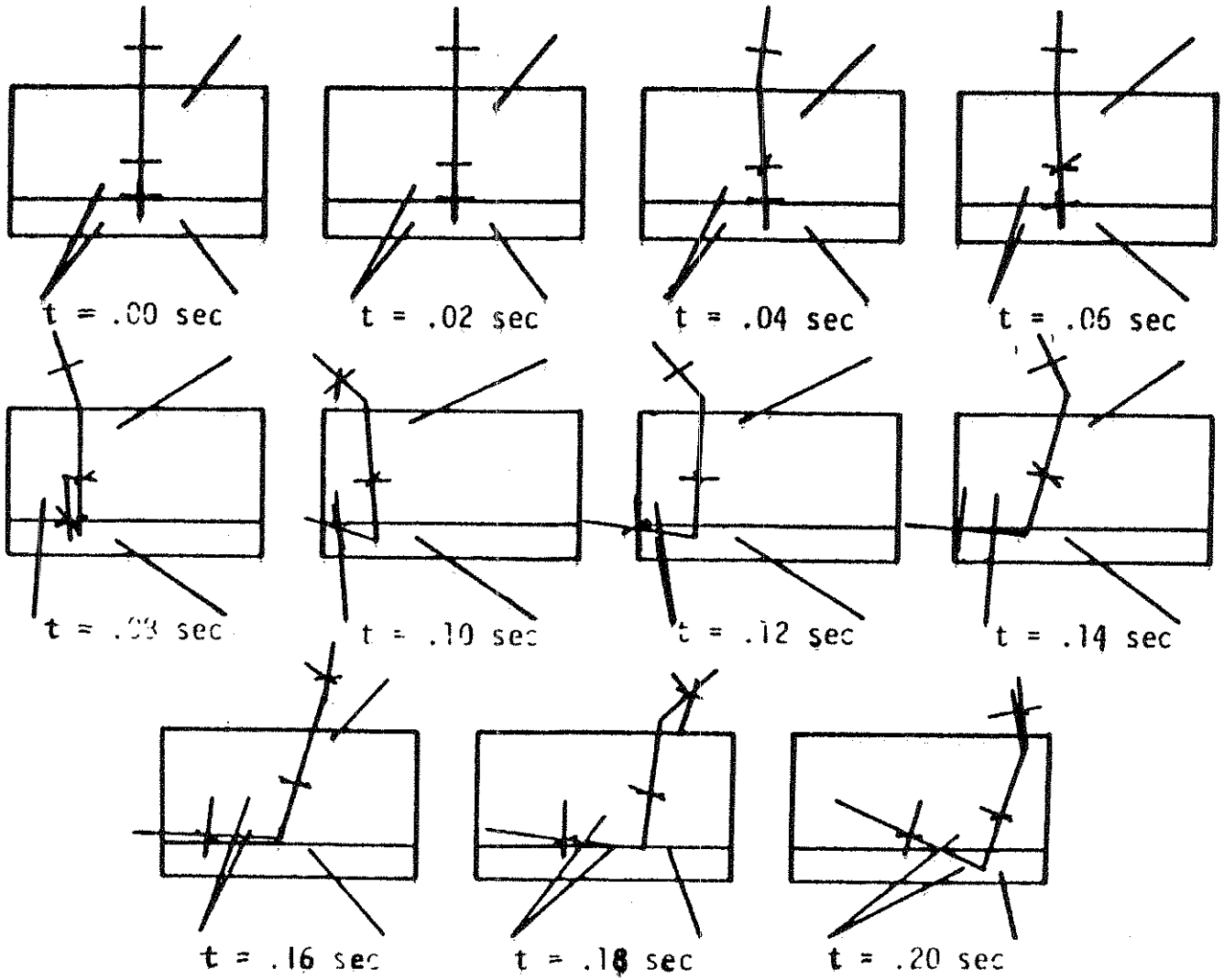

FIGURE 47. SLIDES OF BACK VIEW OF A SIDE COLLISION.

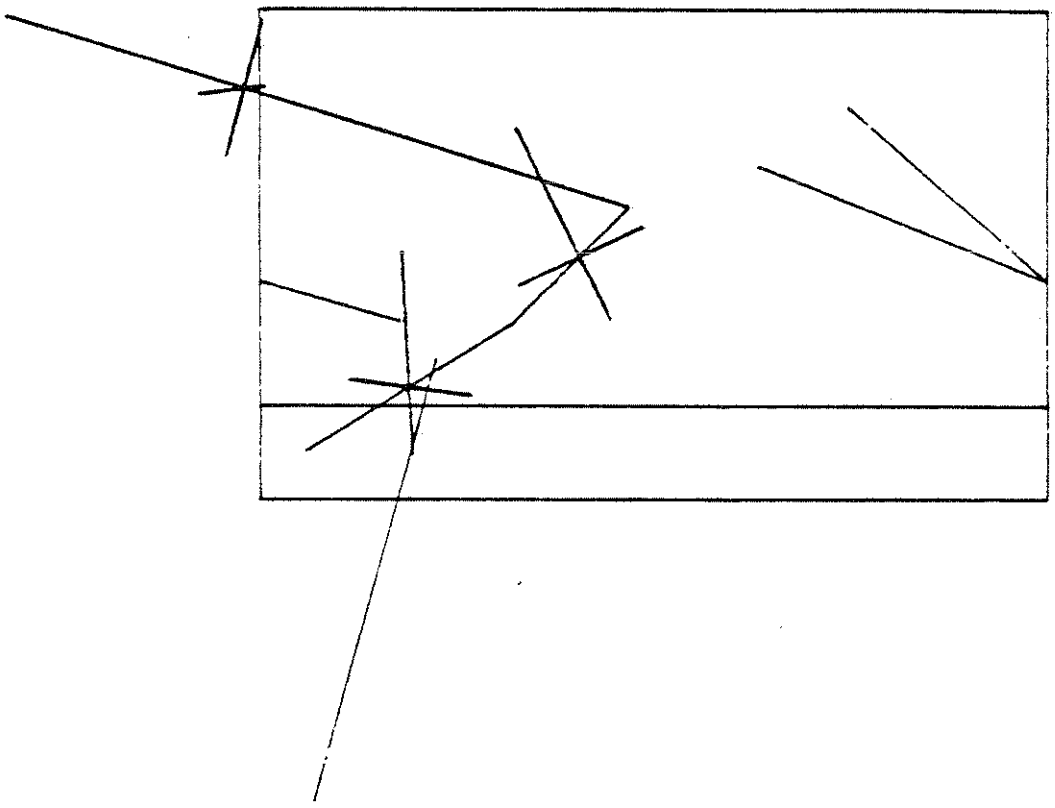

FIGURE 48. CALCOMP PLOT OF A TOP VIEW OF A SIDE COLLISION

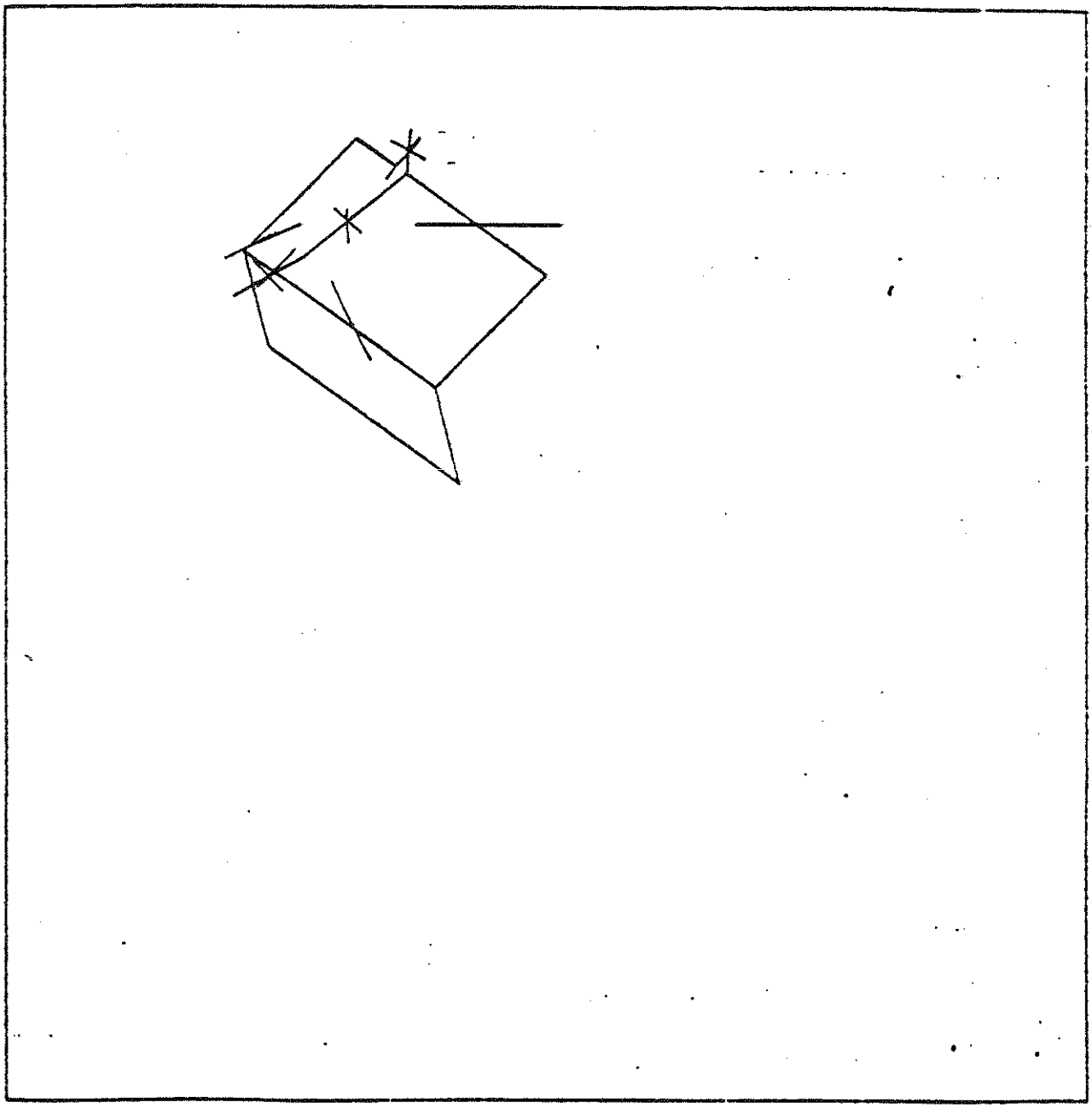

FIGURE 49. CALCOMP RECONSTRUCTION OF A MOVIE FRAME OF A LOWER RIGHT 45 DEGREE BACK OBLIQUE VIEW OF A SIDE COLLISION

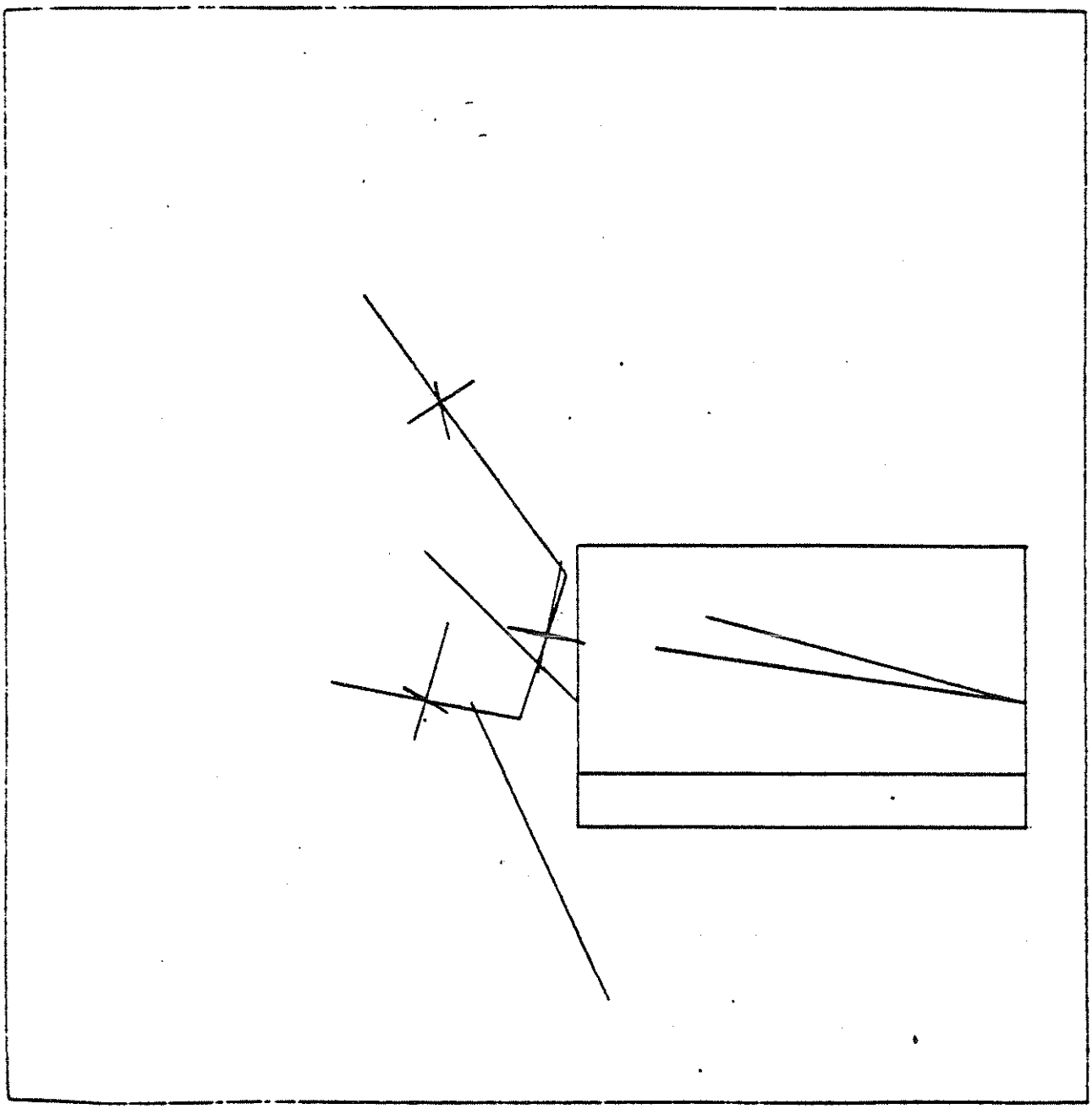

FIGURE 50. CALCOMP RECONSTRUCTION OF A MOVIE FRAME

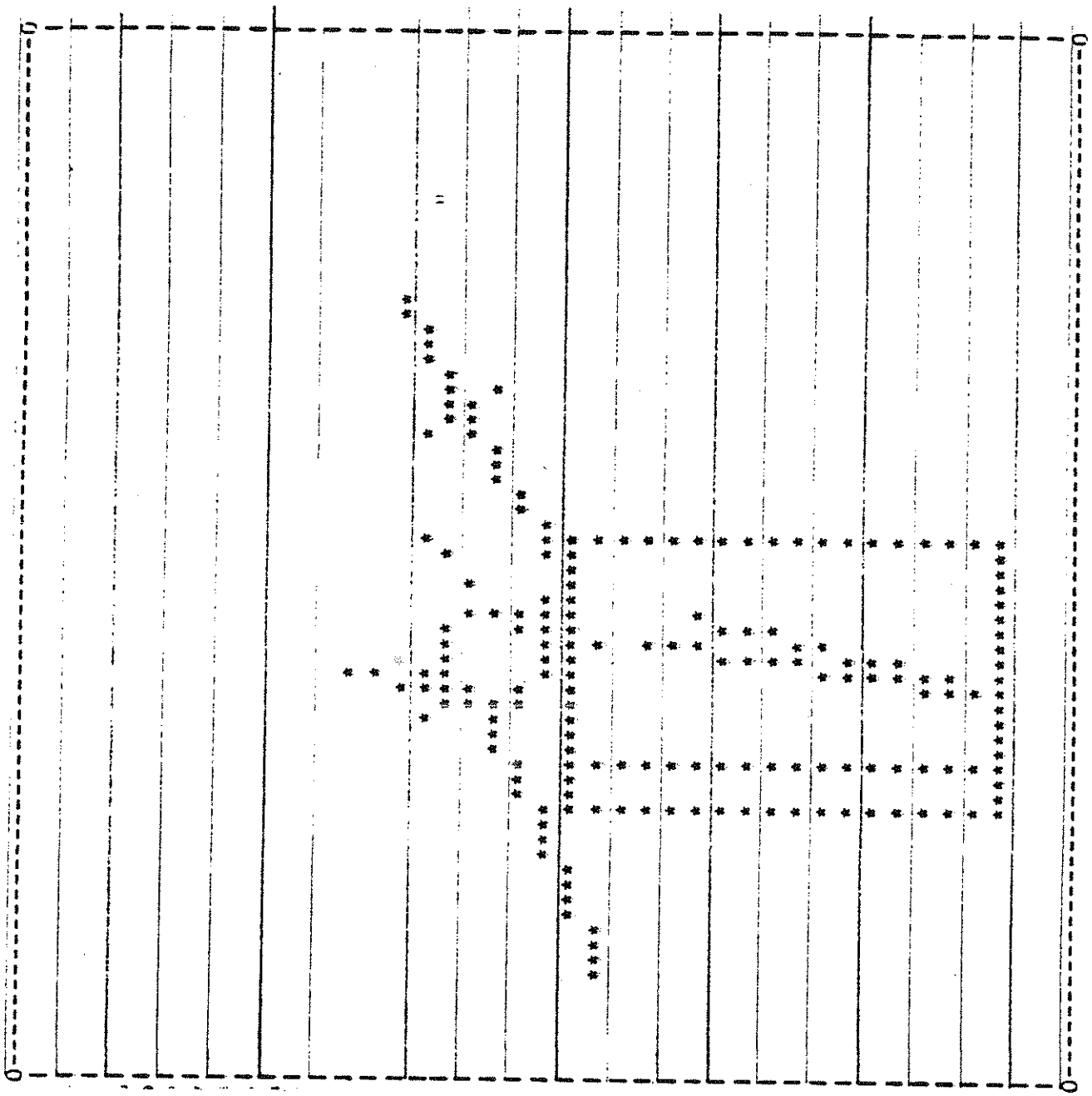

FIGURE 51. PRINTER PLOTTER RECONSTRUCTION OF A MOVIE FRAME

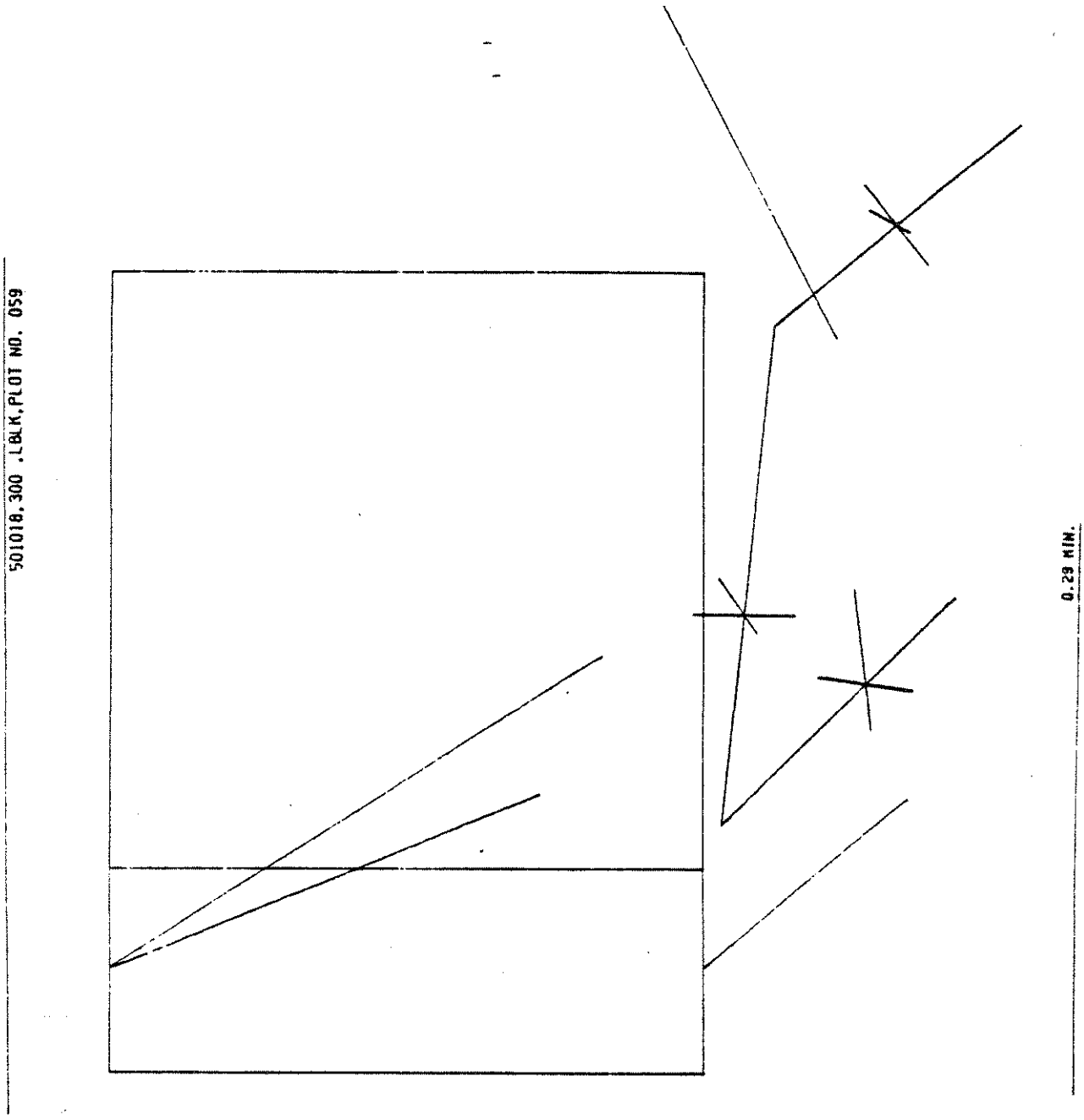

FIGURE 52. CALCOMP PLOT OF A FRONT VIEW OF A SIDE COLLISION WITH WIDE PICTURE BOUNDARIES

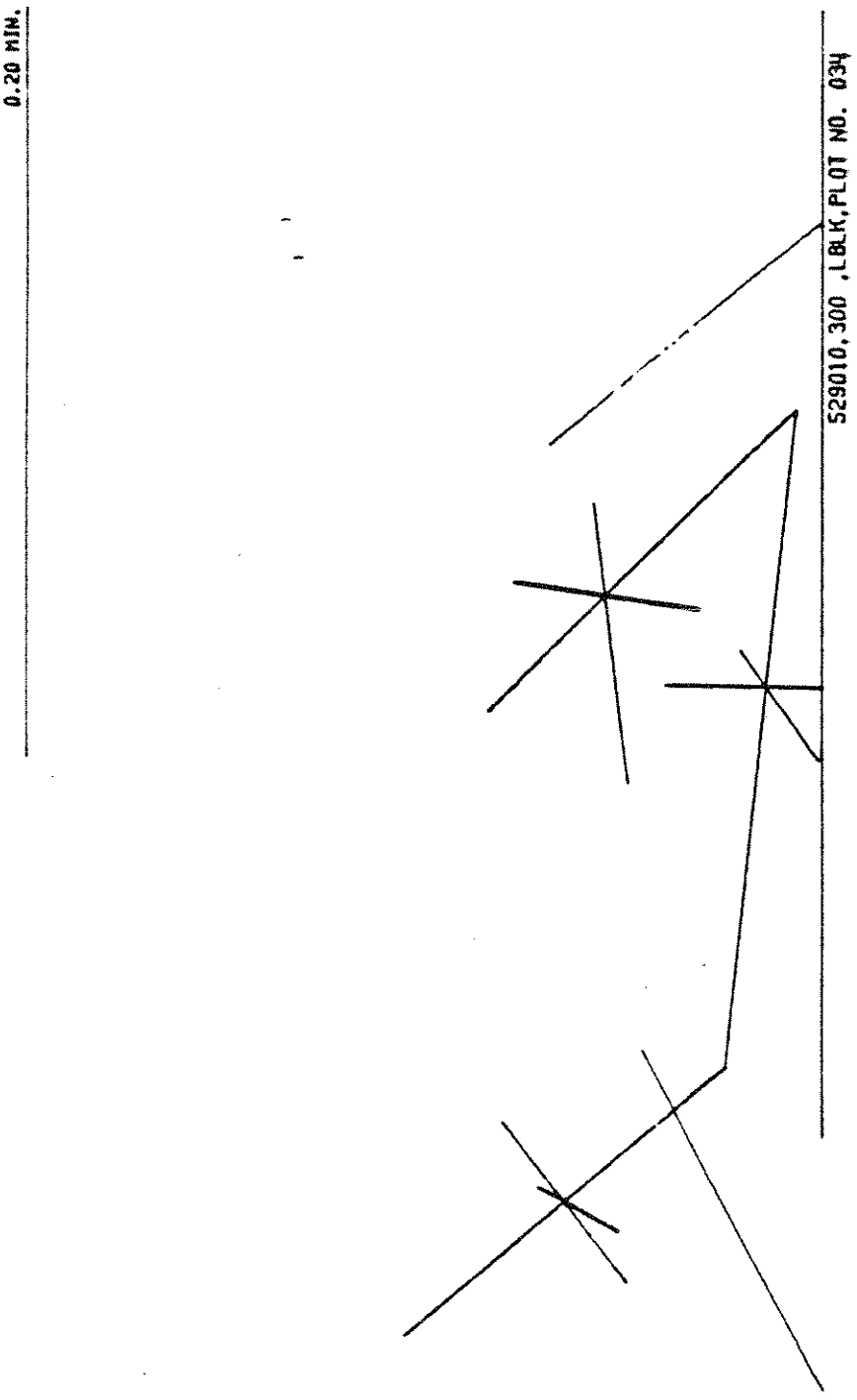

FIGURE 53. CALCOMP PLOT OF A FRONT VIEW OF A SIDE COLLISION WITH PICTURE BOUNDARIES SET TO SHOW ONLY THE EXTENSION BEYOND THE SEAT EDGE

5.2. THE DISPLAY CONTROL SECTION

The display control section of the pictorial output program has the function of handling the communication with the user, the reading of the movie file from the crash victim simulator, the proper transformations from inertial or relative simulator coordinates into coordinates suitable to the Stick Figure Display Section and the appropriate calls to the three entries of the Stick Figure Display Section to obtain the desired pictorial output. The promptings made by this section of the program have been discussed in Section 5.1.

The movie file written by the crash victim simulator is composed of a header block and a block for each of the simulated times which appear in the printed output of the simulator. Once a movie file has been designated for a computer run on the pictorial output program, it cannot be changed until the next loading of the program. This file is rewound automatically before each new pass through the prompting sequence. The contents of this file are set forth in Table 30. The header block consists of the first four lines. Each time block is made up of four lines (numbered in the Table 4M+1, etc.).

The PEEK file and the picture boundary file are shown in Tables 31 and 32, respectively. Each single block of information requires one line in both these files. If the 0 TO BEGIN OVER question is answered with a "one," these two files are rewound. Otherwise, additional lines of the same type will be needed to meet the program requirements. Failure to provide enough lines will cause termination of the run.

TABLE 30. THE MOVIE FILE LAYOUT

Line No.	Col-umns	Description	Coordinate System	Units
1	1	Left Shoulder Belt Switch (0=attached)	-	-
1	2	Right Shoulder Belt Switch	-	-
1	3	Right Top Belt Switch	-	-
1	4	Left Tope Belt Switch	-	-
1	5-10	Left Shoulder Harness Anchor X	Vehicle	Inches
1	11-16	Left Shoulder Harness Anchor Y	Vehicle	Inches
1	17-22	Left Shoulder Harness Anchor Z	Vehicle	Inches
1	23-28	Left Shoulder Harness Attachment X	Torso	Inches
1	29-34	Left Shoulder Harness Attachment Y	Torso	Inches
1	35-40	Left Shoulder Harness Attachment Z	Torso	Inches
1	41-46	Right Shoulder Harness Attachment X	Torso	Inches
1	47-52	Right Shoulder Harness Attachment Y	Torso	Inches
1	53-58	Right Shoulder Harness Attachment Z	Torso	Inches
1	59-64	Right Shoulder Harness Anchor X	Vehicle	Inches
1	65-70	Right Shoulder Harness Anchor Y	Vehicle	Inches
1	71-76	Right Shoulder Harness Anchor Z	Vehicle	Inches
2	1-6	Right Lap Belt Anchor X	Vehicle	Inches
2	7-12	Right Lap Belt Anchor Y	Vehicle	Inches
2	13-18	Right Lap Belt Anchor Z	Vehicle	Inches
2	19-24	Right Lap Belt Attachment X	Torso	Inches
2	25-30	Right Lap Belt Attachment Y	Torso	Inches
2	31-36	Right Lap Belt Attachment Z	Torso	Inches
2	37-42	Left Lap Belt Attachment X	Torso	Inches
2	43-48	Left Lap Belt Attachment Y	Torso	Inches
2	49-54	Left Lap Belt Attachment Z	Torso	Inches
2	55-60	Left Lap Belt Anchor X	Vehicle	Inches
2	61-66	Left Lap Belt Anchor Y	Vehicle	Inches
2	67-72	Left Lap Belt Anchor Z	Vehicle	Inches
3	1-6	Left Top Seat Back Corner X	Vehicle	Inches
3	7-12	Left Top Seat Back Corner Y	Vehicle	Inches
3	13-18	Left Top Seat Back Corner Z	Vehicle	Inches
3	19-24	Left Bottom Seat Back Corner X	Vehicle	Inches
3	25-30	Left Bottom Seat Back Corner Y	Vehicle	Inches
3	31-36	Left Bottom Seat Back Corner Z	Vehicle	Inches
3	37-42	Left Front Seat Bottom Corner X	Vehicle	Inches
3	43-48	Left Front Seat Bottom Corner Y	Vehicle	Inches
3	49-54	Left Front Seat Bottom Corner Z	Vehicle	Inches
3	55-60	Right Front Seat Bottom Corner X	Vehicle	Inches
3	61-66	Right Front Seat Bottom Corner Y	Vehicle	Inches
3	67-72	Right Front Seat Bottom Corner Z	Vehicle	Inches

TABLE 30. THE MOVIE FILE LAYOUT (page 2)

Line No.	Columns	Description	Coordinate System	Units
4	1-6	Right Bottom Seat Back Corner X	Vehicle	Inches
4	7-12	Right Bottom Seat Back Corner Y	Vehicle	Inches
4	13-18	Right Bottom Seat Back Corner Z	Vehicle	Inches
4	19-24	Right Top Seat Back Corner X	Vehicle	Inches
4	25-30	Right Top Seat Back Corner Y	Vehicle	Inches
4	31-36	Right Top Seat Back Corner Z	Vehicle	Inches
4	37-42	Distance from Torso c.g. to Neck Joint	-	Inches
4	43-48	Distance from Neck Joint to Head c.g.	-	Inches
4	49-54	Distance from Torso c.g. to Hip Joint	-	Inches
4	55-60	Distance from Hip Joint to Legs c.g.	-	Inches
4	61-66	Distance from Legs c.g. to Extremity	-	Inches
4	67-72	Distance from Head c.g. to Top of Head	-	Inches
4M+1	1-10	Current Simulated Time	-	sec.
4M+1	11-20	Leg c.g. X	Inertial	Inches
4M+1	21-30	Leg c.g. Y	Inertial	Inches
4M+1	31-40	Leg c.g. Z	Inertial	Inches
4M+1	41-50	Torso c.g. X	Inertial	Inches
4M+1	51-60	Torso c.g. Y	Inertial	Inches
4M+1	61-70	Torso c.g. Z	Inertial	Inches
4M+2	1-10	Head c.g. X	Inertial	Inches
4M+2	11-20	Head c.g. Y	Inertial	Inches
4M+2	21-30	Head c.g. Z	Inertial	Inches
4M+2	31-40	Vehicle X	Inertial	Inches
4M+2	41-50	Vehicle Y	Inertial	Inches
4M+2	51-60	Vehicle Z	Inertial	Inches
4M+3	1-10	Leg Yaw	Inertial	Radians
4M+3	11-20	Leg Roll	Inertial	Radians
4M+3	21-30	Leg Pitch	Inertial	Radians
4M+3	31-40	Torso Yaw	Inertial	Radians
4M+3	41-50	Torso Roll	Inertial	Radians
4M+3	51-60	Torso Pitch	Inertial	Radians
4M+4	1-10	Head Yaw	Inertial	Radians
4M+4	11-20	Head Roll	Inertial	Radians
4M+4	21-30	Head Pitch	Inertial	Radians
4M+4	31-40	Vehicle Yaw	Inertial	Radians
4M+4	41-50	Vehicle Roll	Inertial	Radians
4M+4	51-60	Vehicle Pitch	Inertial	Radians

TABLE 31. THE PEEK FILE LAYOUT

Line No.	Columns	Description	Coordinate System	Units
1	1-6	Time to Read Another PEEK	-	Secs.
1	7-12	Point of Interest X	As Specified	Inches
1	13-18	Point of Interest Y	As Specified	Inches
1	19-24	Point of Interest Z	As Specified	Inches
1	25-30	Vantage Point X	As Specified	Inches
1	31-36	Vantage Point Y	As Specified	Inches
1	37-42	Vantage Point Z	As Specified	Inches
1	43-48	Focal Length	-	Inches

TABLE 32. THE PICTURE BOUNDARY FILE LAYOUT

Line No.	Columns	Description	Coordinate System	Units
1	1-6	Minimum Picture Boundary X	Picture Plane	Inches
1	7-12	Maximum Picture Boundary X	Picture Plane	Inches
1	13-18	Minimum Picture Boundary Y	Picture Plane	Inches
1	19-24	Maximum Picture Boundary Y	Picture Plane	Inches

5.3. THE STICK FIGURE DISPLAY SECTION

This program displays a stick figure of the three-dimensional crash victim together with seat backs, seat cushions, and the four individual belt segments. The displays take place on any combination of four types of display units.

CALLING SEQUENCES:

Normal Entry: STICK (PEEK, GUY, IAC, IER)

Alternate Entry: STICK1 (GUY, IAC, IER)

Alternate Entry: STICK2

Where: PEEK is an array of length eleven whose contents are depicted in Table 33.

TABLE 33. PEEK ARRAY LAYOUT

Index	Description
1	X Coordinate of Point of Interest
2	Y Coordinate of Point of Interest
3	Z Coordinate of Point of Interest
4	X Coordinate of Vantage Point
5	Y Coordinate of Vantage Point
6	Z Coordinate of Vantage Point
7	Focal Length or Distance from the Vantage Point to the Viewing Plane. The viewing plane is always between the point of interest and the vantage point and perpendicular to the line joining those two points. If this quantity is negative, orthographic projection is used.
8	Minimum X Coordinate of Image on Viewing Plane
9	Maximum X Coordinate of Image on Viewing Plane
10	Minimum Y Coordinate of Image on Viewing Plane
11	Maximum Y Coordinate of Image on Viewing Plane

GUY is a double subscripted array which contains the 3D coordinates for the thirty points to be plotted to form the stick figure. This array is dimensioned GUY (30,3). The thirty points are specified in Table 34.

TABLE 34. THE GUY ARRAY LAYOUT

Point No.	Description
1	Knee or Foot
2	Top of Leg C.G. Coordinate
3	Bottom of Leg C.G. Coordinate System
4	Right of Leg C.G. Coordinate System
5	Left of Leg C.G. Coordinate System
6	Hip
7	Front of Torso C.G. Coordinate System
8	Back of Torso C.G. Coordinate System
9	Right of Torso C.G. Coordinate System
10	Left of Torso C.G. Coordinate System
11	Neck
12	Front of Head C.G. Coordinate System
13	Back of Head C.G. Coordinate System
14	Right of Head C.G. Coordinate System
15	Left of Head C.G. Coordinate System
16	Top of Head
17	Left Shoulder Harness Anchor
18	Left Shoulder Harness Attachment
19	Right Shoulder Harness Attachment
20	Right Shoulder Harness Anchor
21	Right Lap Belt Anchor
22	Right Lap Belt Attachment
23	Left Lap Belt Attachment
24	Left Lap Belt Anchor
25	Left Top Seat Back Corner
26	Left Bottom Seat Back Corner
27	Left Front Seat Bottom Corner
28	Right Front Seat Bottom Corner
29	Right Bottom Seat Back Corner
30	Right Top Seat Back Corner

These points are connected by lines as illustrated in Figure 54 and shown in Table 35.

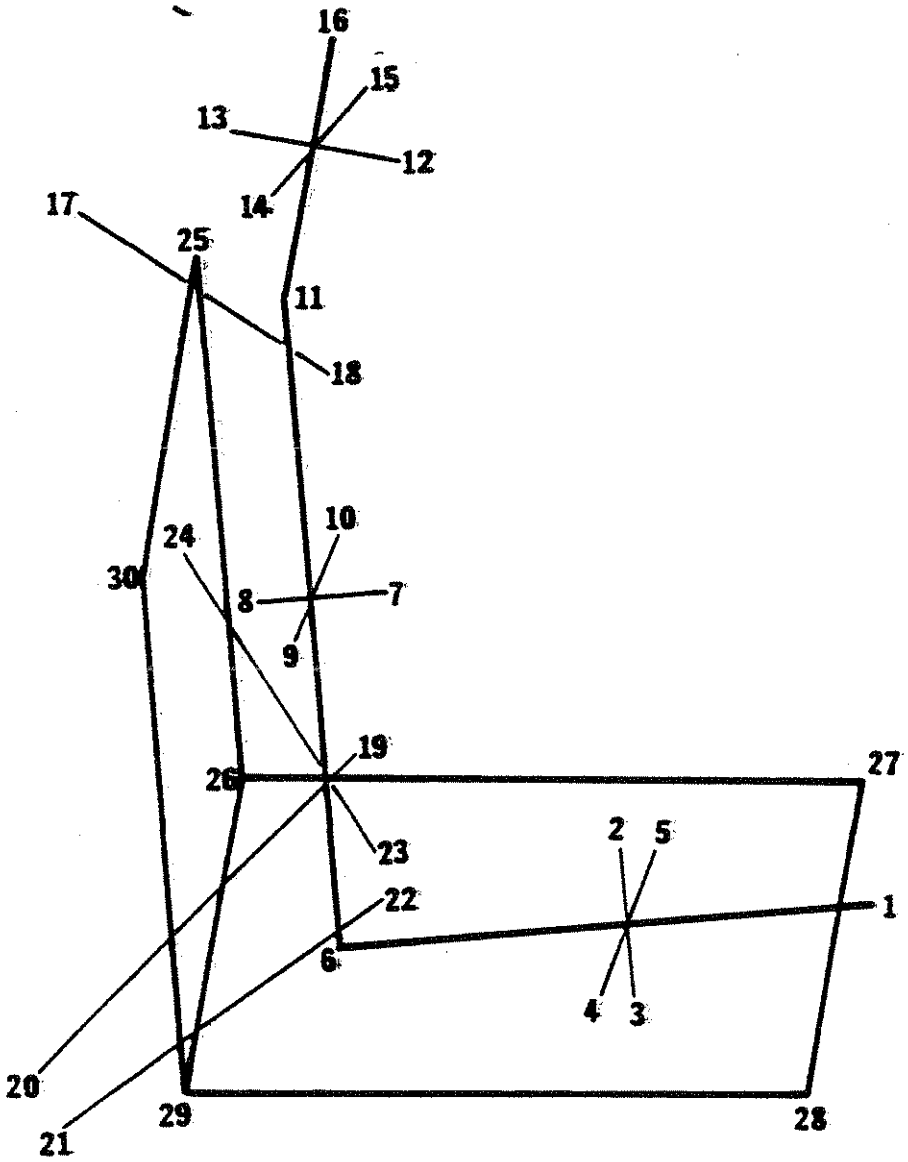

FIG. 54
STICK FIGURE LAYOUT

TABLE 35. CONNECTIVITY TABLE

Point	Connects to Points	Intensity	May Be Absent
1	6	2	no
2	3	2	no
4	5	2	no
6	11	2	no
7	8	2	no
9	10	2	no
11	16	2	no
12	13	2	no
14	15	2	no
17	18	1	yes
19	20	1	yes
21	22	1	yes
23	24	1	yes
25	26,30	1	no
26	27,29	1	no
27	28	1	no
28	29	1	no
29	30	1	no

The double intensity lines are written twice. If single intensity lines coincide, only one is written. The lines that may disappear are absent when both endpoints are at the origin.

All coordinates are relative to a right-handed set of coordinate axes whose X coordinate is pointed forward, whose Y coordinate is pointed up, and whose Z coordinate is pointed right. The point at which the line of sight intersects the viewing plane serves as the origin for the image limit X and Y coordinates.

IAC is the output option switch. Four output options are available from this subroutine which will be controlled by using the integer values of IAC from zero through fifteen. The IAC value is decoded by converting it to a four bit binary number.

TABLE 36. OUTPUT OPTION SWITCH BIT POSITIONS

Position	Output Requested
1	338 CRT
2	Movie frame
4	28-inch CALCOMP off line
8	10-inch CALCOMP on line

If IAC is zero, that is, none of the four options are exercised, the output is a printout of the thirty points in CRT coordinates.

IER is an error code which is zero upon normal return and set to a designated non-zero value in case of error. In particular if IER is set to one, STICK1 was called before STICK.

The following table of logical device numbers is used by this program.

TABLE 37. LOGICAL DEVICE NUMBER USAGE

L.D.N.	USE
0	Scratch for CALCOMP Routines
1	Unused
2	Scratch for Pictorial
3	PEEK Input for Control Section
4	Picture Boundary File Input for Control Section
5	Simulator Movie File Input for Control Section
6	Normal Printed Output
7	Movie Output Tape
8	Offline CALCOMP Output
9	CRT Communication
SCARDS	Teletype Input (User's Typed Responses)
SPRINT	Teletype Output (Prompting)

LIST OF REFERENCES

1. Roberts, V. L. and Robbins, D. H. "Multidimensional Mathematical Modeling of Occupant Dynamics Under Crash Conditions," SAE Paper No. 690248, January 1969.

2. McHenry, R. R. and Naab, K. N. "Computer Simulation of the Crash Victim -- A Validation Study," Proc. of the Tenth Stapp Car Crash Conference 1966.

3. Haley, J. L., et al. "Crashworthiness Study for Passenger Seat Design," Arizona State University Engrg. Rept. No. 65-01, 1966.

4. Thompson, J. E. "Occupant Response Versus Vehicle Crush: A Total System Approach," Proc. of the Twelfth Stapp Car Crash Conference, 1968.

5. Furusho, H., et al. "Analysis of Occupant Movements in Rear-End Collision. Part I. Simulation of Occupant Movements," SAE of Japan Safety Research Tour Publication, 1969.

6. Robbins, D. H. "Three-Dimensional Simulation of Advanced Automotive Restraint Systems," 1970 International Automobile Safety Conference Compendium, SAE Publication No. P-30, pp. 1008-1023.

7. Young, R. D. "A Three-Dimensional International Model to Predict the Dynamic Response of an Automobile's Occupant," to be presented at the Annual Meeting of the Highway Research Board, 1971.

8. Segal, D. "Computer Simulation of Body Kinematics Associated with Rapid Deceleration," Dynamic Response of Biomechanical Systems, published by ASME, 1970.

9. Beckett, R. and Chang, K. "An Evaluation of the Kinematics of Gait by Minimum Energy," J. Biomechanics 1(2), 1968.

10. Lissner, H. R. and Williams, M. "Biomechanics of Human Motion," W. B. Sanders, Philadelphia, Pa., 1962.

11. Weber, W. and Weber, E. "Mechanik der menschlichen Gehwerkzeuge," Göttingen, 1836.

12. Kane, T. R. and Scher, M. P. "Human Self-Rotation by Means of Limb Movements," J. Biomechanics 3(1), 1970.

13. Hanavan, E. P. "A Personalized Mathematical Model of the Human Body," AIAA Paper No. 65-498, 1965.

14. Kulwicki, P. V., et al. "Weightless Man: Self-Rotation Technique," AMRL - TDR-62-129, 1962.

15. Chaffin, D. B. "A Computerized Biomechanical Model - Development of and Use in Studying Gross Body Actions," ASME Paper No. 69-BHF-5, 1969.

16. Damon, A., Stoudt, H. M. and McFarland, R. A. "The Human Body in Equipment Design," Harvard University Press, Cambridge, Mass., 1966.

17. Fischer, O. "Theoretische Grundlagen fur eine Mechanik der lebenden Körper mit speziallen Anwendungen auf den Menschen, sowie auf einige Bewegungs-vorgange an Maschinen," B. G. Teubner, Berlin, 1905.

18. Weaver, J. R. "A Simple Occupant Dynamics Model," J. Biomechanics 1(3): 185-191, 1968.

19. Aldman, B. and Asberg, A. "Impact Amplification in European Compacts," Proc. of the Twelfth Stapp Car Crash Conference, 1968.

20. Rennecker, D. N. "A Basic Study of Energy-Absorbing Vehicle Structure and Occupant Restraint by Mathematical Model," SAE Automotive Safety Dynamic Modeling Symposium, Anaheim, Ca., 1967.

21. Martinez, J. L. and Garcia, D. J. "A Model for Whiplash," J. Biomechanics 1(1), 1968.

22. Mertz, H. J. "Kinematics and Kinetics of Whiplash," Ph.D. Thesis, Wayne State University, 1967.

23. Roberts, S. B., et al. "Head Trauma - A Parametric Dynamic Study," J. Biomechanics 2(4), 1969.

24. Hansen, H. M. and Chenea, P. F. "Mechanics of Vibration," John Wiley and Sons, Inc., New York, 1952, pp. 128-137.

25. Hanavan, E. P. "A Mathematical Model of the Human Body," AMRL Technical Report No. TR-64-102, 1964.

26. Patten, J. S. and Theiss, C. M. "Auxiliary Program for Generating Occupant Parameter and Profile Data," CAL Report No. VJ-2759, V-1R.

27. Robbins, D. H., Bennett, R. O. and Roberts, V. L. "HSRI Two-Dimensional Crash Victim Simulator: Analysis, Verification, and Users' Manual," Final Report on U.S. DOT Contract No. FH-11-6962, December 1970, 256 pp.

28. Robbins, D. H., Snyder, R. G. and Roberts, V. L. "Injury Criteria Model for Restraint System Effectiveness Evaluation," HSRI Report No. Bio M-70-7, First Draft, Final Report under DOT Contract FH-11-6962, October 1970.

29. System/360 Scientific Subroutine Package (360A-CM-03X) Version II H20-0205-2, pp. 122-128.

30. Ralston "Runge-Kutta Methods with Minimum Error Bounds," MTAC, Vol. 16, No. 80 (1962), pp. 431-437.

31. Scarborough, J. B. "Numerical Mathematical Analysis," John Hopkins Press pp. 84, 1962.

32. Hamming, R. W. "Numerical Methods for Scientists and Engineers," Chapters 14, 15 and 16, McGraw-Hill, 1962.

33. Boettner, D. W. and Solisbury, R. A. "The Michigan Terminal System, Volume 3: Subroutine and Macro Descriptions," Third Edition, The University of Michigan Computing Center, June 1970.